

February 22, 2013

Attn: Grants Officer
United States Department of Energy
Golden Field Office
1617 Cole Boulevard
Golden, Colorado 80401-3305

Dear Grants Officer:

Attached to this letter is the final scientific report for work done on the DOE grant entitled "Finite Volume Based Computer Program for Ground Source Heat Pump Systems." This grant was part of the Recovery Act – Geothermal Technologies Program: Ground Source Heat Pumps. The Grant Award Number is DE-EE0002805 and the principal investigator at Wright State is Dr. James Menart. The DOE Project Manager for this grant is Yana Rasulova, the Project Monitor is Michael Wofsey, the Contract Officer is Laura Merrick, and the Financial Assistant Specialist is Melissa Jacobi.

This report is a compilation of the work that has been done on grant DE-EE0002805. The goal of this project was to develop a GSHP (ground source heat pump) system simulation program. The period covered by this grant was March 1, 2010 to August 31, 2012. As part of this grant both two-dimensional and three-dimensional GSHP simulation tools have been developed. We feel that the two-dimensional simulation tool we have developed will be well received by the GSHP community as it provides a wealth of results on GSHP systems in a short computational time. The three-dimensional tool that we have developed provides more results than the two-dimensional tool; however, the computational times are longer. Overall a great deal of work was done under this grant that should help to advance the field for GSHPs.

At this time, I would personally like to thank DOE and the Geothermal Technologies Program: Ground Source Heat Pump staff for working with Wright State on this project. I believe this was a worth-while project that will provide benefits for the country in the future.

Sincerely,



James A. Menart
Department of Mechanical Engineering
Wright State University
3640 Colonel Glenn Highway
Dayton, OH 45435
Phone: (937) 775-5145
e-mail: james.menart@wright.edu

FINAL SCIENTIFIC REPORT
For DOE Grant Entitled
**Finite Volume Based Computer Program
for Ground Source Heat Pump System**

Principal Investigator:
Dr. James Menart
Professor
Wright State University
Mechanical and Materials Engineering
3640 Colonel Glenn Highway
Dayton, OH 45435-0001
(937) 775-5145 (phone)
(937) 775-5009 (fax)
james.menart@wright.edu (e-mail)

Business Personnel:
Jackie Frederick, Director Pre-award
Research and Sponsored Programs
Wright State University
201J University Hall
3640 Colonel Glenn Highway
Dayton, OH 45435-0001
(937) 775-2423
(937) 775-3781
jackie.frederick@wright.edu (e-mail)

PI Signature and Date: James A. Menart, February 22, 2013

Federal Agency and Organization: DOE EERE – Geothermal Technologies Program: Ground Source Heat Pumps

Award Number: DE-EE0002805

Recipient Organization: Wright State University

DUNS Number: 047814256

Recipient Address: 3640 Colonel Glenn Highway, Dayton, Ohio 45435-0001

Date of Report Submission: February 22, 2013

Period Covered by Report: March 1, 2010 to August 31, 2012

Duration of Project: March 1, 2010 to August 31, 2012

Reporting Period: March 1, 2010 to August 31, 2012

DOE Project Team: Project Manager - Yana Rasulova
Project Monitor - Michael Wofsey
Contract Officer - Laura Merrick
Financial Assistant Specialist - Melissa Jacobi.

TABLE OF CONTENTS

TABLE OF CONTENTS.....	3
LIST OF FIGURES.....	5
LIST OF TABLES.....	8
NOMENCLATURE.....	9
EXECUTIVE SUMMARY.....	12
1. INTRODUCTION.....	13
2. INPUTS.....	15
2.1. GUI DESIGN.....	15
2.1.1. Building Specifics.....	15
2.1.2. Heat Pump Selection.....	19
2.1.3. Ground Loop Inputs.....	20
2.2. BUILDING LOAD CALCULATIONS.....	22
2.2.1. ENERGYPLUS.....	24
3. CALCULATIONS.....	28
3.1. FLUID FLOW.....	28
3.1.1. Laminar Flow.....	28
3.1.2. Turbulent Flow.....	28
3.2. HEAT TRANSFER IN GROUND AND GROUND LOOP.....	32
3.2.1. Energy Equation.....	32
3.2.2. Grids.....	33
3.2.3. BOUNDARY CONDITIONS.....	41
3.3. HEAT PUMP.....	47
3.3.1. COP Trend Study.....	47
3.3.2. Correction Factors.....	51
3.3.3. Entering Water Temperature.....	53
3.3.4. Wet Bulb Temperature.....	54
3.4. ECONOMICS.....	56
3.4.1. Unit and Installation Costs.....	56
3.4.2. Operational Costs.....	56
3.4.3. Payback Period.....	58

4. PROGRAM OUTPUTS	60
4.1. GEO2D	60
4.2. GEO3D	66
5. OTHER GSHP SYSTEM MODELING WORK.....	74
5.1. RESEARCH ORIENTATED.....	74
5.1.1. Analytical Methods	74
5.1.2. Numerical Methods	75
5.2. AVAILABLE COMMERCIAL CODES	77
5.2.1. RETScreen	78
5.2.2. TRNSYS	80
5.2.3. GLHEPRO	83
5.2.4. Ground Loop Design.....	84
5.2.5. Earth Energy Designer.....	85
5.2.6. GS2000	88
6. PUBLICATIONS	91
6.1. Presentations and publications	91
6.2. Patents and Intellectual property	92
6.3. training and professional development.....	92
6.4. Other Products / Deliverables	92
7. SUMMARY	93
REFERENCES	95
APPENDIX I: Simulation RESULTS FOR DAYTON, OHIO	100
APPENDIX Ii: Simulation RESULTS FOR BOSTON, MASSACHUSETTS.....	128
APPENDIX Iii: Simulation RESULTS FOR OMAHA, NEBRASKA.	156

LIST OF FIGURES

Figure 1: Building specifics options window.	15
Figure 2: Flow chart of the building specifics GUI.	16
Figure 3: Novice load calculator.	17
Figure 4: Expert options for load calculations.....	18
Figure 5: Heat pump selection window.....	19
Figure 6: Fluid properties selection window.....	20
Figure 7: Pipe material selection window.....	21
Figure 8: Soil properties selection GUI.....	22
Figure 9: Loop configuration selection window.	23
Figure 10: Other simulation details selection.....	23
Figure 11: Calculated friction factor compared to Moody diagram.....	29
Figure 12: Velocity profiles.	30
Figure 13: Three regions modeled in turbulent flow.	31
Figure 14: Effective thermal conductivity profiles.....	32
Figure 15: An example of the control volume layout.	34
Figure 16: Heat transfer coefficient as a function of the number of grid points in the bulk fluid. 35	
Figure 17: Heat transfer coefficient as a function of the number of grid points in the sublayer region.....	36
Figure 18: Heat transfer coefficient as a function of the number of grid points in the bulk flow region.....	36
Figure 19: Equation for number of grid points in the bulk flow region.	37
Figure 20: Soil grid study for different exponents.	38
Figure 21: Error in entering water temperature.	38
Figure 22: Accuracy with changing time step.....	39
Figure 23: The grid system used for a vertical GLHE in GEO3D.	40
Figure 24: The grid system in GEO3D for a vertical GLHE.....	41
Figure 25: Section of a vertical GLHE and some inputs used to develop the model.	41
Figure 26: The total heat extracted from the ground loop at various boundary condition radii using an adiabatic boundary condition.....	42
Figure 27: The total heat extracted from the ground loop at various boundary condition radii using a constant temperature boundary condition.	43
Figure 28: Far field boundary radius required for 0.1% error in simulations as a function of simulation period in years.....	44
Figure 29: Coefficient A for 60% heating ratio.....	45
Figure 30: Coefficient B for 60% heating ratio.....	45
Figure 31: <i>The boundary condition for a vertical GLHE in GEO3D.</i>	46
Figure 32: Cooling capacity versus fluid flow for different EWT (Trane November 2010).....	48
Figure 33: Coefficient A versus EWT for 3 ton unit #8.....	48
Figure 34: Coefficient B vs. EWT for 3 ton unit #8.....	49
Figure 35: Coefficient C vs. EWT for 3 ton unit #8.	49

Figure 36: COP for 3 ton unit number 8 at rated volume flow (Trane November 2010).	51
Figure 37: Correction factors for entering air temperature (Trane November 2010).	51
Figure 38: Correction factor for indoor air volume flow (Trane November 2010).	52
Figure 39: Correction factor for capacity as a function of antifreeze concentration (Trane November 2010).	53
Figure 40: Temperature profiles for flow in a tube	54
Figure 41: Adiabatic saturation process (Cengel and Boles 2008).	55
Figure 42: Vapor pressure, fluid enthalpy, and vapor enthalpy plotted and fit.	55
Figure 43: Price per foot of geothermal tubing.	57
Figure 44: COP for air-to-air heat pump in cooling mode.	57
Figure 45: COP for air-to-air heat pump in heating mode.	58
Figure 46: Screen shot of the economics page.	59
Figure 47: Home screen for case study.	60
Figure 48: Daily COP.	61
Figure 49: Histogram of COP's.	61
Figure 50: Entering water temperature to the heat pump.	62
Figure 51: Heat exchanged with the working fluid.	63
Figure 52: Indoor and outdoor dry-bulb temperatures.	63
Figure 53: Hourly heat loads from ENERGYPLUS.	64
Figure 54: Temperatures at different locations in the earth and tube.	65
Figure 55: Example of a temperature field during heating season.	65
Figure 56: Example of a temperature field during the cooling heating season.	66
Figure 57: Temperature profiles in a horizontal plane at a depth of 0.00 meters below the earth's surface. Note that the $x = 0, y = 0$ position is the center of the bore hole and the temperature scale shown is in degrees Celsius.	68
Figure 58: Temperature profiles in a horizontal plane at a depth of 0.22 meters below the earth's surface. Note that the $x = 0, y = 0$ position is the center of the bore hole and the temperature scale shown is in degrees Celsius.	69
Figure 59: Temperature profiles in a horizontal plane at a depth of 13.56 meters below the earth's surface. Note that the $x = 0, y = 0$ position is the center of the bore hole and the temperature scale shown is in degrees Celsius.	69
Figure 60: Temperature profiles in a horizontal plane at a depth of 49.11 meters below the earth's surface. Note that the $x = 0, y = 0$ position is the center of the bore hole and the temperature scale shown is in degrees Celsius.	70
Figure 61: Temperature profiles in a horizontal plane at a depth of 93.55 meters below the earth's surface. Note that the $x = 0, y = 0$ position is the center of the bore hole and the temperature scale shown is in degrees Celsius.	70
Figure 62: Temperature profiles in a horizontal plane at a depth of 100.00 meters below the earth's surface. Note that the $x = 0, y = 0$ position is the center of the bore hole and the temperature scale shown is in degrees Celsius.	71

Figure 63: Zoomed in view of temperature profiles in a horizontal plane at a depth of 13.55 meters below the earth's surface. Note that the $x = 0, y = 0$ position is the center of the bore hole and the temperature scale shown is in degrees Celsius.....	71
Figure 64: Bulk temperature of working fluid exiting the ground loop as a function of time.	72
Figure 65: Heat delivered from the heat pump to the house, heat taken from the fluid by the heat pump, and heat delivered by the ground to the fluid.	72
Figure 66: COP of the heat pump as a function of time.....	73
Figure 67: RETScreen's method for determining entering water temperature as a function of outside temperature.	79
Figure 68: Example project in TRNSYS Simulation Studio (TRNSYS 2009).	81
Figure 69: The finite difference model for a single buried pipe in TRNSYS (Giardina 1995).	82
Figure 70: TRNSYS's thermal resistance approach for the heat transfer analysis (Giardina 1995).....	82
Figure 71: The average fluid temperature from GEO2D and Earth Energy Designer.	86
Figure 72: The average fluid temperature difference between GEO2D and Earth Energy Designer.....	86
Figure 73: The minimum and maximum average fluid temperature for EED and the daily entering water temperature for GEO2D, for a 5 year simulation.....	87
Figure 74: The minimum and maximum average fluid temperature for EED and the daily entering water temperature for GEO2D, for 25 th year.....	87
Figure 75: GS2000 and GEO2D entering water temperature comparison for 10 years of simulation using a constant heating load.....	89
Figure 76: GS2000 and GEO2D entering water temperature comparison for 10 years of simulation using heating and cooling loads for a home in Dayton, Ohio.	89

LIST OF TABLES

Table 1: Coefficients for outside convection algorithm (Yazdanian and Klems 1994).	25
Table 2: Roughness factor multiplier (EnergyPlus 2010).	25
Table 3: Computation time required for changing exponent and time step.	39
Table 4: Input conditions for geothermal program.	67
Table 5: Development of models and techniques for sizing ground loop geothermal systems (Haberl and Sung 2008).	77
Table 6: A brief description of 6 commercial GLHE programs available today in comparison to GEO2D.	90

NOMENCLATURE

$\%af$	Percentage of antifreeze concentration
A	Area
B	resistance shape factor coefficient
cv	Control volume
C	Thermal capacitance of a layer
C_p	Specific heat
COP	coefficient of performance
COP_C	Coefficient of performance for cooling
COP_H	Coefficient of performance for heating
CC	Cooling capacity
CP	Cooling compressor power
D	diameter
D_m	neutral stability momentum transfer coefficient
D_h	stability correction
eff_{ng}	Natural gas furnace efficiency
eff_{oil}	Fuel oil furnace efficiency
eff_{pr}	Propane gas furnace efficiency
EWT	Entering Water Temperature
FV	Future value dollars
g	g-function
h	Convective heat transfer coefficient
h_n	Natural Convective heat transfer coefficient
h_r	Radiation heat transfer coefficient
h_{glass}	Convective heat transfer coefficient on a smooth glass surface
h_f	Enthalpy of the fluid
h_g	Enthalpy of the vapor
H	borehole depth
HC	Heating capacity
HP	Heating compressor power
i	Interest rate
I^o	Total available irradiation
I_b	Intensity of direct beam radiation
I_s	Intensity of sky diffuse radiation
I_g	Intensity of ground reflected diffuse radiation
k_t	Turbulent thermal conductivity of the fluid
k_{eff}	Effective thermal conductivity of the fluid
k	Thermal conductivity of the fluid
k_{soil}	Thermal conductivity of the soil
\dot{m}	mass flow rate
ncv	number of control volumes
n_z	number of control volumes in axial direction
n_r	number of control volumes in radial direction
n_σ	number of control volumes in azimuthal direction

Pe_t	Turbulent Peclet number
Pr	Prandtl number
Pr_t	Turbulent Prandtl number
P_g	Vapor pressure
P_{atm}	Atmospheric pressure
PV	Present value dollars
\dot{q}	Heat flux
\dot{Q}	Total heat rate
\dot{Q}/L	Heat rate per unit length
r	radius or radius index number
R	Thermal resistance
Re	Reynolds number
R_f	Roughness factor multiplier
Ri	Richardson number
t	Time
T	Temperature
$T(r)$	Temperature at distance r from the center of the pipe
T_{db}	Indoor dry bulb temperature
T_{wb}	Indoor wet bulb temperature
T_m	Mean fluid temperature
T_{bulk}	Bulk fluid temperature
T_{wall}	Temperature of the pipe wall surface
u	Velocity at distance r from the center of the pipe
u_*	Friction velocity
U	fluid node temperature
U^+	Dimensionless axial velocity
U_m	Maximum centerline velocity
\dot{v}	Volume flow of the fluid
V	volume
\dot{V}	Volume flow of the air
V_z	Local wind speed calculated at the height of the surface centroid
V_{ave}	Average fluid velocity
x	axial direction or distance between nodes
y^+	$= \frac{yu_*}{\nu}$, dimensionless normal distance from the wall
y	Distance from the pipe wall
z	axial node index number

Greek Symbols

α	Thermal diffusivity
α_a	Solar absorptance of a surface
ε	Solar emissivity of a surface
ϵ_r	Relative eddy momentum diffusivity
ϵ_m	Eddy momentum diffusivity
λ	Friction factor

ν	Kinematic viscosity of the fluid = μ/ρ
ρ	Solar reflectivity of a surface or density
σ	azimuthal node index number
τ	Solar transmissivity of a surface
ω	Humidity ratio

EXECUTIVE SUMMARY

This report is a compilation of the work that has been done on the grant DE-EE0002805 entitled "Finite Volume Based Computer Program for Ground Source Heat Pump Systems." The goal of this project was to develop a detailed computer simulation tool for GSHP (ground source heat pump) heating and cooling systems. Two such tools were developed as part of this DOE (Department of Energy) grant; the first is a two-dimensional computer program called GEO2D and the second is a three-dimensional computer program called GEO3D. Both of these simulation tools provide an extensive array of results to the user. A unique aspect of both these simulation tools is the complete temperature profile information calculated and presented. Complete temperature profiles throughout the ground, casing, tube wall, and fluid are provided as a function of time. The fluid temperatures from and to the heat pump, as a function of time, are also provided. In addition to temperature information, detailed heat rate information at several locations as a function of time is determined. Heat rates between the heat pump and the building indoor environment, between the working fluid and the heat pump, and between the working fluid and the ground are computed. The heat rates between the ground and the working fluid are calculated as a function time and position along the ground loop. The heating and cooling loads of the building being fitted with a GSHP are determined with the computer program developed by DOE called ENERGYPLUS. Lastly COP (coefficient of performance) results as a function of time are provided. Both the two-dimensional and three-dimensional computer programs developed as part of this work are based upon a detailed finite volume solution of the energy equation for the ground and ground loop. Real heat pump characteristics are entered into the program and used to model the heat pump performance. Thus these computer tools simulate the coupled performance of the ground loop and the heat pump. The price paid for the three-dimensional detail is the large computational times required with GEO3D. The computational times required for GEO2D are reasonable, a few minutes for a 20 year simulation. For a similar simulation, GEO3D takes days of computational time. Because of the small simulation times with GEO2D, a number of attractive features have been added to it. GEO2D has a user friendly interface where inputs and outputs are all handled with GUI (graphical user interface) screens. These GUI screens make the program exceptionally easy to use. To make the program even easier to use a number of standard input options for the most common GSHP situations are provided to the user. For the expert user, the option still exists to enter their own detailed information. To further help designers and GSHP customers make decisions about a GSHP heating and cooling system, cost estimates are made by the program. These cost estimates include a payback period graph to show the user where their GSHP system pays for itself. These GSHP simulation tools should be a benefit to the advancement of GSHP systems.

1. INTRODUCTION

The purpose of this DOE (Department of Energy) funded project was to develop a GSHP (ground source heat pump) computer simulation tool. This has been done; in fact, two GSHP computer simulations have been developed. The first program developed is called GEO2D and the second program developed is called GEO3D. Essentially, as the names imply, one of the programs is a two-dimensional program and the other is a three-dimensional program. GEO2D models the GSHP system in the radial and axial directions, while GEO3D does the radial, axial and azimuthal directions. Both of these programs provide a great deal of results for GSHP systems. These two computer simulation tools should be assets to the GSHP community, as well as to the future development of GSHP systems in the United States.

Both GEO2D and GEO3D use a detailed finite volume technique to solve the unsteady energy equation in the ground and the ground loop. So that accurate performance information may be obtained, the GSHP loop and the heat pump are modeled as a coupled system. The programs model the performance of the GSHP system over a period of hours or years as chosen by the user. Essentially any time frame greater than one hour, can be chosen. We believe that these programs produce some of the most detailed information available for GSHP systems. For the GSHP designer this program may be used to design GSHP systems for any type of building or perform many “what if” type scenarios and improve the operation of such systems.

At the present time most commercial GSHP computer codes use a technique called the g-function technique. Essentially this is an approximate one-dimensional technique that provides limited information on the geothermal field. Unlike these one-dimensional GSHP computer simulations based on the g-function technique, GEO2D and GEO3D provide complete temperature field information as a function of time and position. Of course GEO2D does not show changes in the azimuthal direction, while GEO3D does. Temperature field information such as this can help the GSHP designer provide proper spacing of the ground loops, whether they are vertical or horizontal. This temperature information also provides information on the sizing of the system. It is believed that this will be useful information to GSHP designers. In addition to providing the most extensive temperature field information of any GSHP commercial computer code, GEO2D and GEO3D provide extensive heat rate information. Heat flows between the ground and working fluid are calculated in total or as a function of length along the ground loop, heat rates between the working fluid and the heat pump, and heat rates between the heat pump and the building are obtained. These heat rates are all a function of time and are indicators of the performance of the GSHP system. Lastly heat pump COP information as a function of time is provided. This may be one of the most telling parameters on how well the GSHP system is designed. It is believed that GEO2D and GEO3D are the only commercial GSHP computer simulations to provide detailed COP information.

It needs to be stated here that the price paid for extending GEO2D to GEO3D is computational time. To simulate 20 years of GSHP operation takes GEO2D a few minutes while it takes GEO3D a few days. This is a huge penalty to pay for the extra detail included in GEO3D. It is believed that the computational time of GEO3D can be reduced substantially, but this will have to be the goal of another project. Because of the small simulation times with GEO2D, a number of attractive features have been added to it. GEO2D has a user friendly interface where inputs and outputs are all handled with GUI (graphical user interface) screens. These GUI screens make the program exceptionally easy to use. To make the program even easier to use, a number of standard input options for the most common GSHP situations are

provided to the user. For the expert user, the option still exists to enter more detailed information. To further help designers and GSHP customers make decisions about a GSHP heating and cooling system, cost estimates are made by GEO2D. These cost estimates include a payback period graph to show the user where a GSHP system pays for itself.

In this report a number of details on GEO2D and GEO3D are provided. The description of these codes is divided into three main parts. These three main parts are:

- Inputs – presented in Section 2,
- Calculations – presented in Section 3, and
- Outputs – presented in Section 4.

In the input section are included the GUI used for GEO2D and the line data input used for GEO3D. Most of the discussion is carried out for GEO2D which has a very user friendly GUI interface. Also include in the Input section is the building heating and cooling load calculation. The reason for including this in the input section is that the DOE program ENERGYPLUS is used to do these calculations. ENREGYPLUS outputs are directly usable by the GSHP codes developed here. Included in the Calculation section are the working fluid flow modeling, the heat transfer modeling, the heat pump modeling, and the economic analyses. In the Output section results from both GEO2D and GEO3D are presented. GEO2D results are presented in user friendly GUIs while the GEO3D results are presented using external plotting tools. A large amount of additional results are given in the Appendices. After discussing the three main parts of the computer codes a fourth section entitled,

- Other Commercial and Research Orientated Simulation Work – presented in Section 5.

is given. In this section a discussion of all the major commercial codes for performing GSHP system simulations that are known to the Wright State geothermal group are given. In addition, a review of the computational research is given. This will allow the reader of this report to gauge where GEO2D and GEO3D stand in the field of GSHP simulations. Lastly a brief summary is given.

2. INPUTS

2.1. GUI DESIGN

For GEO2D a user friendly GUI was designed implemented. The user interface was written in MATLAB and was designed to allow the user to easily input the many design parameters needed for a GSHP system design. The home screen was written so the user will be guided through the program, enabling screens and buttons when the necessary information has been entered. Upon selection of a new project, the user designates a folder in the 'project files' directory where the raw data is stored. A file in the 'project files' directory with the name supplied is stored and needs to be selected when the user returns to the project in the future. Once the user names a new project, the units and location are selected and are locked in throughout the rest of the program run. Upon selection of the location, the weather file associated with that location is copied to 'in.epw' for use in the ENERGYPLUS simulator.

2.1.1. Building Specifics

The next step in the program is for the user to design the building or home. The user can do this on their own or use an already drawn '.idf' input file to adjust to mimic their home. As seen in Figure 1 the user is asked to choose whether they want to the 'novice' or 'expert' version of input for use with ENERGYPLUS.

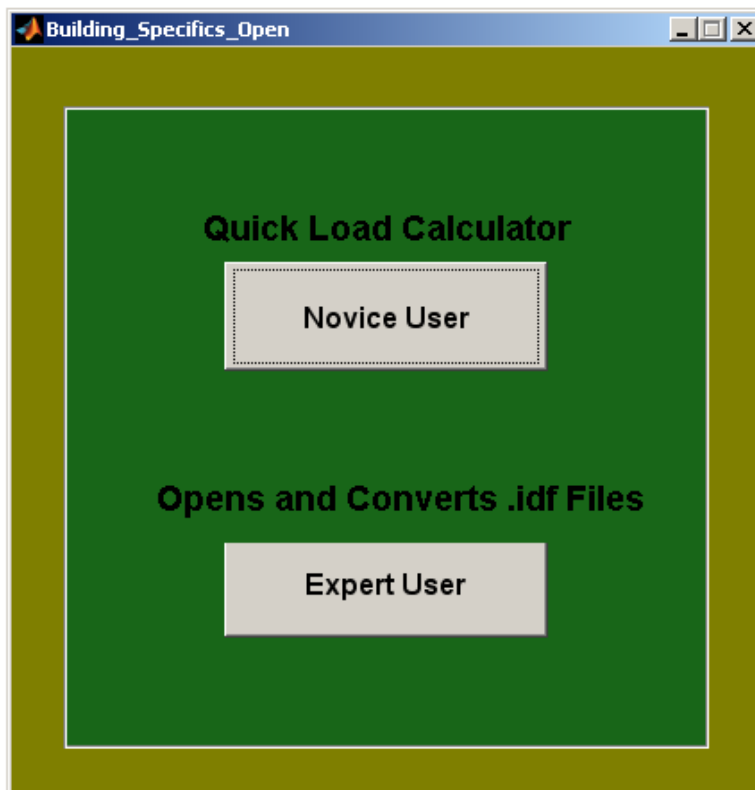


Figure 1: Building specifics options window.

The flow through the 'Building Specifics' screen can best be described by the flow chart in Figure 2 where both choices lead to hourly loads and other data needed for the geothermal analysis.

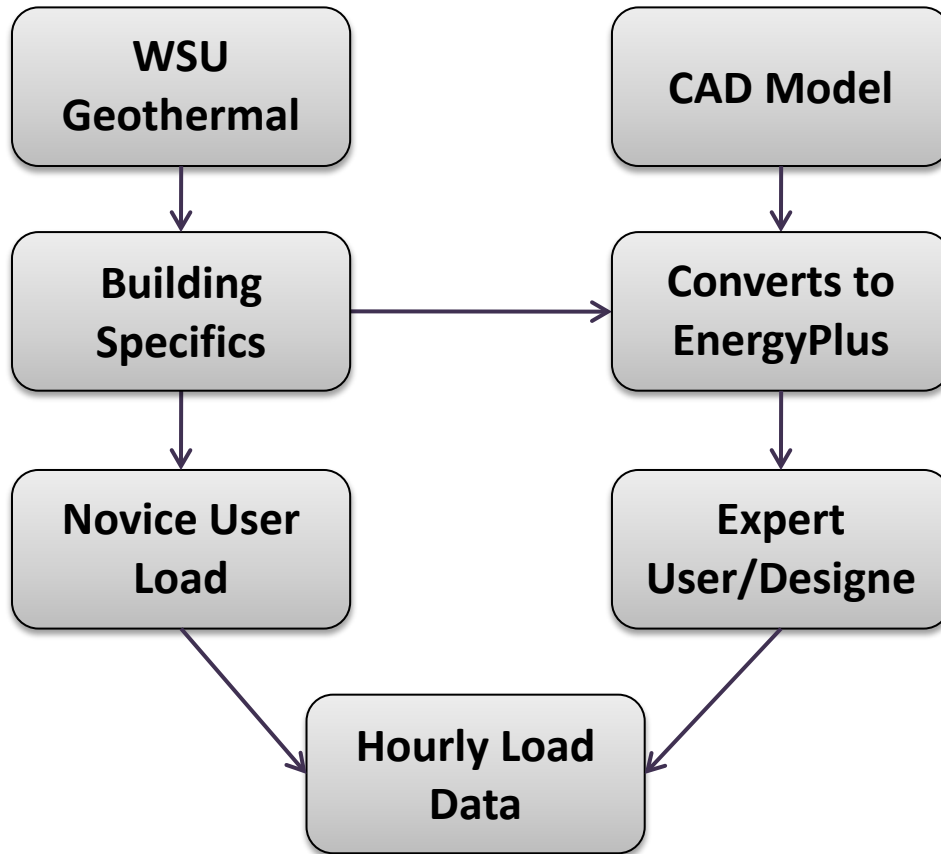


Figure 2: Flow chart of the building specifics GUI.

2.1.1.1. Novice User

The 'novice' choice does not require the user to know anything about ENERGYPLUS or how it exports data. The user is displayed a screen which consists of different shaped floor plans from which he or she can choose. When the user selects one, boxes are enabled for the dimensions of the areas. The '.idf' input file is written specifically to these shapes and any complex geometry or overhangs should be done in the expert section. An example of the building specifics GUI can be seen in Figure 3.

Once the user has selected the floor plan and dimensions of the space, second story and basement options are chosen. The second floor option allows the user to input dimensions up to the same size as the first floor. The basement option is modeled as the four most common types; unconditioned basement, conditioned basement, crawl space, or slab. These conditions are all modeled differently in ENERGYPLUS, but are easily chosen and sized in the GUI.

The unconditioned basement is modeled as a separate zone with concrete walls, slab floor, eight foot ceilings, and no insulation. The concrete walls are modeled using the C-Factor method of construction in ENERGYPLUS. The value for the C-factor was chosen from the ACM Joint Appendix on page 4-37, in a table of C-factors for masonry walls (ASHRAE n.d.). The chosen C-factor is for empty, medium density, concrete masonry units. The concrete floor is modeled using the F-factor method and the value for the F-factor is modeled as having no insulation. The

conditioned basement model is done in the same manner, with the exception of being modeled with wood framed insulated walls and floors, and equipped with a thermostat that is set to maintain the desired temperature. The concrete slab option is modeled using the F-factor method for on-grade with 36 inches of insulation around the perimeter of the slab. The crawl space is modeled using an option in ENERGYPLUS called 'OtherSideCoefficients', where the floor is given a convective heat transfer coefficient of $0.51 \frac{W}{m^2 \cdot ^\circ C}$ to simulate a vented space.

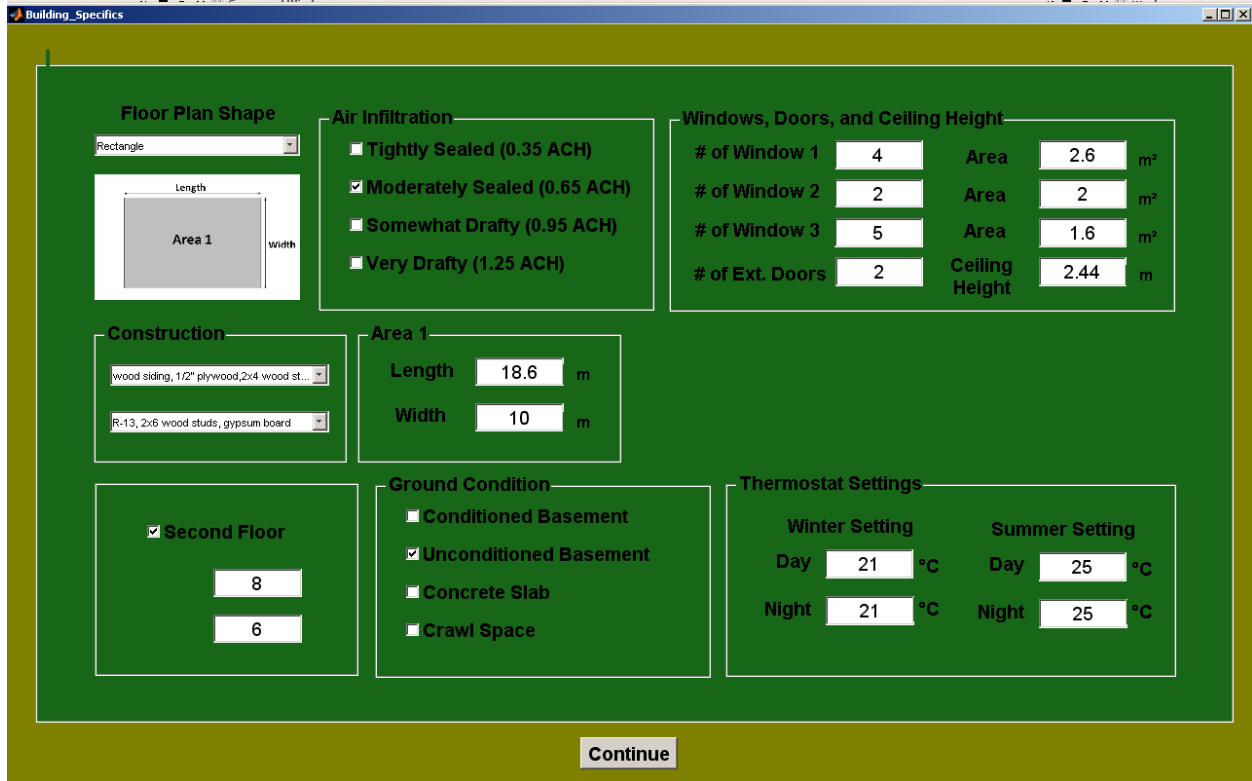


Figure 3: Novice load calculator.

The user must now select the air infiltration desired to be modeled. Equally spaced values, from a tightly sealed construction to a loosely constructed home are available. The values are given in ACH (air changes per hour), which indicates how many times all of the air in the zone is exchanged with outdoor air in a one hour time period. This is also how this heat exchange process is entered into ENERGYPLUS. Anything below 0.35 ACH is not recommended due to a lack of fresh air in the zone which can cause health problems (ASHRAE n.d.). Any value above 1.25 ACH is considered to be extremely drafty; any other infiltration conditions should be modeled in the expert option.

The novice user is given the option to enter three different sized windows, but does not have to specify their location; the model treats it as a square area of window and divides it equally among the wall areas. The exterior door is modeled as a multiplier and is set to a standard size of 3 feet wide by 7 feet tall. The material is modeled with layers of metal with insulation board between. Any complex door conditions should be modeled in the expert option.

The user must now select the construction of the exterior walls and ceiling using the dropdown menu. These constructions were supplied in the ENERGYPLUS's 'compositewallconstruction.idf' file and could be added to for more options in the future. The

ceiling height is then entered and the user can now enter the desired thermostat temperatures for the heating and cooling seasons for both day and night settings. With these values selected, the user clicks on the 'continue' button; the input file is written, the thermostat template is expanded, ENERGYPLUS is executed, and the load simulation begins.

2.1.1.2. Expert User

If the user selects the 'expert' button, a window will pop up providing the option of converting an already existing input file, from a CAD drawing, or simply opening without converting. The 'convert' button, seen in Figure 4, should only be used to input a file drawn in CAD using 'OpenStudio' and not for already started projects. This button collects all of the geometry needed to virtually draw the building in the simulation and adds it to some scheduling, materials, constructions, and outputs so that the tedious process of adding these things can be avoided.

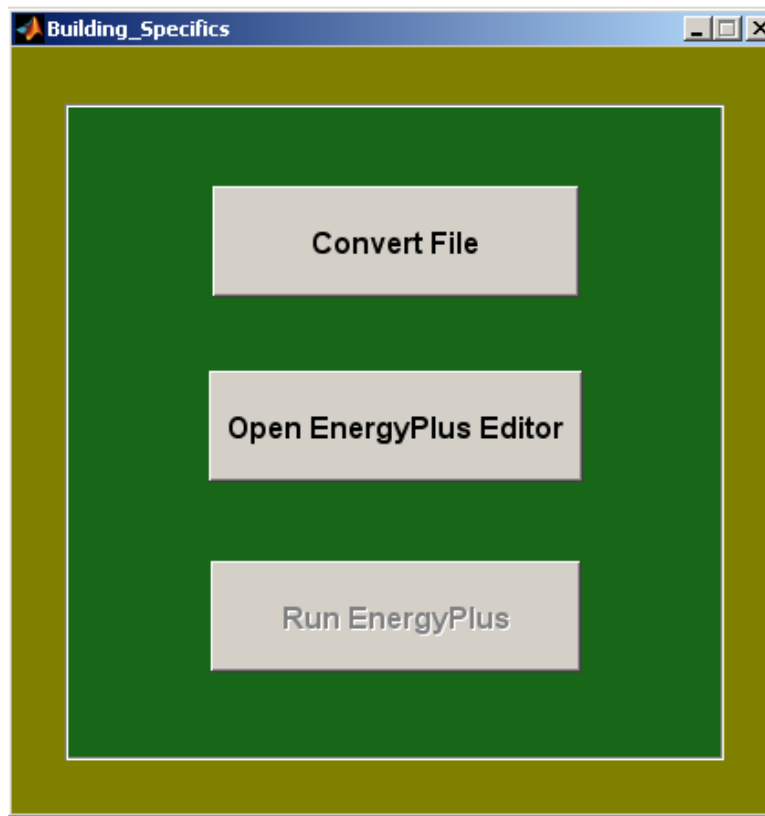


Figure 4: Expert options for load calculations.

Once a file has been converted, the user is asked to select the zones that are to be analyzed for a single heat pump, and the ENERGYPLUS editor is launched for the designer to make any changes. The designer now has full access to the entire ENERGYPLUS program. It is important to preselect some items to insure the geothermal program has the proper data to continue, otherwise an error will occur. The designer can then save any changes such as internal loads, schedules, material properties, shading, etc. The designer clicks on the 'continue' button; the input file is written, the thermostat template is expanded, ENERGYPLUS is executed, and the load simulation begins.

If the user selects the 'open ENERGYPLUS' button, they are asked to select their '.idf' file and it is then opened for editing. This should only be used for already converted files so that when all of the editing is complete, the file will run with the GUI.

2.1.2. Heat Pump Selection

The information obtained from ENERGYPLUS is all on an hourly time step basis and includes the temperatures, humidity ratios, individual zone loads, outside air temperatures, and wind speeds. The next step is to read this information based on the zones selected by the user. The maximum cooling and heating loads are then determined and the 'heat pump select' window is launched. The maximum loads are displayed for the user in kilowatt-hours along with the recommended heat pump selected from the heat pump performance study in Section 3. The user can simply click continue to use the recommendation or can choose any machine in the program via the drop down menu. If the building energy analysis comes back with a peak load that is larger than the rated capacity of the heat pump, then a warning message is displayed. An example of a heat pump selection window can be seen in Figure 5.

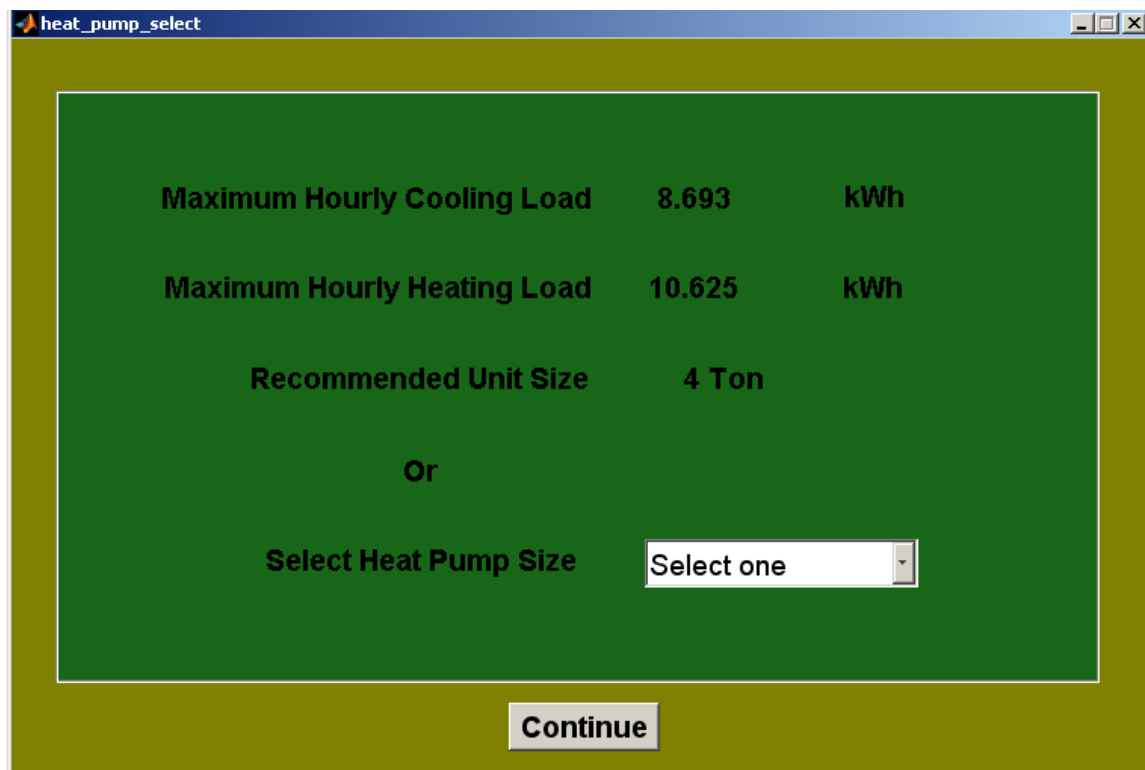


Figure 5: Heat pump selection window.

The rated volume flow for the heat pump selected is used along with the manufacturer's recommended pipe diameter to calculate a recommended fluid velocity. It is important to note that all of these values can be changed by the designer and are only displayed as a guide. The value for the air flow across the heat exchanger is set to the manufacturer's rated volume for the selected heat pump.

2.1.3. Ground Loop Inputs

With the building simulated and the heat pump selected, the user will now begin to design the thermal system. The first step is to define the type of fluid to be used in the analysis. The user will first notice that any antifreeze concentration can be selected with the thermal properties automatically determined as they are selected. Also a value for the initial fluid temperature to start the simulation is calculated as the average ground temperature. The fluid velocity will also have a calculated default value based on the rated volume flow and pipe size of the heat pump selected in the previous step. The values for these inputs are only recommended values and can be changed by the user. An example of the fluid selection window can be seen in Figure 6.

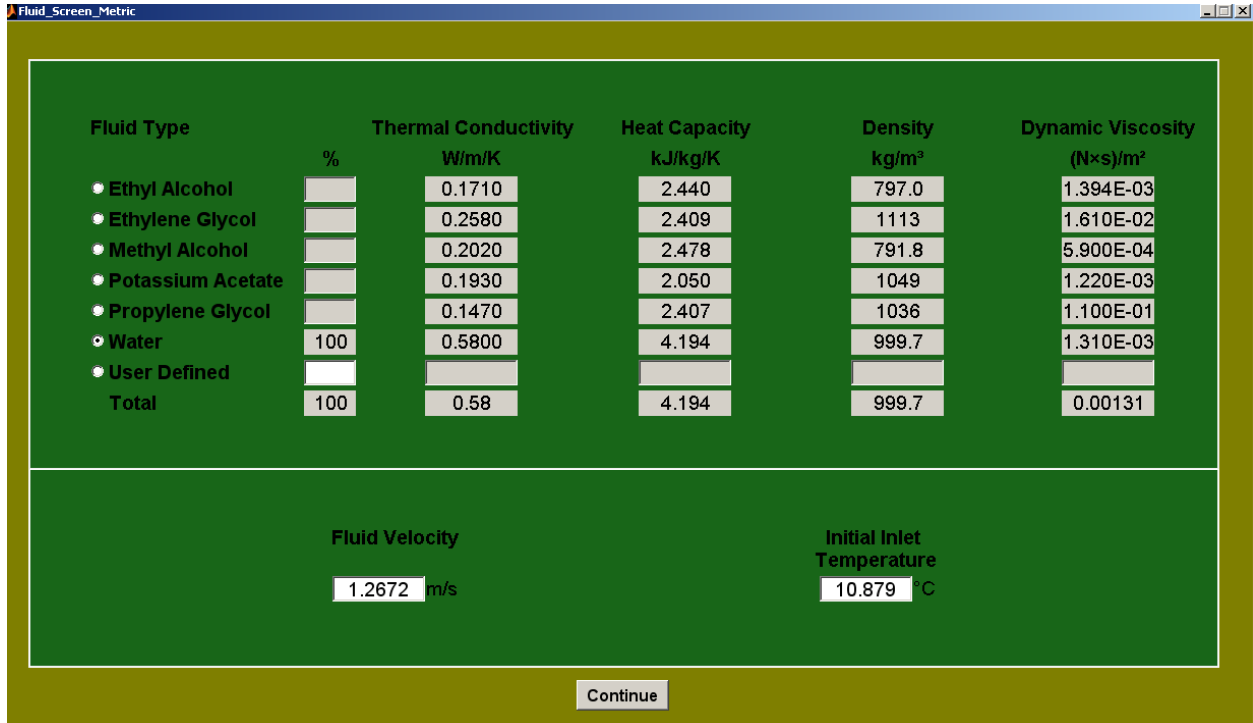


Figure 6: Fluid properties selection window.

Upon completion of the fluid section, the user might notice the values showing up on the home screen for inspection. The next step takes the user to the pipe selection, where the recommended pipe based on the heat pump selected is displayed. The user can define their own properties or select from the three supplied materials and their corresponding pipe size. Copper was used to give the designer options with other heat transfer design work. An example of the pipe selection page can be seen in Figure 7.

The only thermal properties left to enter are for the soil. The user can select from nine different types of soil or enter their own properties. A future grout selection option, currently being developed, will allow for an added layer of material used mainly in vertical loops. An example of the soil properties page can be seen in Figure 8.

The loop configuration button will open a figure that allows the user to choose between the two main types of geothermal systems; horizontal closed loop and vertical closed loop. The recommended pipe length is calculated as a starting point for the geothermal design and is based on a rule of thumb of 100 meters per ton. This recommendation is on the high end what is generally recommended by geothermal designers, but it is a good place to start the design

process. The user can easily change any recommend inputs to values of their choosing. Other essential information about the loop is given here such as depth of trench, number of boreholes, etc. An example of the loop configuration screen can be seen in Figure 9.

Moving on to the 'Calculate GSHE' button, the suggested ground temperature is displayed. This value is calculated by simply averaging the outside dry bulb temperatures supplied by the ENERGYPLUS output files. The suggested values for the fluid grid points are calculated based on the study performed in Section 3. Once the number of time steps and time step size is selected, the soil radius and corresponding suggested number of grid points is displayed. These values are also based on the grid study performed in Section 3. Once all other values have been selected and the 'Continue' button is pushed, the variables for the geothermal analysis are all checked to make sure they have been defined. The input file for the geothermal program is then written and the FORTRAN executable is called. An example of the page used to collect the final simulation parameters can be seen in Figure 10.

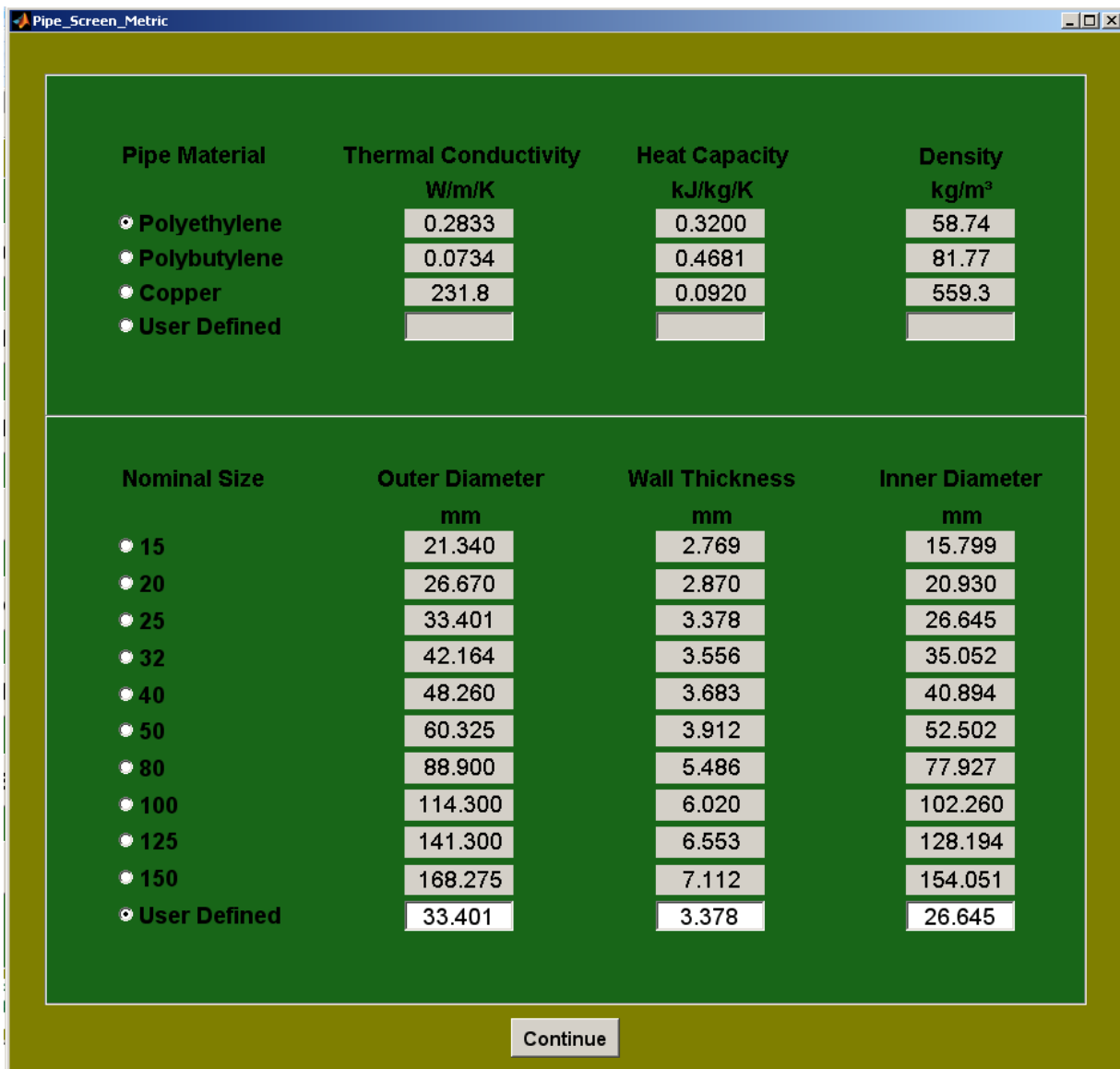


Figure 7: Pipe material selection window.

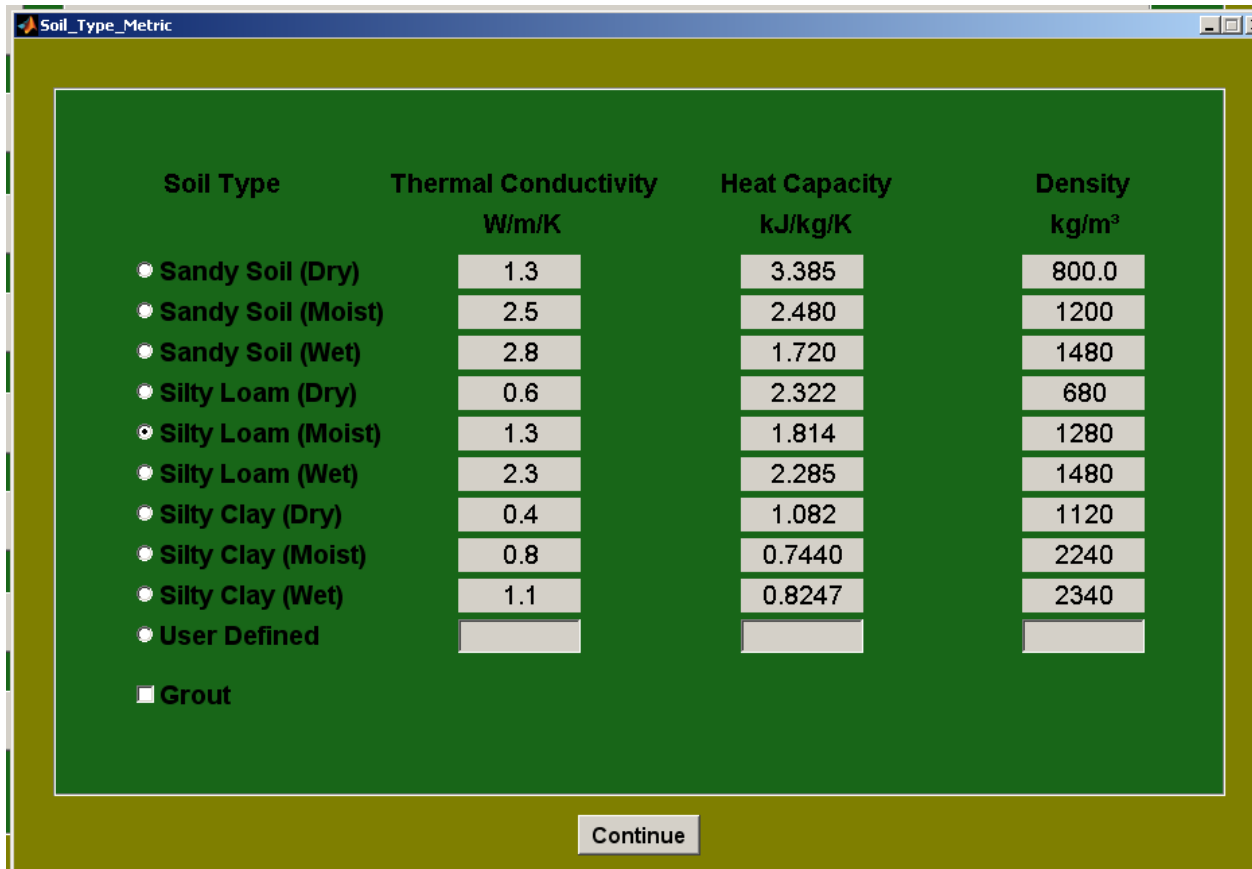


Figure 8: Soil properties selection GUI.

Upon completion of the calculations, the 'Economics' and 'Outputs' buttons are enabled. Careful attention was taken to ensure the user would have as much access to the data as possible. This is ensured by allowing the user full use of the plotting tools in the MATLAB figures.

2.2. BUILDING LOAD CALCULATIONS

Before doing a geothermal analysis an accurate hourly building load calculation is required. Due to the complex nature of a building load calculation and the accuracy desired, ENERGYPLUS (EnergyPlus 2010) is interfaced with the newly developed geothermal program. The latest ENERGYPLUS program gives the geothermal analysis program the ability to make a quick residential type novice calculator, as well as provide the expert designer the access to all of ENERGYPLUS through the editor. The numerous '.epw' weather files supplied by ENERGYPLUS allow the geothermal analysis program more versatility to all regions of the country.

Loop Configuration_Metric

Horizontal Closed Loop

Length of Pipe: m

Depth of Pipe: m

Vertical Closed Loop

Depth of Borehole: m

Diameter of Borehole: m

Number of Boreholes:

Pond Closed Loop

Length of Pipe: m

Depth of Pipe: m

Vertical Open Loop

Depth of Borehole: m

Diameter of Borehole: m

Number of Boerholes:

Figure 9: Loop configuration selection window.

Soil_Properties_New_2

Other Simulation Details

Ground Temperature: °F

No. of Time Steps:

Time Step Size:

Output Frequency:

Soil Thickness (Boundary Condition): m

Number of Control Volumes

Fluid:

Pipe Wall:

Grout:

Soil:

Axial:

Grid Exponent

Fluid:

Pipe Wall:

Grout:

Soil:

Axial:

Figure 10: Other simulation details selection.

2.2.1. ENERGYPLUS

Developed as a result of the BLAST (Building Loads Analysis and System Thermodynamics) and DOE-2 programs, ENERGYPLUS was designed as an energy and load simulation tool (EnergyPlus 2010). The intended use was for architects and HVAC (heating, ventilation, and air conditioning) designers to perform cost analysis and optimize energy performance. Although ENERGYPLUS was designed to simulate different HVAC systems, the integration of the HVAC template allows for an ideal system simulation. Using this template, the building can be modeled at user defined thermostat set points to ultimately calculate hourly load data. Based on the physical description of the building, entered by the user through CAD software, the heating and cooling loads are calculated to meet the thermostat set points. ENERGYPLUS is integrated directly into the GUI design as a first step in the geothermal design. The text based input files make it possible to design a 'novice' load calculator so that a user with no ENERGYPLUS knowledge can use the program. While the expert user has full access to the ENERGYPLUS editor to change material properties, constructions, internal loads and all other modeling inputs in the editor. This option does require some knowledge of ENERGYPLUS, even though the necessary inputs to ensure a successful simulation are prewritten.

2.2.1.1. Conduction Heat Gains and Losses

Using the 'HVAC:Template' to simulate an ideal load on the building, the conduction transfer function module is used. This function uses a state space technique using the environmental temperatures to solve for the heat flux. The set of matrix equations becomes

$$\begin{bmatrix} \frac{dT_1}{dt} \\ \frac{dT_2}{dt} \end{bmatrix} = \begin{bmatrix} -\frac{1}{RC} - \frac{hA}{c} & \frac{1}{RC} \\ \frac{1}{RC} & -\frac{1}{RC} - \frac{hA}{c} \end{bmatrix} \begin{bmatrix} T_1 \\ T_2 \end{bmatrix} + \begin{bmatrix} \frac{hA}{c} & 0 \\ 0 & \frac{hA}{c} \end{bmatrix} \begin{bmatrix} T_o \\ T_i \end{bmatrix} \quad (1)$$

and

$$\begin{bmatrix} q_o \\ q_i \end{bmatrix} = \begin{bmatrix} 0 & -h \\ h & 0 \end{bmatrix} \begin{bmatrix} T_1 \\ T_2 \end{bmatrix} + \begin{bmatrix} 0 & h \\ -h & 0 \end{bmatrix} \begin{bmatrix} T_o \\ T_i \end{bmatrix}, \quad (2)$$

where $R = \frac{l}{kA}$ is the thermal resistance of the layer and $C = \frac{\rho c_p l A}{2}$ is the thermal capacitance. The inner and outer surface convection heat transfer coefficients are found in the following subsection. This technique is preferred to the previously used Laplace transform method which required solving for roots in the Laplace domain. The accuracy of the conduction transfer function was found to be within 1% of the analytical solution when an adequate number of nodes were used. This method has caused the entire simulation to diverge when used with sub-hourly time steps and with materials that are considered thermally massive due to a large number of terms in the transfer function. The inside and outside surface temperatures and heat fluxes are solved for and used in the convective calculations.

2.2.1.2. Convection Heat Gains and Losses

The convection algorithm uses a correlation between the convective heat transfer coefficient, surface orientation, and the temperature difference. The algorithm was taken directly from Walton (1983) where a curve fit is added as a function of the cosine of the tilt angle to give values between vertical and horizontal. The curve fits were compared to the ASHRAE Handbook of Fundamentals values and were found to fit well. This is determined differently depending on the difference in temperature between the surface and the indoor air along with the orientation. The equations for the convective heat transfer coefficient become:

- for ($\Delta T < 0$ and upward facing surface) or ($\Delta T > 0$ and downward facing surface) the following equation is used, (Walton 1983)

$$h_n = \frac{9.482|\Delta T|^{\frac{1}{3}}}{7.283 - |\cos\theta|} \text{ (W/m}^2 \text{ K)} \quad (3)$$

- for ($\Delta T > 0$ and upward facing surface) or ($\Delta T < 0$ and downward facing surface) the following equation is used, (Walton 1983)

$$h_n = \frac{1.810|\Delta T|^{\frac{1}{3}}}{1.382 + |\cos\theta|} \text{ (W/m}^2 \text{ K)} \quad (4)$$

where θ is the surface tilt angle. This algorithm is the default indoor convection algorithm for ENERGYPLUS (EnergyPlus 2010).

The algorithm used for outside convection is in part comprised of the natural convection equations from the inside convection algorithm. The convective heat transfer coefficient is broken into the natural convection and forced convection terms. The coefficient for smooth glass is calculated using the root mean square of the natural convection term and a correlated forced term,

$$h_{glass} = \sqrt{h_n^2 + [aV_z^b]^2} \text{ in (W/m}^2 \text{ K)} \quad (5)$$

where V_z is the local wind speed calculated at the height of the surface centroid, and terms 'a' and 'b' are correlated coefficients given in Table 1.

Table 1: Coefficients for outside convection algorithm (Yazdanian and Klems 1994).

Wind Direction	a	b
Windward	2.38	0.89
Leeward	2.86	0.617

The natural convective heat transfer coefficient is subtracted from the coefficient for smooth glass and multiplied by a roughness factor. h_{glass} is then used to calculate the forced term in the following surface convection heat transfer coefficient equation,

$$h_c = h_n + R_f(h_{glass} - h_n) \text{ (W/m}^2 \text{ K)} \quad (6)$$

where R_f is given in Table 2.

Table 2: Roughness factor multiplier (EnergyPlus 2010).

Roughness Index	R_f	Example Material
1 (Very Rough)	2.17	Stucco
2 (Rough)	1.67	Brick
3 (Medium Rough)	1.52	Concrete
4 (Medium Smooth)	1.13	Clear Pine
5 (Smooth)	1.11	Smooth Plaster
6 (Very Smooth)	1.00	Glass

Summing the natural term with the forced term gives the overall surface convection heat transfer coefficient.

2.2.1.3. Solar Heat Gains and Losses

The default solar irradiance model used in the ENERGYPLUS calculations is the ASHRAE Clear Sky model. The calculation starts with the direct normal irradiation on the earth's surface

on a clear day. This does not yield the maximum direct normal irradiation, but rather values that are representative of conditions on cloudless days. The total available irradiation is calculated using

$$I^o = \frac{A}{e^{(B/\sin\beta)}} \quad (7)$$

where A is the apparent solar irradiation with air mass of zero, B is the atmospheric extinction coefficient and β is the declination angle in degrees. The value for solar irradiance must then be multiplied by clearness numbers from ASHRAE. The values calculated for extraterrestrial solar irradiance tend to overestimate the amount of solar radiation available to the building. The total solar gain on any surface in the model is then calculated by including a combination of the direct and diffuse radiation using

$$Q_{solar} = \alpha \left(I_b \cos\theta \frac{S_s}{S} + I_s F_{ss} + I_g F_{sg} \right) \quad (8)$$

where

- α = solar absorptance of the surface,
- θ = angle of incidence of the sun's rays,
- S = area of the surface,
- S_s = sunlit area,
- S = area of the surface,
- I_b = intensity of direct beam radiation,
- I_s = intensity of sky diffuse radiation,
- I_g = intensity of ground reflected diffuse radiation,
- F_{ss} = angle factor between the surface and the sky, and
- F_{sg} = angle factor between the surface and the ground.

For external long wave radiation calculations, the heat exchange between surfaces is a function of material properties, surface temperature, and spatial properties. The general agreement is that for building load calculations, some assumptions are reasonable such as (Chapman n.d.):

- each surface emits or reflects diffusely and is gray and opaque ($\alpha = \varepsilon, \tau = 0, \rho = 1 - \varepsilon$),
- each surface is at uniform temperature,
- energy flux leaving a surface is evenly distributed across the surface, and
- the medium within the enclosure is non-participating.
- the ground temperature is assumed to be the same as the air temperature
- the long wave emittance is defined by the user in the material properties.

Using these assumptions the long wave radiation heat flux is calculated as the sum of the components from the ground, sky, and air. These constituents are further broken down into the fundamental radiation heat transfer equation

$$q_{lwr}'' = \varepsilon\sigma F_{gnd}(T_{surf}^4 - T_{gnd}^4) + \varepsilon\sigma F_{sky}(T_{surf}^4 - T_{sky}^4) + \varepsilon\sigma F_{air}(T_{surf}^4 - T_{air}^4). \quad (9)$$

This equation is then linearized to produce heat transfer coefficients. These coefficients are combined with another term β used to split the sky and air view factors based on the tilt angle of the surface

$$\beta = \sqrt{0.5(1 + \cos\varphi)}. \quad (10)$$

The final equations for the long wave radiation heat transfer coefficients become

$$h_{r,gnd} = \frac{\varepsilon\sigma F_{gnd}(T_{surf}^4 - T_{air}^4)}{(T_{surf} - T_{air})} (\text{W/m}^2 \text{ K}), \quad (11)$$

$$h_{r,sky} = \frac{\varepsilon\sigma F_{sky}\beta(T_{surf}^4 - T_{sky}^4)}{(T_{surf} - T_{sky})} (\text{W/m}^2 \text{ K}) \quad (12)$$

and

$$h_{r,air} = \frac{\varepsilon\sigma F_{sky}(1-\beta)(T_{surf}^4 - T_{air}^4)}{(T_{surf} - T_{air})} (\text{W/m}^2 \text{ K}). \quad (13)$$

2.2.1.4. *Weather Data*

Simple weather files available consist of observations of temperature, humidity, wind speed and direction, atmospheric pressure, and solar radiation made on an hourly basis. The data for simulation software are derived from this hourly set for a specific location. The typical data such as TMY2 and WYEC2 contain more solar radiation and illumination data and have been found to be more accurate over longer lengths of time than averaging (Crawley, 1998). The 'epw' file used in ENERGYPLUS was developed based on the TMY2 format, but with the ability to interpolate sub-hourly. Another difference is the infrared sky field used to calculate effective sky temperatures for re-radiation at night (EnergyPlus 2010).

The ENERGYPLUS input files converted from a CAD drawing, or written by the novice load calculator, use the option to run a simulation for 'weather file run periods'. This uses the weather file for an hourly simulation rather than a peak load or design load. The 'typical' weather supplied by the weather files are loaded into the model upon the selection of the location by the user.

2.2.1.5. *Quantities Delivered to GEO2D and GEO3D*

For the purposes of modeling a geothermal heat pump system, the hourly load data for all of the modeled zones is necessary. Other necessary building simulation data include the inside dry bulb temperature and humidity ratios for all of the simulated zones. The outside dry bulb temperature and wind speeds are also output automatically whether in expert or novice modes. This is a critical and necessary step in interfacing ENERGYPLUS with the geothermal program since it supplies the user with crucial data for a complete design. The indoor dry bulb and humidity ratios are used in the heat pump model discussed in Section 3. The outdoor dry bulb temperature is used to suggest a soil temperature specific to a location. This is done by averaging the outdoor temperature.

3. CALCULATIONS

This section of this report will discuss the details of the calculations used in GEO2D and GEO3D. Details on the fluid flow model, the heat conduction model, the grids used, the boundary conditions, heat pump model, and the economics model are given.

3.1. FLUID FLOW

First the fluid mechanics model used in GEO2D and GEO3D is discussed. The control volumes that are set up in the fluid region have a velocity profile across the diameter based on the Reynolds number. The flow parameters for each control volume are modeled using empirically correlated equations for frictional velocities, eddy momentum, and turbulent thermal conductivity.

GSHP systems generally use turbulent flow with Reynolds numbers greater than 20,000 (Trane November 2010). For this reason the most time is spent on the turbulent model of the fluid flow. However, to make the programs capable of handling laminar flow situations, a laminar flow model is also included in both GEO2D and GEO3D. In the subsections below the laminar flow model is discussed first and then the turbulent flow model.

3.1.1. Laminar Flow

The equation used to calculate the laminar velocity at a given radius from the centerline of the pipe to edge of the pipe wall is

$$u(r) = 2V_{avg} \left(1 - \frac{r^2}{R^2}\right), \quad (14)$$

where the user inputs the average velocity V_{avg} and inner pipe radius R . The velocity $u(r)$ is calculated for each control volume assuming fully developed flow. This model is only used when the Reynolds number is less than 2300. Unlike turbulent flow, no adjustments need to be made to the material thermal conductivity for laminar flow. Thus for laminar flow the effective thermal conductivity of the fluid remains the thermal conductivity of the fluid.

3.1.2. Turbulent Flow

The equation used in the case of Reynolds numbers between 2300 and 100,000 for the velocity profile is the empirically derived power law (Fox, McDonald and Pritchard 2006),

$$\frac{u}{U_m} = \left(\frac{y}{R}\right)^{1/n}, \quad (15)$$

where u is the velocity, y is the distance from the wall, n is an empirically derived exponent, and U_m is the maximum centerline velocity. The value for the exponent n is calculated using the log relationship with the Reynolds number written as (Fox, McDonald and Pritchard 2006)

$$n = -1.7 + 1.8 \log_{10}(Re). \quad (16)$$

Using the calculated exponent n and the average velocity supplied by the user, the maximum centerline velocity can be calculated from the average velocity using (Fox, McDonald and Pritchard 2006)

$$\frac{V_{avg}}{U_m} = \frac{2n^2}{(n+1)(2n+1)}. \quad (17)$$

To further broaden the applicability of the geothermal analysis program, the velocity profile for Reynolds numbers greater than 100,000 is also included in GEO2D and GEO3D. This high of a Reynolds number would normally not be seen in a geothermal application, but the widest

range of conditions was included in these programs. For Reynolds numbers greater than 100,000 the velocity profiles are determined with (Swearingen 2009)

$$\frac{u}{V_{avg}} = 1 + 1.44\sqrt{\lambda} + 2.15\sqrt{\lambda}\log_{10}\left(1 - \frac{r}{R}\right). \quad (18)$$

With the velocity profile modeled for a wide range of Reynolds numbers, the friction factor, for a smooth pipe should be calculated using the equation (Fox, McDonald and Pritchard 2006)

$$\sqrt{\frac{8}{\lambda}} = 2.44\ln\left(\sqrt{\frac{\lambda}{32}} Re_d\right) + 2.0. \quad (19)$$

While this equation produces friction factors that closely follow friction factors from the Moody diagram, it requires an iterative solution. To save as much computational time as possible a direct-solve equation for the friction factor was investigated. The direct solve equation investigated is the Petukhov equation (BS. 1970)

$$\lambda = (0.79\ln(Re) - 1.64)^{-2}. \quad (20)$$

This is a one-step calculation of the friction factor, rather than an iterative process. A comparison of the factors obtained with equation (19) and that from equation (2) is plotted in Figure 11. The difference between the two equations is less than 6%, and generally within 3%. These errors in the friction factors are insignificant in the geothermal calculations being done. It has been found that these errors affect the calculated heat transfer coefficient minimally in the range of Reynolds numbers typically used in geothermal systems, Reynolds numbers from 15,000 to 30,000 (Trane 2009).

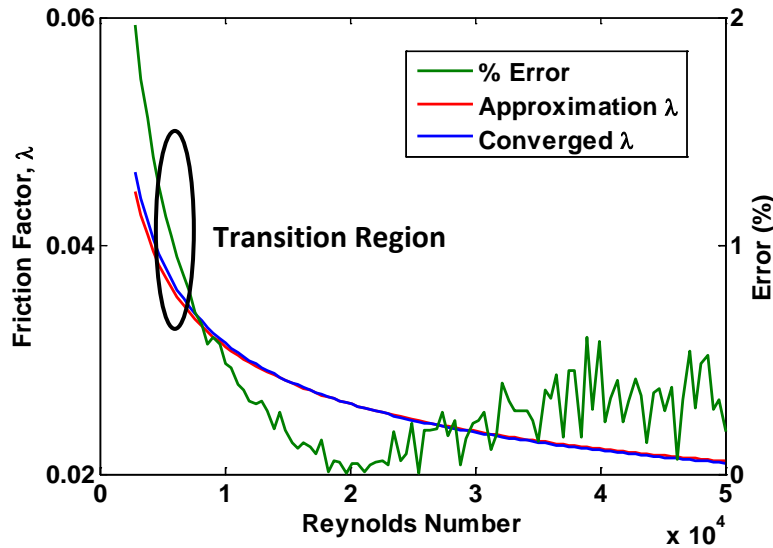


Figure 11: Calculated friction factor compared to Moody diagram.

The friction factor for smooth pipes is used to calculate the friction velocity (Datta 1993)

$$u_* = V_{ave}\sqrt{\frac{\lambda}{8}}. \quad (21)$$

The friction velocity is a function of the wall shear τ_w and can also be described as $\sqrt{\frac{\tau_w}{\rho}}$, where; in the region very close to the wall the viscous shear dominates the turbulent shear. This becomes more evident when the effective thermal conductivity is calculated. With all three of the velocity profiles complete, covering a wide range of Reynolds numbers, a plot of the non-

dimensional profiles was produced and can be seen in Figure 12. The profile for the high Reynolds numbers using equation (18), shows some of its shortcomings as it does not quite reach a non-dimensional velocity of one at the centerline of flow tube. The profile for turbulent flow shows asymptotic behavior close to the wall and the laminar velocity profile is parabolic.

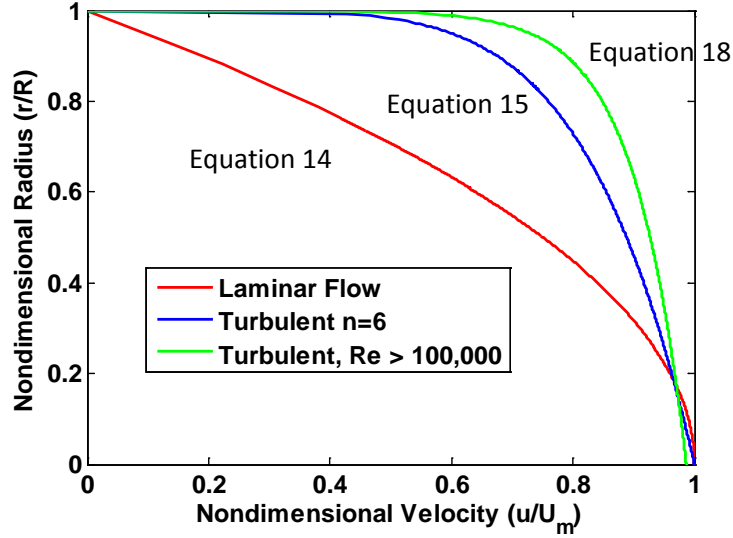


Figure 12: Velocity profiles.

The asymptotic behavior for the turbulent flow is important for determining the effective thermal conductivity of the fluid. The effective thermal conductivity is calculated by dividing the flow field into three different regions: a viscous sublayer, a buffer layer, and a bulk flow. These regions are found by first calculating

$$y^+ = \frac{yu_*}{\nu} \quad (22)$$

where ν is the kinematic viscosity and y is the distance from the wall. The viscous sublayer, the region where $y^+ \leq 10.5$, is extremely close to the wall. The dimensionless axial velocity U^+ can be calculated for this region as

$$U^+ = \frac{yu_*}{\nu} = y^+. \quad (23)$$

The second layer, or buffer layer, is empirically derived for values of $10.5 < y^+ < 30$. The viscous shear and turbulent shear both play an important role in this region. The scattered data in the buffer layer is fit using a natural log relationship that is a function of the distance from the wall, the frictional velocity, and the viscosity of the fluid. The dimensionless axial velocity U^+ for the buffer layer now become (Fox, McDonald and Pritchard 2006)

$$U^+ = 5 \ln \frac{u_* y}{\nu} - 3.05. \quad (24)$$

In the bulk flow, where $y^+ \geq 30$, the axial velocity is dominated by turbulent shear and the empirical correlation for U^+ becomes (Fox, McDonald and Pritchard 2006)

$$U^+ = 2.5 \ln \frac{u_* y}{\nu} + 5.5. \quad (25)$$

An example of the three regions and the corresponding equations for the axial velocity can be seen in Figure 13.

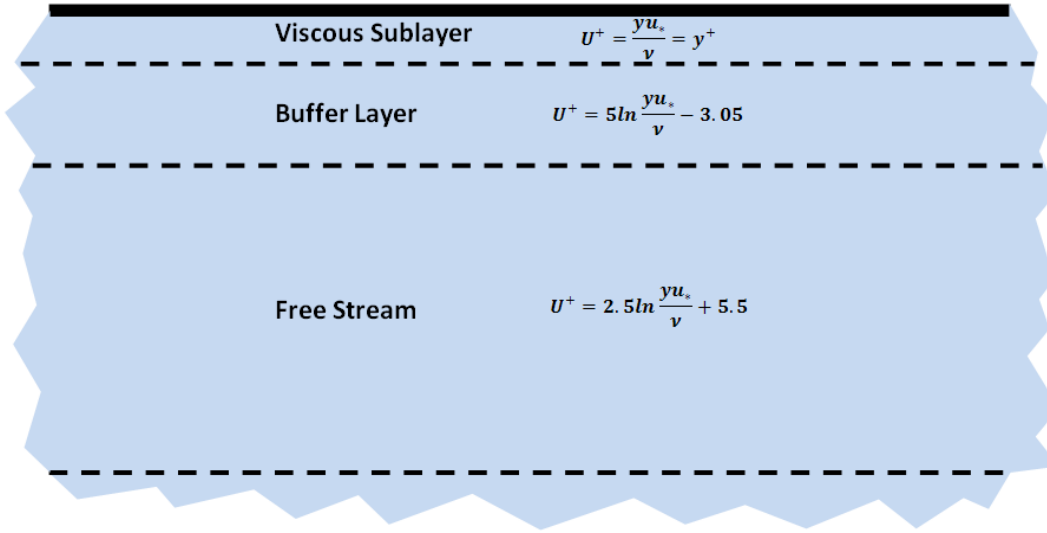


Figure 13: Three regions modeled in turbulent flow.

With the values for U^+ fully defined in the three regions, the transport of energy by means of heat diffusion and momentum are now discussed. A model for the eddy momentum diffusivity is used that comes from the dimensional analysis by Datta (Datta 1993),

$$\epsilon_r = \frac{\epsilon_m}{\nu} = \sinh^4 \left(\frac{U^+}{\alpha} \right) \left\{ 1 - \frac{\sinh \left(\frac{\beta U^+}{\alpha} \right)}{\sinh \left(\frac{\delta \beta U_{max}^+}{\alpha} \right)} \right\}, \quad (26)$$

where it is determined that the universal constants α , δ , and β are equal to 10.25, 1.008 and 4.17 respectively. This model ensures that the eddy momentum becomes $\frac{\epsilon_m}{\nu} = \sinh^4 \left(\frac{U^+}{\alpha} \right)$ as y^+ approaches zero. The eddy momentum is then used to describe how the bulk flow of the fluid transports the heat using the Péclet number for turbulent flow. This is calculated by multiplying the ratio of the inertial and viscous forces in the Eddy momentum and kinematic viscosity by the dimensionless Prandtl number to get a turbulent Peclet number,

$$Pe_t = \epsilon_r Pr. \quad (27)$$

The turbulent Péclet number is then used to calculate the turbulent Prandtl number which describes the ratio of molecular diffusion due to momentum transport to the molecular diffusion of heat, (Kays 1994)

$$Pr_t = \frac{2.0}{Pe_t} + 0.85. \quad (28)$$

With the eddy momentum already calculated from equation (25), the turbulent thermal conductivity can be calculated using

$$k_t = \frac{c_p \epsilon_m \rho}{Pr_t}, \quad (29)$$

which is simply added to the thermal conductivity of the fluid to arrive at the effective thermal conductivity for turbulent flow in the tube,

$$k_{eff} = k + k_t. \quad (30)$$

Plotting the effective thermal conductivity as a function of nondimensional radius for several Reynolds numbers is done in Figure 14. This plot shows that turbulent eddies greatly affecting the effective thermal conductivity; and thus greatly affecting the heat transfer in the fluid. The plot shows the turbulent thermal conductivities being two orders of magnitude higher

than the laminar thermal conductivities. This is the reason why turbulent flow should be maintained in the ground loop. Figure 14 also reveals an area in the middle of the pipe where the eddies are less prominent and result in lower thermal diffusion. Though it is difficult to see in the plot, the effective thermal conductivity receives no contribution from the turbulent equations when $\frac{r}{R}$ is very close to one, making $k_{eff} = k$.

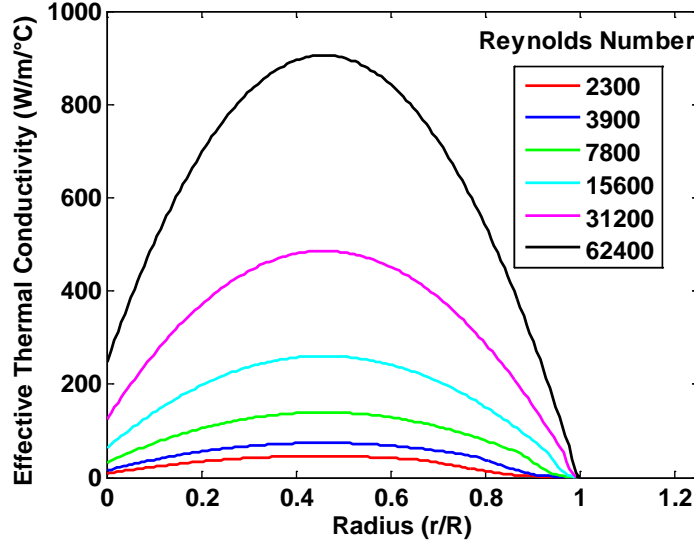


Figure 14: Effective thermal conductivity profiles.

3.2. HEAT TRANSFER IN GROUND AND GROUND LOOP

3.2.1. Energy Equation

The governing differential equations used to solve for the heat transfer and temperature field in a GSHP system for both GEO2D and GEO3D is the energy equation. The energy equation, also called the first law of thermodynamics, is nothing more than a statement that says energy is conserved. The energy equation can be written in many forms depending on the energy mechanisms involved. For a GLHE (ground loop heat exchanger) there are two energy flow mechanisms and one storage energy mechanism. The energy flow mechanisms are conduction and advection and the energy storage mechanism is thermal energy storage. All three of these energy mechanisms are included in the governing differential equations presented below.

3.2.1.1. GEO2D

For GEO2D changes in the temporal direction and both the radial and axial spatial directions are included. This is more than most commercial programs do, which generally consider a GLHE to be essentially a one dimensional, unsteady problem. The governing differential equation solved by GEO2D for the two-dimensional unsteady heat transfer occurring is

$$\rho C_p \frac{\partial T}{\partial t} + \frac{\partial(\rho u C_p T)}{\partial z} = \frac{\partial}{\partial z} \left(k \frac{\partial T}{\partial z} \right) + \frac{1}{r} \frac{\partial}{\partial r} \left(kr \frac{\partial T}{\partial r} \right) \quad (31)$$

where ρ is the density, C_p is the specific heat, T is the temperature, t is the time, u is the velocity, k is the thermal conductivity, and z and r are the radial and axial positions.

3.2.1.2. GEO3D

Even though GEO2D is a very good program for a GSHP system, only accounting for heat transfer in 2 dimensions causes some limitations. GEO2D does not account for the asymmetry for a U-tube pipe in a vertical ground loop system. This requires a 3-dimensional heat transfer analysis. For these reasons, we have expanded GEO2D to three-dimensions. The three-dimensional form of GEO2D is called GEO3D.

GEO3D uses a third spatial dimension, the azimuthal direction, to account for the ground surface heat transfer and the heat transfer between the U-tube pipes within a vertical borehole. The third dimension adds physical detail to the model, but increases the computation time as well. The governing differential equation used to solve the heat transfer in GEO3D is

$$\frac{\partial(\rho c_p T)}{\partial t} + \frac{\partial(\rho u c_p T)}{\partial z} = \frac{\partial}{\partial z} \left(k \frac{\partial T}{\partial z} \right) + \frac{1}{r} \frac{\partial}{\partial r} \left(kr \frac{\partial T}{\partial r} \right) + \frac{1}{r^2} \frac{\partial}{\partial \theta} \left(k \frac{\partial T}{\partial \theta} \right) \quad (32)$$

where the meaning of the symbols used are the same as used in Equation (31) and θ is the azimuthal coordinate in radians. Thus only one term has been added to Equation (31) to obtain Equation (32). This is the last term on the right-hand side of Equation (32) and it accounts for heat conduction in the azimuthal direction. This adds a considerable amount of complexity to the solution of the governing differential equation.

3.2.2. Grids

Neither Equation (31) or (32) can be solved analytically. Thus a finite volume numerical representation is used for both of these equations. Numerical models are developed by replacing the differential equations, with a set of algebraic equations. In the case of the finite volume method, this is done by writing algebraic representations of the differential equations over a large number of small volumes which subdivide the overall computational domain. The center point of these control volumes is called a grid point (Y. A. Cengel 2007). The collection of these grid points and control volumes will be called the grid. Since this grid is different for GEO2D and GEO3D, each will be discussed in its own sub-section.

3.2.2.1. GEO2D

The computation time needed to run a multi-year analysis with a geothermal heat exchanger program was a concern from the beginning of the project. In order to minimize the computational time, and therefore make the program useful for optimizing a design, research effort was taken to minimize the number of control volumes used to model the ground loop and ground. A grid study was performed to reduce the number of grid points, while not compromising the accuracy of the solution. A broad range of conditions were evaluated in this grid study to ensure that the program maintain its versatility. In the sub-sections below a number of critical regions for the GLHE heat transfer analysis are looked at separately.

3.2.2.1.1. Fluid Grid Study

The number of grid points necessary in the fluid region is particularly important since this is where the energy to and from the ground is transferred. With the use of the effective thermal conductivity discussed above, the heat transfer to the fluid is calculated. Knowing the temperature of the first grid point in the fluid as well as the first grid point in the wall, the temperature on the pipe wall is calculated using Fourier's law. In Figure 15, an example of the grid layout can be seen where each control volume lies a distance from the pipe surface and has a corresponding thermal conductivity and temperature.

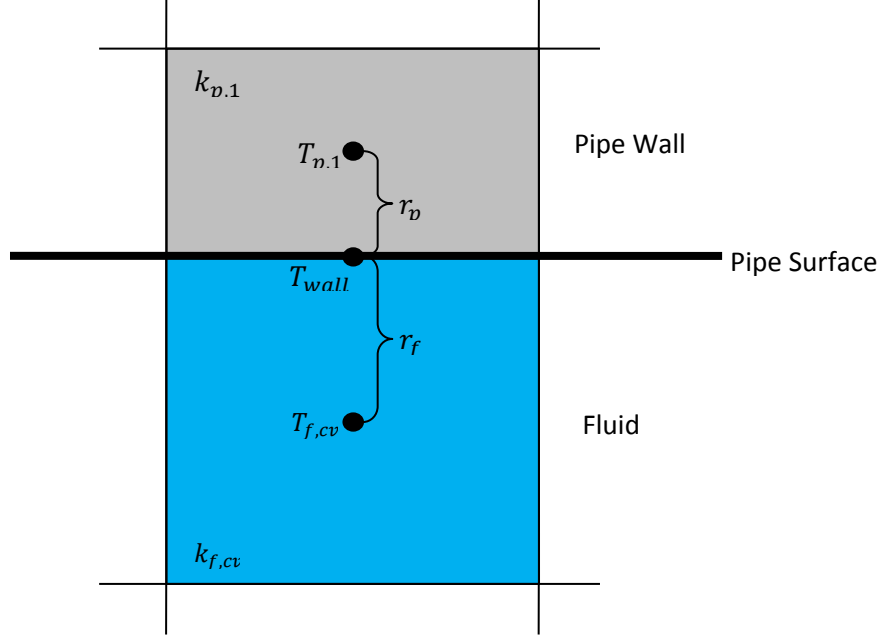


Figure 15: An example of the control volume layout.

The equations for the heat flux at the pipe surface from either side can be set equal to each other and solved for T_{wall} using

$$k_{p,1} \left(\frac{T_{p,1} - T_{wall}}{r_p} \right) = k_{f,cv} \left(\frac{T_{wall} - T_{f,cv}}{r_f} \right) = \dot{q}. \quad (33)$$

Rearranging this equation for the temperature of the surface gives

$$T_{wall} = \frac{(T_p k_{p,1} r_f) + (T_{f,cv} k_{f,cv} r_p)}{(k_{p,1} r_f + k_{f,cv} r_p)} \quad (34)$$

where cv represents the last control volume in the fluid region. To determine when the number of grid points used is enough, the calculated heat transfer coefficient on the tube inside wall is used. To calculate the convective heat transfer coefficient at any point along the length of the pipe, the bulk temperature T_{bulk} must first be determined. This is done using the same integration technique discussed in Section 3.3. The convective heat transfer coefficient can be determined as

$$h = \frac{\dot{q}}{(T_{wall} - T_{bulk})}. \quad (35)$$

It is important to note, the value for h , in a steady state condition, is used to determine what the converged solution is in the grid study. This value is not used in the unsteady energy equation solution, and no empirically derived equations were used. They are not needed in this model.

The hydrodynamic entry length for fully developed flow, for turbulent velocities is small compared to laminar flow. Therefore a long length of pipe was used to make sure it supports a fully developed flow region for all Reynolds numbers. The grid study was performed over a range of Reynolds numbers from 2,300 to 1,000,000 using different diameters and dynamic viscosities. For the purposes of this study, the results extend past the high and low ends of typical conditions in geothermal systems. A pipe diameter of 2 centimeters is used in this study.

The convective heat transfer coefficient is now plotted versus the total number of grid points in the fluid. The grid spacing exponent was set to 1 and 0.1 to further understand its effect. With 15 grid points in the viscous sublayer region, the number of grid points in the fluid was altered and plotted. The converged value for a grid exponent of 0.1 was determined quickly. It can be

seen in Figure 16 that the grid exponent of 1 slowly converges and requires an order of magnitude more grid points. As the number of grid points is increased, numerical instability can be seen for the grid exponent of 0.1. The reason for this is the grid points are too close together for the number of significant figures held by the computer.

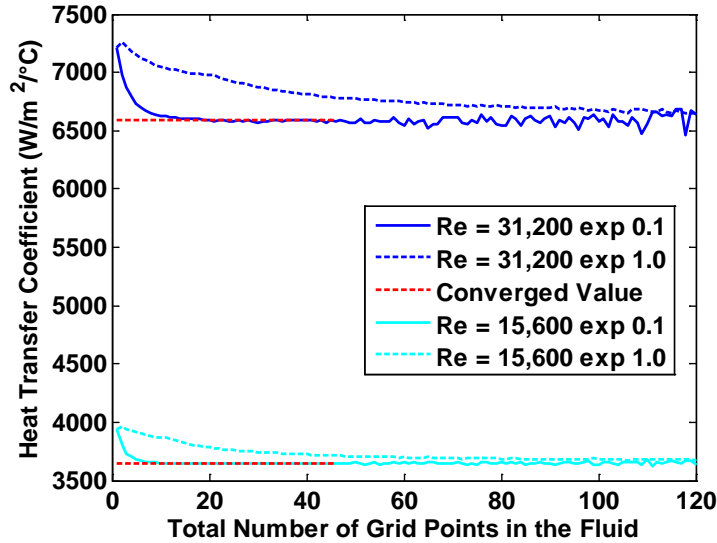


Figure 16: Heat transfer coefficient as a function of the number of grid points in the bulk fluid.

With a converged value determined by inspection, the number of grid points in the viscous sublayer region is minimized. The viscous sublayer region plays an important role in the calculation of the convective heat transfer coefficient due to the viscous shear and its role in the effective thermal conductivity. With the number of grid points in the bulk flow set to 60, the number of grids in the viscous sublayer region is analyzed. The behavior can be seen in Figure 17, where the grid exponents of 0.1 and 1 are again utilized for the same Reynolds numbers shown in Figure 16. This study is comprised of pipe radii ranging from one millimeter to half a meter for all of the Reynolds numbers mentioned. The number of grid points necessary in the viscous sublayer region was determined to be five. Five grid points in this region was enough to cover all of the different cases in the study. Numerical instability was recognized when the grid points in this region were increased above 20.

The next step in the study was to minimize the number of points necessary in the bulk flow region. With the viscous sublayer region already determined and set, the number of grid points in the bulk flow was varied. It is found that with a grid exponent of 0.1, the number of points necessary for Reynolds numbers of 15,600 and 31,200 are 5 and 6 respectively. This was chosen as the minimum number of points needed to be within 1% error from the converged value as seen in Figure 18.

The same procedure was used for a range of Reynolds numbers and diameters to determine an equation. The results of the study for the grid exponent of 0.1 was determined to be

$$Grid_{free\ stream} = ceil(1.4612 * ln(Re) - 9.1534) \quad (36)$$

This equation can be used to suggest to the user the minimum number of grid points that can be used to ensure an error of less than 1% from the converged value. The equation plotted with a before and after the ceiling function can be seen in Figure 19, along with the actual data points.

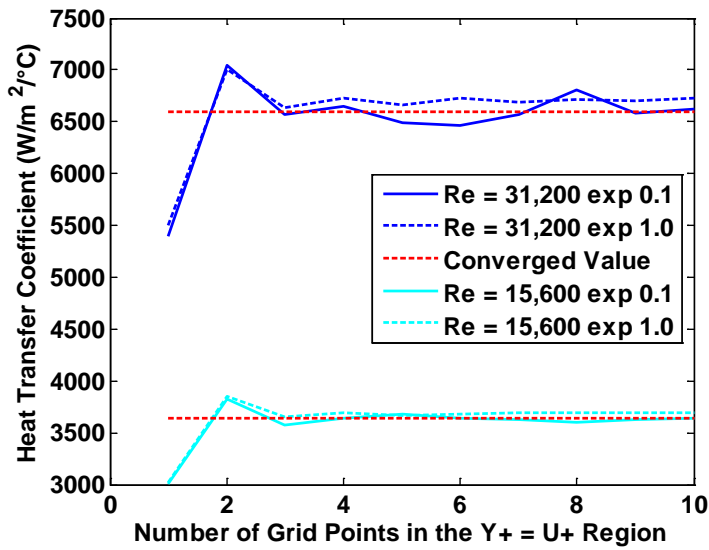


Figure 17: Heat transfer coefficient as a function of the number of grid points in the sublayer region.

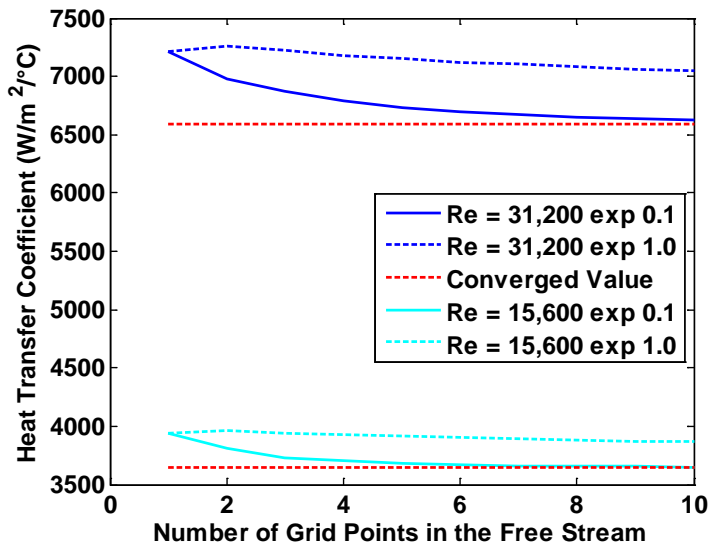


Figure 18: Heat transfer coefficient as a function of the number of grid points in the bulk flow region.

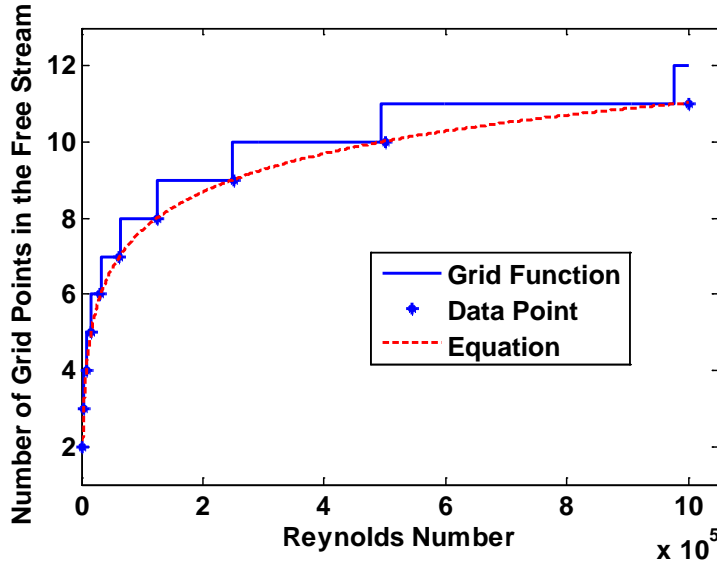


Figure 19: Equation for number of grid points in the bulk flow region.

3.2.2.1.2. Earth Grid Study

The earth grid study was done using a number of heating ratios. First a minimal number of grid points was determined that maintained accuracy. The grid study was conducted using exponents of 1, 2, 3, and 4. The total energy moving to and from the pipe is used to show convergence for different earth grid point numbers. The number of control volumes was doubled for boundary condition radii ranging from 2 to 128 meters. The converged value was decided by inspection and used as the target result in the earth grid studies.

The number of grid points required to meet a 1% tolerance is determined and plotted as a function of radius in Figure 20. An exponential regression analysis is completed and a ceiling function is applied to ensure an integer value for the number of grids is obtained. The equation obtained for the number of grid points needed in the earth for a corresponding exponent and radius is

$$Grid_{soil} = \text{ceil}(A \cdot \text{radius}^B). \quad (37)$$

The curve fit of equation (37) with and without the ceiling function is plotted in Figure 20 along with the original data points.

A study was also undertaken to determine the error encountered because of the exponent value chosen for the soil grid calculation. The errors associated with different exponent values for the soil grid can be seen in Figure 21. The difference in temperatures never exceeds more than 0.2 °C for any grid exponent number. Because of other reasons besides accuracy, it is recommended that a grid exponent of three be used. The reason for this is so the model avoids numerical instability that can occur when the grid exponent is set four and the number of grid points is increased. The amount of grid points necessary for an exponent of one leads to a long computational time.

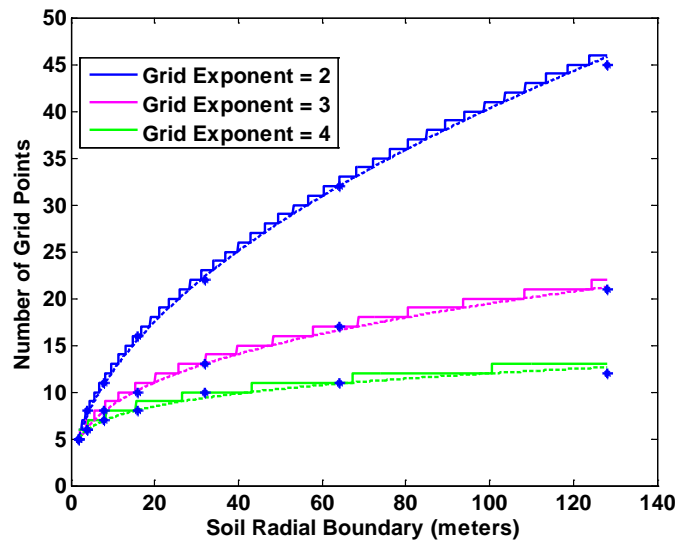


Figure 20: Soil grid study for different exponents.

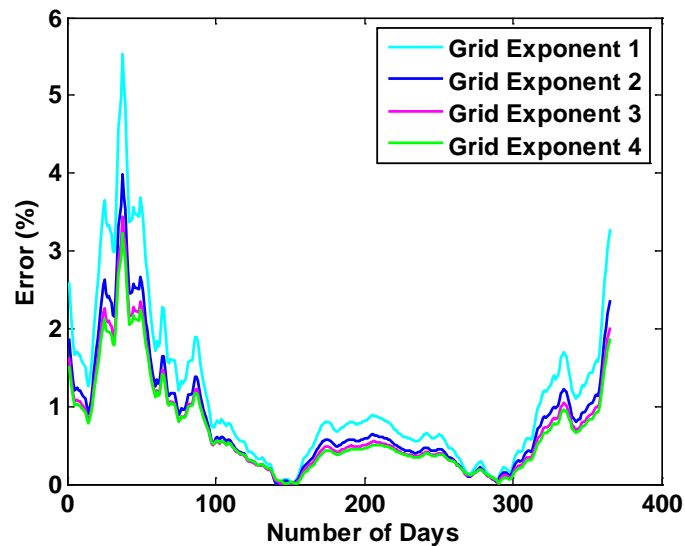


Figure 21: Error in entering water temperature.

Using the unique feature of the grid exponent can greatly reduce the computation time by reducing the necessary number of control volumes in the earth. The number of iterations can also be reduced significantly by using the daily time step over the hourly time step. A typical residential case was run to compare the computation time saved using a larger grid exponent and using hourly and daily time steps. The results can be seen in Table 3. Figure 22 shows the EWT for four different time steps and a grid exponent of three. From these results it can be seen that as the time step is increased from the hourly value the oscillations in the results diminishes. However, it also can be seen that 1 day and 5 day time steps produce reasonable average results. The one day results are especially good and reduce computational times by over an order of magnitude as compared to the one hour simulation. Another factor of four reduction

computational time is achieved by going to a 5 day time step. The computational time reductions as a function of time step and the earth grid exponent can be seen in Table 3. All the results shown in Table 3 are for a 10 year simulation period.

Table 3: Computation time required for changing exponent and time step.

Time step	Years	Earth Grid Exponent	Earth Control Volumes	Computation Time (sec.)
Hourly	10	2	44	214
		3	28	168
Daily	10	2	44	14.1
		3	28	13.4
5 Day	10	2	44	3
		3	28	2.7
Monthly	10	2	44	1
		3	28	.75

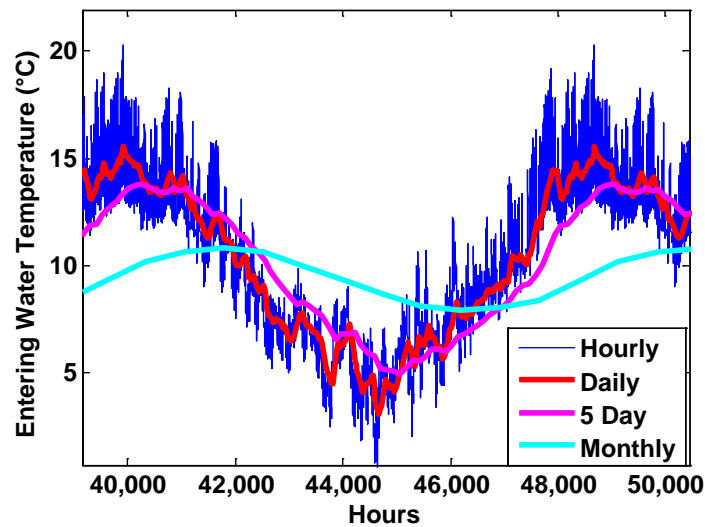


Figure 22: Accuracy with changing time step.

3.2.2.2. GEO3D

For GEO3D the gridding system used is shown in Figure 23. To reduce computational time, the computational domain is divided along the axial direction as shown in Figure 23. Since the GLHE acts the same on either side, a single half can be simulated and produce the same results as a whole model would.

Developing a grid system for a vertical GLHE has some difficulties. Since the origin of the grid is taken at the center of the borehole, the grid volumes continuously grow as the radius increases, causing modeling problems in the fluid and tube wall regions, which are circular cross

sectional regions off the centerline of the computational domain (see Figure 24 and Figure 25). This causes these regions to have a jagged cross sectional shape as opposed to a smooth circular shape. The black lines in Figure 24 show the actual shape of the fluid and tube, but the computational shape of these objects has to follow the closest grid lines. The computational shape of these objects is dictated by the material properties applied to each control volume.

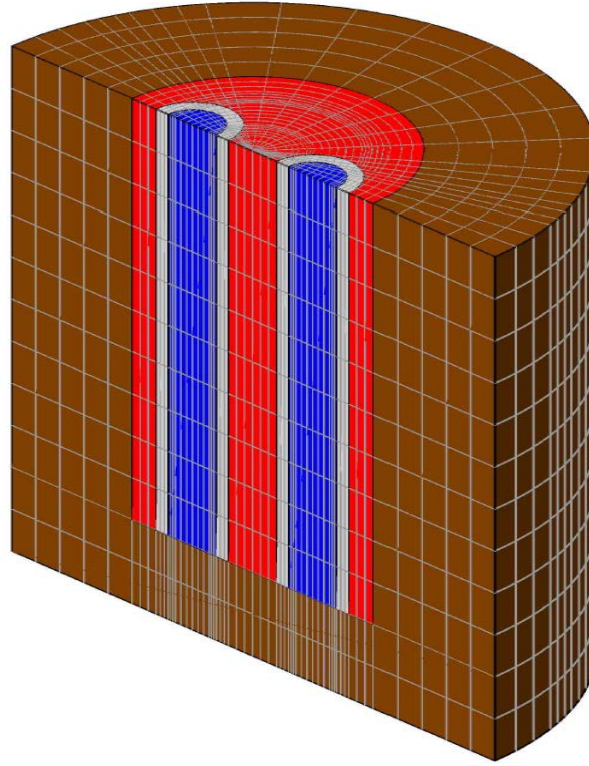


Figure 23: The grid system used for a vertical GLHE in GEO3D.

GEO3D uses special program routines to find the locations of the nodes in the fluid, pipe and grout so that the appropriate material properties can be applied to them. The following equations are used to find the grid points that lie within the fluid and tube wall regions:

$$x = abs(r(j) \cdot \cos(\theta(k))), \quad (38)$$

$$y = r(j) \cdot \sin(\theta(k)), \quad (39)$$

and

$$r_{tube} = sqrt((r_{center} - x)^2 + y^2). \quad (40)$$

If r_{tube} is found to be less than or equal to R_{tube} , the thermal properties are set equal to the specified fluid values. If r_{tube} is greater than or equal to R_{tube} and r_{tube} is less than or equal to $(R_{tube} + pipe\ thickness)$, the nodes are set to the tube wall properties.

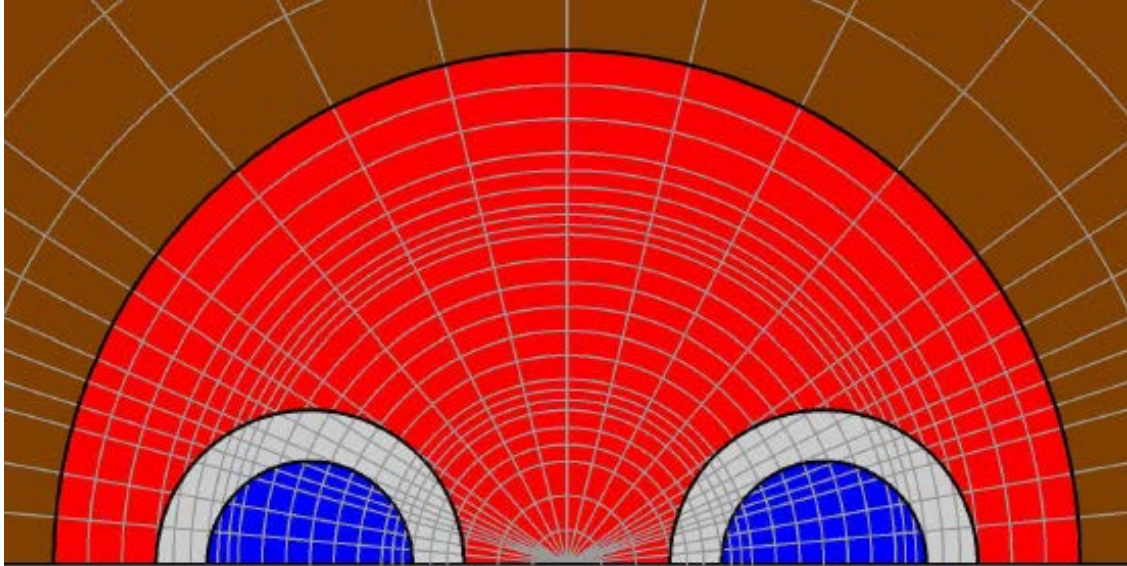


Figure 24: The grid system in GEO3D for a vertical GLHE.

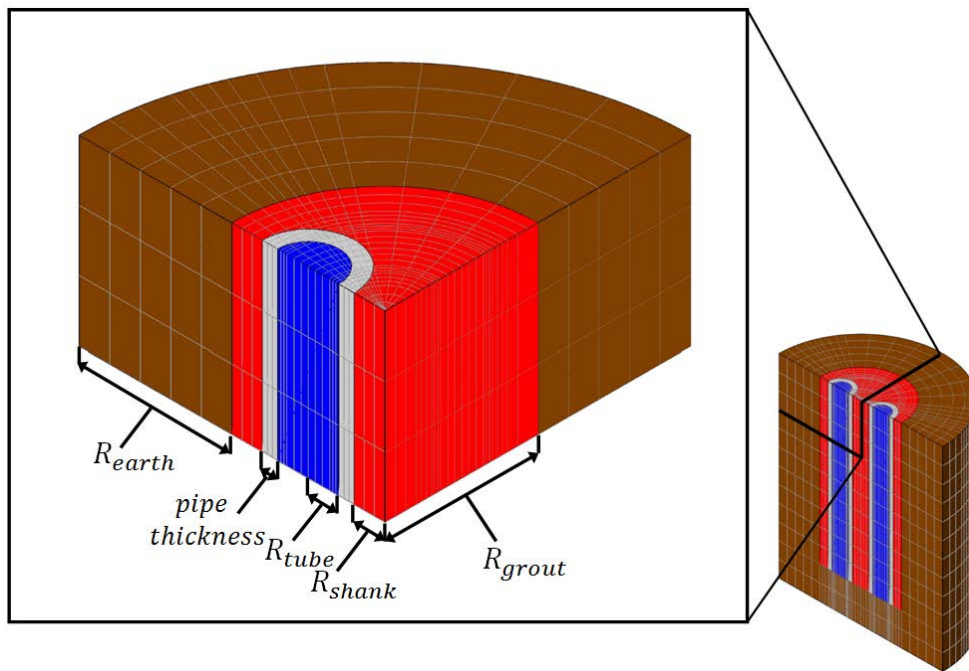


Figure 25: Section of a vertical GLHE and some inputs used to develop the model.

3.2.3. BOUNDARY CONDITIONS

3.2.3.1. GEO2D

All boundary conditions in GEO2D are taken as being adiabatic except the fluid inlet temperature in the flow tube. This inlet temperature is determined by the heat pump model.

3.2.3.1.1. Far Field Boundary Condition

Two boundary conditions can be used for the far field boundary condition in the ground for this type of analysis; an adiabatic boundary condition or a constant temperature boundary condition. A study was performed to determine which one of these boundary conditions should be used.

This study was performed using GEO2D and used a constant entering water temperature of 5 °C. The geothermal system was simulated for a 1 year period. The thermal properties, velocities, grid variability, number of control volumes and geometry of the GSHP system were the same for the adiabatic and constant temperature boundary condition cases. GEO2D was run for both boundary conditions with soil radii of 0.8, 1.6, 3.2, 6.4, 12.8 and 25.6 m. The total heat extracted from the pipe at the end of a day, week, month and year was found. The results from the adiabatic boundary condition and the constant temperature boundary condition can be seen in Figure 26 and Figure 27, respectively.

For each study, the portion of the line that levels off demonstrates a soil radius that provides a converged solution. At the end of the first day, while using a radius of 0.8 m, both boundary conditions are shown to have little influence on the heat being extracted. For both boundary conditions, a soil radius greater than 1.6 m is necessary for an analysis exceeding a month. Similarly, a full year's analysis requires a soil radius of at least 6.4 m. The results show that both the adiabatic and the constant temperature boundary conditions provide similar convergence. However, using a constant temperature boundary condition can show unrealistic temperature results in the soil at the far field boundary for very long simulation times since the temperature along this boundary is held constant. Thus, an adiabatic far-field boundary condition was used for GEO2D and GEO3D.

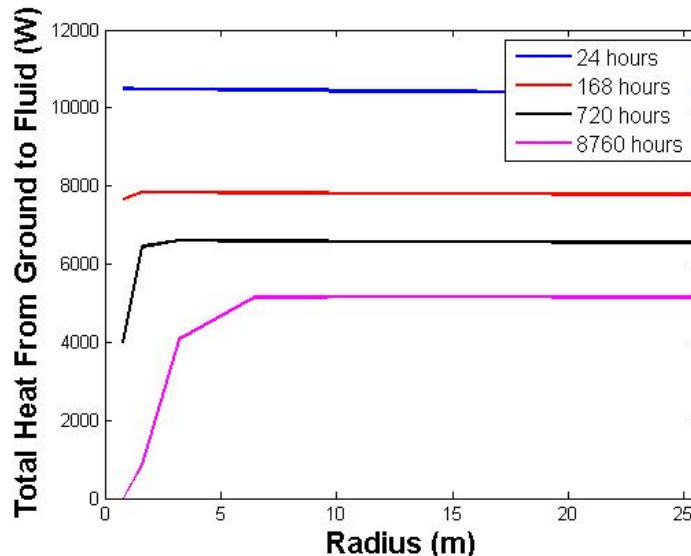


Figure 26: The total heat extracted from the ground loop at various boundary condition radii using an adiabatic boundary condition.

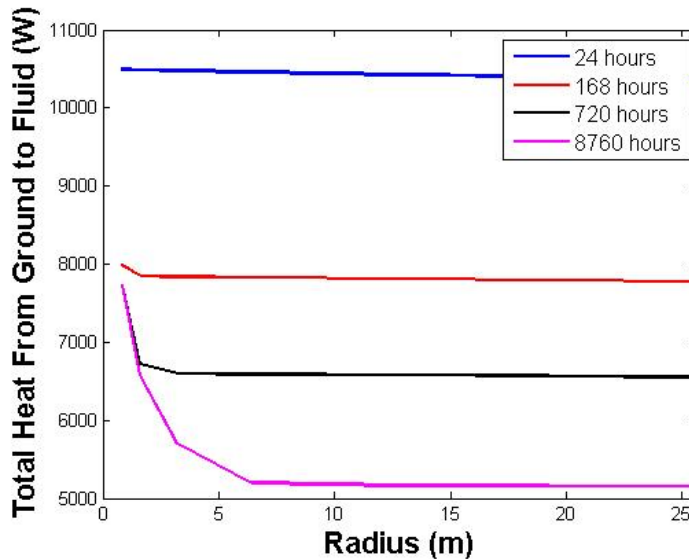


Figure 27: The total heat extracted from the ground loop at various boundary condition radii using a constant temperature boundary condition.

To get a better handle on the radius that should be used for the far-field boundary condition a more detailed outer radius study was undertaken using the adiabatic type boundary condition. Extreme scenarios were simulated using a 3½ ton heat pump and hourly loads that were appropriate for this heat pumps capacity. A range of heating ratios from 0% to 100% is used and each ratio is studied with a range of thermal conductivities and simulation times. Simulation times up to forty years are tested. The length of pipe is itself a function of these variables and its value was decided through an extensive trial and error process. The length was determined by not letting the exiting fluid temperature drop below -5 °C or go above 43°C so as to simulate a worst case scenario without exceeding the performance range of the heat pump. With the length of pipe iteratively determined, it was decided that interpolation between heating ratios helped to reduce the complexity of the study; therefore an equation for each of six heating ratios is reduced to functions of thermal conductivity and time.

The procedure used for each heating ratio is the same, but for purposes of this work the 60% case is explained here. The first step after finding the length necessary to stay within the heat pump curves, is to find a converged value for the amount of energy moving in and out of the pipe at the end of each run. The converged solution is found by setting the soil radius to 100 meters and doubling the number of grid points in the soil until a converged solution results. Simulation times of 1, 3, 10, 20 and 40 years were correlated in this study with soil thermal conductivities of 0.5, 1, 2, and $4 \frac{W}{m^2 \cdot ^\circ C}$. It is important to note that a grid exponent of three was used for the entire study and is recommended to the user as well.

The minimum radius was determined by increasing the radius 1 meter at a time and comparing the final time step's energy value to the converged value. An error of just 0.1% was set as the tolerance and the final radius is determined by linearly interpolating between the integer values. As a result, four different curves as a function of time can be plotted for each thermal conductivity. Exponential regression analysis reveals an equation for each curve and these can be seen in Figure 28.

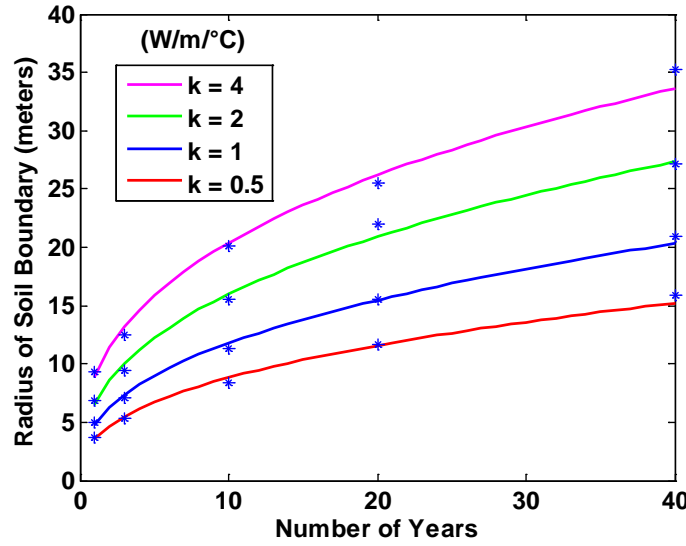


Figure 28: Far field boundary radius required for 0.1% error in simulations as a function of simulation period in years.

The equation for a radius with a 60% heating ratio as a function of time in years is

$$\text{soil radius} = A(\text{years})^B \quad (41)$$

where the coefficients A and B are both functions of the thermal conductivity of the soil. Plotting the coefficient A and determining its behavior as a function of the soil thermal conductivity can be seen in Figure 29. A second order polynomial equation was derived to fit the data points tightly which is important since the behavior is dominated by this coefficient. The quadratic fit for coefficient A now takes the form

$$A = ak_{soil}^2 + bk_{soil} + c \quad (42)$$

where the coefficients a , b , and c were found for six different heating ratios. The coefficient B is now plotted as a function of the soil thermal conductivity. The behavior of the data points appears to be linear and does not change in magnitude much. A linear regression was performed for this coefficient, though an average value would work fine in this case. A plot of this curve can be seen in Figure 30. The equation for coefficient B is

$$B = dk_{soil} + e \quad (43)$$

Combining equations (41), (42), and (43) into one equation for the radial soil boundary condition gives

$$\text{Boundary Radius} = (ak_{soil}^2 + bk_{soil} + c)\text{years}^{(dk_{soil}+e)} \quad (44)$$

Plugging in the values for soil thermal conductivity and years used in the correlation study, reveals errors no greater than 7%. The larger errors are seen in the shorter runs, which can most likely be contributed to the initial conditions fading away in time. In GEO2D the earth radius boundary condition is a default number, calculated for the user, but can be changed by the user.

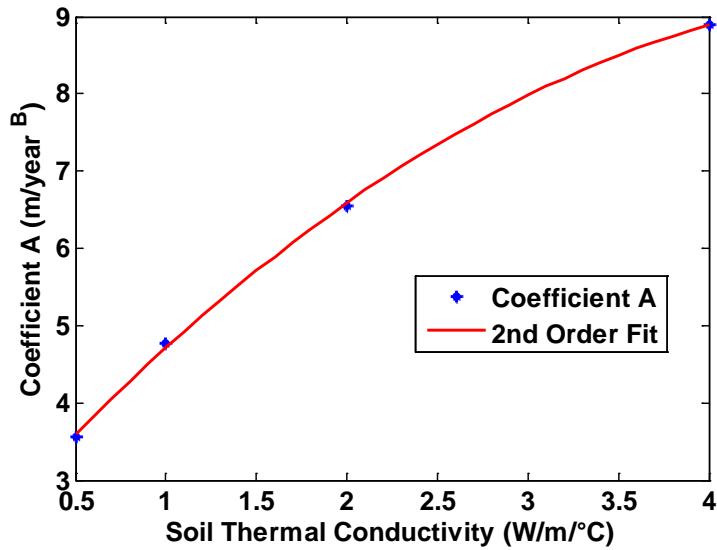


Figure 29: Coefficient A for 60% heating ratio.

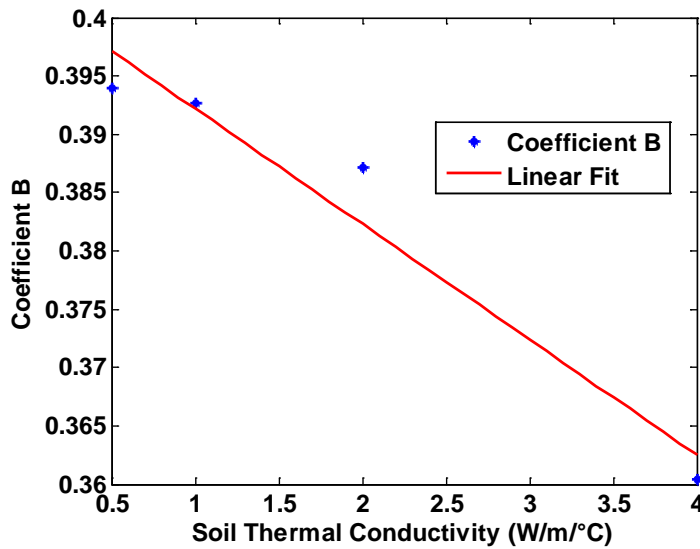


Figure 30: Coefficient B for 60% heating ratio.

3.2.3.2. *GEO3D*

A few types of boundary conditions are implemented into the grid system when modeling a three-dimensional GSHP system. Most boundaries in the model are taken as being adiabatic, but some important ones are not. The boundary condition along the outer radius for a vertical well is set to $\frac{dT}{dr} = 0$ (see Figure 31), except this time the outer radial boundary does not intersect with the ground surface; an axial surface does this. Thus the entire outer radial surface is taken as adiabatic. At the inner radius a symmetry boundary condition is used, $\frac{dT}{dr} = 0$. The axial surfaces for the vertical computational domain are located at $z = 0$ and $z = L$. The surface at $z = L$ uses the adiabatic boundary condition, $\frac{dT}{dz} = 0$. The surface at $z = 0$ is the ground surface and uses the convective boundary condition

$$-k \frac{\partial T}{\partial z} = h(T_s - T_\infty) \quad (45)$$

for all non-fluid areas. A unique aspect of GEO3D is the inclusion of ground surface heat transfer. To determine the ground surface heat transfer a surface heat transfer coefficient is entered into the program. The area where the working fluid enters the ground loop is given the temperature of the fluid exiting the heat pump. For the first time step this temperature is set equal to the ground temperature. For the area where the fluid leaves the ground loop, the boundary condition $\frac{dT}{dz} = 0$ is used. The boundary conditions for the areas that divide the model for symmetry in the azimuthal direction at $\theta = 0$ and $\theta = \pi$ are $\frac{dT}{d\theta} = 0$.

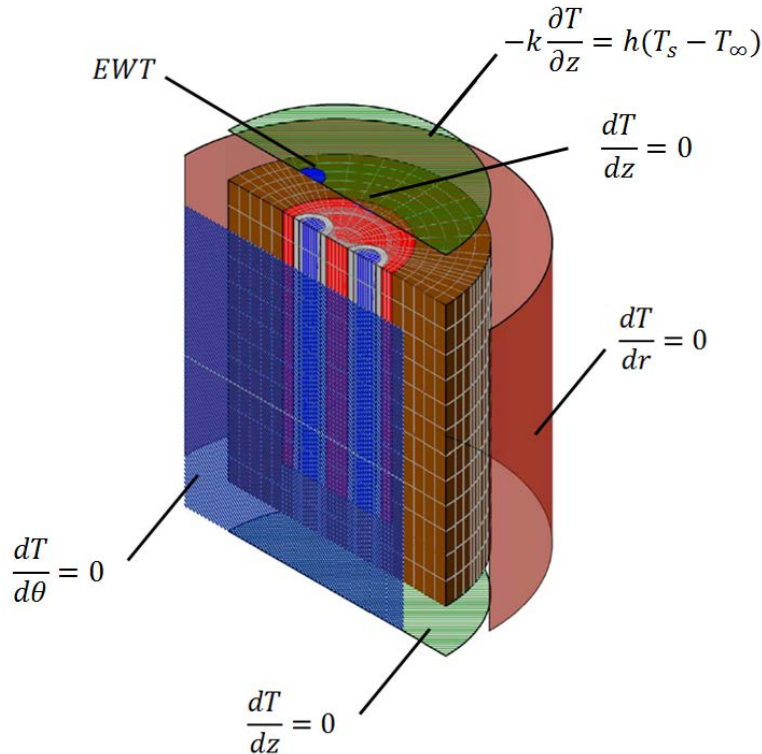


Figure 31: The boundary condition for a vertical GLHE in GEO3D.

The material properties that need to be allocated are density, specific heat, and thermal conductivity, as can be seen in the governing differential equations shown in Equations (31) and (32). For the fluid region two types of thermal conductivity are required; they are the material thermal conductivity of the fluid and the turbulent thermal conductivity. The actual determination of the turbulent thermal conductivity was discussed in Section 3.1. GEO3D allows these properties to be a function of position, which they must be if different materials are involved. They also can even vary within a single material, but the program cannot automatically adjust these properties as a function of temperature. This is not needed because the temperature variations in GSHP systems are relatively small. To implement temperature dependent material properties would make the computational time for GEO3D more excessive than it already is.

3.3. HEAT PUMP

The geothermal analysis program is coupled with a heat pump model that uses an extensive coefficient of performance (COP) trend study, correction factors, and energy balance. This model is developed by using the performance data from 18 units in the Trane line of water to air heat pumps (Trane November 2010). The data analyzed provides the necessary information to define the COP as a function of the entering fluid temperature, fluid volume flow, entering air temperature, air volume flow, and antifreeze concentration. The method used and the equations that result can be seen in the following sections.

3.3.1. COP Trend Study

A subroutine modeling a geothermal heat pump unit is executed at each time step of the GSHP system simulation. The performance data is supplied with COP's for different fluid volume flows and entering water temperatures. A crude model could be developed using this data although this would neglect the indoor air temperature, air flow, and antifreeze concentration factors. The most accurate model possible must include these factors and that is why the COP will be dissected into its constituents for a complete correlation study. That is to say, equations for the capacity and power are individually studied. The hourly EER (energy efficiency ratio) value can be calculated and converted to a COP value for rated conditions using the following equations for cooling and heating respectfully,

$$COP_C^u = \frac{CC^u}{CP^u} \times 0.29287 \quad (46)$$

and
$$COP_H^u = \frac{HC^u}{HC^u} \times 0.29287 \quad (47)$$

where

CC^u is the gross cooling capacity in Mbtuh of unit number u ,
 CP^u is the compressor power in kW of unit number u ,
 HC^u is the gross heating capacity in Mbtuh of unit number u , and
 HC^u is the compressor power in kW of unit number u , and
0.29287 is the unit conversion from EER to COP.

To develop an equation for cooling capacity, the data is plotted versus the fluid volume flow in $\frac{m^3}{sec}$ for all eight EWT (entering water temperatures) provided in the performance data. A plot of each curve for a 3 ton unit can be seen in Figure 32. It is important to note that the capacity data is in English units, while all other data is in metric units. This was done to easily check the gross capacity and compressor power calculations against performance data, while also being necessary to calculate the EER properly. Each of the curves in Figure 32 can now be described as a second order quadratic equation taking the form

$$CC^u = A_{CC}^u \dot{v}^2 + B_{CC}^u \dot{v} + C_{CC}^u. \quad (48)$$

It is recognizable that the curve and slope of each of the different sets of data appears to be somewhat constant.

The coefficient A_{CC}^u from equation (48) is then plotted versus the entering water temperature for every heat pump unit size. A second order polynomial is fit to the data and the curve describing the 3 ton unit number 8 can be seen in Figure 33. The coefficient A_{CC}^u can be written as

$$A_{CC}^u = a_{CC}^u EWT^2 + b_{CC}^u EWT + c_{CC}^u \quad (49)$$

where EWT is the entering water temperature in Celsius. The coefficients a_{CC}^u , b_{CC}^u and c_{CC}^u for all eighteen heat pump sizes have been determined and are in the computer program. This

coefficient describes how much the data in Figure 32 bends as the volume flow changes. At lower EWT's, the coefficient A_{CC}^u has larger magnitudes suggesting that the capacity is changing more with volume flow. The behavior of coefficient A_{CC}^u at higher EWT's suggests that the cooling capacity is dominated more by the water temperature than the volume flow.

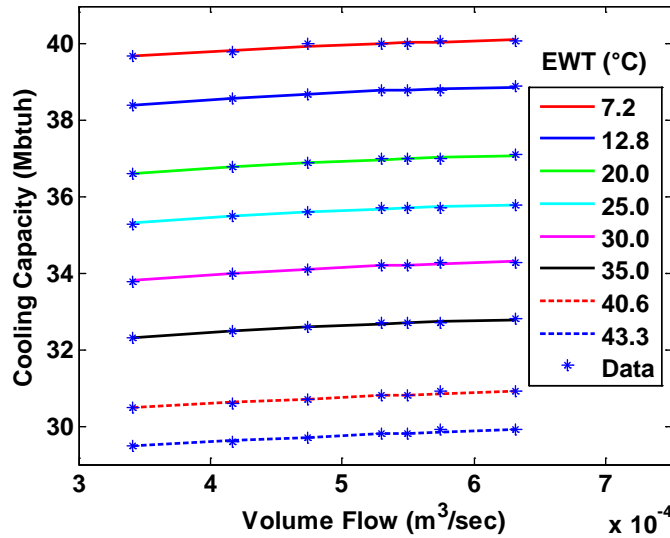


Figure 32: Cooling capacity versus fluid flow for different EWT (Trane November 2010).

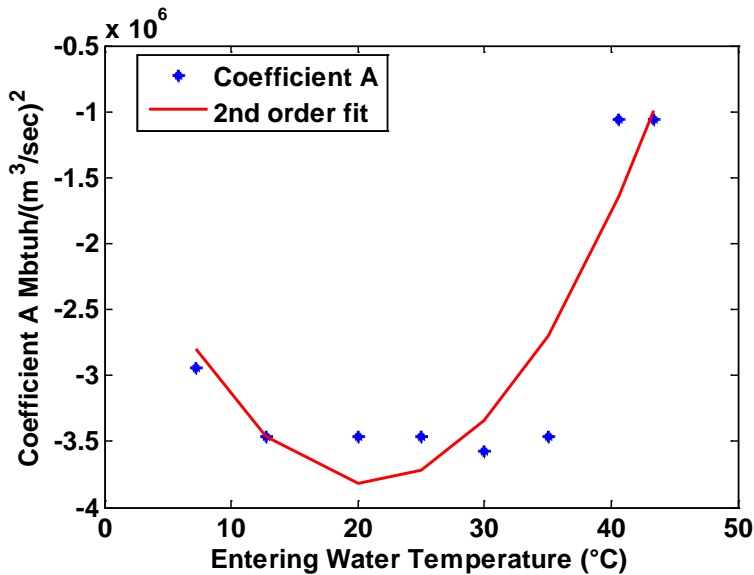


Figure 33: Coefficient A versus EWT for 3 ton unit #8.

The next coefficient to describe the cooling capacity CC^u in equation (48), is the linear term B_{CC}^u . Plotting each of the coefficients versus the respective entering water temperature can be seen in Figure 34. The coefficient B_{CC}^u can now be written as

$$B_{CC}^u = d_{CC}^u EWT^2 + e_{CC}^u EWT + f_{CC}^u \quad (50)$$

where again, the coefficients d_{CC}^u , e_{CC}^u and f_{CC}^u for all eighteen heat pump sizes can be found in the appendix. This curve fit can be seen in Figure 34. The behavior of coefficients A_{CC}^u and B_{CC}^u appear to be mirror images of each other and somewhat sporadic. The behavior of coefficient B_{CC}^u is describing the slope of the curve shown in Figure 32. The slope at higher temperatures has decreased, suggesting that the cooling capacity becomes more dependent on the EWT than the volume flow at higher temperatures.

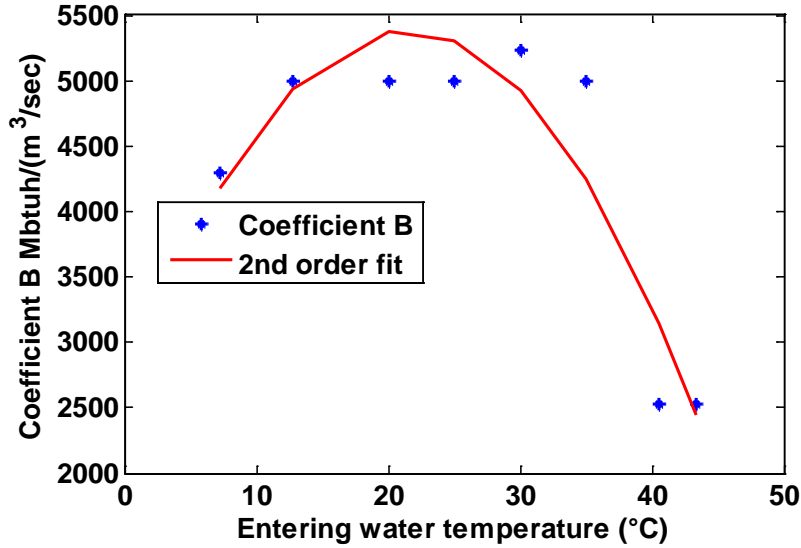


Figure 34: Coefficient B vs. EWT for 3 ton unit #8.

The final coefficient describing the cooling capacity described by equation (48) is the constant term, C_{CC}^u . This term is what truly dominates the equation and after performing a second order regression, Figure 35 shows the correlation between coefficient C_{CC}^u and EWT. The correlation for C_{CC}^u is

$$C_{CC}^u = g_{CC}^u EWT^2 + h_{CC}^u EWT + i_{CC}^u. \quad (51)$$

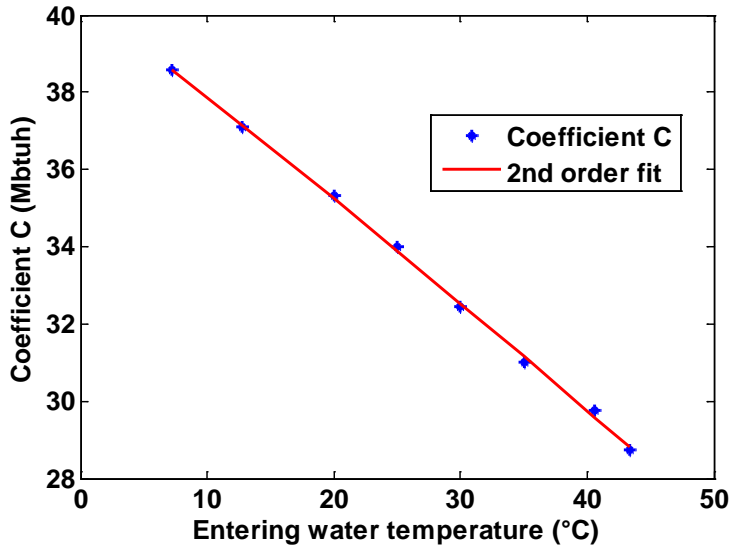


Figure 35: Coefficient C vs. EWT for 3 ton unit #8.

Plugging equations (49), (50), and (51) into equation (48) for the cooling capacity gives

$$CC^u = (a_{CC}^u EWT^2 + b_{CC}^u EWT + c_{CC}^u) \dot{v}^2 + (d_{CC}^u EWT^2 + e_{CC}^u EWT + f_{CC}^u) \dot{v} + (g_{CC}^u EWT^2 + h_{CC}^u EWT + i_{CC}^u). \quad (52)$$

The fit of this equation to the actual heat pump performance is shown in Figure 32. When plugging in the values for the coefficients a_{CC}^u , b_{CC}^u , c_{CC}^u , d_{CC}^u , e_{CC}^u , f_{CC}^u , g_{CC}^u , h_{CC}^u and i_{CC}^u for unit #8, and using the rated volume flow of $8.4 \frac{gal}{min} = 0.0005299 \frac{m^3}{sec}$, and entering a water temperature of 25 °C, the cooling capacity is calculated to be 35.66 Mbtuh. The supplied performance data shows the cooling capacity of unit number 8 at 25°C (77°F) to be 35.7 Mbtuh at the rated volume flow.

Like the cooling capacity first described in equation (48), the cooling compressor power, the heating capacity, and heating compressor power are described as

$$CP^u = A_{CP}^u \dot{v}^2 + B_{CP}^u \dot{v} + C_{CP}^u, \quad (53)$$

$$HC^u = A_{HC}^u \dot{v}^2 + B_{HC}^u \dot{v} + C_{HC}^u, \quad (54)$$

and

$$HP^u = A_{HP}^u \dot{v}^2 + B_{HP}^u \dot{v} + C_{HP}^u. \quad (55)$$

After trend studies of the coefficients were completed in the same manner as the cooling capacity trend studies above, the correlated equations for CP^u , HC^u and HP^u are developed as follows for any unit 1 through 18

$$CP^u = (a_{CP}^u EWT^2 + b_{CP}^u EWT + c_{CP}^u) \dot{v}^2 + (d_{CP}^u EWT^2 + e_{CP}^u EWT + f_{CP}^u) \dot{v} + (g_{CP}^u EWT^2 + h_{CP}^u EWT + i_{CP}^u) \quad (56)$$

$$HC^u = (a_{HC}^u EWT^2 + b_{HC}^u EWT + c_{HC}^u) \dot{v}^2 + (d_{HC}^u EWT^2 + e_{HC}^u EWT + f_{HC}^u) \dot{v} + (g_{HC}^u EWT^2 + h_{HC}^u EWT + i_{HC}^u) \quad (57)$$

$$HP^u = (a_{HP}^u EWT^2 + b_{HP}^u EWT + c_{HP}^u) \dot{v}^2 + (d_{HP}^u EWT^2 + e_{HP}^u EWT + f_{HP}^u) \dot{v} + (g_{HP}^u EWT^2 + h_{HP}^u EWT + i_{HP}^u). \quad (58)$$

Using the rated value for the volume flow, and coefficients for unit 8, CP^8 is calculated to be 2.579 kW. Using the values calculated for CC^8 and CP^8 and plugging into equation (46) gives,

$$COP_c^8 = \frac{35.666}{2.579} \times 0.29287 = 4.050 \quad (59)$$

The COP for unit 8 at the rated volume flow and an entering fluid temperature of 25 °C published in the performance data is 4.053. The COP_H^u is calculated in the same way using equation (47) with equation (57) and equation (58). The COP for heating and cooling are plotted in Figure 36 using entering water temperatures from the performance data with the unit rated volume flow. The performance data used was not extrapolated past the published EWT's.

Using second order polynomials for each coefficient describes the capacities and compressor power well enough to avoid error propagation through to the COP calculation. Evaluating all 18 units in the same manner revealed the largest error to be no more than 0.7% for any of the capacity or compressor power calculations. Note that performing the correlation study on the capacity and compressor power, and not just the COP, results in higher accuracy.

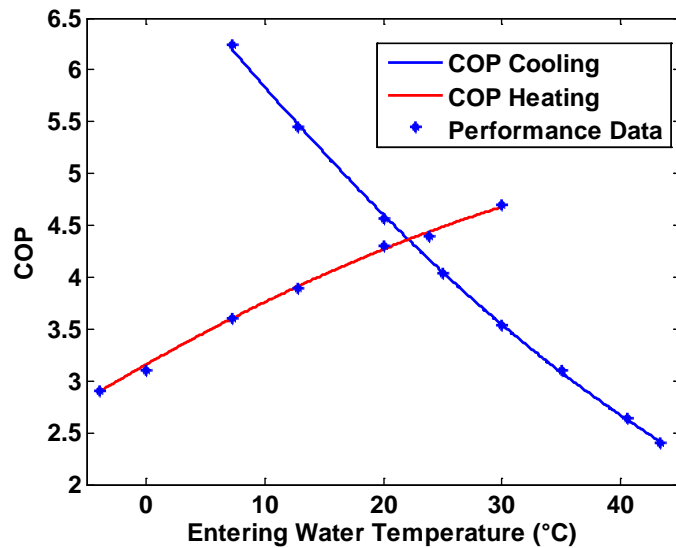


Figure 36: COP for 3 ton unit number 8 at rated volume flow (Trane November 2010).

3.3.2. Correction Factors

The COP for any heat pump is also a function of the air flow, entering air temperature (EAT) over the heat exchanger, and the percent concentration of antifreeze in the working fluid. The previous calculations were all performed at the manufacturers rated air volume flow, air temperatures, and using water as the working fluid. The correction factors for capacities and compressor power as a function of the EAT are plotted in Figure 37. The rated EAT can be seen where the correction factor is equal to one. It is important to note that the EAT for cooling is the wet bulb temperature while for heating it is the dry bulb temperature. Calculation of the wet bulb temperature is discussed in section 3.3.4.

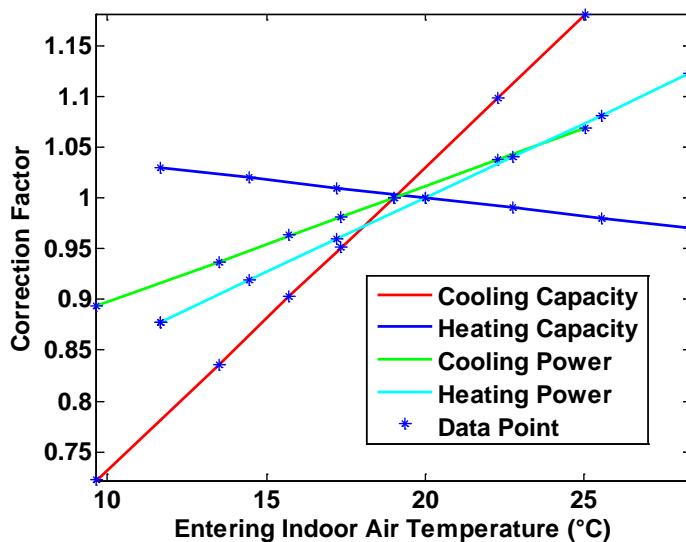


Figure 37: Correction factors for entering air temperature (Trane November 2010).

The need to fit the EAT correction factors with a second order polynomial is more evident in the larger units, while the squared term for smaller units can be set to zero. The entering air temperature correction factor coefficients for all 18 units have been calculated. The equations for the EAT correction factors are

$$CF_{T_{db}}^u = A_{CF}^u T_{db}^2 + B_{CF}^u T_{db} + C_{CF}^u \quad (60)$$

and

$$CF_{T_{wb}}^u = A_{CF}^u T_{wb}^2 + B_{CF}^u T_{wb} + C_{CF}^u, \quad (61)$$

where T_{db} and T_{wb} are the indoor dry bulb temperature and indoor wet bulb temperature respectively.

The second set of correction factors is a function of the air volume flowing over the heat exchanger, which are plotted in Figure 38. Again, the rated air volume flow for this heat pump can be seen where the correction factor is equal to one. These curves can now be expressed as

$$CF_{\dot{V}}^u = A_{CF}^u \dot{V}_{air}^2 + B_{CF}^u \dot{V}_{air} + C_{CF}^u \quad (62)$$

where \dot{V}_{air} is the indoor air volume flow in $\frac{m^3}{sec}$. Equation (62) can be used for both heating and cooling, as well as for capacity and compressor power.

The final set of correction factors is found for concentrations of methanol, ethylene glycol and propylene glycol from zero to fifty percent. The correction factor as a function of percent concentration of ethylene glycol can be seen in Figure 39. A linear regression analysis allows the equation for the capacity correction factor to be written as

$$CF_{\%af}^u = A_{CF}^u (\%af) + B_{CF}^u \quad (63)$$

where $\%af$ is the percent concentration of antifreeze. Coefficients for all three types of antifreeze have been determined.

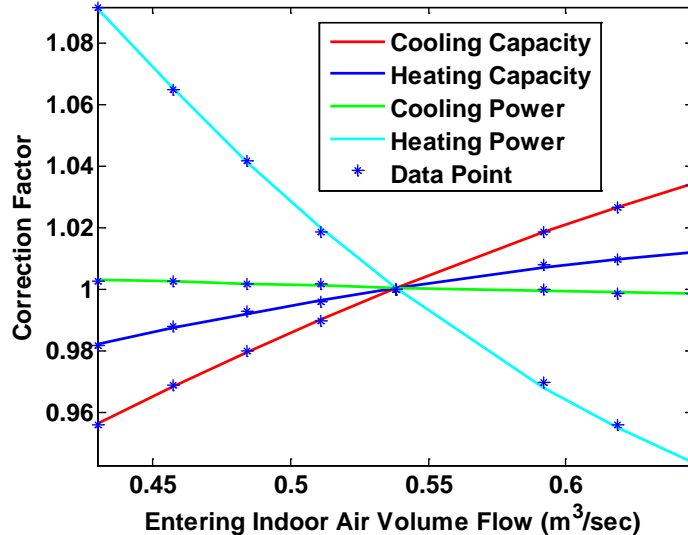


Figure 38: Correction factor for indoor air volume flow (Trane November 2010).

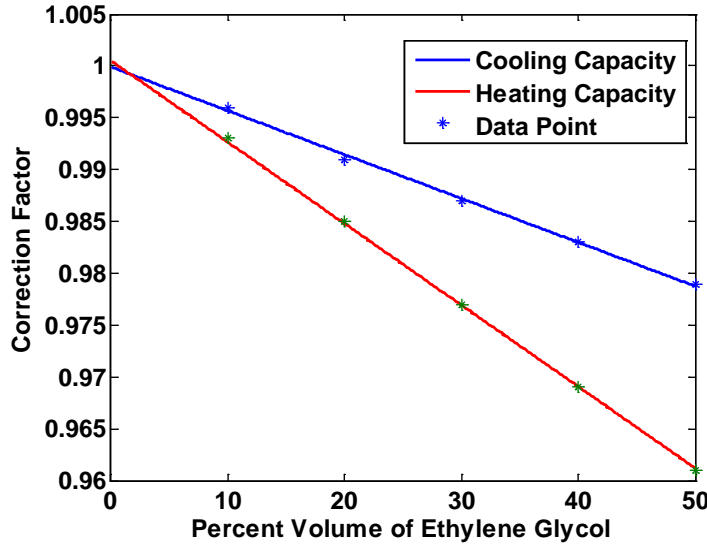


Figure 39: Correction factor for capacity as a function of antifreeze concentration (Trane November 2010).

Finally, with the correction factors $CF_{T_{db}}^u$, $CF_{T_{wb}}^u$, CF_V^u and $CF_{\%af}^u$, the equations for COP become

$$COP_C^u = \frac{CF_{\%af}^u CF_V^u CF_{T_{wb}}^u CC^u}{CF_V^u CF_{T_{wb}}^u CP^u} \times 0.29287 \quad (64)$$

and

$$COP_H^u = \frac{CF_{\%af}^u CF_V^u CF_{T_{db}}^u HC^u}{CF_V^u CF_{T_{db}}^u HP^u} \times 0.29287. \quad (65)$$

The variables necessary to calculate the COP for cooling and heating respectively are

$$COP_C^u(\dot{v}, EWT, T_{wb}, \dot{V}_{air}, \%af) \quad (66)$$

and

$$COP_H^u(\dot{v}, EWT, T_{db}, \dot{V}_{air}, \%af). \quad (67)$$

The variables \dot{v} , \dot{V}_{air} and $\%af$ are user defined and remain constant throughout the calculation. The variable, T_{db} , is determined in the load calculations by ENERGYPLUS and changes every time step. This leaves EWT and T_{wb} to complete the heat pump model.

3.3.3. Entering Water Temperature

Upon convergence of the temperature field in each time step, the temperature of the fluid exiting the loop becomes the entering fluid temperature to the heat pump. The bulk fluid temperature is then determined for the working fluid exiting the ground loop. Using the velocity profile $u(r)$ discussed in Section 3.1 and the temperature profile $T(r)$, calculated at every iteration, the bulk fluid temperature, T_m , is determined from

$$T_m = \frac{\int_0^R c_p T(r) \rho u(r) 2\pi r dr}{\rho V_{ave} (\pi R^2) c_p} = EWT. \quad (68)$$

The idealized result can be seen in Figure 40 where the rate at which the energy is transported with the fluid is the same in either case (Y. A. Cengel 2007).

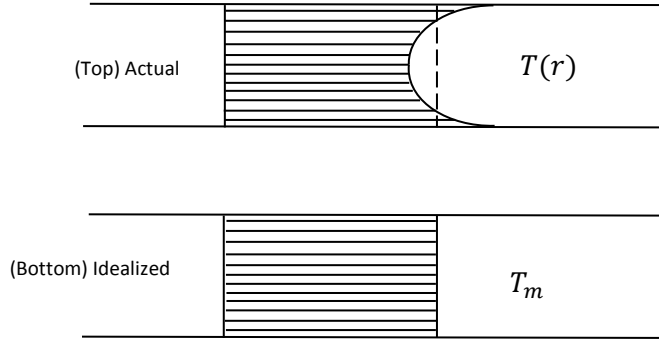


Figure 40: Temperature profiles for flow in a tube

The numerator in Equation (66) is the sum of the energy being delivered to the heat pump from the ground loop. The change in energy across the heat pump is then calculated using the first law of thermodynamics

$$Q_L + W_{in} = Q_H . \quad (69)$$

For heating, Q_L is the change in energy transported by the fluid, Q_H is the simulated hourly building load, and W_{in} is the building load divided by the COP_H , or work done on the system. For cooling, Q_L is the simulated hourly building load, Q_H is the change in energy transported by the fluid, and W_{in} is the building load divided by the COP_C .

The temperature of the fluid leaving the heat pump and entering back into the ground loop is

$$T_{bulk} = T_m - \frac{\Delta E}{\rho V_{ave}(\pi R^2)C_p} . \quad (70)$$

It is important to note that the sign convention must remain negative for cooling and positive for heating throughout the calculation. This uniform temperature profile then becomes the entering fluid temperature to the geothermal ground loop for the next iteration of the time loop.

3.3.4. Wet Bulb Temperature

The ENERGYPLUS building loads output file was set up to provide the inside dry bulb temperature, T_{db} , and the humidity ratio, ω_1 . The wet bulb temperature is the temperature the air would be if allowed to cool adiabatically to saturation by evaporating water into it. In a thermodynamic process the wet bulb temperature can be understood and calculated from knowing the properties of the state. A schematic of the thermodynamic process can be seen in Figure 41.

In order to calculate the indoor wet bulb temperature, a trial and error solution must be followed using the following equation

$$T_{wb} = \frac{(\omega_1(h_{g,1} - h_{f,2}) - (\omega_2 h_{fg,2}) + T_{db} C_p)}{C_p} \quad (71)$$

where h is the enthalpy and C_p is the specific heat of the air. The specific humidity at state two is then calculated using

$$\omega_2 = \frac{0.622 P_{g,2}}{P_{atm} - P_{g,2}} . \quad (72)$$

The values for P_g , h_g and h_f can be found in water tables. These values were plotted and fit with an equation as a function of the temperature. The curves used for P_g , h_g and h_f can be seen in Figure 42.

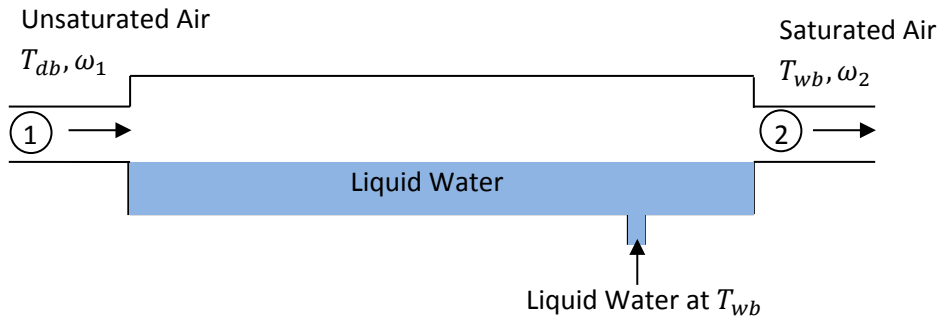


Figure 41: Adiabatic saturation process (Cengel and Boles 2008).

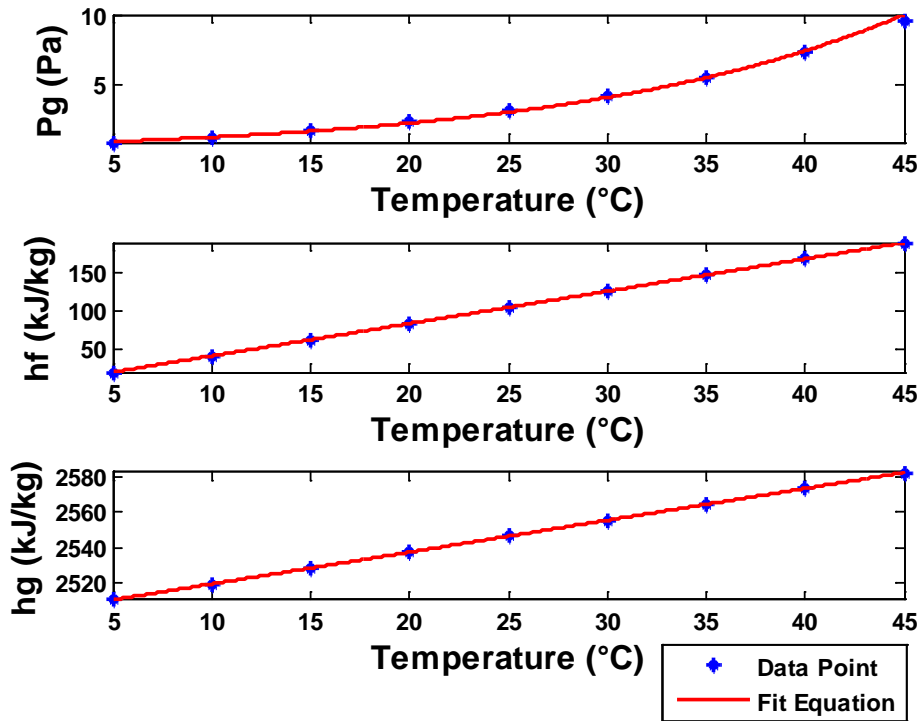


Figure 42: Vapor pressure, fluid enthalpy, and vapor enthalpy plotted and fit.

The pressure as a function of temperature is fit with an exponential function taking the form

$$P_g = 0.6834e^{0.0599T}. \quad (73)$$

The energy in the fluid at temperature T is fit linearly along with the energy in the vapor. These two equations are then subtracted from one another to give h_{fg} as seen in the following equations:

$$h_f = 4.1845T + 0.1789, \quad (74)$$

$$h_g = 1.8097T + 2501.2, \quad (75)$$

and

$$h_{fg} = -2.3748T + 2501.0211. \quad (76)$$

The wet bulb temperature can now be calculated and used in the correction factors for cooling capacity and cooling compressor power. This is done each time step in an iterative process when cooling is needed from the heat pump.

3.4. ECONOMICS

A cost analysis is performed to evaluate whether geothermal heating and cooling is a more attractive option over conventional systems. The size and initial cost of the system, fuel costs, efficiencies, and interest rate all contribute to the cost over time. The hourly loads, hourly COP (in the case of the air-to-air heat pump and the vapor compression air conditioner), and weather information is used to simulate conventional systems for comparison. The time value of money with a user defined interest rate and initial system costs are plotted and show the time required to pay back the initial investment on the geothermal system. The user also has the option of changing the efficiencies of the conventional units for further flexibility.

3.4.1. Unit and Installation Costs

The potential of the data generated from the building load calculations and the geothermal analysis are fully realized when applied to a payback period calculation. The initial cost of the geothermal system is estimated using pricing from heat pump, trenching/drilling, installation, water pump, and material costs. The heat pump unit cost was found to be an average cost of \$835.21/ton (D.O.E. 2010). The trenching costs were estimated from some local companies to be \$2/foot for 5 foot depth including back filling and \$9/foot for 10 foot depth. The drilling costs were estimated at \$10/foot but will vary greatly depending on the specific job. The water pump and material costs were found in a catalog from Geo-Hydro Supply (Geo-Hydro 2011). A function for the price per foot was derived with the catalog information and used to extrapolate other pipe sizes. The cost per linear foot as a function of the diameter can be seen in Figure 43. The water pumps ranged from \$300 to \$2000 and were determined linearly depending on the size of the heat pump. With these initial cost estimations, the designer can determine cost savings based on accurate sizing of the system. These values are all hard coded into the program and will require updating in the future.

3.4.2. Operational Costs

The operating costs for five different systems are calculated using the hourly building load data. The natural gas, fuel oil, and propane systems are simulated with a vapor compression air conditioner for the cooling needs. Every conventional unit has the user option to change its efficiency, with the exception of the geothermal system, since its COP has already been determined in the geothermal analysis. The price for the fuel to run each unit has a default value, but can be changed depending on where the user is located and the particular price of the fuel. It is known that the price of some fossil fuels change from day to day and the cost of electricity can change from region to region. The geothermal systems hourly operational cost is calculated using

$$\text{Hourly Geothermal Cost} = \frac{Q_{Load}(Wh)}{COP_{geo,hourly}} \cdot \frac{1kWh}{1000Wh} \cdot \frac{\$}{kWh_{elect.}} + \frac{W_{pump}}{eff_{pump}} \cdot \frac{\$}{kWh_{elect.}} \quad (77)$$

If the user chooses a run-time step larger than hourly for the geothermal analysis, then the hourly COP is approximated. The air-to-air heat pump operational cost is modeled similar to the geothermal cost calculation, with a few differences. The first difference is that a COP function was developed for cooling and heating as a function of outdoor air temperature. This was done for five different seasonal energy efficiency ratings (SEER). The cooling data is a function of the

air volume flow and wet bulb temperature as well; however, the curves are plotted using the rated values.

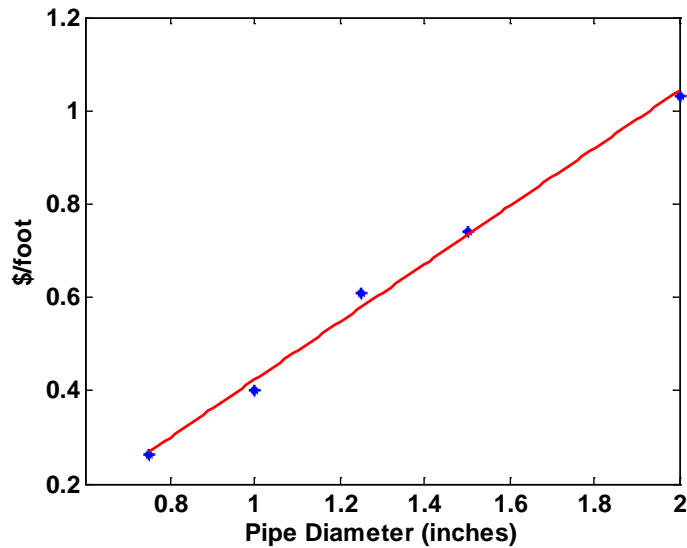


Figure 43: Price per foot of geothermal tubing.

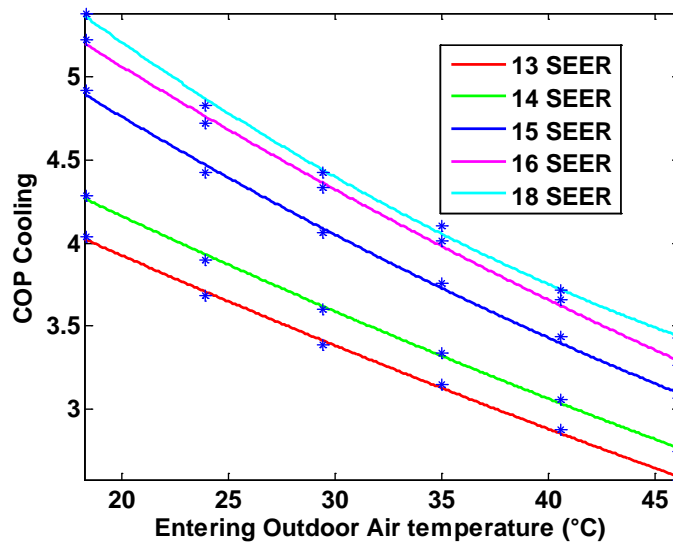


Figure 44: COP for air-to-air heat pump in cooling mode.

The equation developed for each is used in the hourly calculations for air-to-air cost, except when the outdoor temperature is less than -5 degrees Celsius. When this happens the COP is set equal to one to simulate a backup electric resistance heating system. The air-to-air system's hourly operational cost is calculated using

$$\text{Hourly Air - to - Air Cost} = \frac{Q_{Load}(Wh)}{COP_{airhp,hourly}} \cdot \frac{1kWh}{1000Wh} \cdot \frac{\$}{kWh_{elect.}} \quad (78)$$

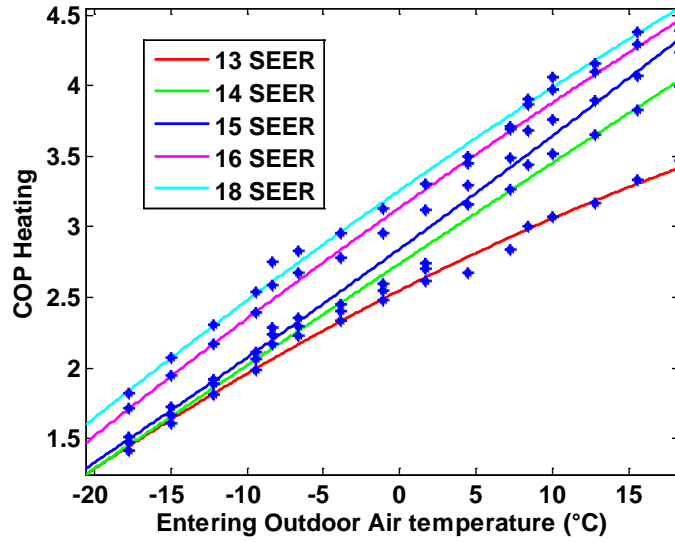


Figure 45: COP for air-to-air heat pump in heating mode.

To model the natural gas furnace operational costs, the hourly heating load is divided by the furnace efficiency. A value for the energy available for combustion per cubic foot of natural gas was found to be approximately $292 \frac{Wh}{ft^3}$ (Cengel and Boles 2008). This makes the hourly cost equation for natural gas heating,

$$\text{Hourly Natural Gas Heating Cost} = \frac{Q_{Load}(Wh)}{eff_{ng}} \cdot \frac{1ft^3}{292Wh} \cdot \frac{\$}{ft^3}. \quad (79)$$

The hourly loads that are negative, referring to cooling needs, are modeled using the COP cooling study from Figure 44. The user-defined SEER values are used to simulate any efficiency of an air conditioner. This will allow the user to model several different combinations of cooling and heating systems including ultra-high efficient systems.

The propane and fuel oil systems are modeled the same way as the natural gas using $40,883 \frac{Wh}{gal}$ for fuel oil and $26,945 \frac{Wh}{gal}$ for propane energy content (Cengel and Boles 2008). The cooling needs of these systems are also modeled using the vapor compression model as discussed above. The equations for fuel oil and propane hourly operational heating are

$$\text{Hourly Fuel Oil Heating Cost} = \frac{Q_{Load}(Wh)}{eff_{oil}} \cdot \frac{1gal}{40,883Wh} \cdot \frac{\$}{gal} \quad (80)$$

and

$$\text{Hourly Propane Heating Cost} = \frac{Q_{Load}(Wh)}{eff_{pr}} \cdot \frac{1gal}{26,945Wh} \cdot \frac{\$}{gal}. \quad (81)$$

The hourly operational costs over an entire year for each system now make it possible to more accurately calculate the operational costs and couple them with the initial system costs for payback periods.

3.4.3. Payback Period

To more accurately calculate the payback period of the geothermal system compared to conventional systems, including the time value of money is necessary. The initial value of the different systems is entered by the user to represent the total installation and equipment costs of the system. In the case of geothermal this would be the cost of the trenching or drilling, pipe

materials, water pumps, installation, and heat pump. With the yearly operational cost for each system calculated as described in the previous section, a multiyear scenario will show which system is the least expensive. To do this, the user will enter the desired number of years to calculate, along with the interest rate to be used. The present day dollar value of the system at year n is calculated by adding the present day value of the operational cost at the end of year n to the previous year's present value using

$$PV = \sum_{t=0}^n \frac{FV_t}{(1+i)^t}, \quad (82)$$

where the present value of the operational cost is calculated for n years at interest rate i . The present value of each system is then plotted and the iteration repeats, giving a curve of present day cost over time. The point at which the geothermal curve crosses the conventional system's curve, is the year at which the geothermal system has paid for itself. A screen shot of the economics page can be seen in Figure 46 as an example of what the user will see.

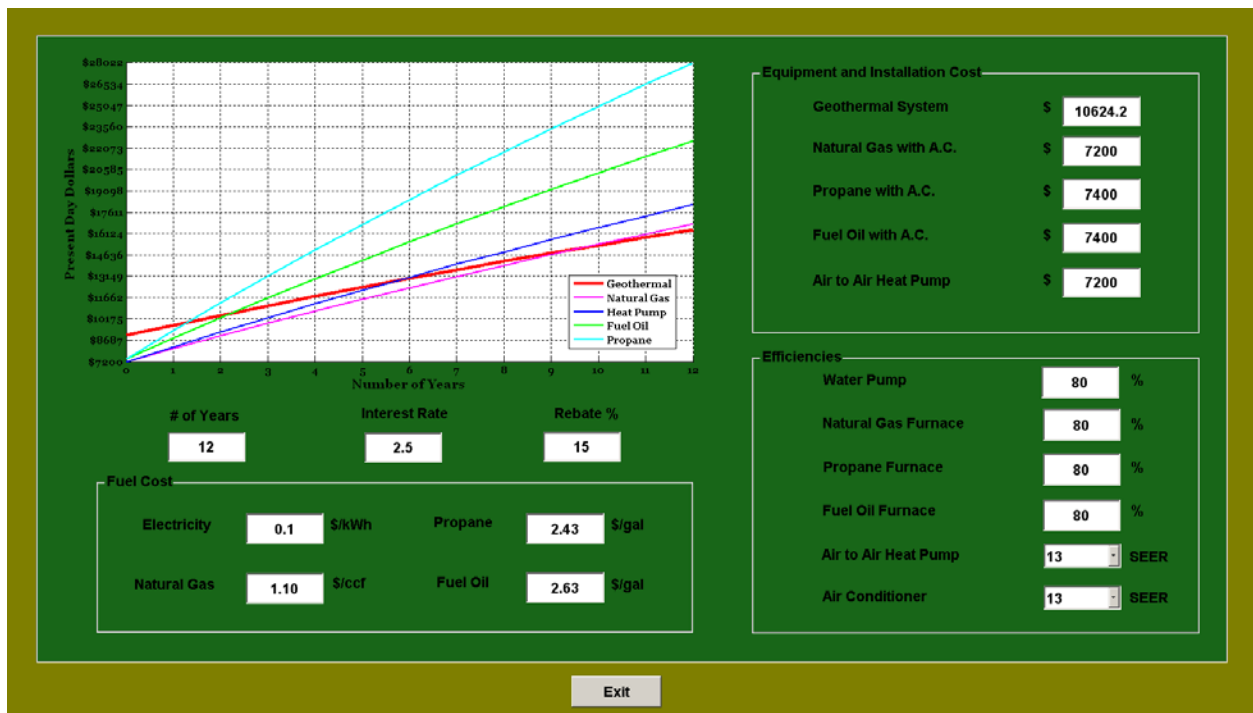


Figure 46: Screen shot of the economics page.

Using this tool, the designer can see how changing certain parameters of the geothermal design will ultimately affect the final cost. By using the hourly load data with the heat pump model, a designer can see what economic impact a system will have by reducing the length or size of pipe, types of fluid, or even the geothermal configuration itself.

4. PROGRAM OUTPUTS

4.1. GEO2D

As the program came together, many case studies were performed to test the completeness of the entire program. One such case study is a hypothetical 2500 square foot house in Dayton, Ohio. This house was virtually constructed using the ‘novice’ load calculator as a typical two story home with an unconditioned basement. A horizontal closed loop system was designed using the recommended 4 ton heat pump. The recommended pipe size, fluid velocity, ground temperature, and grid parameters were used. The working fluid was chosen to be 100% water and the soil type ‘silty loam (moist)’. The length of tubing used in the design was chosen to be 350 meters and the simulation was run on daily time steps for a twenty year analysis. Most of these plots are in terms of days so it should be realized that 20 years is equivalent to 7300 days.



Figure 47: Home screen for case study.

The first output is a daily COP, as seen in Figure 48 for twenty years; this gives the designer a good sense of how the efficiencies change with the different seasons. The outputs available to the designer are intended to allow the user to iterate the design to achieve optimum results. Maximizing the amount of time the COP is a higher value can lead to a more efficient, cost effective design. A histogram of COP’s allows the designer to see the frequency at which a range of efficiencies occur. An example of a COP histogram can be seen in Figure 49.

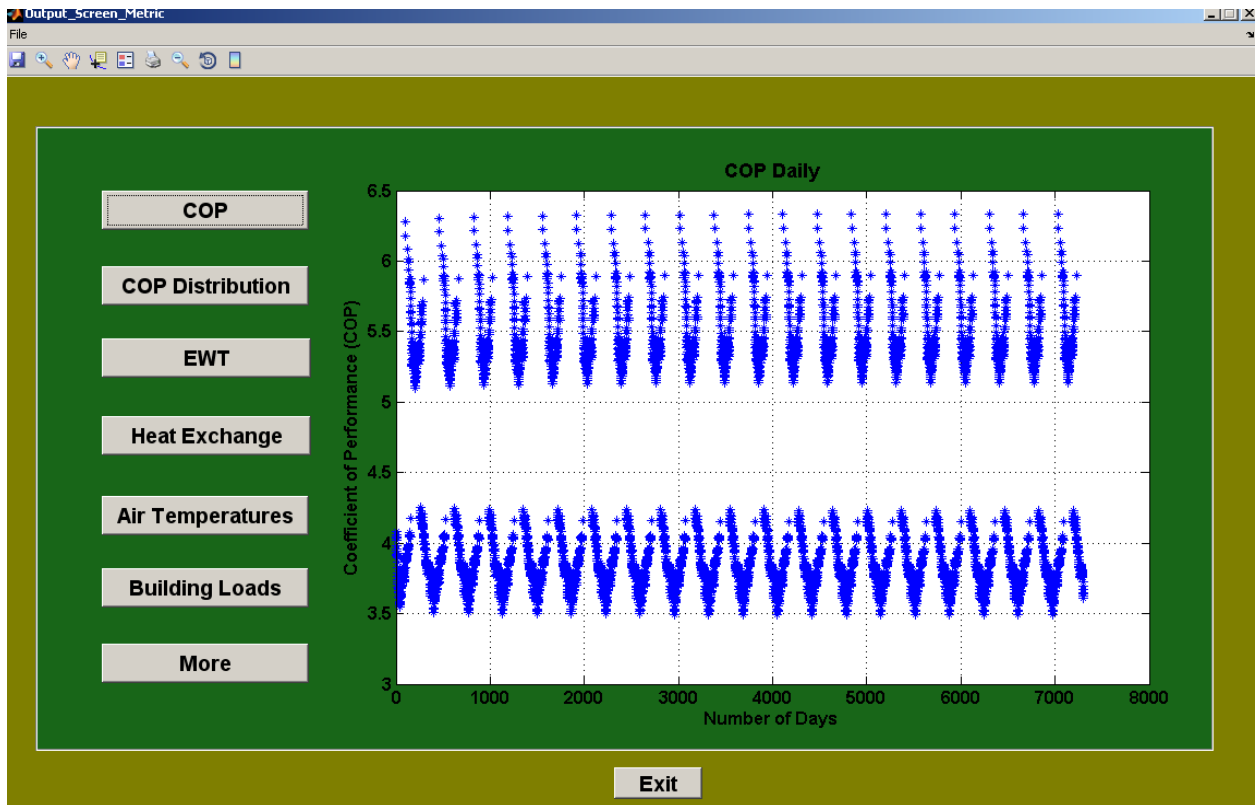


Figure 48: Daily COP.

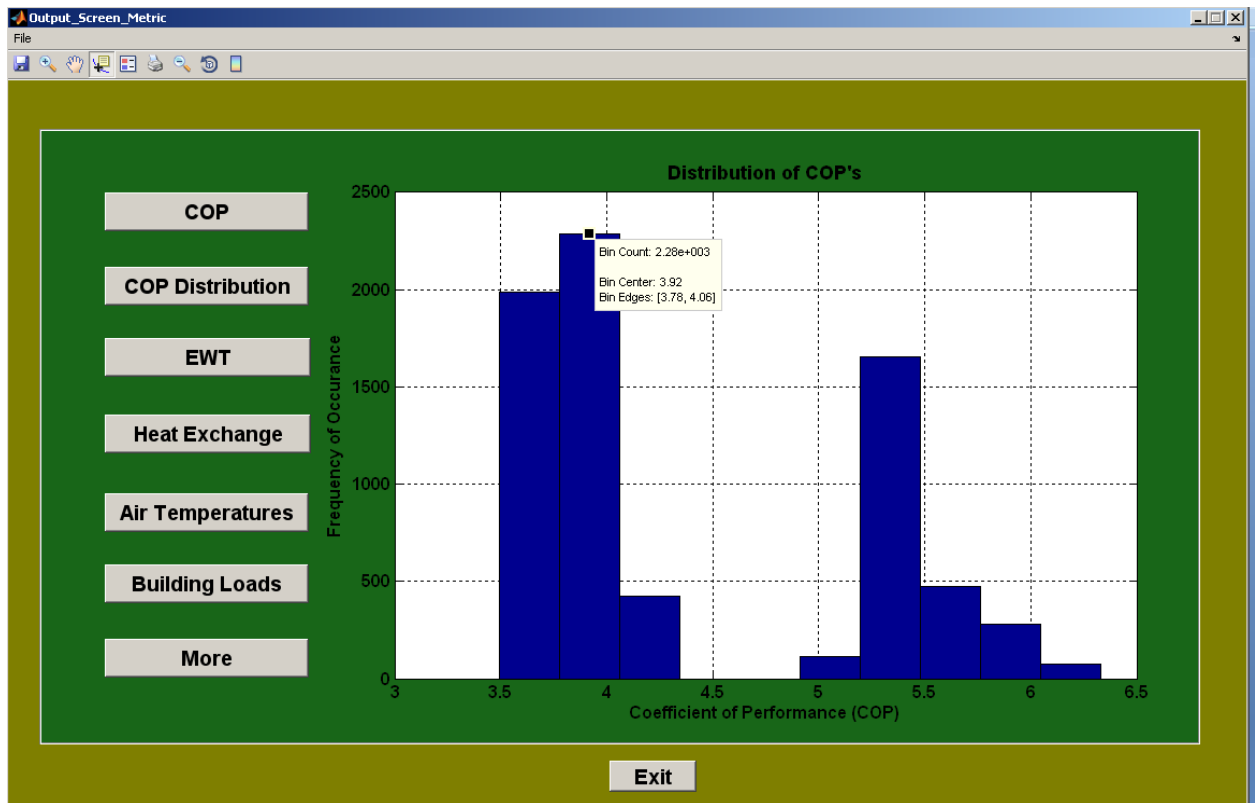


Figure 49: Histogram of COP's.

A cost effective heating dominated design can sometimes require a longer length of tube or the use of antifreeze as the working fluid. The result in Figure 50 allows the designer to reduce unnecessary cost in material by watching how close the fluid gets to the desired temperature. Some geothermal systems will use a higher concentration of antifreeze and allow the entering water temperature to drop below the freezing point of water during extreme winter conditions. In addition, the total amount of heat being exchanged to and from the ground loop is displayed to give the designer better understanding of the thermal response of the system (see Figure 51).

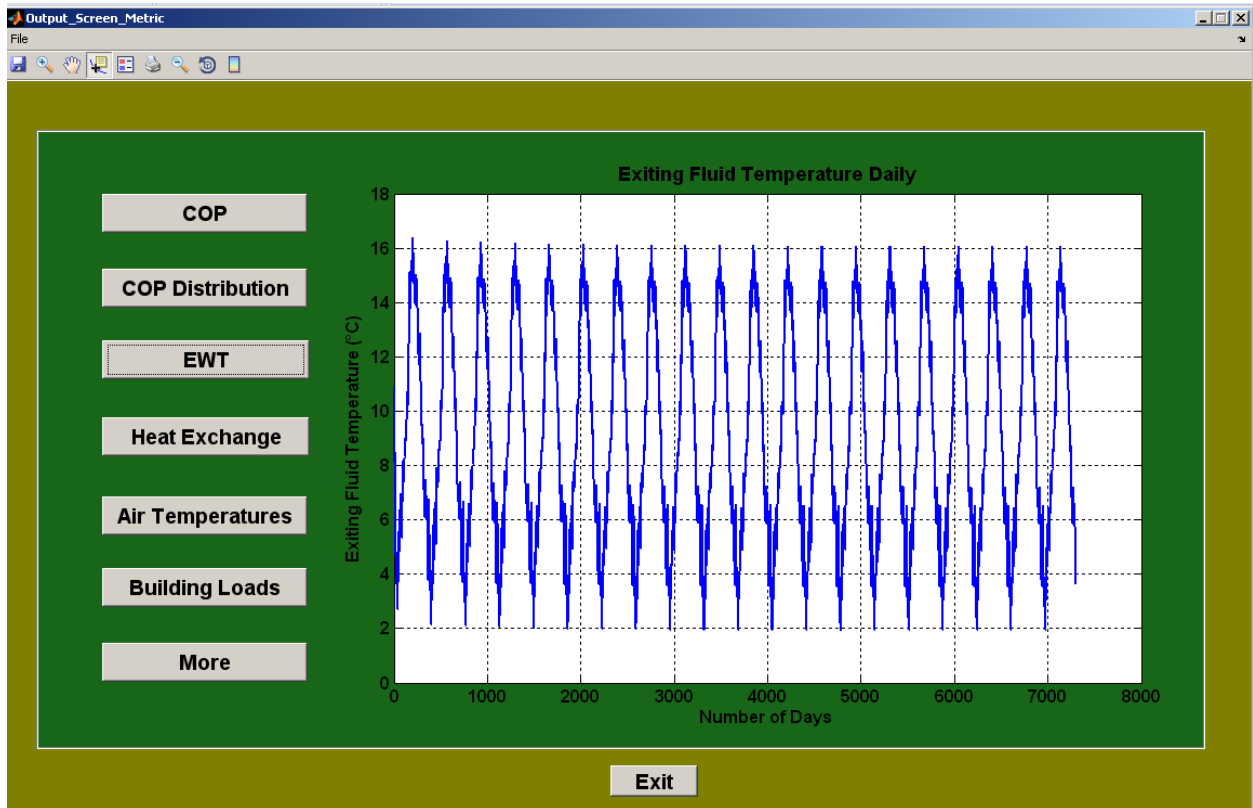


Figure 50: Entering water temperature to the heat pump.

Some ENERGYPLUS data is displayed such as the indoor and outdoor dry bulb temperatures and the hourly building loads as seen in Figure 52 and Figure 53 respectively. The building heating loads are what the GSHP system has to be sized to meet. This is the starting point of the GSHP analysis done in GEO2D.

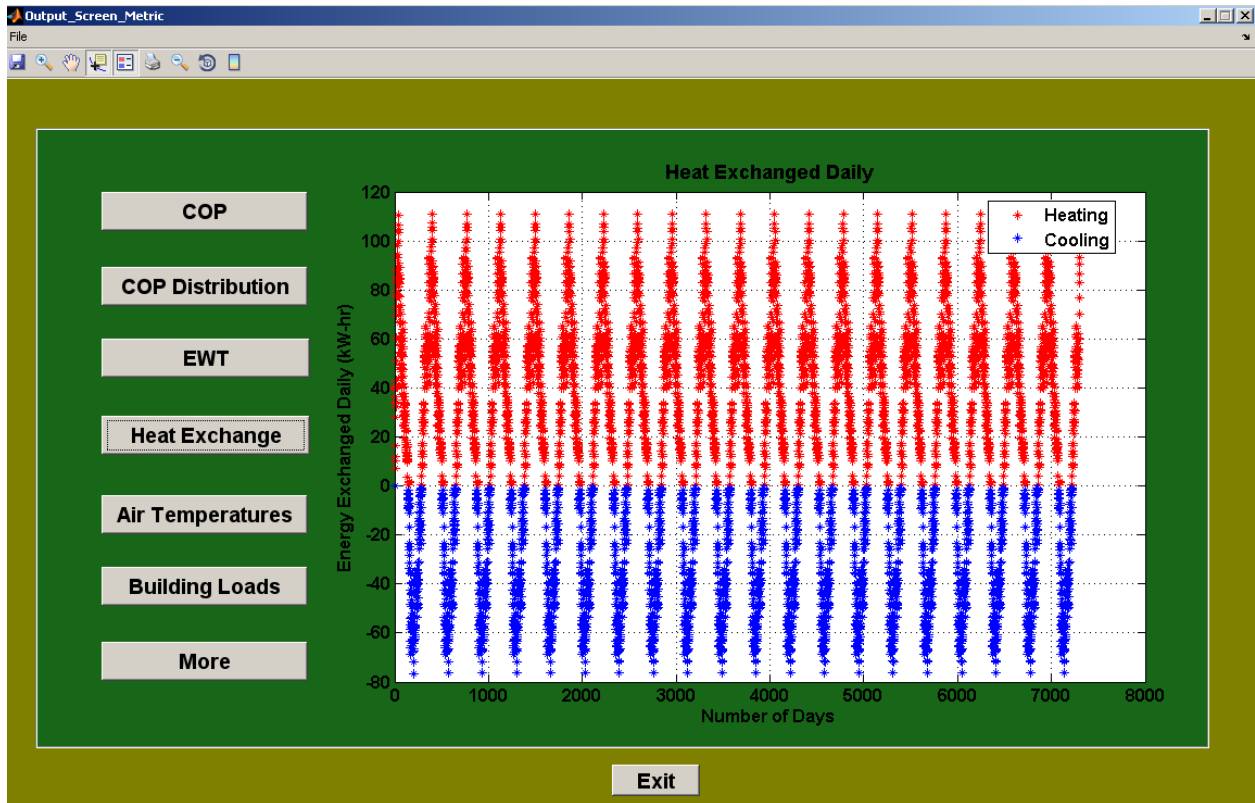


Figure 51: Heat exchanged with the working fluid.

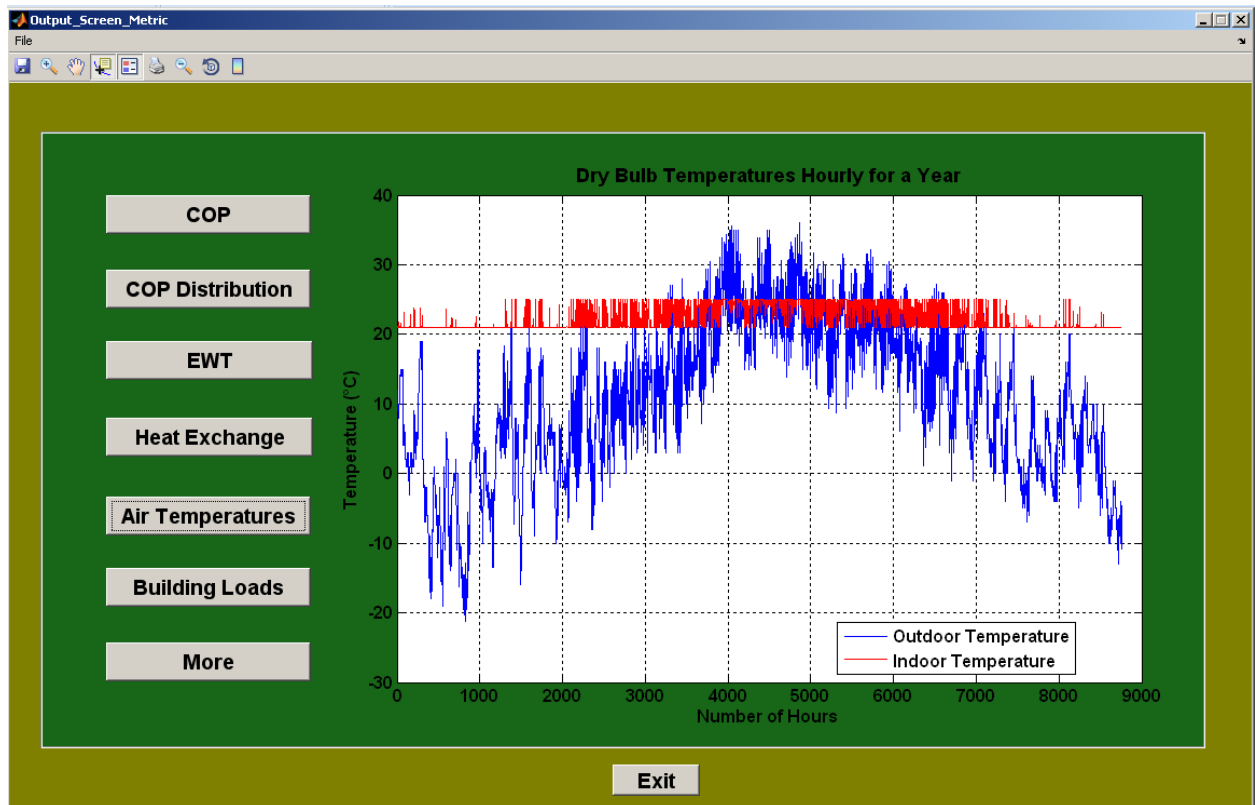


Figure 52: Indoor and outdoor dry-bulb temperatures.

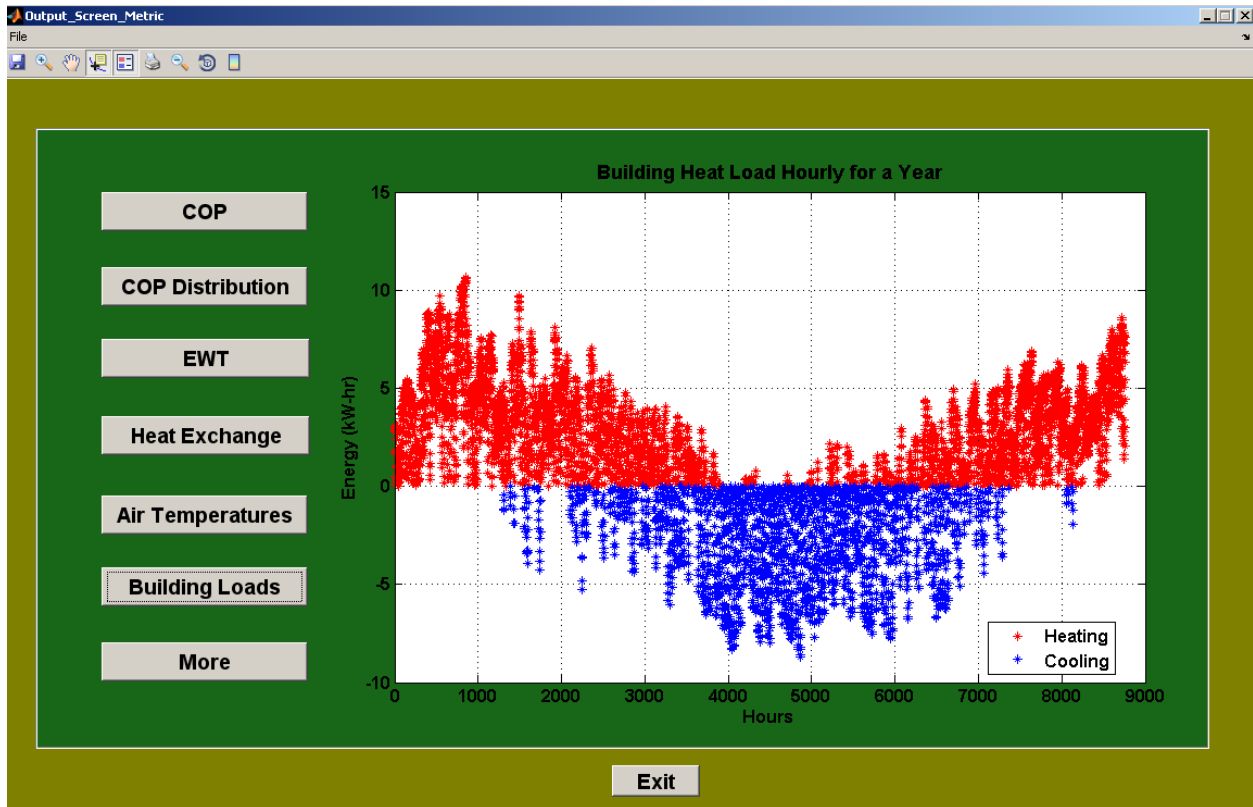


Figure 53: Hourly heat loads from ENERGYPLUS.

Temperatures at six different locations in the earth and tube are displayed to the user as a function of time. These plots are shown in Figure 54. These types of plots allow the user to easily see what is occurring in the tube and ground around the ground loop over a period of time. Entire temperature field information can be obtained at any time by making contour plots of the data found in the projects folder called “temp_contour_plots*.txt” where the asterisks indicates a name of the users choosing. This information allows the designer to analyze the thermal response of the ground and alter the spacing of the tubes based on the heat pulse over time. Contour plots of the temperature field during the heating season after twenty years can be seen in Figure 55 and the temperature profile during the cooling season after 20 years of operation can be seen in Figure 56.

These outputs supplied to the designer in conjunction with the emphasis on accuracy and computation time will help push the geothermal industry forward. A better program and more confidence in the results will ultimately begin to reduce the overall cost of the system making geothermal an even more attractive option for consumers.

A great deal of results produced by GEO2D can be found in the appendices. Appendix I shows results for Dayton, Ohio, Appendix II shows results for Boston, Massachusetts, and Appendix III shows results for Omaha, Nebraska. Each of these appendices presents the building specifics, some peak building load information, the geothermal design inputs, building loads for one year, the calculated fluid temperature exiting the ground loop for a 20 year period, the heat exchange with the ground for a 20 year period, and the temperature distributions over a 20 year period. None of the commercial codes presently in existence is known to produce temperature profiles like those produced by GEO2D and GEO3D.

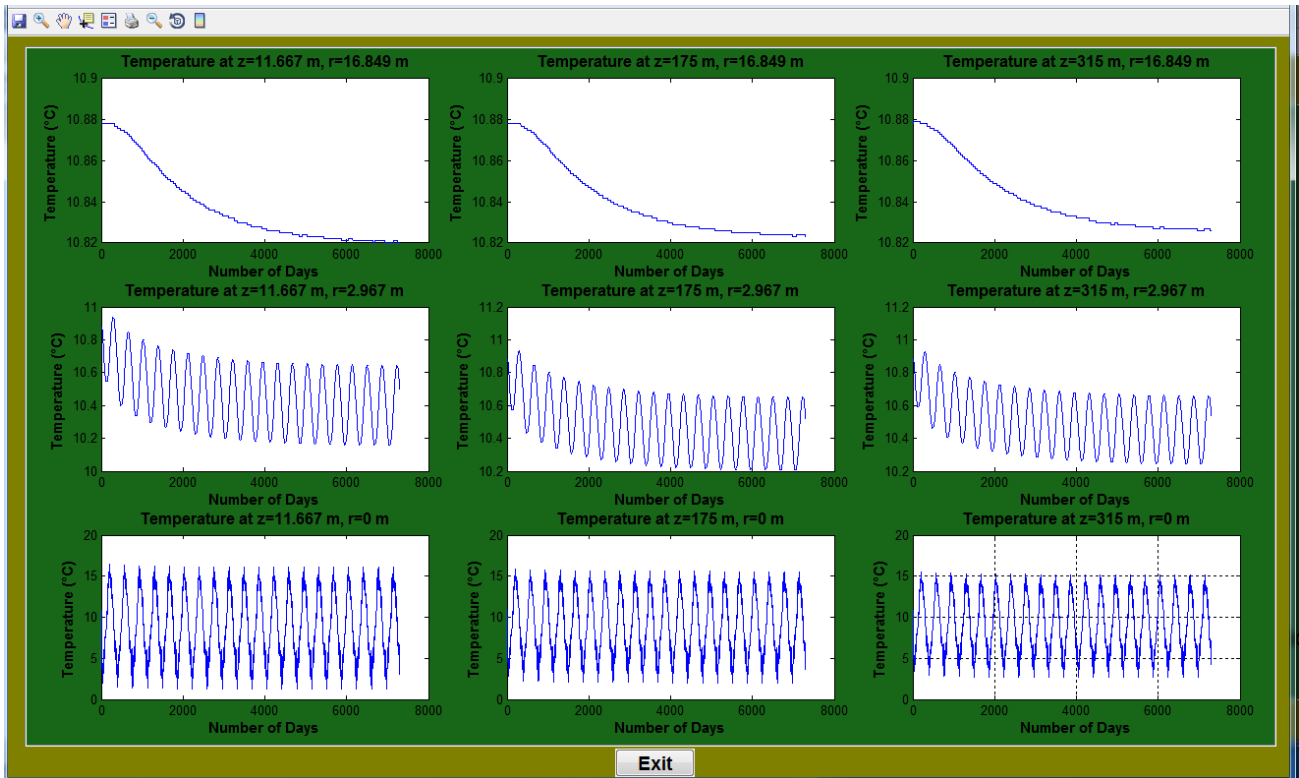


Figure 54: Temperatures at different locations in the earth and tube.

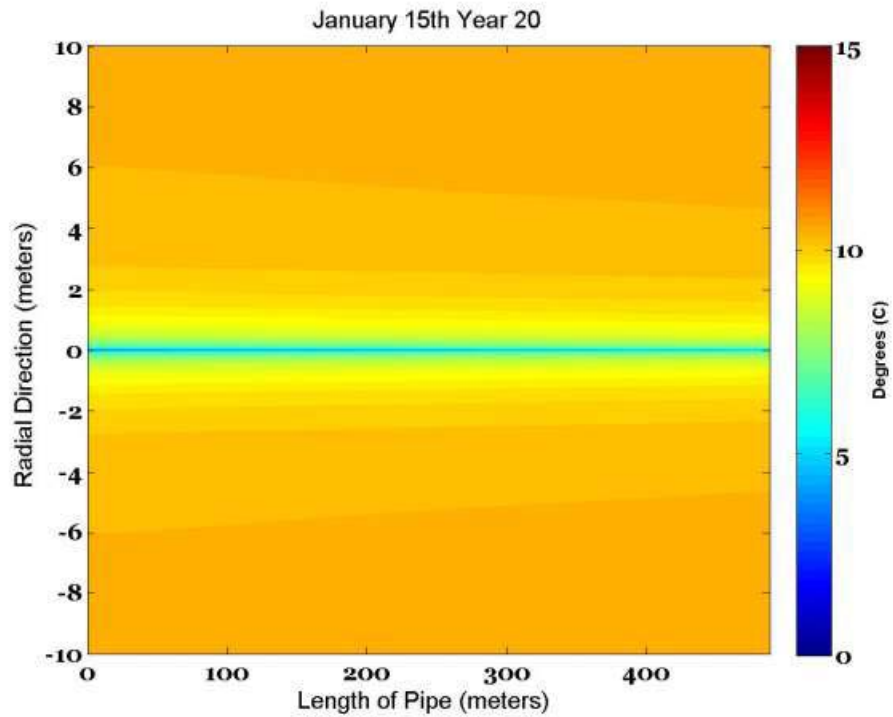


Figure 55: Example of a temperature field during heating season.

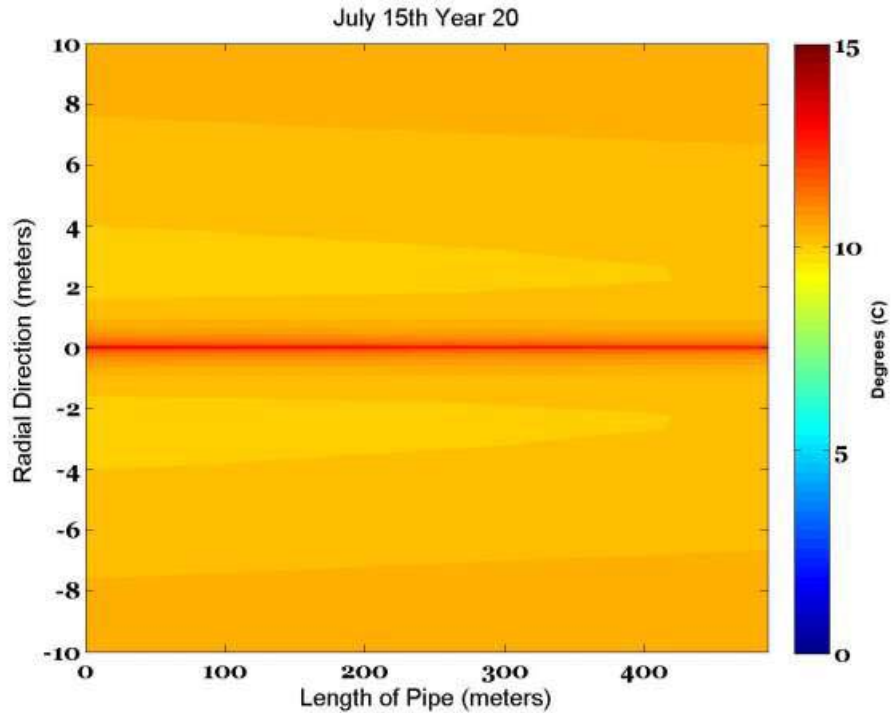


Figure 56: Example of a temperature field during the cooling heating season.

4.2. GEO3D

Results from the three-dimensional GSHP computer code GEO3D are shown in this section of this report. The results shown are for one vertical bore hole that is 100 m deep. This is a deep bore hole and could just as easily have been modeled as two vertical wells 50 m deep. The bore hole has one U-shaped tube such that one side of the U-tube carries the working fluid down the well and the other side carries the fluid up the well. This means the working fluid must travel 200 meters through the well. The details of the input parameters used for this analysis are shown in Table 4 below. This simulation uses heat loads for an average size home in the Dayton, Ohio area. Results are produced for a 2 year period starting on January 1 and going through the second year to December 31. A total of 28,728 cells were used and a time step of 6 hours was used.

Figure 57 through Figure 62 show the temperature profiles in horizontal planes, at different depths along the length of the well. The x-y planes shown in these figures are parallel to the surface of the earth at a depth listed in the caption. The position $x=0$, $y=0$ is at the center of the bore hole. Figure 57 shows the temperature profile at the surface of the well and Figure 62 shows the temperature profile at the bottom of the bore hole. Figure 58 through Figure 61 show temperature profiles at depths of 0.22, 13.56, 49.11, and 93.55 meters. For most of the bore hole the temperature profiles are quite similar, as expected. The differences occur at the top of the bore hole and at the bottom. The temperatures at the top of the bore hole are affected by heat transfer between the air and the ground. Those temperature profiles at the bottom of the bore hole are different because heat transfer that can easily take place in the vertical direction at this position. For much of the bore hole the heat transfer is essentially in the radial direction. All of these temperature profiles show the temperature levels in the bore hole being close to $-10\text{ }^{\circ}\text{C}$. Note that the color of the fluid in the working fluid that flows through the U-tube is dark blue.

This means the fluid is about $-10\text{ }^{\circ}\text{C}$. The reason for this is the bore hole is not big enough to supply all the home's heating needs in December and thus the heat pump is extracting this energy from the working fluid reducing its temperature. The ground is supposed to replenish the heat in the working fluid to raise its temperature closer to $11.7\text{ }^{\circ}\text{C}$. These temperature contours, as well as the plots to be shown below, indicate the length of the ground loop is too short for this home. Because the working fluid in this case is water, freezing will occur.

In Figure 63 a zoomed-in view of the U-tube where the fluid is located is shown. Close to the tubes the heat transfer is three-dimensional. This figure indicates that the computer simulation is determining the temperature profiles in the grout and around the U-tube nicely. Due to the discretization in cylindrical coordinates centered at the center of borehole the working fluid tubes are not exactly round; however, they are close. This can be improved by using more cells.

The temperature of the fluid leaving the ground loop and going into the heat pump as a function of time is shown in Figure 64. This is shown for a two year time period that begins on January 1 of the first year and ends on December 31 of the second year. At time zero the temperature of the fluid in the entire loop is the undisturbed ground temperature, $11.7\text{ }^{\circ}\text{C}$. This temperature drops for the first 800 hours due to the heat pump removing more energy from the working fluid than the ground puts back. This period is the month of January and a little bit of February. In February and March the fluid temperature recovers, even though the home still requires heating. The heat loads of the home for the simulated 2 year time period are shown in Figure 65 as the green line. Net home heating continues through March. The opposite effect, but somewhat less severe, can be seen to occur in the summertime. This would be the hours of 3000 to 7000. Figure 64 shows the temperature of the working fluid increasing to $30\text{ }^{\circ}\text{C}$ and then recovering. The problem with these huge swings in the fluid temperature is the efficiency of the heat pump decreases. These huge swings in fluid temperature are indicating that the length of this single bore hole is not enough for the heat loads required by this home.

Table 4: Input conditions for geothermal program.

Parameter	Value
Length of ground loop	100 meters
Shank distance	0.06 meters
Inner diameter of fluid tubes	0.025 meters
Tube wall thickness	0.003 meters
Grout radius	0.076 meters
Radius of outer boundary condition for earth	20.076 meters
Mean working fluid velocity	1.0 meters per second
Earth undisturbed temperature	$11.7\text{ }^{\circ}\text{C}$
Outside air heat transfer coefficient	$7.0\text{ W/m}^2\text{-}^{\circ}\text{C}$
Thermal conductivity of ground	1.0 W/m-K
Specific heat of ground	1900 J/kg-K

Density of ground	1500 kg/m ³
Thermal conductivity of tube wall	0.12 W/m-K
Specific heat of tube wall	460 J/kg-K
Density of tube wall	900 kg/m ³
Thermal conductivity of working fluid	0.580 W/m-K
Specific heat of working fluid	4205 J/kg-K
Density of working fluid	1000 kg/m ³
Dynamic viscosity of working fluid	0.001499 N-s/m ²
Thermal conductivity of grout	1.4 W/m-K
Specific heat of grout	880 J/kg-K
Density of grout	2300 kg/m ³

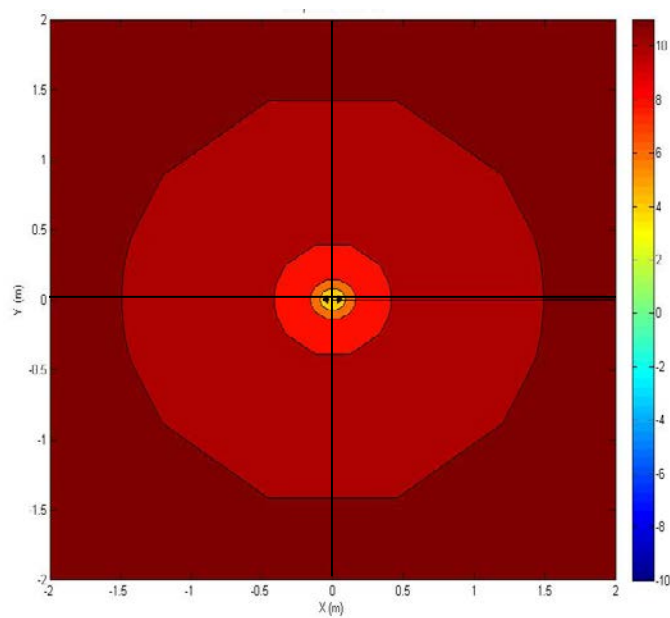


Figure 57: Temperature profiles in a horizontal plane at a depth of 0.00 meters below the earth's surface. Note that the $x = 0, y = 0$ position is the center of the bore hole and the temperature scale shown is in degrees Celsius.

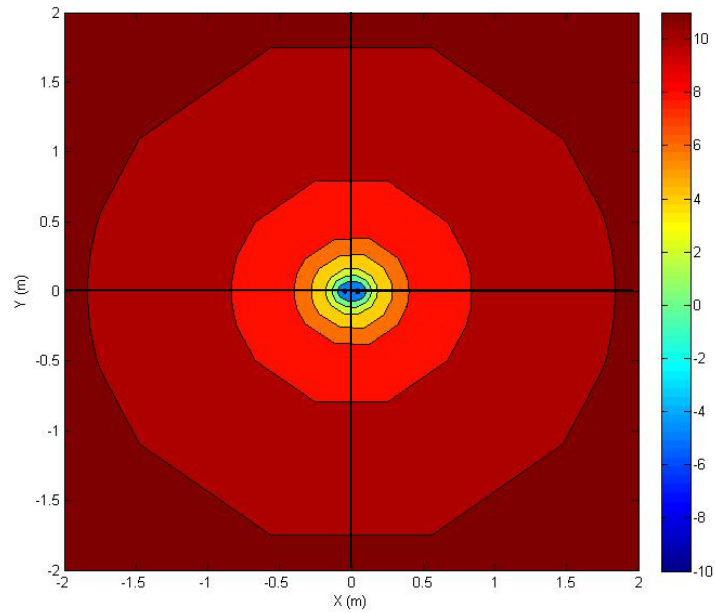


Figure 58: Temperature profiles in a horizontal plane at a depth of 0.22 meters below the earth's surface. Note that the $x = 0, y = 0$ position is the center of the bore hole and the temperature scale shown is in degrees Celsius.

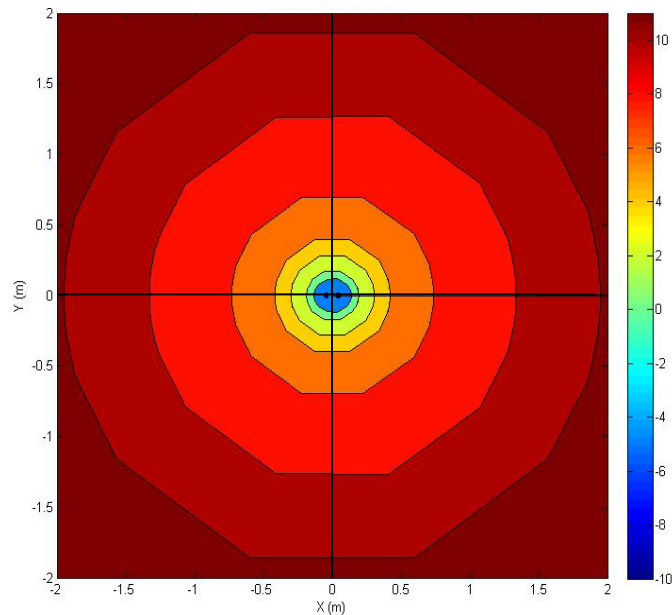


Figure 59: Temperature profiles in a horizontal plane at a depth of 13.56 meters below the earth's surface. Note that the $x = 0, y = 0$ position is the center of the bore hole and the temperature scale shown is in degrees Celsius.

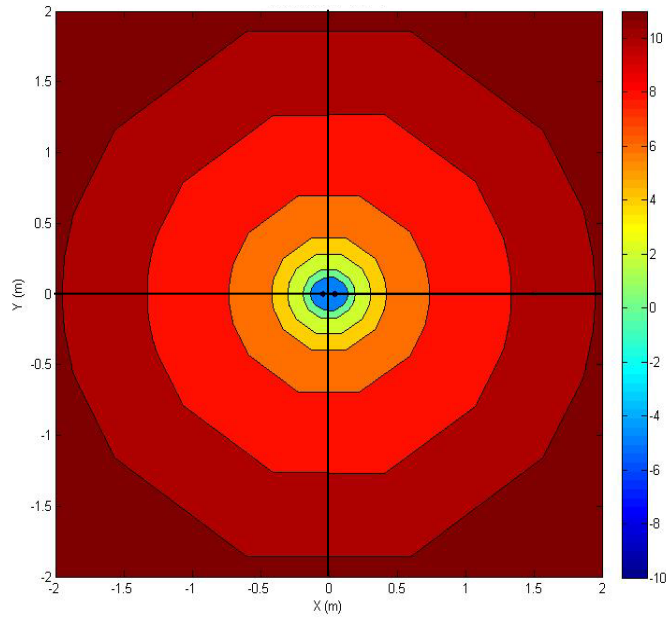


Figure 60: Temperature profiles in a horizontal plane at a depth of 49.11 meters below the earth's surface. Note that the $x = 0, y = 0$ position is the center of the bore hole and the temperature scale shown is in degrees Celsius.

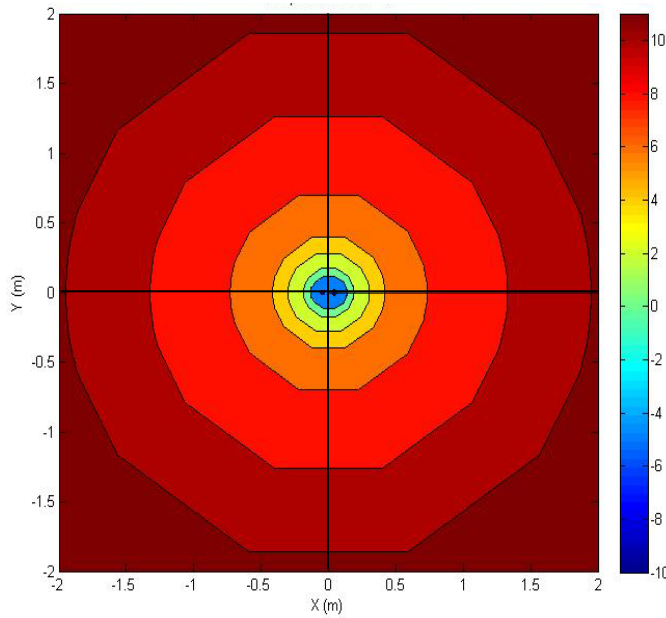


Figure 61: Temperature profiles in a horizontal plane at a depth of 93.55 meters below the earth's surface. Note that the $x = 0, y = 0$ position is the center of the bore hole and the temperature scale shown is in degrees Celsius.

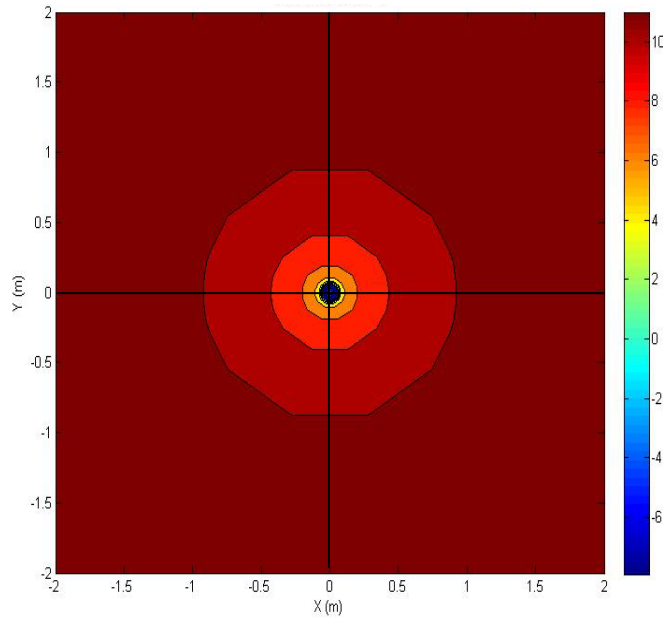


Figure 62: Temperature profiles in a horizontal plane at a depth of 100.00 meters below the earth's surface. Note that the $x = 0, y = 0$ position is the center of the bore hole and the temperature scale shown is in degrees Celsius.

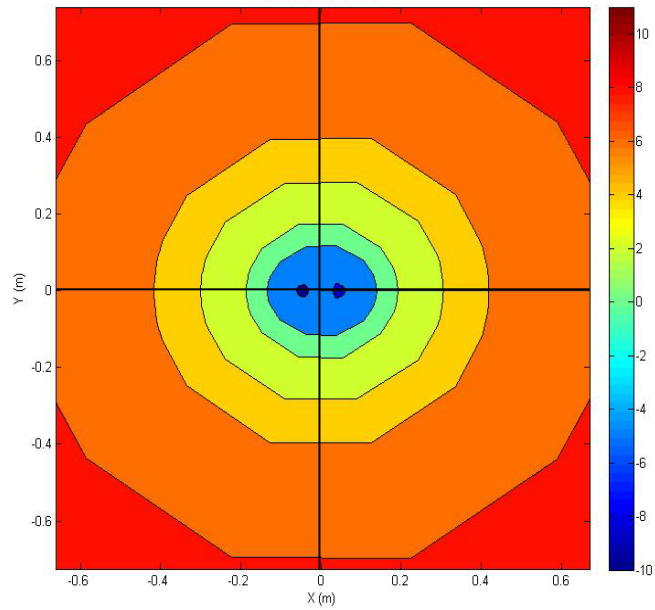


Figure 63: Zoomed in view of temperature profiles in a horizontal plane at a depth of 13.55 meters below the earth's surface. Note that the $x = 0, y = 0$ position is the center of the bore hole and the temperature scale shown is in degrees Celsius.

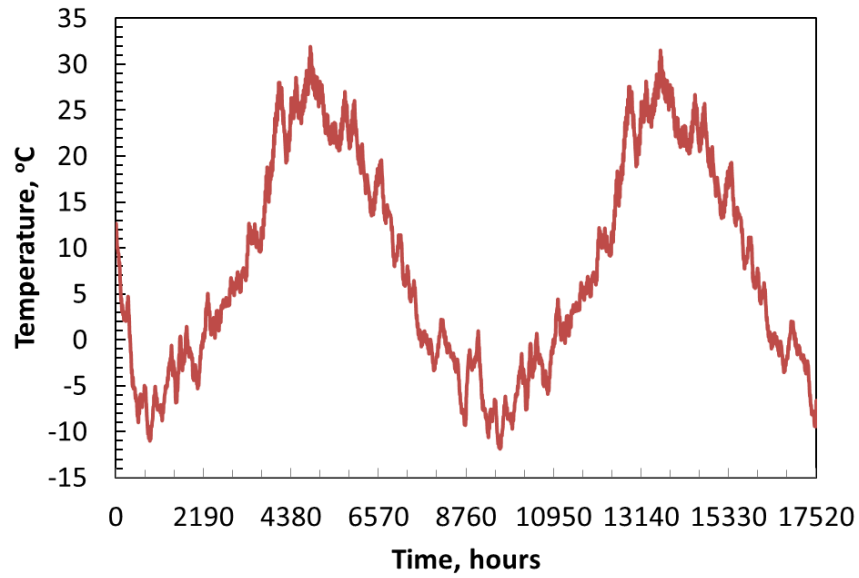


Figure 64: Bulk temperature of working fluid exiting the ground loop as a function of time.

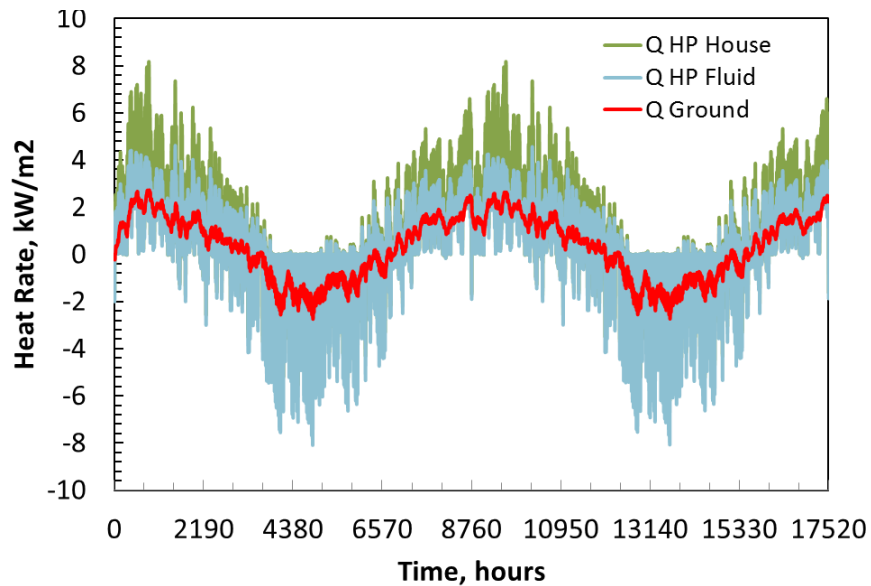


Figure 65: Heat delivered from the heat pump to the house, heat taken from the fluid by the heat pump, and heat delivered by the ground to the fluid.

Also shown in Figure 65 are heat delivered from the heat pump to the home, the heat taken from the working fluid by the heat pump, and the heat delivered by the ground to the working fluid for a two year time period. None of these heat rates are exactly the same, nor should they be. The heat delivered by the heat pump to the home is different from the heat taken from the fluid by the heat pump because the energy from the compressor located in the heat pump is assumed to go into the working fluid. This is a positive effect in the winter and a negative effect

in the summer. The heat from the ground to the working fluid follows the general trend of the heat load, but does not respond to the quick fluctuations. The ground is a rather poor thermal conductor and thus is unable to respond on an hourly or even a daily time scale. This is fine as long as the heat capacity of the working fluid is sufficient to handle these short time fluctuations. This appears to be the case in this design.

The other major concept that can be recognized from both Figure 64 and Figure 65 is that the GSHP system operates on a yearly cycle. The temperatures of the working fluid drop significantly in the winter when the heat pump is extracting heat from the working fluid, and increase substantially in the summer when the heat pump is dumping heat into the working fluid. The goal of a good ground loop design is to reduce these temperature swings while keeping the initial installation cost low. Figure 64 indicates that the ground loop may be undersized for this home's heating loads.

The efficiency or COP of the heat pump used in this simulation is shown in Figure 66. This plot indicates that the COP for the entire 2 years of operation stays above 2. This is good. It would be even better to keep heat pump COP above 3. This could be done if the ground loop were made larger. Notice that it is the heating loads that are drawing the COP below 3.

The results presented in this report indicate that three-dimensional version of the GSHP computer code called GEO3D, developed as part of this DOE grant, is working well and producing a number of useful results. I believe that GEO3D will greatly help in the design and research of better ground loop heat pump systems. The major problem with GEO3D is the long computational times. This will have to be addressed in future work. It is believed that these computational times can be reduced substantially with some algorithm improvements. Right now GEO2D takes a few minutes to do a 20 year simulation. GEO3D takes a few days to perform this same simulation. Thus a factor of 100 decrease in computational time is required. A few days to perform one simulation is too long. I believe that the computational runtime of GEO3D can be reduced substantially with some advanced simultaneous equation solving techniques. This will have to be done as part of another project.

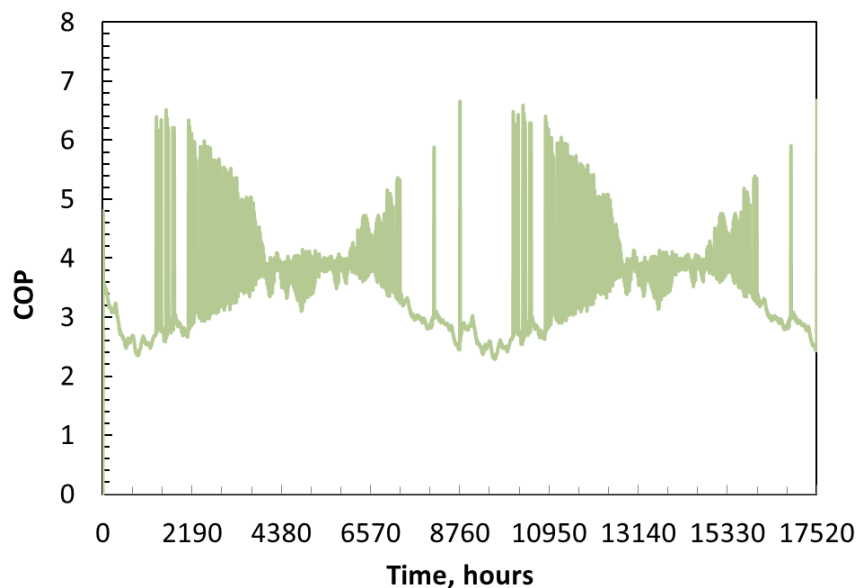


Figure 66: COP of the heat pump as a function of time.

5. OTHER GSHP SYSTEM MODELING WORK

5.1. RESEARCH ORIENTATED

5.1.1. Analytical Methods

Most of the ground loop geothermal sizing programs available today are variations of two analytical methodologies: Kelvin's line source theory (Kelvin 1882) and Carslaw and Jaeger's cylinder source solution (Carslaw and Jaeger 1947). Some programs also use a numerical or combined approach to simulate the GLHE (ground loop heat exchanger). The use of an analytical model allows for a quick computation, but does not always match the real world configuration; while a numerical model mimics the real world equipment well, but consumes more computational time.

Ingersoll (Ingersoll and Plass 1948) (Ingersoll, Zobel and Ingersoll 1954) applies Kelvin's line source theory (Kelvin 1882) to obtain a temperature at any point in an infinite medium. The medium is initially at a uniform temperature in which a line source heat rejection or extraction is applied starting at time zero. Ingersoll's model is valid for a true line source, but can be applied to small pipes after a few hours of operation. For large pipes or small time operation, a "time-to-pipe" ratio ($\frac{at}{R^2}$) must be greater than 20 to meet the applicability criterion. One of the primary assumptions is that the line source must be infinitely long. Thus, this is a one-dimensional analysis. In addition, this model does not account for thermal interference between boreholes or grouting material. The analysis used by Ingersoll is a rough estimation to the actual heat transfer process, but this approach was modified in the following decades to become a more accurate model.

Hart and Couvillion (1986) also utilized Kelvin's line source theory to estimate continuous time-dependent heat transfer between a line source and the ground. Considering the heat rejected by the line source, they introduced a method to calculate the far-field radius r_∞ . The method is only approximate since Kelvin's line source would require r_∞ to be ∞ . Hart and Couvillion developed a standard far-field radius of $r_\infty = 4\sqrt{at}$, which assumes the ground temperature beyond this distance to be undisturbed and constant. This technique can be used for multiple borehole configurations by setting r_∞ equal to the distance between the boreholes. Thermal interference is observed after r_∞ exceeds the distance between the boreholes, but superposition techniques can be used to estimate this interference. Hart and Couvillion's technique introduced a method for calculating more complex ground loop geothermal systems, but still lack the accuracy that can be achieved with the modern computer processor using numerical techniques and precise governing differential equations.

Similar to the line source theory, the cylinder source solution (Carslaw and Jaeger 1947) uses a number of simplifying assumptions. The most significant assumption is the "equivalent diameter" approximation that treats the U-tube from a vertical borehole as a single pipe. This assumption allows the single pipe and borehole to be modeled as co-axial so that the cylinder source may be applied. In the following decade, Ingersoll modified this model to size a buried heat exchanger (Ingersoll, Zobel and Ingersoll 1954). Kavanaugh (1985) furthered this technique to determine the temperature distribution or the heat transfer rate around the pipe. Assumptions made in this technique are: the heat transfer process is of the nature of pure conduction in a perfect ground formation / pipe contact, the pipe is surrounded by an infinite solid with constant properties, and groundwater movements in the earth and thermal interferences between adjacent boreholes are considered negligible. Kavanaugh suggests two methods to correct the thermal

interference within the U-tube borehole. The first method calculates the resistance between the fluid, pipe, and ground to estimate the average fluid temperature. The second method is based on Kalman's work (Kalman 1980). Kalman developed a general equation for heat transfer from an element of differential length and integrates this equation over the entire length of the coupling.

Analytical models provide a quick and fairly accurate solution to ground loop geothermal systems. Unfortunately, Kelvin's line source theory and the cylinder source model neglects one very important heat transfer parameter, changes in the axial direction. A model that neglects axial changes can be inadequate for analyzing the long-term operation of the ground loop geothermal system (Yang, Cui and Fang 2010).

5.1.2. Numerical Methods

Numerical models have a significant advantage over analytical models since they can account for many of the complexities that occur in GSHP systems. Numerical models have been developed to research the heat transfer within the GLHE to predict an optimized system. The models discussed below are more complex than the analytical models and have the disadvantage of being computationally more costly.

Mei and Emerson (1985) were two of the first investigators to develop a numerical model to size horizontal GLHEs that can also account for frozen ground formations around the pipe. The model solves three, one-dimensional partial differential equations (radially through the pipe, frozen formation region, and far field region), using an explicit finite difference scheme. These equations were coupled to a one-dimensional partial differential equation representing the flow of heat along the pipe, resulting in a quasi two-dimensional model. The model uses different time steps for the pipe wall, frozen formation region, and a significantly larger time step for the fluid and unfrozen ground formation region (Yavuzturj, Spitler and Rees 1999). Mei and Emerson reported comparisons with experimental data over a 48 day simulation period.

Eskilson (1987) developed a hybrid model that mixes both analytical and numerical solutions with the g-factor approximation. The use of g-functions allows a program to store predefined factors that can be accessed readily to estimate GLHE length given an input heat load. The g-function is specific to a borehole configuration and demonstrates its response to a heat pulse. With the g-function technique in combination with the principle of superposition, any step change in heat extraction or rejection can be determined. Eskilson's model assumes: homogeneous thermal properties, an evenly distributed heat pulse, and long time steps. Many modifications have been made to Eskilson's g-function technique that account for short time steps and the thermal resistance of the fluid, pipe, and grout.

Hellström (1989) developed a simulation model for vertical ground heat storage, which uses densely packed ground loop heat exchangers for seasonal thermal energy storage (Yang, Cui and Fang 2010). Hellstrom's model is based off a system where heat is stored directly in the ground, otherwise known as a duct ground heat storage system (DST). The model is separated into two regions: the volume that immediately surrounds a single borehole, and the volume of multiple boreholes. Hellstrom defines these regions as the 'local' and 'global' problems. A third problem Hellstrom explains is the steady-flux problem, which describes the heat pulses around a pipe for a constant rejection or extraction. Like Eskilson, the model is a hybrid that uses a numerical solution within the 'local' and 'global' problems and then superimposes them with an analytical solution from the steady-flux input. The numerical model uses a two-dimensional explicit finite difference technique for the 'global' problem and a one-dimensional radial mesh for the 'local' problem. Hellstrom's model is not ideal for determining long time-step system responses for

ground loop geothermal systems since the geometry of the borehole field is assumed to be densely packed, with a minimum surface area to volume ratio (Yavuzturk 1999).

Muraya et al. used a transient two-dimensional finite element model to investigate the thermal interference between the U-tube legs of a borehole (Muraya, O'Neal and Heffington 1996). The thermal short-circuiting is investigated by comparing the numerical model to existing analytical solutions from the single line source and the cylindrical-source. The model is validated against two different applications of the cylindrical-source solution using constant temperature and constant flux conditions. In addition, the model examines the effect of different backfill materials on the heat transfer. This allowed Muraya to define an overall thermal effectiveness and backfill effectiveness. Finally, Muraya investigated the coupling of conduction with moisture transport.

Rottmayer et al. (Rottmayer, Beckman and Mitchell 1997) developed a numerical simulation for a vertical U-tube heat exchanger using an explicit finite-difference technique. Rottmayer uses a three-dimensional transient heat transfer model that includes lateral heat transfer in the fluid every 3 meters. Conduction in the vertical direction was neglected but each section of the model was coupled via the boundary conditions to a model of flow along the U-tube (Yavuzturk 1999). This program allows the user to change borehole depth, flow rate, properties of the fluid, ground, and grout, and temperature of the ground and inlet fluid. The model was found to under-predict the heat transfer from the U-tube by approximately 5% when compared to analytical models.

Thornton et al. (1997) used Hellstrom's approach to model the ground loop geothermal system. The model was implemented in TRNSYS as a detailed component model (Klein 1996). The model was calibrated with an experimental family house unit by adjusting the far-field temperature and the ground formation thermal properties. The model was comparable with measured data.

Shonder and Beck (1999) developed a simple one-dimensional thermal model that describes the temperature field around the borehole. The U-tube pipe is modeled as one, and a thin film may be added to account for the heat capacity of the pipes and fluid. The model assumes one-dimensional transient heat conduction through the film, grout, and soil. These equations are coupled with a time-varying heat flux originating from the film. The far-field radial boundary is assumed to be a constant undisturbed temperature. With this method, ground conductivity can be relatively estimated even though the conditions at the borehole are uncertain (Shonder and Beck 1999).

Yavuzturk and Spitler (1999) furthered Eskilson's long time-step g-function to account for the thermal properties of the fluid, pipe, and grout. The short time-step model uses a transient, two-dimensional numerical, finite volume technique for a vertical GLHE. The numerical model is used to develop a g-function for time intervals as small as three minutes. The parameter estimation method utilizes the downhill simplex minimization algorithm of Nelder and Mead (1965) in conjunction with the numerical model of the borehole to estimate the ground thermal conductivity.

Zeng (2003) developed a quasi-three-dimensional model that accounts for the fluid temperature variation along the borehole depth and its axial convection to determine the thermal resistance inside the borehole analytically. Thermal interference between a single U-tube pipe and a double U-tube pipe are solved on an analytical basis. These analytical expressions are derived based on the following assumptions: 1) the heat capacity of the materials inside the borehole is neglected, 2) the heat conduction in the axial directions is negligible and only the

conductive heat flow between the borehole wall and the pipes in the transverse cross-section is counted, 3) the borehole wall temperature is constant along its depth, 4) the ground outside the borehole and grout are homogeneous, and all the thermal properties involved are independent of temperature. Zeng limited his research to the thermal resistance inside the borehole.

As a summary, a tabulation of the research orientated modeling in geothermal systems that has been covered in this report is given Table 5.

Table 5: Development of models and techniques for sizing ground loop geothermal systems (Haberl and Sung 2008).

Solution Approach	Year	Model
Analytical Solution	1882	Lord Kelvin: Kelvin's Line Source Model
	1948	Ingersoll and Plass: Modified Line Source Model
	1986	Hart and Couvillion: Enhanced Line Source Model
	1947	Carslaw and Jaeger: Cylinder Source Model
	1954	Ingersoll et al.: Modified Cylinder Source Model
	1985	Kavanaugh: Modified Cylinder Source Model
Numerical Solution	1985	Mei and Emerson
	1987	Eskilson
	1989	Hellstrom
	1996	Muraya et al.
	1997	Rottmayer et al.
		Thornton et al.
	1999	Shonder and Beck
		Yavuzturk and Spitler
2003	Zeng et al.	

5.2. AVAILABLE COMMERCIAL CODES

Commercial programs available today offer a variety of methods to analyze a GSHP system. Most of the programs use the g-function method, which limits the borehole geometry and can generate a significant error. This section discusses the heat transfer techniques used, advantages and disadvantages, and outputs from the following commercial programs: RETScreen, TRNSYS, GLHEPRO, GLD2000, Earth Energy Designer, and GS2000. Additionally, results from some of the programs will be compared to GEO2D.

5.2.1. RETScreen

RETScreen is a program developed by CanmetENERGY and a number of other governmental and nongovernmental organizations. The program is used to evaluate the energy production, savings, costs, emission reductions, financial viability, and risk for various types of renewable energy systems. The RETScreen model can be used to evaluate horizontal loops, vertical closed-loops, and vertical open-loops, from large-scale commercial applications to small residential systems. The GSHP systems in RETScreen provide six worksheets in Microsoft Excel to solve and analyze the system through an energy model, heating and cooling load calculation, cost analysis, greenhouse gas emission reduction analysis, financial summary, and sensitivity and risk analysis.

The methodology used in the RETScreen model present many limitations. In some instances, the model cannot capture complex building usage profiles. Additionally, the long-term thermal imbalances are not included in the GLHE calculations. The horizontal GLHE is restricted to a stacked pipe system with a 31.8 mm pipe buried at 1.8 m and 1.2 m below the surface. Likewise, the vertical GLHE configuration is limited to one 31.8 mm U-tube per borehole. Finally, the building's heating and cooling energy consumption and peak loads are evaluated using a simplified version of ASHRAE's modified bin method (ASHRAE 1985) with an interior set point temperature at a constant 23 °C.

A detailed analysis for a GLHE usually requires a dynamic time and temperature model that uses short time-steps. The GSHE model in RETScreen uses a simplified approach, which only uses outside temperature as the critical variable. This approach, called the bin method, distributes the hourly temperature occurrences into the associated temperature bins. The bin method uses temperature and weather data to calculate the building load for each temperature bin. The temperature data is also used to calculate the minimum and maximum ground temperature using (IGSHPA 1988)

$$T_{ground,min} = T_{ground} - A_s \exp\left(-X_s \sqrt{\frac{\pi}{365\alpha}}\right) \quad (83)$$

and

$$T_{ground,max} = T_{ground} + A_s \exp\left(-X_s \sqrt{\frac{\pi}{365\alpha}}\right), \quad (84)$$

where $T_{ground,min}$ is the minimum ground temperature in (°C) or (°F), $T_{ground,max}$ is the maximum ground temperature in °C or °F, T_{ground} is the mean annual surface soil temperature in °C or °F, A_s is the annual surface temperature amplitude in °C or °F, X_s is the soil depth in meters or feet, and α is the soil thermal diffusivity in $\frac{m^2}{s}$ or $\frac{ft^2}{s}$.

There are two options to calculate the load of the building in RETScreen's model. Either the user can use the descriptive data method or the energy use method. The descriptive data method requires the user to enter the physical characteristics of the building. While the energy use method requires the user to enter the design loads and typical energy use of the building. The descriptive data method accounts for: transmission losses (conductive and convective), solar gains (sensible), fresh air loads (latent and sensible), internal gains (latent and sensible), and occupant loads (latent and sensible). The building loads are calculated for the hourly bin temperatures that occur throughout the year.

The temperature of the water entering the heat pump can be calculated with

$$T_w = T_{min} + \left(\frac{T_{ewt,max} - T_{ewt,min}}{T_{d,cool} - T_{d,heat}}\right) (T_{bin,i} - T_{d,heat}). \quad (85)$$

The maximum and minimum design entering water temperatures are estimates based off of a literature review by ASHRAE, Kavanaugh and IGSHPA and can be expressed as (ASHRAE 1995), (Kavanaugh and Rafferty 1997), and (IGSHPA 1988)

$$T_{ewt,min} = T_{g,min} - 15^{\circ}\text{F} \quad (86)$$

and

$$T_{ewt,max} = \min(T_{g,max} + 20^{\circ}\text{F}, 110^{\circ}\text{F}). \quad (87)$$

The heating design temperature, $T_{d,heat}$, and the cooling design temperature, $T_{d,cool}$, are specified by the user in the heating and cooling load worksheet. A graphical representation of equation (85) is given in Figure 67 where T_{min} represents the point where the curve crosses the y-axis.

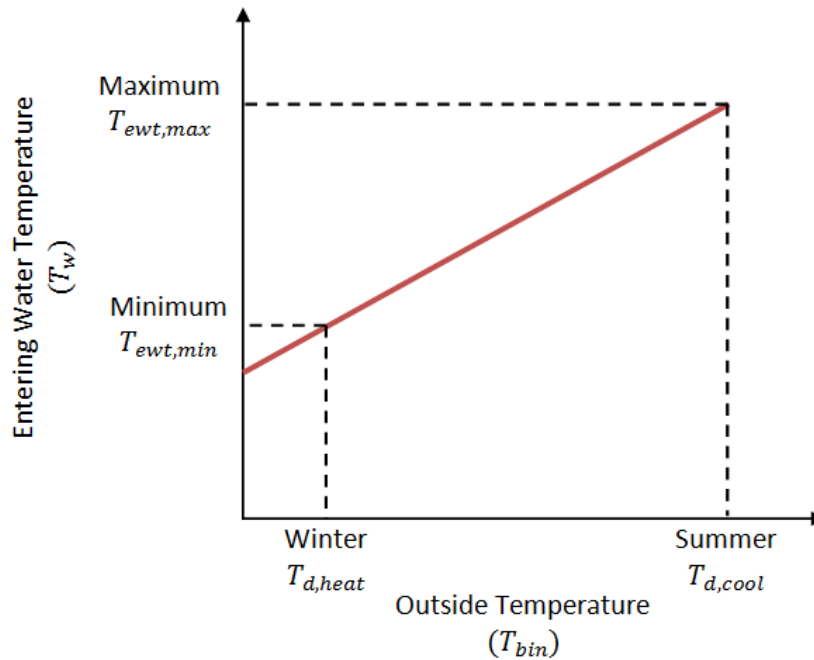


Figure 67: RETScreen’s method for determining entering water temperature as a function of outside temperature.

Once a function for entering water temperature is determined, the coefficient of performance is calculated by

$$COP_{actual} = COP_{baseline}(k_0 + k_1T_{ewt} + k_2T_{ewt}^2), \quad (88)$$

where COP_{actual} is the actual COP of the heat pump, $COP_{baseline}$ is the nominal COP of the heat pump, T_{ewt} is the entering water temperature for the heat pump in °C or °F, and the k 's are the correlation coefficients. For cooling, k_0 is 1.53105836, k_1 is -2.296095×10^{-2} , and k_2 is 6.87440×10^{-5} . For heating, k_0 is 1.0000, k_1 is $1. \times 10^{-2}$, and k_2 is -1.59310×10^{-4} .

Finally, sizing of the GLHE is completed using a method developed by IGSHPA (1988). The required length based on heating requirements is determined with

$$L_h = q_{d,heat} \left[\frac{\frac{(COP_h - 1)(R_p + R_s F_h)}{COP_h}}{T_{g,min} - T_{ewt,min}} \right] \quad (89)$$

where L_h is the length required in meters or feet, $q_{d,heat}$ is the design heating load in kW or Btu , COP_h is the design heating coefficient of performance, R_p is the pipe thermal resistance in $\frac{^\circ C}{W}$ or $\frac{^\circ F}{Btu}$, R_s is the soil field thermal resistance in $\frac{^\circ C}{W}$ or $\frac{^\circ F}{Btu}$, F_h is the ground heat exchanger part load factor for heating, $T_{g,min}$ is the minimum undisturbed ground temperature in $^\circ C$ or $^\circ F$, and $T_{ewt,min}$ is the minimum design entering water temperature in $^\circ C$ or $^\circ F$. Similarly, the required length based on cooling loads can be calculated by

$$L_c = q_{d,cool} \left[\frac{\frac{(COP_c+1)}{COP_c}(R_p+R_sF_c)}{T_{ewt,max}-T_{g,max}} \right] \quad (90)$$

where L_c is the length required in meters or feet, $q_{d,cool}$ is the design cooling load in kW or Btu , COP_c is the design cooling coefficient of performance, R_p is the pipe thermal resistance in $\frac{^\circ C}{W}$ or $\frac{^\circ F}{Btu}$, R_s is the soil field thermal resistance in $\frac{^\circ C}{W}$ or $\frac{^\circ F}{Btu}$, F_h is the ground heat exchanger part load factor for cooling, $T_{ewt,max}$ is the maximum design entering water temperature at the heat pump in $^\circ C$ or $^\circ F$, and $T_{g,max}$ is the maximum undisturbed ground temperature in $^\circ C$ or $^\circ F$. The soil thermal resistance is determined from geometrical and physical considerations given by IGSHPA (1988).

The methodology used by RETScreen provides a quick estimate for sizing a GLHE. When compared to other commercial programs, RETScreen oversizes their GLHEs by 23%, resulting in a higher initial cost (CANMET 2005). For purposes of a ballpark solution on a variety of renewable energy systems with an economic analysis, RETScreen is acceptable; however, for a detailed geothermal analysis, RETScreen lacks the accuracy and output information.

5.2.2. TRNSYS

TRNSYS is an extremely flexible, graphical based, commercial, simulation program package developed at the University of Wisconsin that simulates the behavior of transient systems, including renewable energy systems. It is used by engineers and researchers around the world to validate new energy concepts, from simple domestic hot water systems to the design and simulation of buildings and their components, including strategies, occupant behavior, and alternative energy systems (wind, solar, photovoltaic, hydrogen systems, etc.) (TRNSYS 2009). Using the short time-step g-function technique and a 3-D conduction model, several TRNSYS component models for numerous GLHE were developed. These models include a vertical U-tube borehole, a horizontal single buried pipe, a horizontal twin buried pipe, and a horizontal multi-level pipe. TRNSYS provides a graphical interface, a simulation engine, and a library of components that are standard for HVAC equipment. The simulation package used in TRNSYS is Simulation Studio and can be seen in Figure 68.

The vertical U-tube GLHE is modeled in TRNSYS is called ‘type 557’ and is solved using Hellstrom’s Duct Storage Model (DST) (Hellström 1989). Yavuzturk and Spitler (Yavuzturk and Spitler 1999) also incorporated their short time-step g-function model into TRNSYS. The model assumes that the boreholes are placed uniformly throughout the ground. Also, the model accounts for convective heat transfer within the pipes and conductive heat transfer throughout the ground. The model is separated into two regions: the ground that immediately surrounds a single borehole (local region) and the ground that surrounds multiple boreholes (global region).

The global and local regions are solved using an explicit finite-difference technique, while the steady-flux solution is obtained analytically.

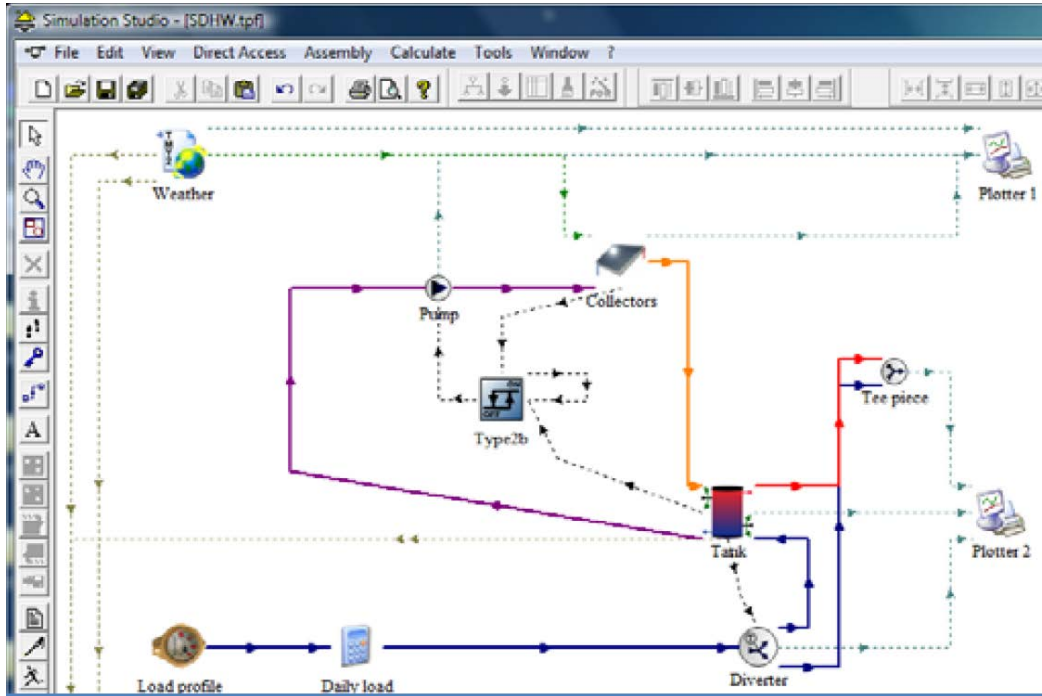


Figure 68: Example project in TRNSYS Simulation Studio (*TRNSYS 2009*).

The horizontal single buried pipe (type 952), horizontal twin buried pipe (type 951), and horizontal multi-level pipe (type 997) are all solved using a three-dimensional finite difference method. The model from the Oak Ridge National Lab for a GLHE is used as the basis for the horizontal models in TRNSYS. Oak Ridge National Lab models a buried pipe within the ground, where the heat transfer is solved radially and circumferentially. Temperatures along the outer radius are assumed undisturbed by the heat transfer of the pipe and the soil properties are assumed to be homogeneous. Also, there are no moisture migrations or soil freezing within the model. The model simulates a pipe located in the center of a large volume of soil with homogeneous thermal properties. The heat transfer is symmetric along the ‘z’ by ‘i’ plain, so only half the cylinder is needed. The model accounts for heat transfer in the radial and circumference direction, but not in the axial direction. Figure 69 illustrates a sample grid layout, where the section, radius, and rotation from the top are indicated by j , i , and m , respectively. The fluid temperature is saved in a matrix $U(j, k)$. Similarly, The ground temperatures are saved in a matrix $S(i, j, m, k)$, where k marks the updated node. TRNSYS users may select minute or hourly time-steps.

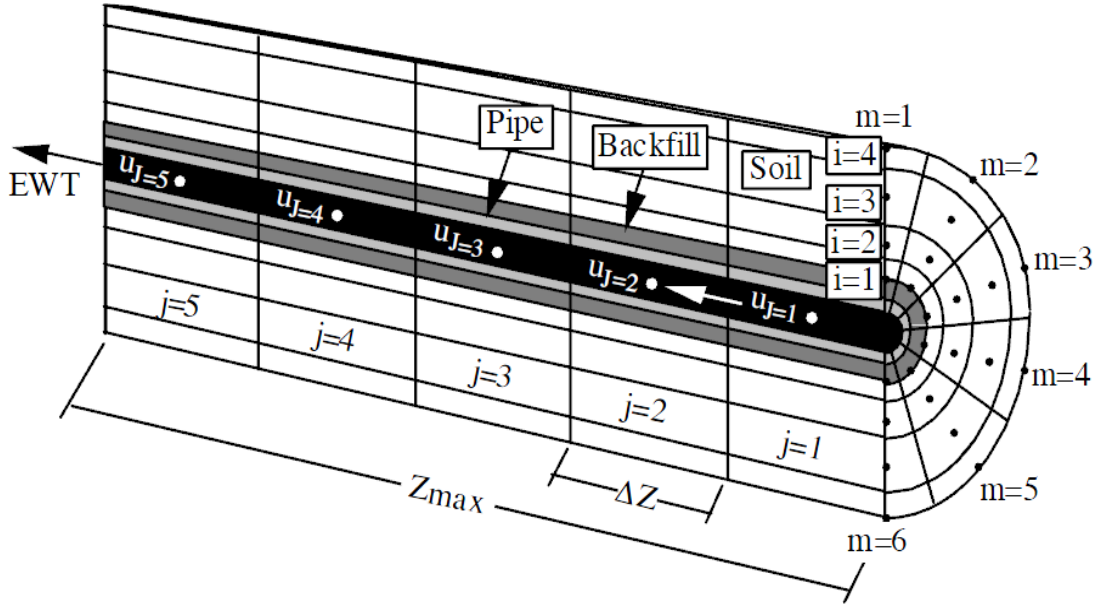


Figure 69: The finite difference model for a single buried pipe in TRNSYS (Giardina 1995).

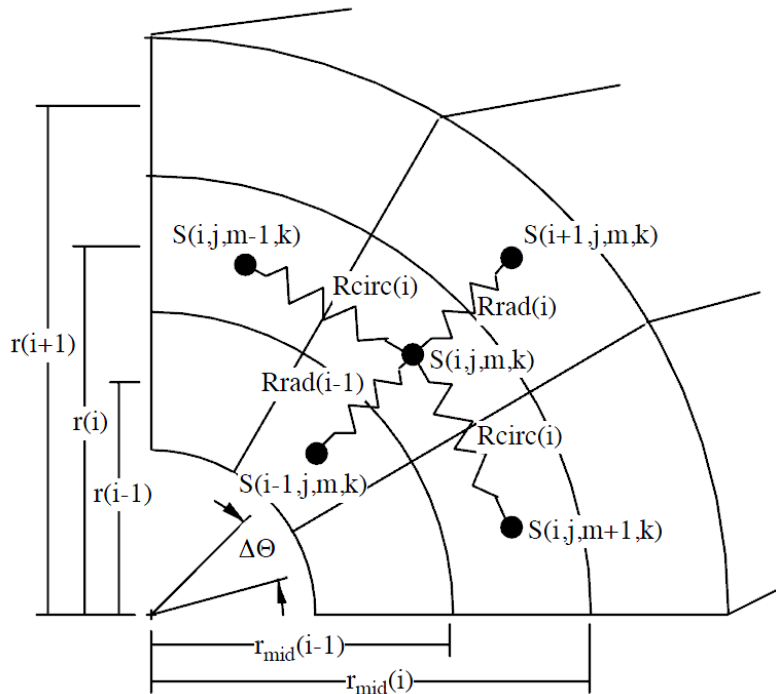


Figure 70: TRNSYS's thermal resistance approach for the heat transfer analysis (Giardina 1995).

For ease, TRNSYS uses a simplistic thermal resistance approach for solving the heat transfer problems. The temperature of the soil $S(i, j, m, k)$, is determined by

$$(\rho V(i) c_p)_{soil} \frac{(S(i, j, m, k + 1) - S(i, j, m, k))}{dt} = \frac{(S(i + 1, j, m, k) - S(i, j, m, k))}{R_{rad}(i)} + \frac{(S(i - 1, j, m, k) - S(i, j, m, k))}{R_{rad}(i - 1)} + \frac{(S(i, j, m + 1, k) - S(i, j, m, k))}{R_{circ}(i)} + \frac{(S(i, j, m - 1, k) - S(i, j, m, k))}{R_{circ}(i)} \quad (91)$$

where

$$R_{circ}(i) = \frac{r(i) * \Delta \theta}{k_{soil} * (r_{mid}(j) - r_{mid}(j - 1)) * \Delta Z} \quad (92)$$

and

$$R_{rad}(i) = \frac{\ln\left(\frac{r(i + 1)}{r(i)}\right)}{\Delta \theta * k_{soil} * \Delta Z} \quad (93)$$

TRNSYS also accounts for the convective heat transfer from the fluid, followed by the conductive heat transfer through the pipe and backfill. The energy transfer in the fluid can be solved by

$$U(j, k + 1) = U(j, k) + \frac{\dot{m} dt}{(\rho V)_{fluid}} (U(j - 1, k) - U(j, k)) - \frac{dt}{(\rho c_p V)_{fluid}} \dot{Q}_{out} \quad (94)$$

where U is the fluid node temperature and the energy transfer from the fluid to the ground, \dot{Q}_{out} , is determined by

$$\dot{Q}_{out} = \frac{(U(j, k) - avg S_j)}{R_{total}} \quad (95)$$

where

$$R_{total} = R_{fluid} + R_{pipe} + R_{backfill} \quad (96)$$

and the average temperature of the inner soil ring is calculated by

$$avg S_j = \frac{\sum_{m=1}^{m_{max}} S(i, j, m, k)}{m_{max}} \quad (97)$$

and the resistances are determined with

$$R_{fluid} = \frac{1}{h_{conv} * A}, \quad (98)$$

$$R_{pipe} = \frac{\ln\left(\frac{r_{pipe, out}}{r_{pipe, in}}\right)}{\pi * k_{pipe} * \Delta Z}, \quad (99)$$

and

$$R_{backfill} = \frac{\ln\left(\frac{r_{backfill, out}}{r_{backfill, in}}\right)}{\pi * k_{backfill} * \Delta Z}. \quad (100)$$

TRNSYS provides an accurate simulation of the GLHE, as well as an advanced and very flexible graphical user interface. However, the user must have detailed information about the system, such as, building design, heat pump coefficients, and values for the thermal properties throughout the GLHE. Most of these inputs are not assumed or suggested in TRNSYS, and therefore makes the program complicated for the common user. Due to its high cost, stiff learning curve, and significant computation time, TRNSYS is not used frequently (Liu and Hellstrom 2006).

5.2.3. GLHEPRO

GLHEPRO was developed as an aid in the design of vertical GLHE, typically for commercial sized systems, though GLHEPRO may be used for sizing residential systems. GLHEPRO is composed of numerous borehole configurations and performs three tasks. First, it allows the user to perform a simulation period, up to 100 years, and determines the monthly peak

and average entering fluid temperature, the power consumed by the heat pump, and the heat extraction rate per unit length. Second, GLHEPRO determines the required depth of the borehole(s), to meet the user specified minimum and maximum entering fluid temperature into the heat pump. Third, the program sizes hybrid ground source heat pump systems by determining the required depth of the borehole(s) after the user designs a supplemental cooling tower and/or boiler system. The g-function method, developed by Eskilson (Eskilson 1987), is implemented in the GLHEPRO program.

There are 307 pre-computed g-function configurations included in GLHEPRO, as of 2007. Additionally, functions have been developed that approximate larger rectangular borehole fields, with a reasonable degree of accuracy (GLHEPRO 4.0 for Windows 2007). GLHEPRO is limited to modeling vertical closed-loop heat exchangers. Also, GLHEPRO requires an outside heating and cooling load program to determine monthly loads and monthly peaks.

5.2.4. Ground Loop Design

Ground Loop Design (GLD) is a prestigious geothermal sizing program developed by Gaia Geothermal. The program provides heating and cooling loads for a building designed by the user and determines lengths for vertical, horizontal and surface water GLHE. Additionally, the coefficient of performance (COP) can be determined from a heat pump model to let the user know how efficiently the system is operating. One major advantage of GLD is the internationalization. Not only does that program provide an option for metric and English units, the program is also capable of communicating in multiple languages.

Ground Loop Design uses two methods to solve the heat transfer problem for a vertical borehole GLHE. The first method is based on the cylindrical source method, while the second is based on Eskilson's g-function technique. The first method uses Ingersoll's (Ingersoll and Plass 1948) modification to Carslaw and Jaeger's (1947) cylinder buried in the earth model to size GLHE. Additionally, the model uses Kavanaugh and Deerman's (1991) method to account for the U-tube arrangement and hourly time steps. It also accounts for the borehole resistance, such as the pipe placement, grout conductivity, and borehole size, as suggested by Remund and Paul (1996). The second method uses Eskilson's (1987) g-function technique.

The two vertical GLHE models do not always agree, but both are available for the user to compare the results. Additionally, the program calculates the energy extracted or rejected into the ground based on the load information and heat pump model chosen. The two methods calculate the long-term condition of the borehole. The system is then optimized to allow for acceptable heat extraction/rejection from the earth.

The horizontal ground loop heat transfer analysis used in Ground Loop Design uses a combination of Carslaw and Jaeger's cylindrical buried in the earth and the multiple pipe methodology developed by Parker et al. (1985). The model includes modifications suggested by Kavanaugh and Deerman (1991) that accounts for the physical arrangement and an hourly heat variation. The slinky loop option in GLD provides a theoretical approximation to the pipe length. The loop models a 36" diameter slinky coil that assumes it to be a single U-tube buried pipe in a horizontal configuration. The heat transfer analysis performed is identical to the cylindrical source method used in the vertical borehole model. The calculated length is then divided by 250 feet and multiplied by a factor determined from both the run fraction and the slinky pitch (distance between adjoining loops).

The surface water heat exchanger used in GLD is based off experiments performed by Kavanaugh and Rafferty (1997) for different sized pipes in coiled and slinky configurations. A

polynomial fit of this experimental data is used to determine the amount of pipe necessary for a given heating and cooling load.

Ground Loop Design offers a fairly accurate solution for a GLHE, while maintaining a certain degree of user friendliness. The heat transfer techniques used to solve the vertical, horizontal and surface water heat exchangers have been used for the past few decades and give a fairly good solution for a short computation time. However, a more accurate numerical heat transfer analysis can be solved with little additional computational time in exchange for more detailed results.

5.2.5. Earth Energy Designer

Earth Energy Designer (EED) is a GLHE program that is easy to use and provides a quick means of providing the average fluid temperature in the ground loop. EED was designed for commercial buildings, but residential houses can be modeled with this program as well. The methods used to solve the heat transfer problem for a GLHE are g-function techniques developed by Eskilson (1987) and Hellstrom (1989). Only vertical GLHEs can be modeled in EED. EED contains g-functions for 798 different borehole configurations, which vary from vertical lines, L-shapes, U-shapes and rectangles. The pipe selections available are coaxial (one tube inside another), single U-tube, double U-tube and triple U-tube per borehole.

EED uses monthly, average heating and cooling loads with an additional heating and cooling pulse to solve the average, monthly fluid temperature. Calculating the borehole thermal resistance using the borehole geometry, grout material properties, and pipe material properties solves the fluid temperature. For a simulation period of 20 years (EED does a maximum of 25 years), the output from EED includes: design data entered, required length of boreholes, average monthly specific heat extraction rate, end of the month mean fluid temperature for years 1, 2, 5, 10 and 20, and minimum and maximum mean fluid temperature with month of occurrence for the final year of simulation.

When making comparisons between GEO2D to the demo version of EED, certain modeling constraints have to be made. First, EED's demo version has limited ground properties. The demo version of EED uses a thermal conductivity, volumetric heat capacity, ground surface temperature, and geothermal heat flux set to $3.5 \frac{W}{m \cdot K}$, $2.16 \frac{MJ}{m^3 \cdot K}$, $8.0 \text{ }^\circ\text{C}$ and $0.06 \frac{W}{m^2}$, respectively. To replicate EED's properties, the properties entered into GEO2D are a soil thermal conductivity of $3.5 \frac{W}{m \cdot K}$, the soil heat capacity of $0.8247 \frac{kJ}{kg \cdot K}$ and the soil density of $2619 \frac{kg}{m^3}$. Secondly, to model the same GLHE, the borehole diameter in EED was simulated as 10 meters and was filled with a grout that has a thermal conductivity equal to that of the ground. The U-tube pipe was then modeled with a shank spacing that places the inlet and outlet pipe at the edge of either side of the borehole, with the intention of virtually eliminating the thermal interference between the U-tube. The fluid properties used in both programs are a dynamic viscosity of $0.00131 \frac{N \cdot s}{m^2}$, a heat capacity of $4.194 \frac{kJ}{kg \cdot K}$ and a density of $999.7 \frac{kg}{m^3}$.

Comparison of results from the two programs was completed using two methods. The first method assumed a constant extraction of 2070 watts every hour, while the second method used heating and cooling data from a home located in Dayton, OH. Since EED only produces average monthly fluid temperatures, the program does not accurately account for the peak heating and cooling loads, even with the hourly heating and cooling input for each month. A comparison of EED's average monthly fluid temperature and GEO2D's daily entering water temperature can be

seen in Figure 71. Results from the two programs have the same trend and are comparable in magnitude with temperature differences less than 0.5 °C as shown in Figure 72. The temperature difference between the two programs results may not seem like much, but it has to be remembered that GLHEs only operate with temperature differences that run from 0 (°C) to about 20 (°C).

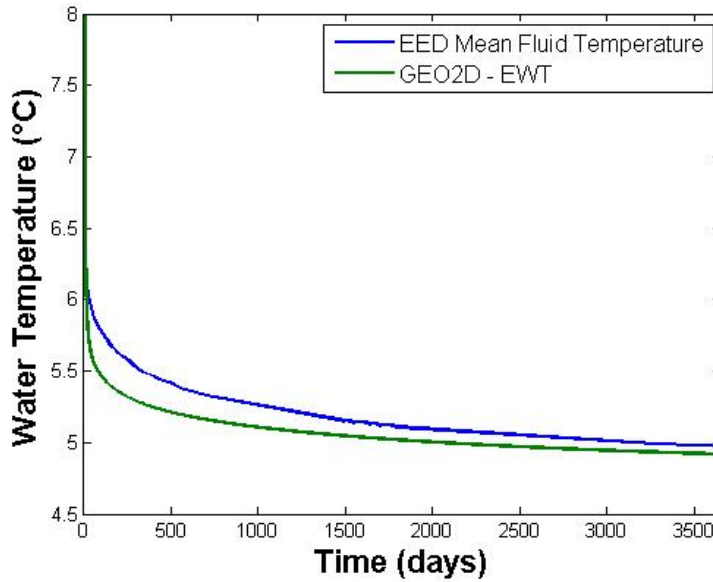


Figure 71: The average fluid temperature from GEO2D and Earth Energy Designer.

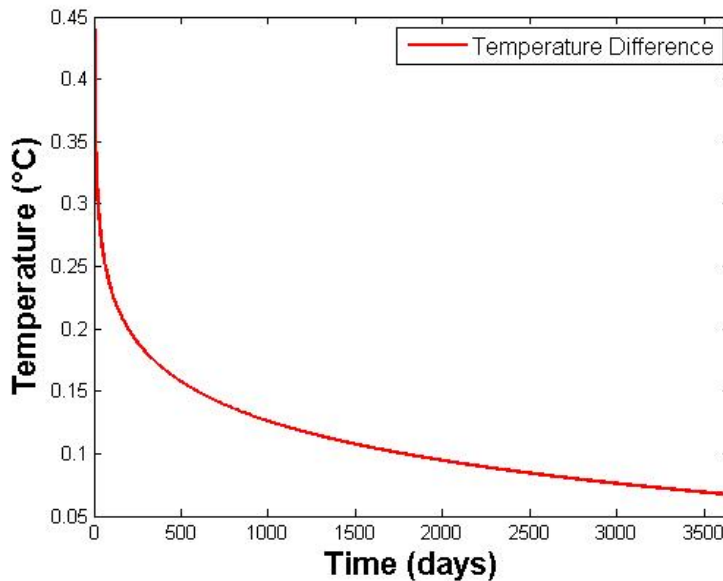


Figure 72: The average fluid temperature difference between GEO2D and Earth Energy Designer.

In order to simulate the same GLHE for an actual case study in Dayton, OH, GEO2D was run for a home with weather data from Dayton, OH. Once completed, the hourly home heating and cooling load was added for each month, keeping track of the hourly peak load. The base

loads and peak loads were entered into EED for comparison. Based on the monthly peak loads, EED yields maximum and minimum average monthly fluid temperatures as seen in Figure 73 for a 5 year simulation and Figure 74 for a 25 year simulation. Also shown in these figures are the daily entering fluid temperatures from GEO2D. The entering water temperature from GEO2D follows the same trend as EED, but shows a more rapid variation because of its much finer time steps. In general, GEO2D predicts fluid temperatures that lie between the minimum and maximum values predicted by EED except for the coldest temperatures. It should be noticed that the temperature difference predicted by GEO2D and EED are significant in the case. The temperature differences can be 2 to 4 (°C).

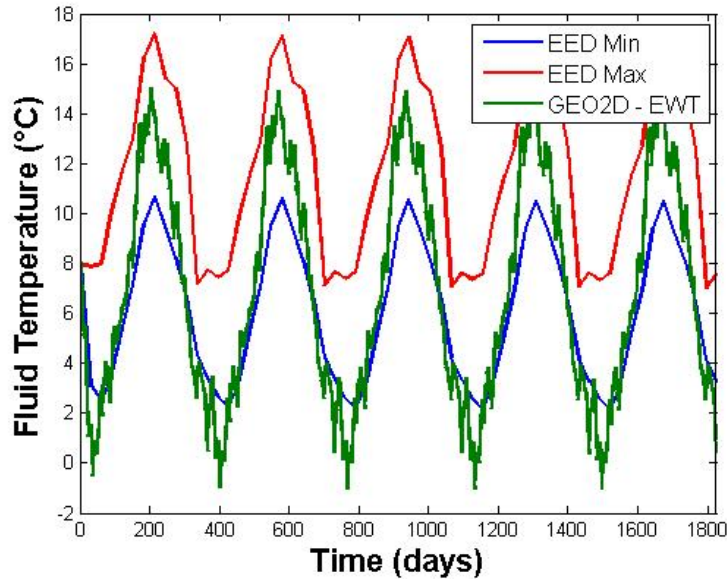


Figure 73: The minimum and maximum average fluid temperature for EED and the daily entering water temperature for GEO2D, for a 5 year simulation.

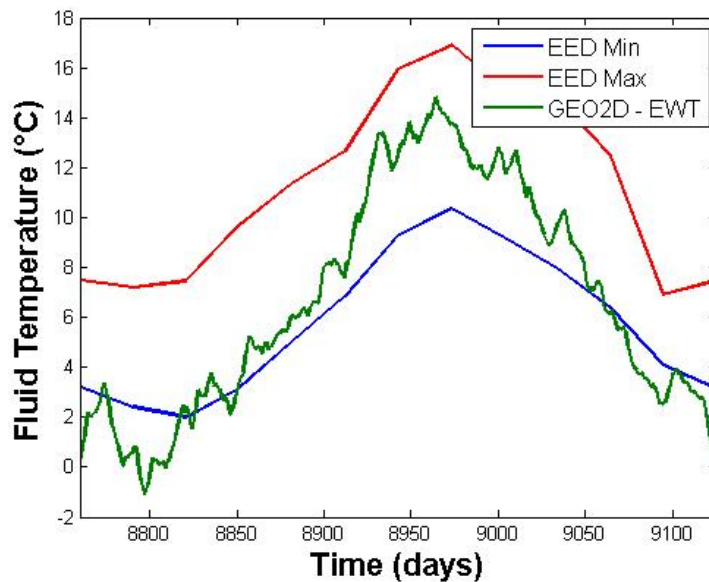


Figure 74: The minimum and maximum average fluid temperature for EED and the daily entering water temperature for GEO2D, for 25th year.

Overall the GLHE program EED provides a quick calculation for the average fluid temperature in the ground loop, but lacks accuracy due to the large time step used in the heat transfer analysis. To account for the peak loads for a GLHE system, a model needs more than just a single hourly peak heating load and single hourly peak cooling load during each month. The user friendliness of EED allows for a quick learning curve, but lacks accuracy, generality and useful outputs.

5.2.6. GS2000

GS2000 was first developed in 1995 by Caneta Incorporated for CETC-Ottawa as a GSHP sizing program. A simple GUI allows the user to select soil properties, fluid properties, pipe properties, and heat pump design information to easily design a GSHP system. The program can model 34 different loop configurations consisting of horizontal and vertical ground loops. Ground temperature data from 129 locations in the United States and Canada are available for selection. Once a design of the GLHE is complete and heating and cooling loads are entered, the program runs a single year or multi-year analysis (up to 25 years). GS2000 recommends a length or depth of the GLHE. Also, the fluid entering water temperature is provided for the user on a monthly basis.

The heat transfer analysis used in GS2000 is the cylinder and line source method developed by Carslaw and Jaeger (1947). The line source analysis is performed on a single pipe and the results are superimposed for a multi-pipe GLHE (Purdy and Morrison 2003). During heating season, the freezing soil is modeled as an ice ring, with an estimated diameter and assumes the outside temperature of the ring remains a constant 0 °C. This does not accurately model the latent energy in the soil, but provides a reasonable solution to the fluid temperature.

To compare results from GS2000 and GEO2D two cases were considered. First, a constant heat extraction was performed; followed by a varying heating and cooling load. The fluid selected for both programs was water with a velocity of 3.166 m/s and a dynamic viscosity, thermal conductivity, heat capacity and density of $0.00131 \frac{N*s}{m^2}$, $0.58 \frac{W}{m*K}$, $4.194 \frac{kJ}{kg*K}$ and $999.7 \frac{kg}{m^3}$, respectively. A thermal conductivity of $0.391 \frac{W}{m*K}$, heat capacity of $0.32 \frac{kJ}{kg*K}$ and a density of $58.74 \frac{kg}{m^3}$ was selected for a pipe of 26.67 mm diameter and thickness of 2.87 mm. The soil thermal properties consisted of $1.3 \frac{W}{m*K}$ for the thermal conductivity, $1.814 \frac{kJ}{kg*K}$ for the heat capacity and $1280 \frac{kg}{m^3}$ for the density. Finally, a constant building heat load of 1500 W-h was used for this analysis. Results from the two programs can be seen in Figure 75. Since GS2000 first outputs a recommended pipe length, GEO2D was executed after the recommended length was found from GS2000, so that the same ground loop length was used in each simulation. From Figure 75 it can be seen that the difference between the two programs is about 1.5 °C. This could be a result of the long, monthly time steps that GS2000 uses or the inaccuracy of the heat transfer method used by GS2000. Regardless, a GSHP system following the results from GS2000 would be undersized.

Next a varying heating and cooling load comparison is performed. This comparison used actual heating and cooling loads for a home located in Dayton, Ohio. The heating and cooling loads were taken from GEO2D and the loads were summed to obtain monthly values to enter into GS2000. The entering water temperature results are shown in Figure 76. Entering water temperature results from GS2000 and GEO2D follow the same pattern, but GS2000 calculates a

higher entering water temperature during peak heating and a lower entering water temperature during peak cooling. Again, this could be from the long monthly time steps or the inaccuracy of the heat transfer analysis. A system modeled by GS2000 would be considerably oversized, causing a higher initial cost; and thus a longer payback period.

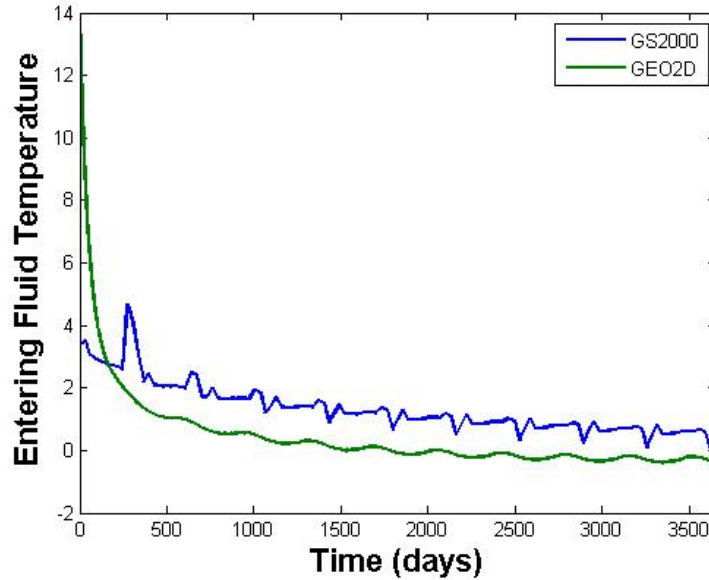


Figure 75: GS2000 and GEO2D entering water temperature comparison for 10 years of simulation using a constant heating load.

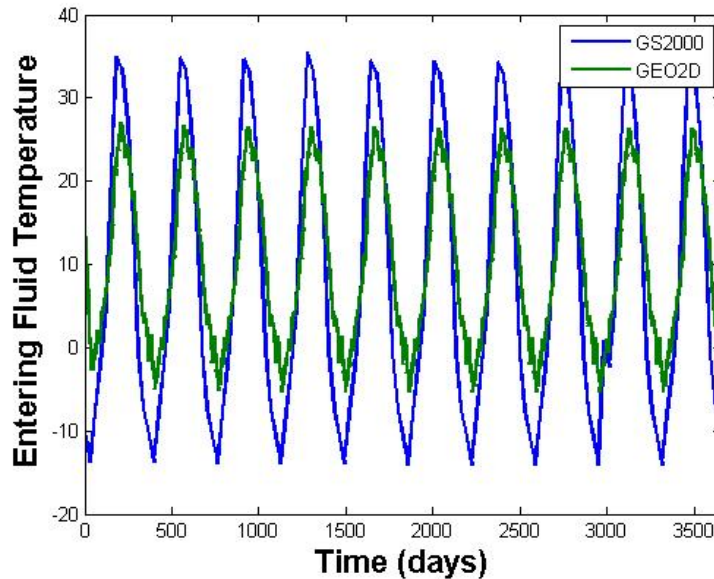


Figure 76: GS2000 and GEO2D entering water temperature comparison for 10 years of simulation using heating and cooling loads for a home in Dayton, Ohio.

For ease of comparison, the six commercial programs discussed above and GEO2D are tabulated with a list of traits in Table 6. First, the user-friendliness of each of the computer codes is estimated. For instance, TRNSYS requires a high learning curve, but produces an accurate

GLHE solution. For this reason, TRNSYS appeals to researchers rather than the typical GSHP system installers. Secondly, the program's heat load calculation methods are compared. The heating and cooling load calculations play a significant role in determining the optimized size for a GSHP system. An accurate hourly heating and cooling prediction, such as those used in TRNSYS, GLD2000 and GEO2D, account for peak loads accurately. Next, the types of ground loops considered by the program are compared. A program limited to sizing vertical GLHE eliminates the option for installers to simulate a horizontal GLHE, which overall, is less expensive to install. The heat transfer analysis technique used by each program presents the most important aspect of each program. A more accurate technique, such as those used by GEO2D and TRNSYS, provides a more accurate simulation, but require more computation time. On the other hand, programs such as GS2000, RETScreen, GLHEPRO and EED give quick solution, but lack accuracy. Whether the programs offered a cost analysis was the final point of interest to analyze. The programs that provide a cost analysis are shown in Table 6. These programs estimate the cost for the modeled GLHE and also give an estimated payback period compared to conventional HVAC systems. It should be noted that the major factor in motivating costumers to install a GLHE is the payback period.

Table 6: A brief description of 6 commercial GLHE programs available today in comparison to GEO2D.

	User Friendly	Heat Load Calculation Method	Loops Capable of Modeling	Heat Transfer Technique	Cost Analysis
GS 2000	Yes	Monthly averaged loads	Horizontal and Vertical	Cylinder & line source method and g-function	No
RETScreen	No	Built in	Horizontal and Vertical	Bin Method	Yes
TRNSYS	No	TRNBuild	Horizontal and Vertical	Multiple methods	Yes
EED	Yes	Monthly averaged loads (built in)	Vertical	g-function	No
GLHEPRO	Yes	User Supplied	Vertical	g-function	No
Ground Loop Design	No	LEADPlus	Horizontal and Vertical	Cylinder & line source method and g-function	Yes
GEO2D	Yes	EnergyPlus	Horizontal (Vertical)	2-D, Unsteady Finite Volume	Yes
GEO3D	No	EnergyPlus	Vertical	3-D, Unsteady Finite Volume	No

6. PUBLICATIONS

6.1. PRESENTATIONS AND PUBLICATIONS

The following presentations have been made.

1. Menart, J., Prasad, S., Gross, P., and Hughes, K., (2010), “New Commercial Ground Source Geothermal Design Computer Code,” *6th Annual ASME Dayton Engineering Sciences Symposium*, Dayton, OH, October 25.
2. Prasad, S., Menart, J., Hughes, K., and Gross, P., (2010), “Imbalanced Heat Load in Ground Source Heat Pump (GSHP) Systems – Is this a Problem?,” *6th Annual ASME Dayton Engineering Sciences Symposium*, Dayton, OH, October 25.
3. Hughes, K., Menart, J., Prasad, S., and Gross, P., (2010), “Ground Source Heat Pump Sizing Codes,” *6th Annual ASME Dayton Engineering Sciences Symposium*, Dayton, OH, October 25.
4. Gross, P., Menart, J., Prasad, S., and Hughes, K., (2010), “Using EnergyPlus in a Ground Source Heat Exchanger Code,” *6th Annual ASME Dayton Engineering Sciences Symposium*, Dayton, OH, October 25.
5. Hughes, K., Gross, P., Menart, J., and Prasad, S., (2011), “Heat Load Calculations, Cost Analysis, GUI, and G-Factor Comparisons for a General Geothermal Design and Analysis Program,” *5th Annual University Clean Energy Alliance Organization*, Columbus, OH, April 26-27, 2011.
6. Menart, J., Prasad, S., Hughes, K., and Gross, P. (2011), “Numerical Model of a Geothermal System’s Ground Loop Heat Exchanger,” *5th Annual University Clean Energy Alliance Organization*, Columbus, OH, April 26-27, 2011.
7. Gray, E., (2011), “Computational Analysis for Differing Variables of a Closed-Loop geothermal Heating and Cooling System”, Honors Thesis, Wright State University, Dayton, OH, May, 27.
8. Hughes, K. and Menart, (2011), “Comparison of Commercial Ground Source Heat Pump Sizing Codes,” *7th Annual ASME Dayton Engineering Sciences Symposium*, Dayton, OH, October 24.
9. Gross, P., (2011), “Commercial Program Development for a Ground Loop Geothermal System: Energy Loads, GUI, Turbulent Flow, Heat Pump Model, and Grid Study,” Master Thesis, Wright State University, Dayton, OH, December 7.
10. Hughes, K. (2011), “Commercial Program Development for Ground Loop Geothermal System: g-function, Commercial Codes, and 3D Grid, Boundary, and Property Extension,” Master Thesis, Wright State University, Dayton, OH, December 9.
11. Meyer, K., Menart, J., and Hughes, K., (2011), “Computational Determination of Guidelines for the Length of the Heat Exchanger Tube in a Ground Loop Geothermal Heating and Cooling System,” *7th Annual ASME Dayton Engineering Sciences Symposium*, Dayton, OH, October 24.
12. Menart, J., Gross, P., and Hughes, K., (2012), “Status Report on the Development of a Three-Dimensional Commercial Code for Ground Source Heat Pump Systems,” *8th Annual ASME Dayton Engineering Sciences Symposium*, Dayton, OH, October 24.

13. Meyer, K., (2012), “Computational Determination of Guidelines for the Length of the Heat Exchanger Tube in a Ground Loop Geothermal Heating and Cooling System,”, Honors Thesis, Wright State University, Dayton, OH, January, 31.

6.2. PATENTS AND INTELLECTUAL PROPERTY

No patents have been applied for. The intellectual property that has been developed is a two-dimensional geothermal modeling code called GEO2D and a three-dimensional geothermal modeling code called GEO3D.

6.3. TRAINING AND PROFESSIONAL DEVELOPMENT

Two graduate students have been trained in the methods of geothermal modeling and computer programming. Both of these students have graduated and are employed by government and industrial. In addition, two undergraduate students finished their honors thesis as part of this project. Both of these students are currently employed as engineers. Lastly a research scientist has worked on this project. After leaving this project the research scientist went to work at General Electric.

6.4. OTHER PRODUCTS / DELIVERABLES

The following products have been developed as part of this work:

1. A two-dimensional geothermal computer code called GEO2D. This code has a user friendly GUI interface and produces a plethora of results, many of which are graphically displayed.
2. A three-dimensional geothermal computer code called GEO3D. This code produces a plethora of results in all three dimensions.
3. A web site showing a number of geothermal results. The web address is http://oldwww.cs.wright.edu/bie/rce_program/papersandpresentations.shtml

7. SUMMARY

The geothermal industry has proven its place in the HVAC market even with some of the barriers and misconceptions it faces. With technological advances in the industry and more accurate modeling tools, geothermal designers can begin to optimize a design and reduce the payback periods. The work done as part of this Department of Energy grant has added two new computer modeling tools to the arsenal of ground source heat pump designers and installers. These two computational tools are called GEO2D and GEO3D. GEO2D is a two-dimensional model of the ground and ground loop and GEO3D is a three-dimensional model of the ground and ground loop. Both of these models also include the analysis of the heat pump.

Both GEO2D and GEO3D used a detailed analysis of the heat transfer occurring throughout the system. For the heat transfer occurring in the ground and ground loop a detailed solution of the differential form of the energy equation is solved using a finite volume technique. Coupled to this ground loop and ground heat transfer analysis is a computational model of the heat pump. These two coupled models provide detailed and accurate results of the operation of the GSHP system. It is felt that GEO2D and GEO3D produced some of the most detailed results of any commercial GSHP system computer code currently available. GEO2D and GEO3D produce temperature results and heat fluxes at any location in the computational domain. Contour plots of the temperature field in the ground loop and the earth are presented to the user as a function of time. Heat rates are presented to the user for the ground loop and heat pump as a function of time. COP and other useful results are also presented to the user as a function of time. Simulations can be carried out for any period of time in hour increments or longer time increments.

GEO2D goes on to provide an economic analysis of the GSHP system. The costs of the GSHP system are compared to conventional systems such as propane furnaces, natural gas furnaces, air-to-air heat pumps, and vapor compression air-conditioners. A payback period relative to the conventional systems mentioned is calculated including the initial capital outlays, maintenance, and the cost of the energy input to the heating and cooling system. This is all done accounting for the time value of money. The user can enter an interest rate that describes the value of time in monetary terms.

To perform a detailed GSHP system analysis the heating and cooling loads of a building are required. The sizing of the system is critical to the overall efficiency which is why the most reliable load calculator, ENERGYPLUS, is used to supply building heating and cooling load information to GEO2D and GEO3D. ENERGYPLUS provides the designer with all of the necessary building inputs to ensure an accurate building load on an hourly basis using trusted Typical Meteorological Year version 2 (TMY2) format weather files. GEO2D provides the user with some standard home layouts that can be altered easily and allow a user to bypass many of complicated inputs required by ENERGYPLUS.

A complete Graphical User Interface was employed in GEO2D to ease the designer through the process of selecting the geothermal design parameters. The data collected from the building simulation is used to help suggest values for heat pump size, pipe size, fluid velocity, and soil temperature. The user is left with full control over all of the inputs including the number of control volumes, time steps, and even the exponent used for grid spacing.

Finally, in this report, a number of results from GEO2D and GEO3D have been presented. These results indicated the detail of the model used in these two programs. It is believed that the array of results determined by these programs will be useful to GSHP designers and installers. In

addition results have been compared to results from a number of popular commercial geothermal programs. In general the results compare, but due there are some differences due to the more detailed model used in our program relative to the commercial codes used for comparison.

REFERENCES

- ASHRAE. *Commercial/ Institute Ground-Source Heat Pump Engineering Manual*. Atlanta, GA: American Society of Heating, Refrigerating and Air-Conditioning Engineers, Inc., 1995.
- . *Handbook Fundamentals, American Society of Heating, Refrigerating and Air-Conditioning Engineers, Inc.* Atlanta, GA: American Society of Heating, Refrigerating and Air-Conditioning Engineers, Inc., 1985.
- . "U-factor, C-factor, and Thermal Mass Data." *2008 Joint Appendices – June 2007 Workshop Draft*. n.d. Page 4-1.
- BS., Petukhov. *Advances*. Vols. 6:503–564. 1970.
- California Energy Commission*. n.d.
http://www.consumerenergycenter.org/home/heating_cooling/geothermal.html (accessed 2011 йил 24-08).
- CANMET. *RETSscreen International - Ground-Source heat Pump Project Analysis*. Minister of Natural Resources Canada, 2005.
- Carslaw H.S., J.J.C. *Conduction of Heat in Solids*. 2d ed Great Britain: Oxford Science Publications., 1959.
- Carslaw, H, and J Jaeger. *Conduction of Heat in Solids*. Oxford, U.K.: Clarendon Press, 1947.
- Cengel, Yunus A. *Heat and Mass Transfer: A Practical Approach*. McGraw-Hill, 2007.
- Cengel, Yunus A. 3rd. Vol. Heat and mass transfer a practical approach. New York: McGraw-Hill, 2007.
- Cengel, Yunus A., and Michael A. Boles. sixth. Vol. Thermodynamics. New York: McGraw-Hill, 2008.
- Chapman, A.J. "Heat Transfer." (Macmillan Publishing Company) 4th Edition (n.d.).
- Cheng, Nian-Sheng. "Formulas for friction factor in transitional regimes." (*Journal of Hydraulic Engineering, ASCE*) 134, no. 9 (2008): 1357-1362.
- Crawley, Drury B. "Which Weather Data Should You Use for Energy Simulations of Commercial Buildings." Washington DC, 1998, 104 Part 2.
- D.O.E. "Geothermal Heat Pump Manufacturing Activities." (U.S. Energy Information Administration), no. <http://www.eia.gov/fuelrenewable.html> (2010).
- Datta, Ravindra. *Eddy Viscosity and Velocity Distribution in Turbulent Pipe Flow Revisited*. Vol. 39. Iowa City, IA: AIChE Journal, 1993.
- Deru, M. *A model for Ground-Coupled Heat and Moisture Transfer from Buildings*. Golden, Colorado: National Renewable Energy Laboratory, 2003.

- EnergyPlus. "Engineering Reference." *The reference to EnergyPlus calculations*, 2010: 1-1075.
- Eskilson, P. "Thermal Analysis of Heat Extraction Boreholes. Doctoral Thesis." University of Lund, Department of Mathematical Physics. Lund, Sweden, 1987.
- Fox, Robert W., Alan T. McDonald, and Phillip J. Pritchard. *Introduction to Fluid Mechanics*. sixth. Danvers, MA: John Wiley & Sons, 2006.
- Gemelli, Alberto. "GIS-based energy-economic model of low temperature geothermal resources:." (Elsevier Ltd. All rights reserved.) *Renewable Energy* 36 (2011) 2474e2483 (2011).
- GeoEnergy. "Energy Information Administration/Geothermal Heat Pump Manufacturing Activities." (<http://www.eia.doe.gov/cneaf/solar.renewables/page/ghpsurvey/geothermalrpt.pdf>) 2008.
- GeoExchange. *GeoExchange*. n.d. <http://www.geoexchange.org/> (accessed 2011).
- GEO-FLO. *GEO-FLO TM ALL*. www.recochem.com. Montréal • Toronto • Edmonton • Vancouver, n.d.
- Geo-Hydro. "MAY 2011 Price & Product Catalog." (www.geohydrosupply.com) 2011.
- geothermalgenius. "sizing up a geothermal system." (<http://www.geothermalgenius.org/thinking-of-buying/industry-issues/sizing.html>) 2011.
- Giardina, Jonathan J. *Evaluation of Groun Coupled Heat Pumps for The State of Wisconsin. Master's Thesis*. University of Wisconsin-Madison, 1995.
- Gilat, Amos. *MATLAB an introduction with applications*. second. Danvers, MA: John Wiley & Sons, 2005.
- Gross, Paul Allen. *Commercial Program Development for Ground Loop Geothermal System: Energy Loads, GUI, Turbulent Flow, Heat Pump Model, and Grid Study. Master's Thesis*. Dayton, OH: Wright State University, 2011.
- Ground Loop Design. "Geothermal Design Studio." *Ground Loop Design™ Premier Version 5.0 for Windows*®. Celsia, 2007.
- Haberl, J S, and L D Sung. *A Review of Ground Coupled Heat Pump Models Used in Whole-Building Computer Simulation Programs*. College Station, TX: Energy Systems Laboratory Department of Architecture. Texas A&M University, 2008.
- Hamada, Yasuhiro, Makoto Nakamura, Kiyoshi Ochifuji, Shintaro Yokoyama, and Katsunori Nagano. "Development of a database of low energyhomes around the world and analyses of their trends." (www.elsevier.com) *Renewable Energy* 28 (2002): 321–328.
- Hart, D, and R Couvillion. *Earth Coupled Heat Transfer*. National Water Well Association, 1986.
- Hellström, G. *Duct ground heat storage model: Manual for computer code*. Lund, Sweden: University of Lund, Department of Mathematical Physics, 1989.

- IGSHPA. *Closed-Loop/Ground-source Heat Pump Systems - Installation Guide*. Stillwater, OK, Oklahoma: International Ground-source Heat Pump Association, 1988.
- Ingersoll, L R, and H J Plass. "Theory of the Ground Pipe Heat Source for the Heat Pump." In *Fundamentals of Heat Transfer*, by F.P. DeWitt, D.P. Incropera. John Wiley and Sons, 1948.
- Ingersoll, L, O Zobel, and A Ingersoll. *Heat Conduction with Engineering, Geological, and Other Applications*. New York: McGraw-Hill, 1954.
- International Ground Source Heat Pump Association*. n.d.
<http://www.igshpa.okstate.edu/geothermal/faq.htm> (accessed 2011 йил 24-08).
- Jensen, M E. *Consumption Use of Water and Irrigation Water Requirement*. New York: American Society of Civil Engineers, 1973.
- Kalman, M D. *Earth Heat Exchangers for Ground Source Heat Pumps. Master's Thesis*. Georgia institute of Technology, 1980.
- Kavanaugh, P K, and K Rafferty. *Ground-source Heat Pumps – Design of Geothermal Systems For Commercial and Institutional Buildings*. Atlanta, GA: American Society of Heating, Refrigerating and Air-Conditioning Engineers, 1997.
- Kavanaugh, S P, and J D Deerman. *Simulation of vertical U tube ground coupled heat pump system*. Vol. 97. ASHRAE Transactions, 1991.
- Kavanaugh, S. *Simulation and experimental verification of vertical ground-coupled heat pump systems. Ph.D dissertation*. Stillwater, OK: Oklahoma State University, 1985.
- Kays. *Turbulent Prandtl Number-Where are we?* Vol. 116. J.Heat Transfer, 1994.
- Kelvin, W Thomson. *Mathematical and Physical Papers*. cited by Ingersoll, et al (1954), 1882, 41.
- Klein, S A. *TRNSYS Manual, a Transient Simulation Program*. Madison, WI: Solar Engineering Laboratory. University of Wisconsin-Madison, 1996.
- Liu, Xiaobing, and Goran Hellstrom. *Enhancement of an Integrated Simulation Tool for Ground Source Heat Pump System Design and Energy Analysis*. Lund, Sweden: Department of Mathematical Physics, Lund University of Technology, 2006.
- M.Conde Engineering. "Thermophysical properties of brines." Zurich, 2002.
- Marchand, Patrick, and O.Thomas Holland. *Graphics and GUIs with MATLAB*. third. Boca Raton: Chapman & Hall/CRC, 2003.
- Mei, L R, and C J Emerson. *New approach for analysis of ground-coupled design for applied heat pump systems*. ASHRAE Transactions 91(2):1216-1224, 1985.

- Mogensen, P. "Fluid to Duct Wall Heat Transfer in Duct System Heat Storages." (The international Conference on Subsurface Heat Storage in Theory and Practice) 1983.
- Monzo, Patricia M. "Comparison of different Line Source Model approaches for analysis of Thermal Response Test in a U-pipe Borehole Heat Exchanger." Stockholm, Sweden, 2011.
- Muraya, N, D O'Neal, and W Heffington. *Thermal interference of adjacent legs in a vertical U-tube heat exchanger for a ground-coupled heat pump.* ASHRAE Transactions 102(2):12-21, 1996.
- Nelder, J A, and R Mead. *A Simplex Method for Function Minimization Computer Journal.* Computer Journal 7(1):308-313, 1965.
- Oregon Residential Energy Code. "Residential thermal performance calculations." no. No. 10. Oregon, april 2008.
- Parker, J D, J E Bose, and F C McQuiston. *ASHRAE Design/Data Manual for Ground-Coupled heat Pumps.* ASHRAE, 1985.
- Paul, N D. *The Effect of Grout Thermal Conductivity on Vertical Geothermal Heat Exchanger Design and Performance. Master's Thesis.* South Dakota State University, 1996.
- Purdy, Julia, and Andrew Morrison. "Ground-Source Heat Pump Simulation Within A Whole-Building Analysis." *Proc. 8th International IBPSA Conference* . Eindhoven, Netherlands, 2003. 1077-1084.
- Purdy, Julia, and Andrew Morrison. "GROUND-SOURCE HEAT PUMP SIMULATION WITHIN A WHOLE-BUILDING ANALYSIS." (Eighth International IBPSA Conference) 2003.
- Rafferty, Kevin. "Scaling in Geothermal Heat Pump Systems." Department of Energy, Klamath Falls, OR, 1999.
- Rees, Daniel E. Fisher and Simon J. "MODELING GROUND SOURCE HEAT PUMP SYSTEMS IN A BUILDING." (Ninth International IBPSA Conference), no. pp 311 (2005).
- Roadmap. "Ground-source Heat Pump Roadmap - Version 2.2." (http://ghpsrus.com/documents/GHP%20Roadmap_Version%202.2.pdf) n.d.
- Rottmayer, S, W Beckman, and J Mitchell. *Simulation of a single vertical U-tube ground heat exchanger in an infinite medium.* ASHRAE Transactions 103(2): 651-659, 1997.
- Shonder, J, and J Beck. *Determining effective soil temperature thermal properties from feild data using parameter estimation technique.* ASHRAE Transaction 105(1), 1999.
- Stathers, R J, T A Black, and M D Novak. *Modelling Soil Temperature in Forest Clearcuts Using Climate Station Data.* Vancouver B.C. 2A2 Canada: Department of Soil Science, university of British Cumbia, 1985.

Swearingen, Corte.

http://www.coleparmer.com/techinfo/techinfo.asp?htmlfile=V_PDeviations.htm&ID=815. Cole-Parmer Technical Library. September 25, 2009.

Thornton, J, T McDowell, J Shonder, and D P Hughes. *Residential Vertical Geothermal Heat Pump System Models: Calibration to Data*. ASHRAE Transactions 103(2): 660-674, 1997.

Trane. "Axiom Horizontal/Vertical Water-Source Heat Pump." *GEHE/GEVE - R - 410A 1/2 to 5 tons - 60 hz*. no. WSHP-PRC017-EN. Trane, 2009.

—. "Water Source Heat Pump." *Axiom™ Horizontal/Vertical — GEH/GEV*. no. WSHP-PRC016-EN. Trane, November 2010.

TRNSYS. *TRNSYS 17 - a TRAnSient SYstem Simulation program*. 2009.

Ubeg. "Geothermal Heat Pumps." (Zum Boden), no. ubeg@ubeg.de (1998).

University, School of Mechanical and Aerospace Engineering: Oklahoma State. *GLHEPRO 4.0 for Windows*. International Ground Source Heat Pump Association, 2007.

Vanek, Francis M., and Louis D. Albright. *Energy Systems Engineering evaluation and implementation*. McGraw-Hill, 2008.

Walton, G. N. *Thermal Analysis Research Program Reference Manual*. National Bureau of Standards, 1983.

Yang, H, P Cui, and Z Fang. *Vertical-borehole ground-coupled heat pumps: A review of models and systems*. Elsevier, 2010.

Yavuzturk, C, J.D. Spitler, and S.J. Rees. *A Transient Two-dimensional Finite Volume Model for the Simulation of Vertical U-tube Ground Heat Exchanger*. ASHRAE Transactions 105(2), 1999.

Yavuzturk, C. *Modeling of vertical ground loop heat exchangers for ground source heat pump systems*. Stillwater, OK: Oklahoma State University: ASHRAE Transactions 105(2), 1999.

Yavuzturk, C, and J Spitler. *A short time step response factor model for vertical ground loop heat exchangers*. ASHRAE Transactions 105(2), 1999.

Yazdanian, M, and J H Klems. *Measurement of the Exterior Convective Film Coefficient for Windows in Low-Rise Buildings*. Vols. 100, Part 1, p.1087. ASHRAE Transactions, 1994.

Young, Thomas R. *Development, Verification, and Design Analysis of The Borehole Fluid Thermal Mass Model for Approximating Short Term Borehole Thermal Response*. Master's Thesis. Stillwater, OK: Oklahoma State University, 2004.

Zeng, Heyi, Nairen Diao, and Zhaohong Fang. *Heat transfer analysis of boreholes in vertical ground heat exchangers*. International Journal of Heat and Mass Transfer. 46(23): 4467-4481, 2003.

APPENDIX I: SIMULATION RESULTS FOR DAYTON, OHIO

Building Specifics

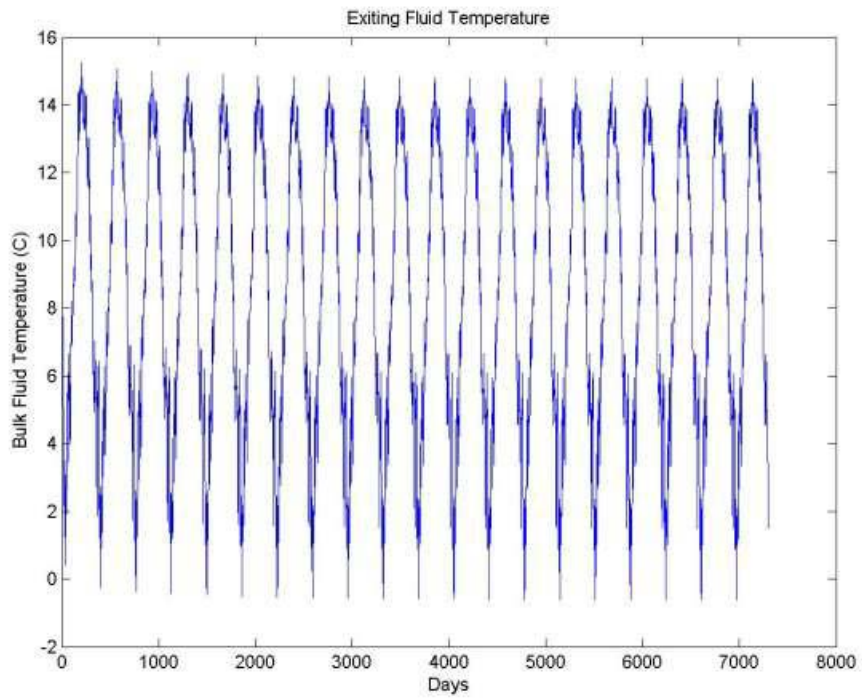
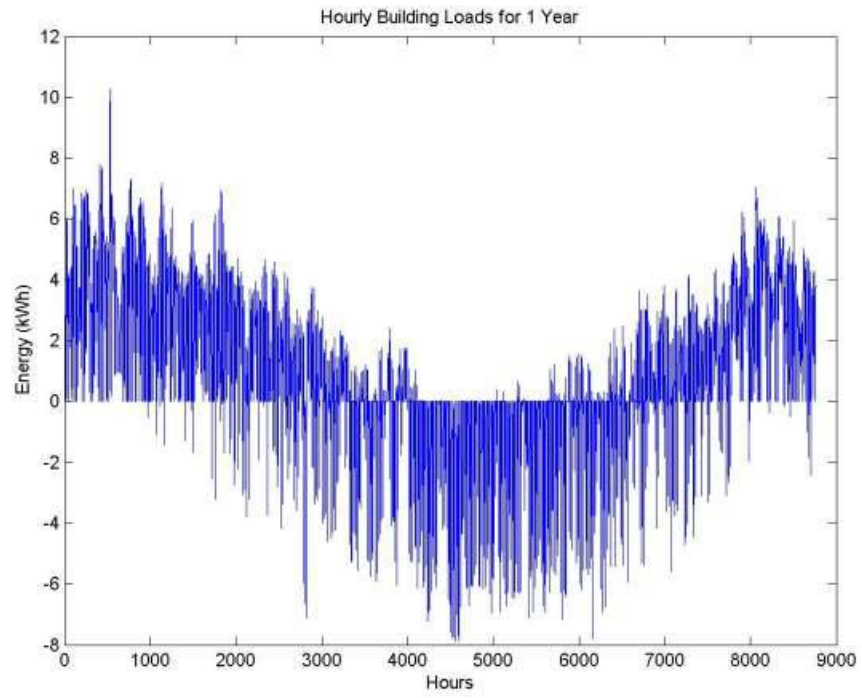
Floor plan Rectangle (18.6m x 10 m)	2000 ft ² / 186 m ²
Air Infiltration	'Moderately Sealed' (.65 ACH)
Window area	22.4 m ² / 241 ft ²
Number of exterior doors	2
Ceiling Height	8 ft. / 2.44 m
Winter Thermostat	70 °F / 21 °C
Summer Thermostat	77 °F / 25 °C
Exterior wall material layers	wood siding, 1/2" plywood, 2x4 wood studs and R11 insulation, 1/2" gypsum board
Exterior Ceiling/Attic material Layers	R-13, 2x6 wood studs, gypsum board

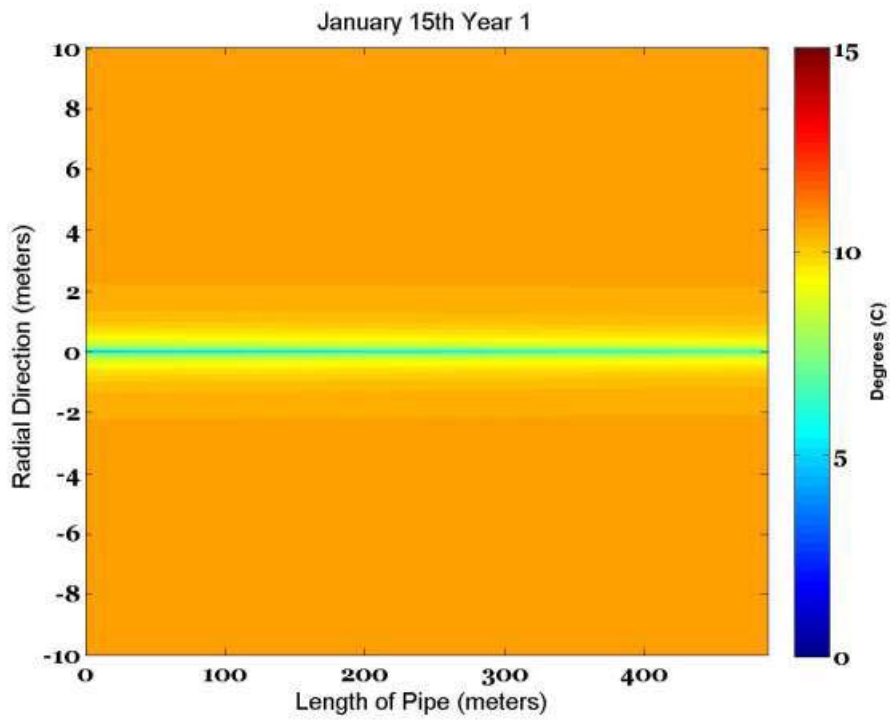
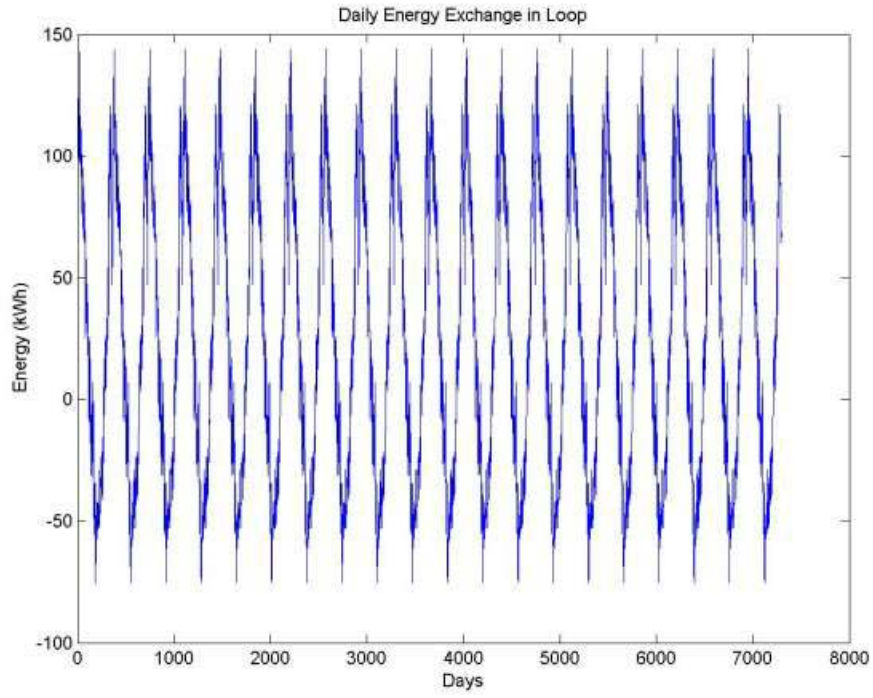
Building Load Analysis

Peak Cooling Load	7880 Whr
Peak Heating Load	8439 Whr
Extreme Low Outdoor Drybulb	-21.2 °C
Extreme High Outdoor Drybulb	36.1°C
Chosen Heat Pump Size	3 ton unit

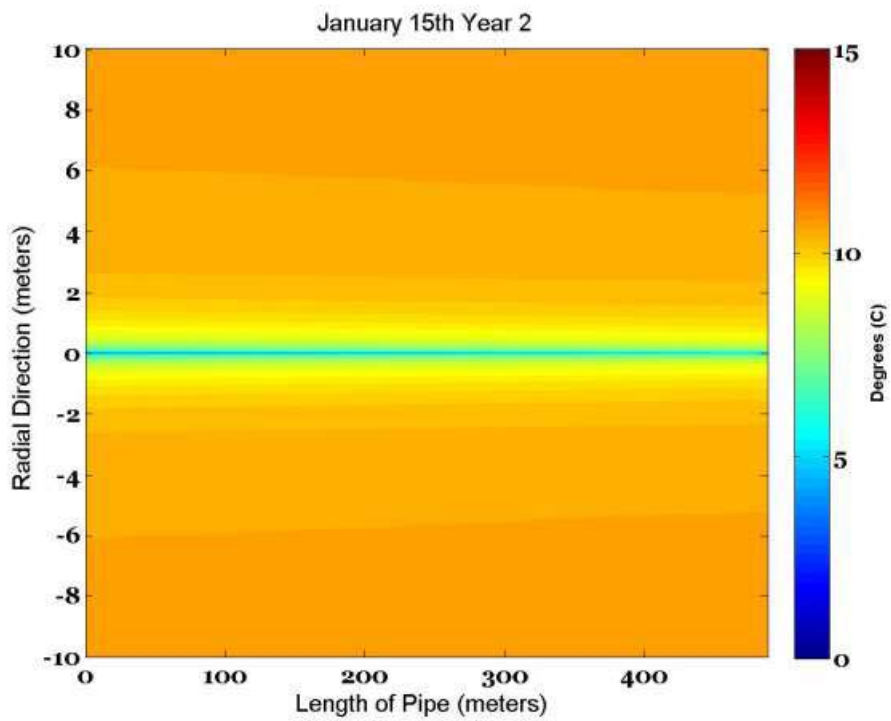
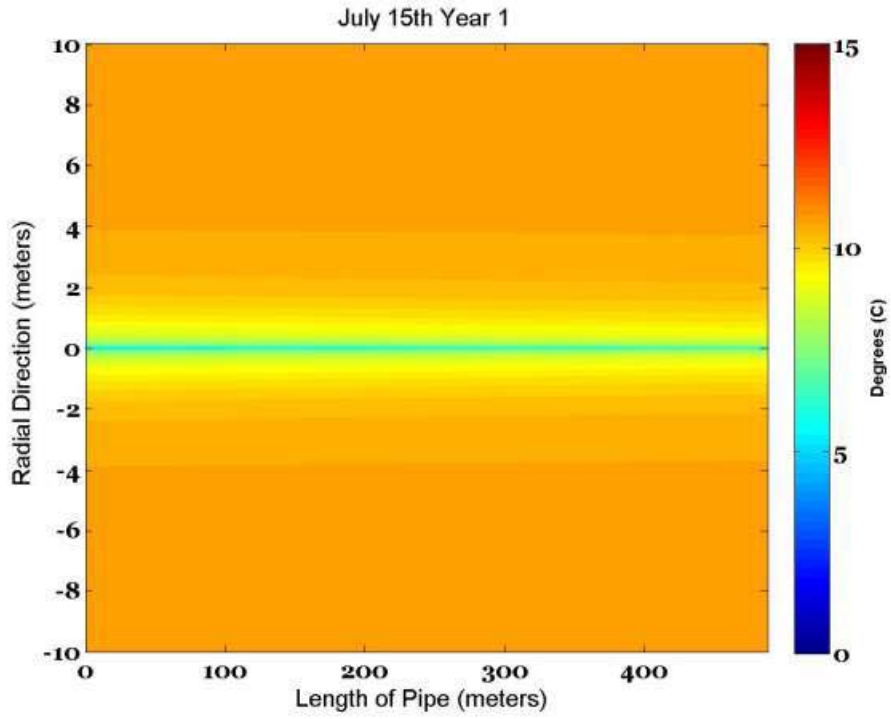
Geothermal Design Inputs

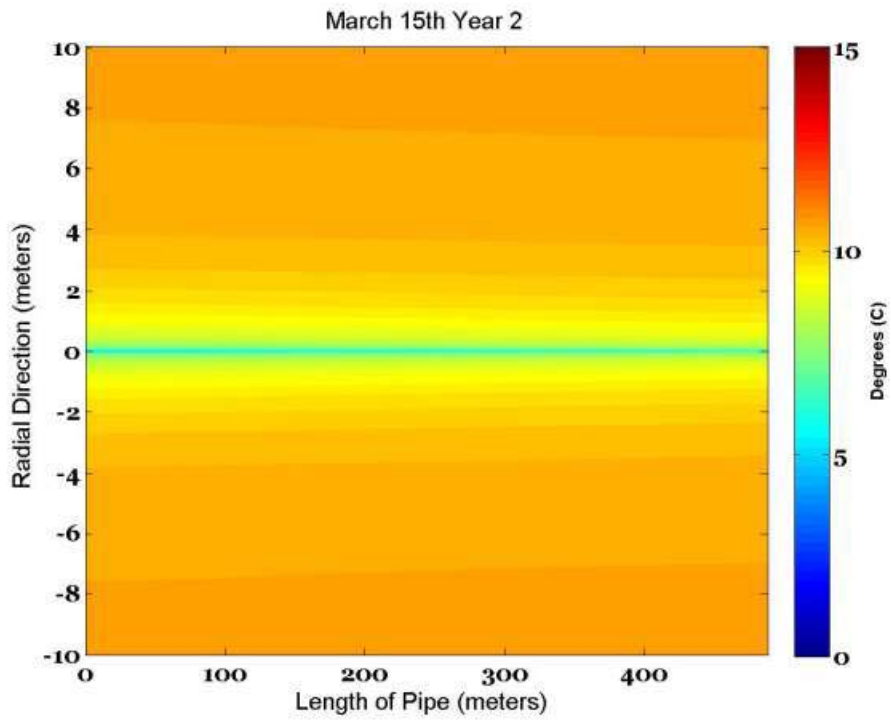
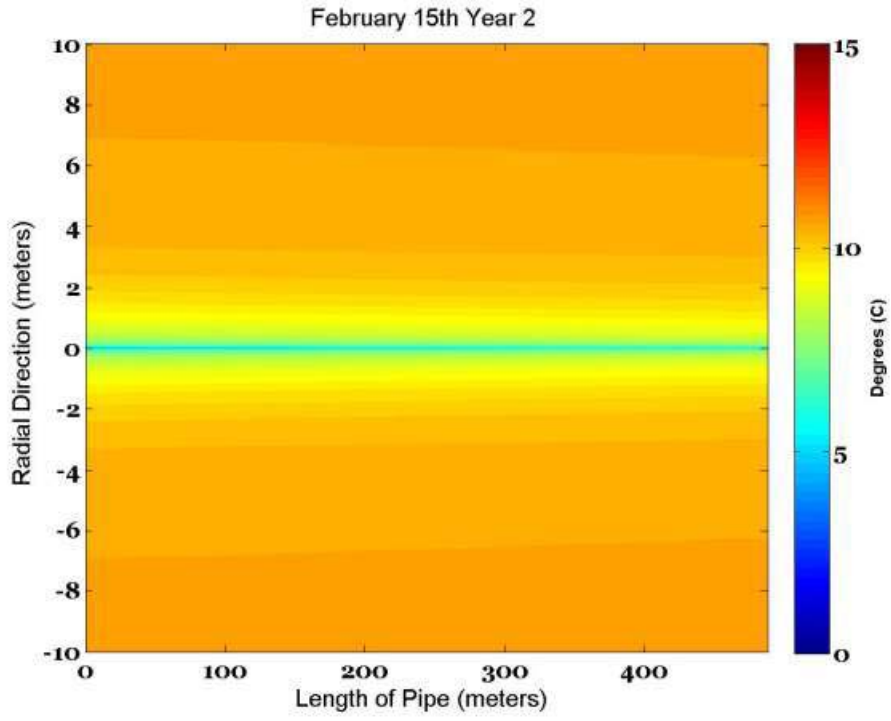
Time step	Daily
Years simulated	20 years
Length of tube	366 m
Inner Radius of pipe	11.646 mm
Thickness of Pipe Wall	2.87 mm
Fluid Thermal Conductivity (water)	0.58 W/m-C
Fluid Specific Heat	4220 J/kg-C
Fluid Density	1002 kg/m ³
Fluid Dynamic Viscosity	0.001 N-s/m ²
Tube Thermal Conductivity	0.49 W/m-C
Tube Specific Heat	1340 J/kg-C
Tube Density	941 kg/m ³
Earth Thermal Conductivity	1.3 W/m-C
Earth Specific Heat	1813 J/kg-C
Earth Density	1280 kg/m ³
Fluid Velocity	1.2438 m/s
Earth Temperature	10.87 °C
Fluid Initial Temperature	5 °C

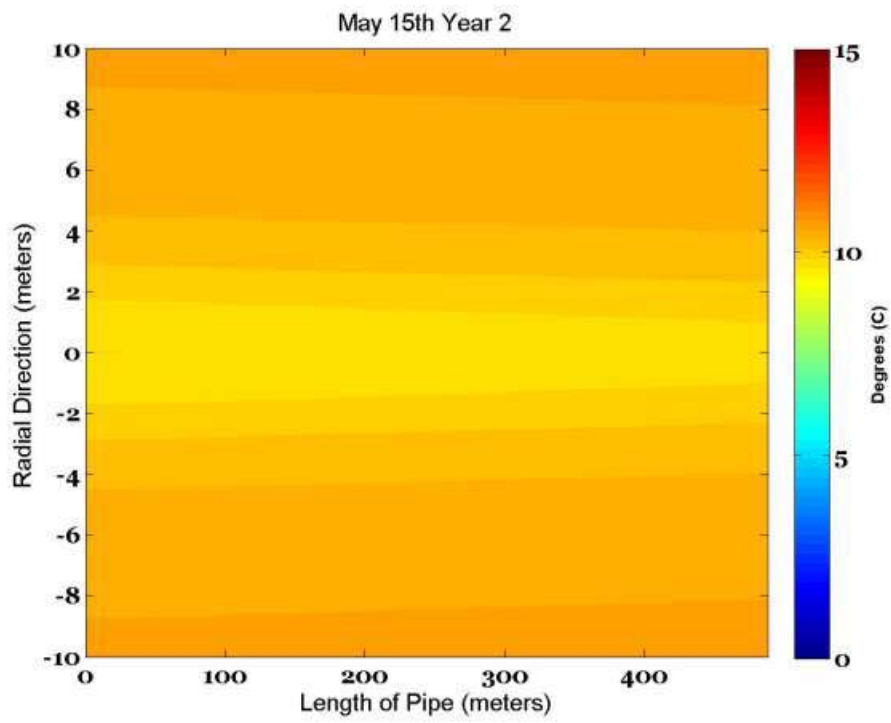
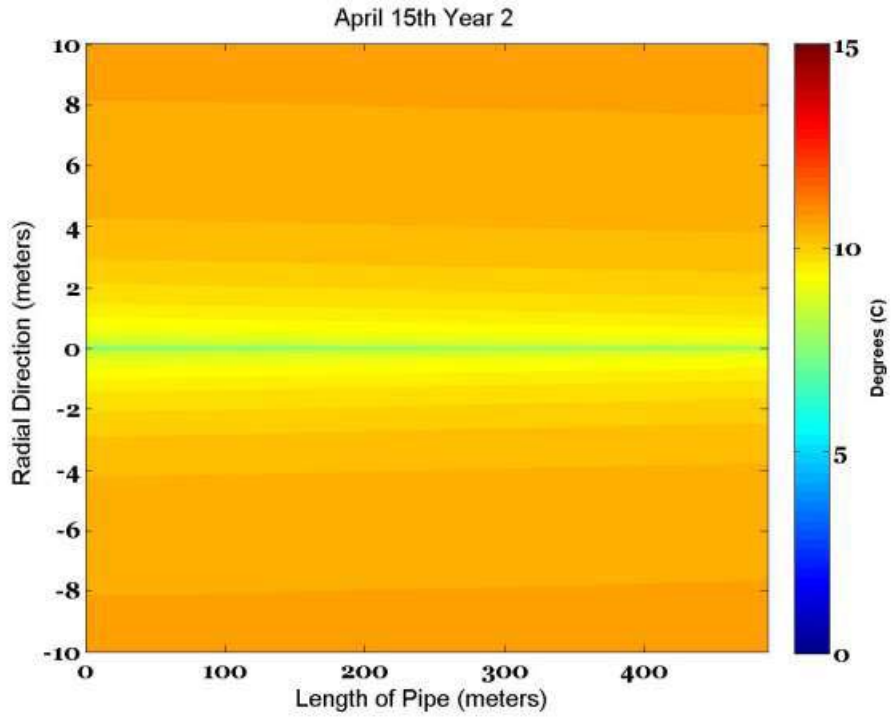


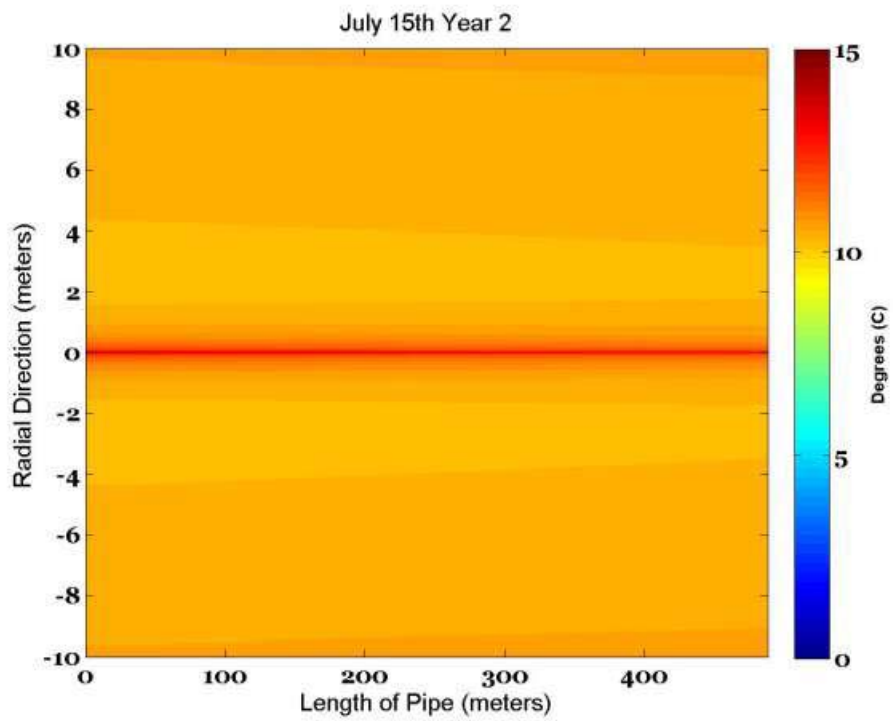
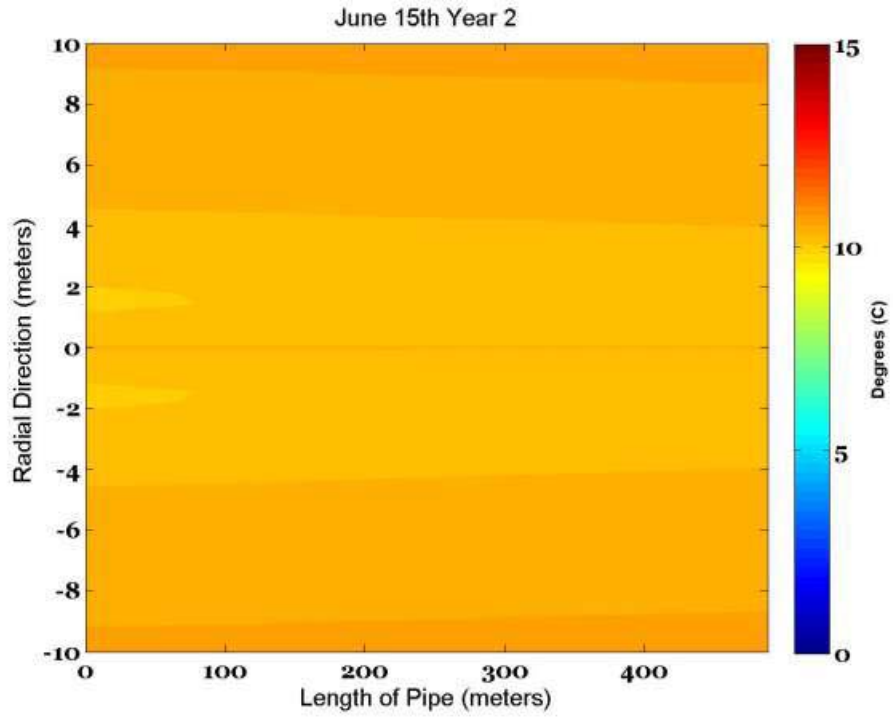


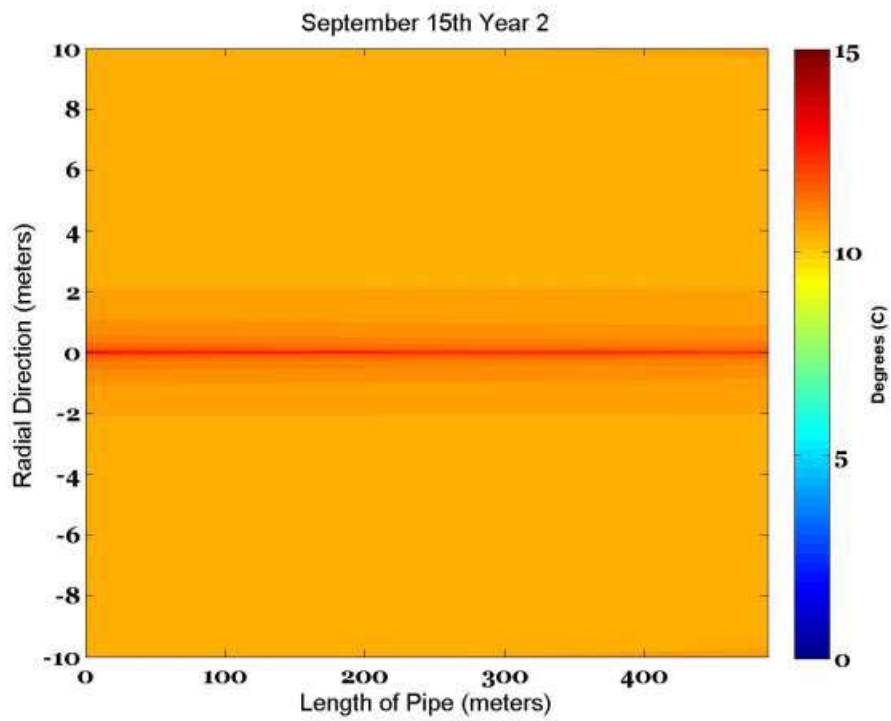
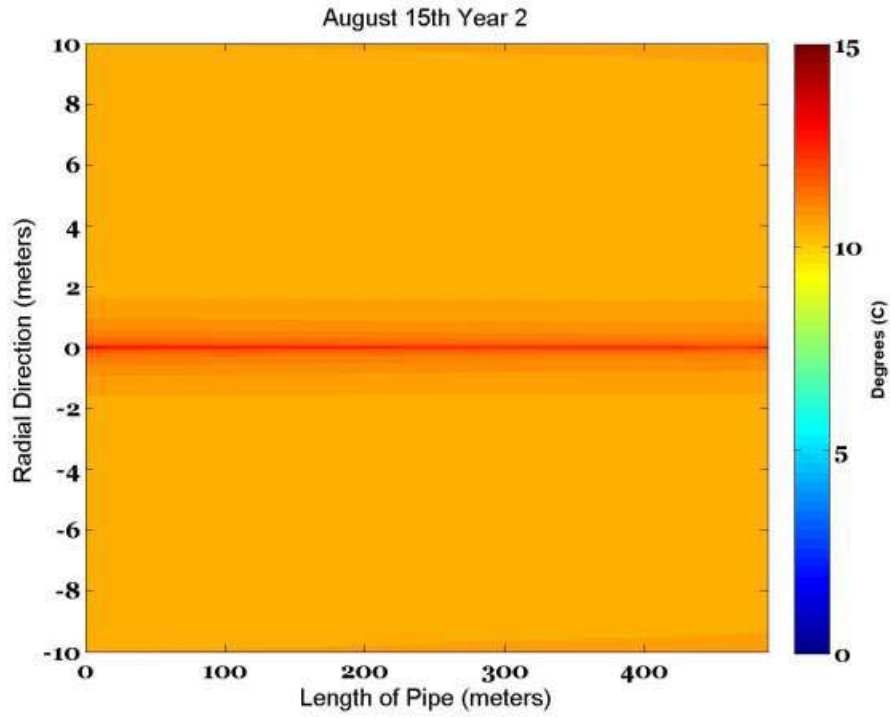
*These are temperature contour plots.

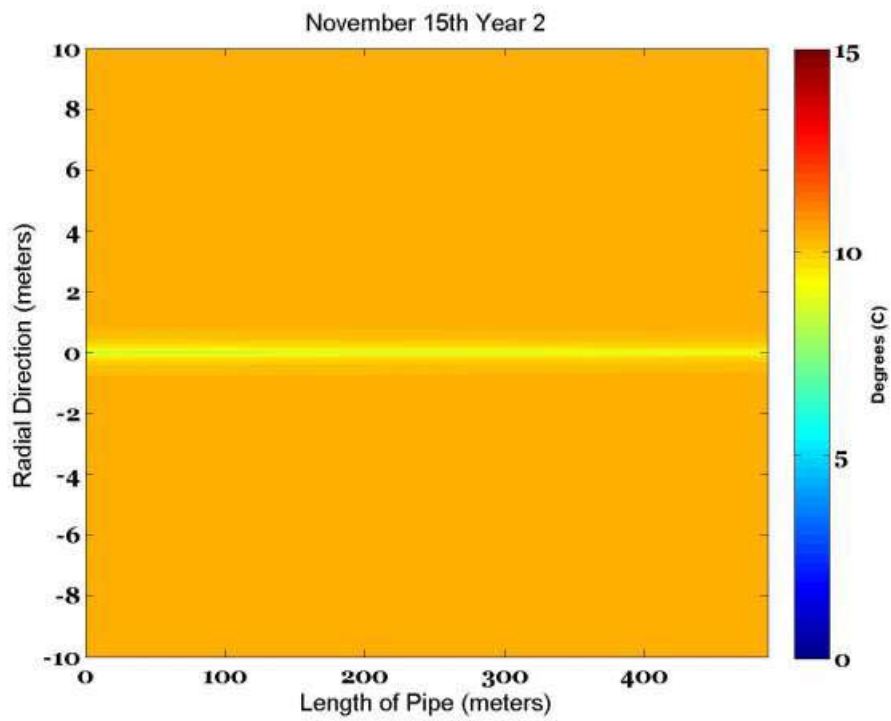
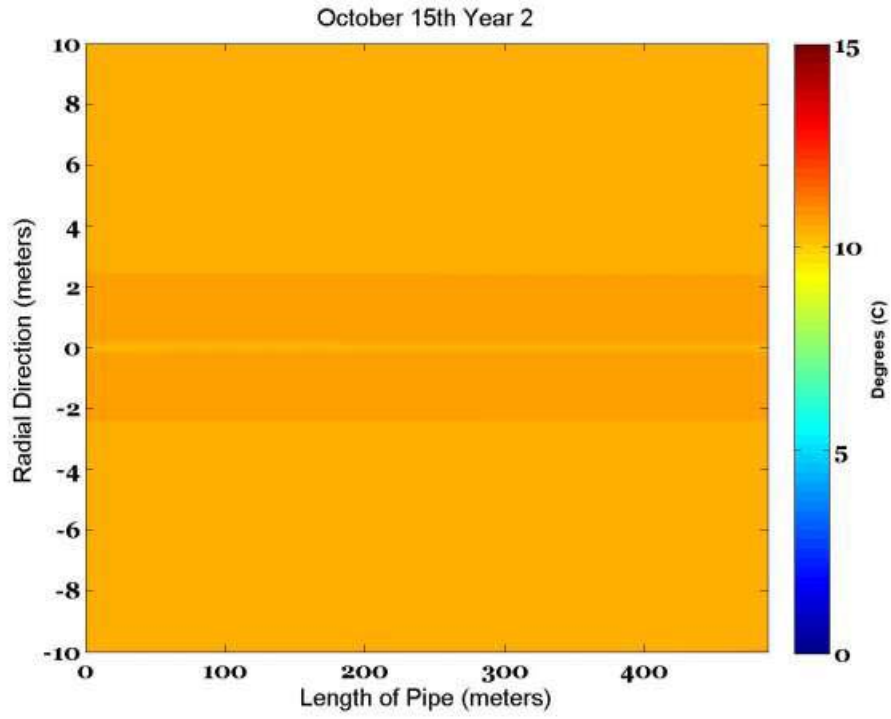


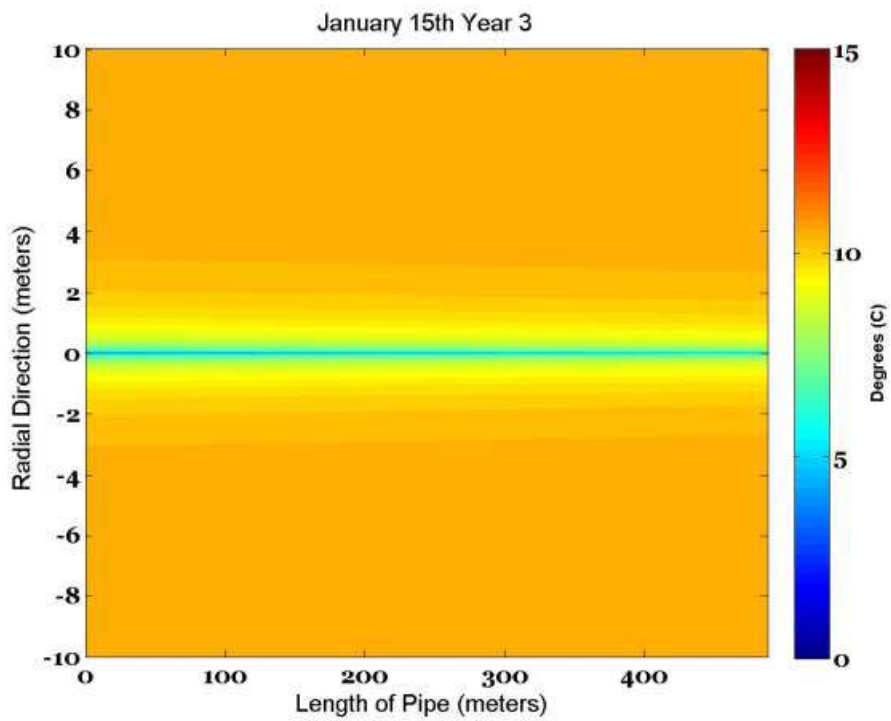
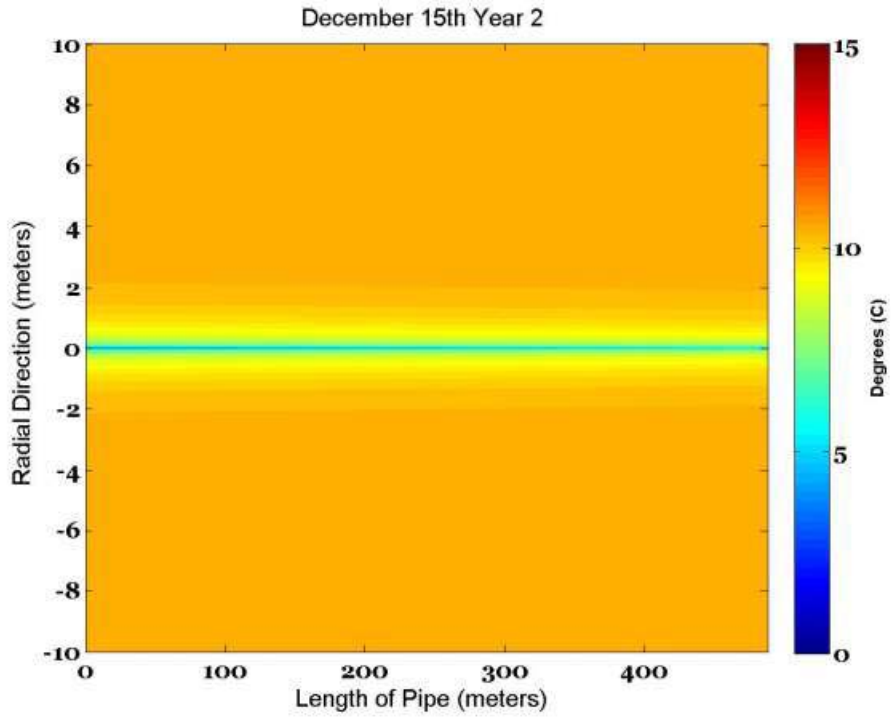


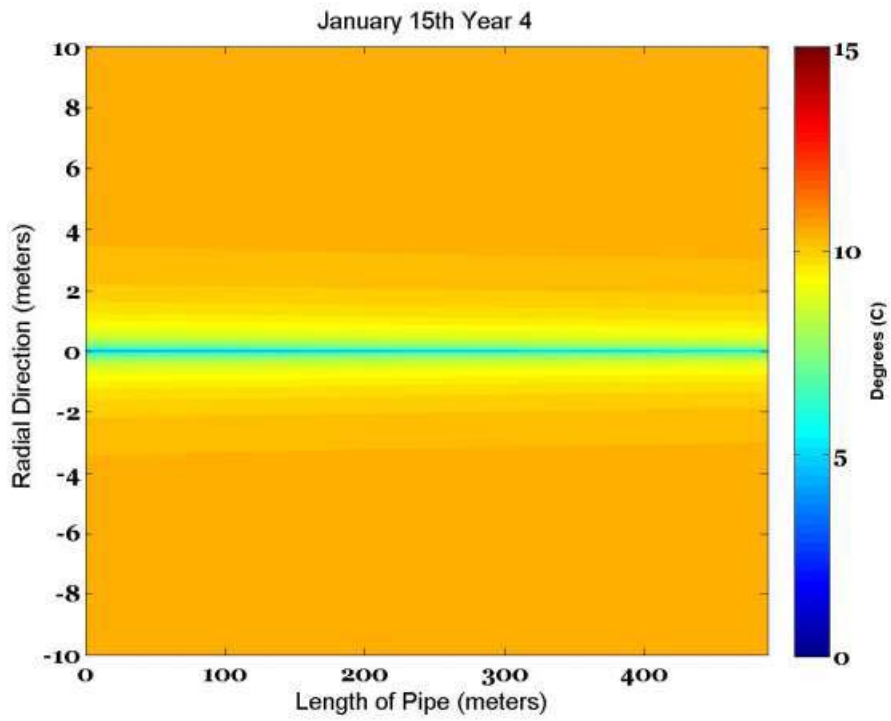
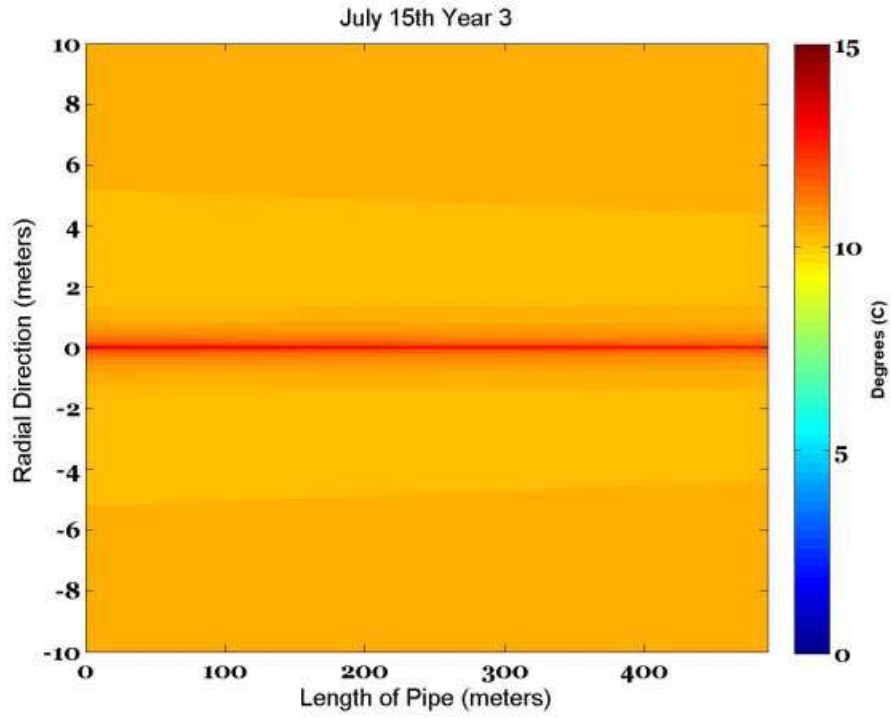


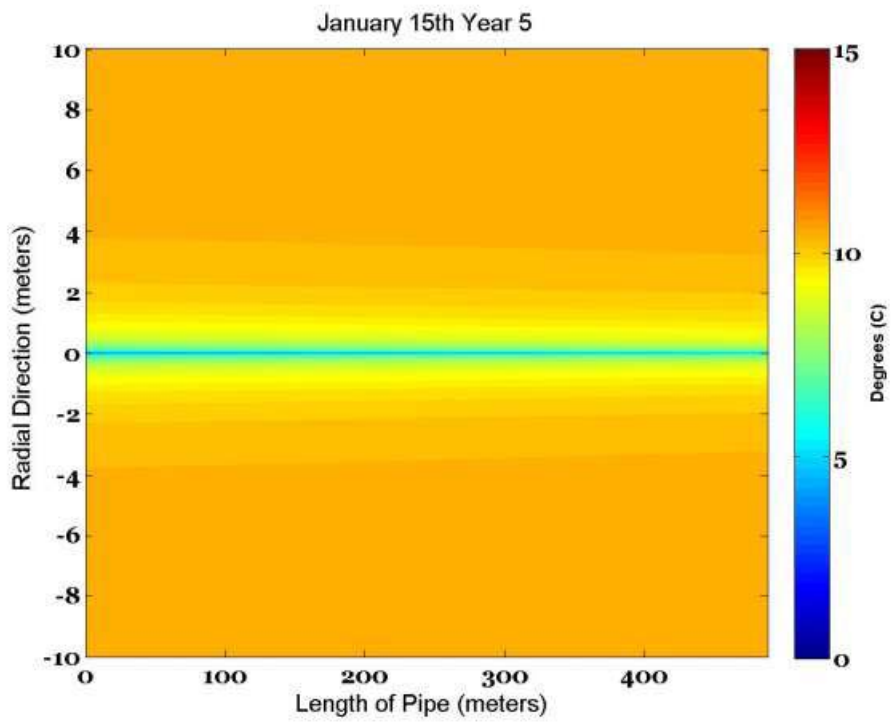
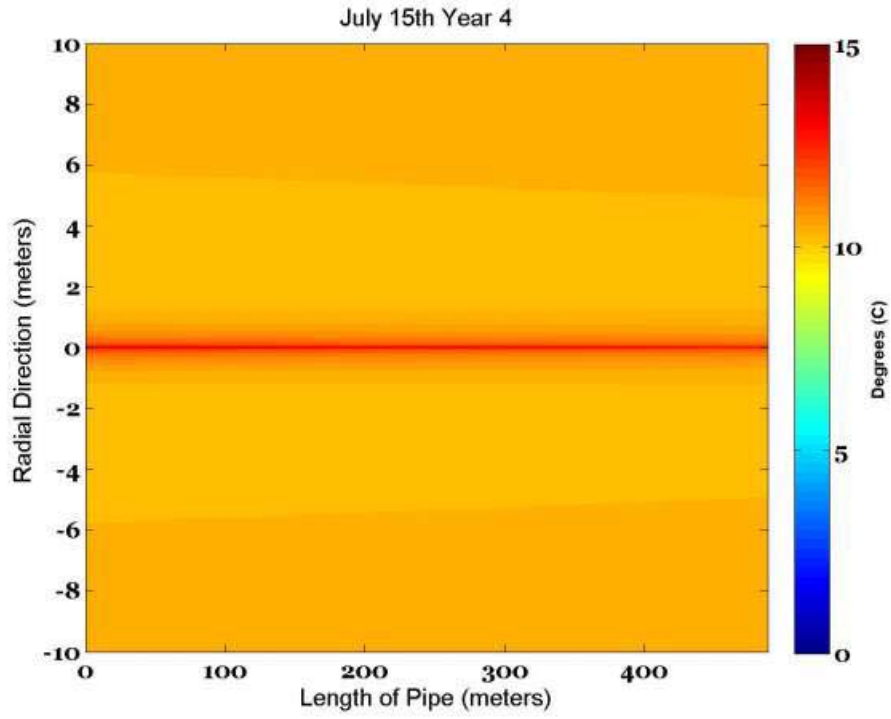


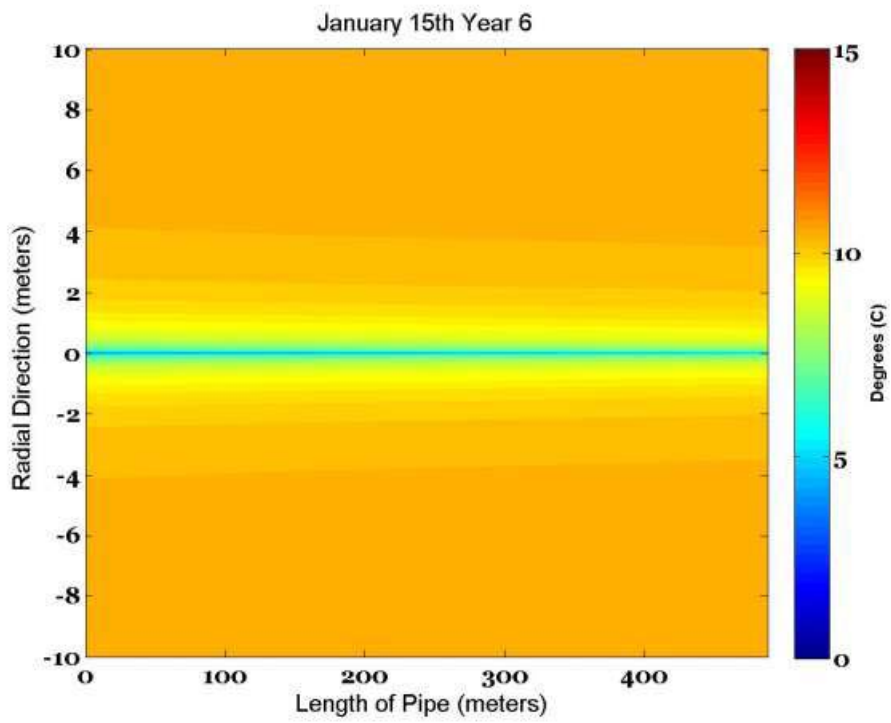
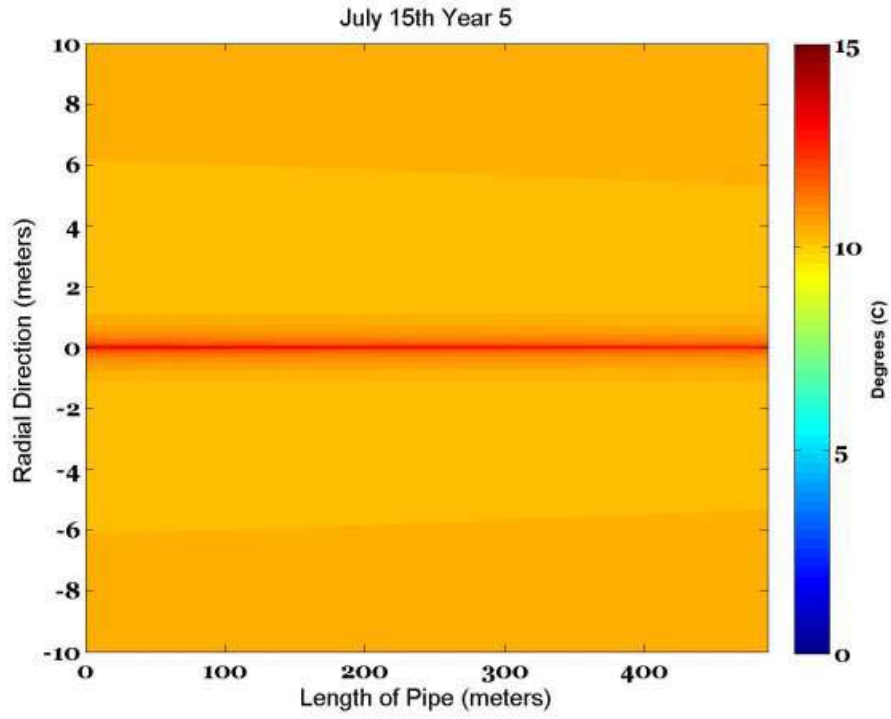


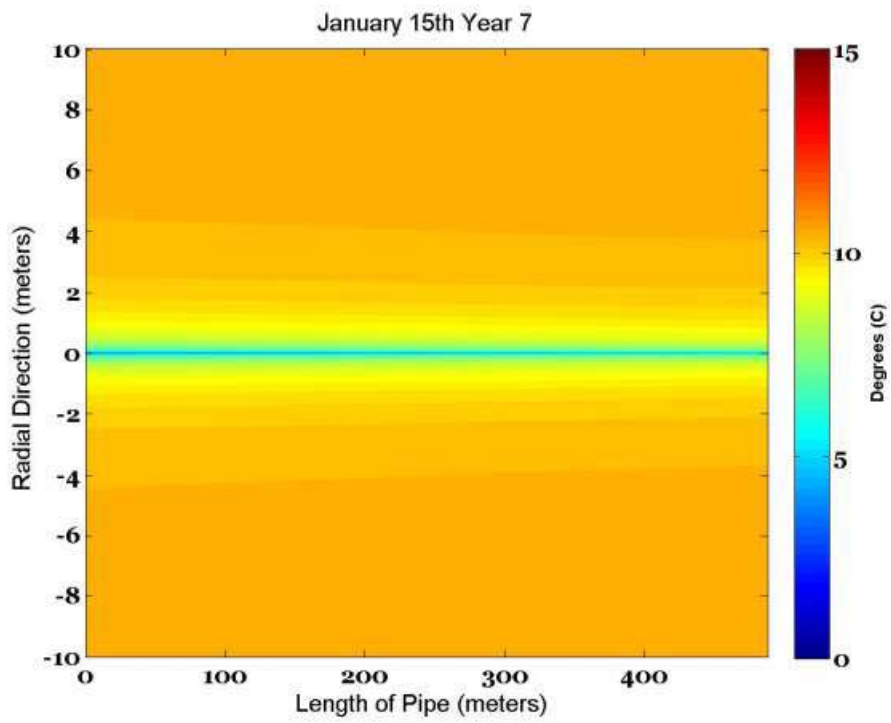
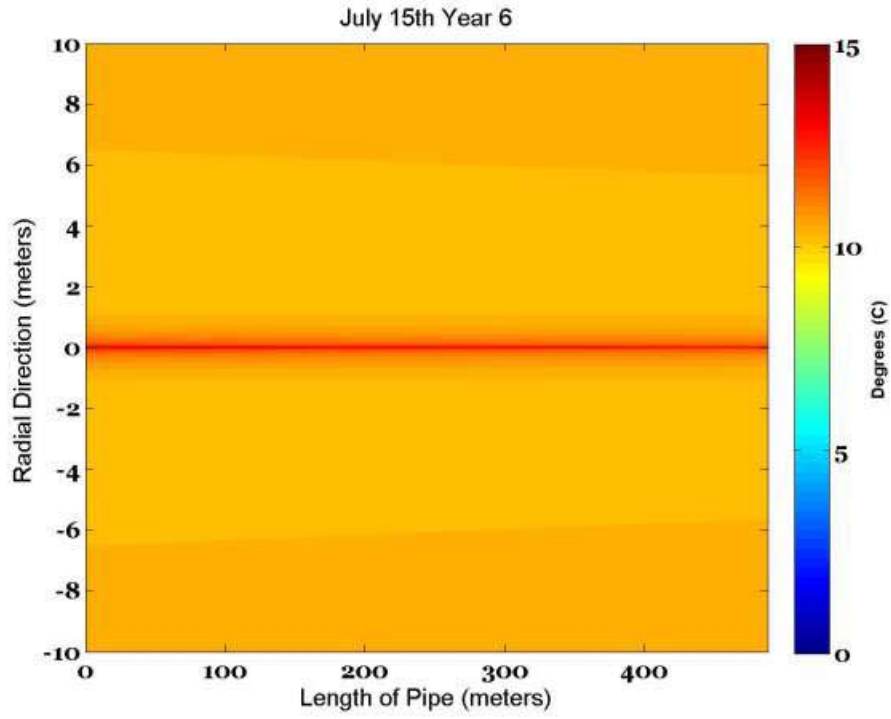


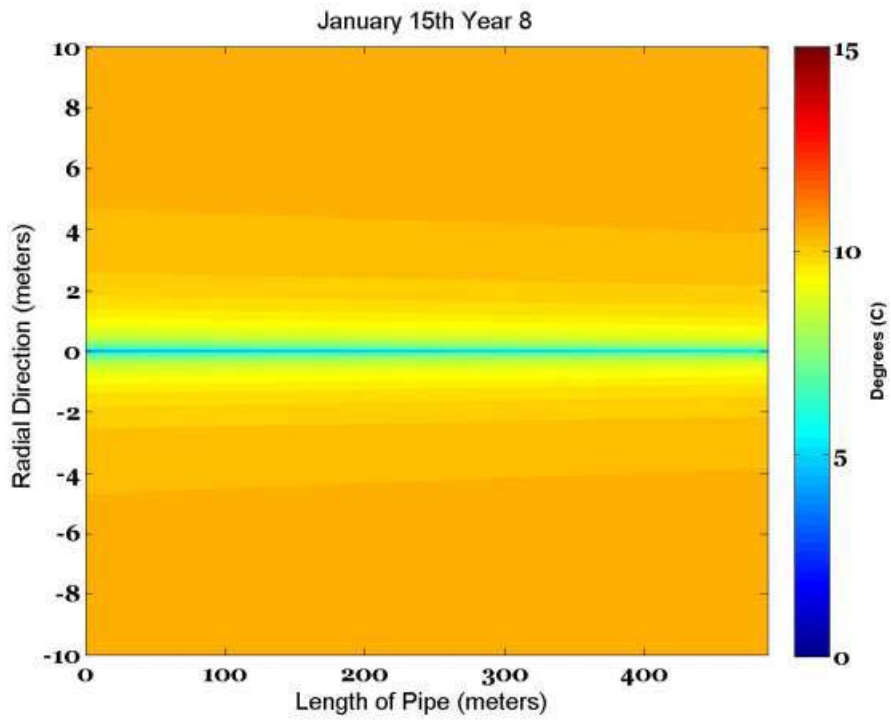
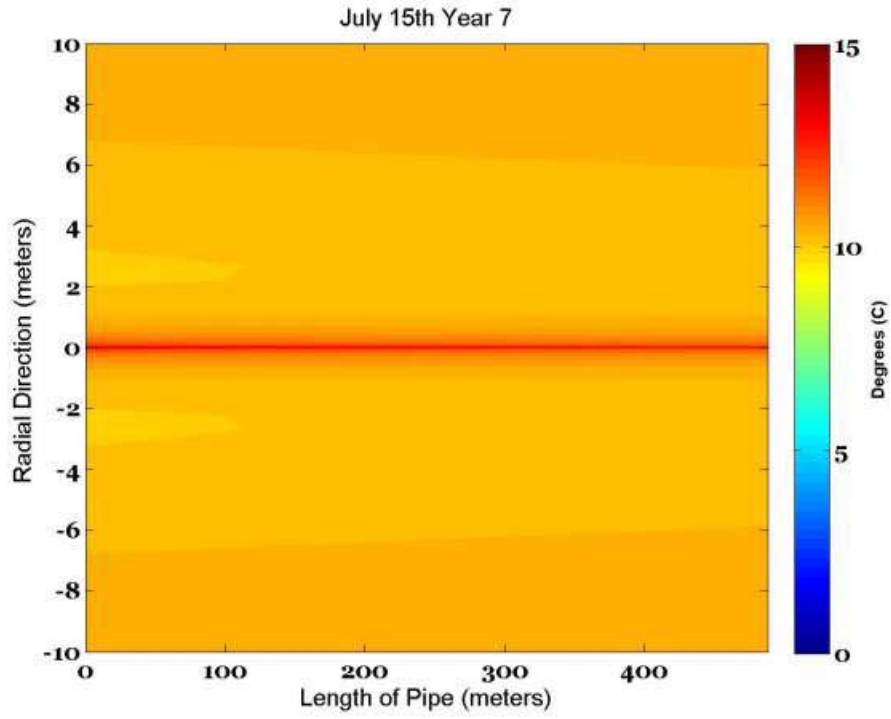


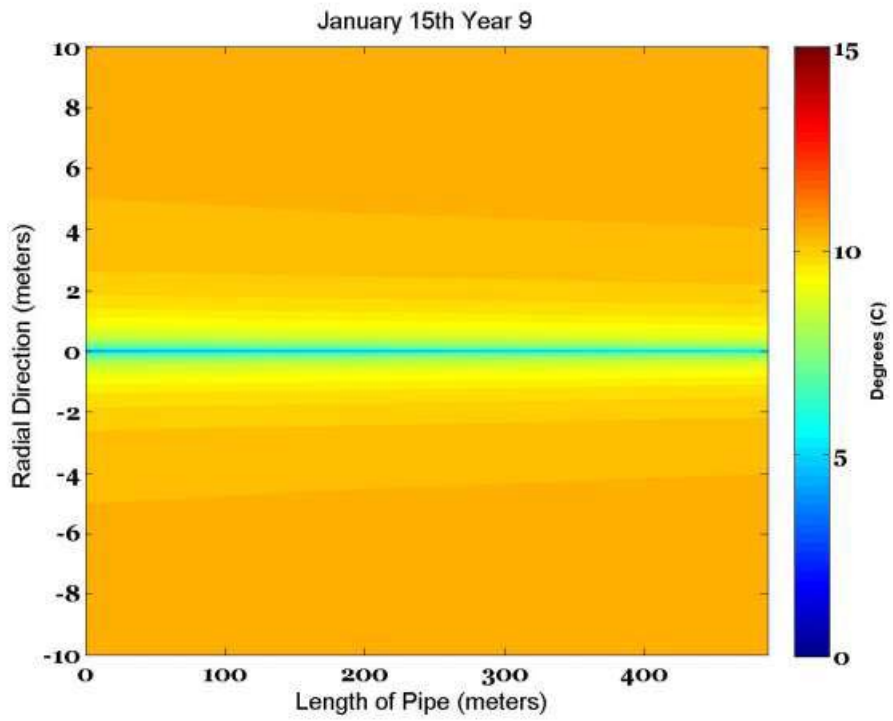
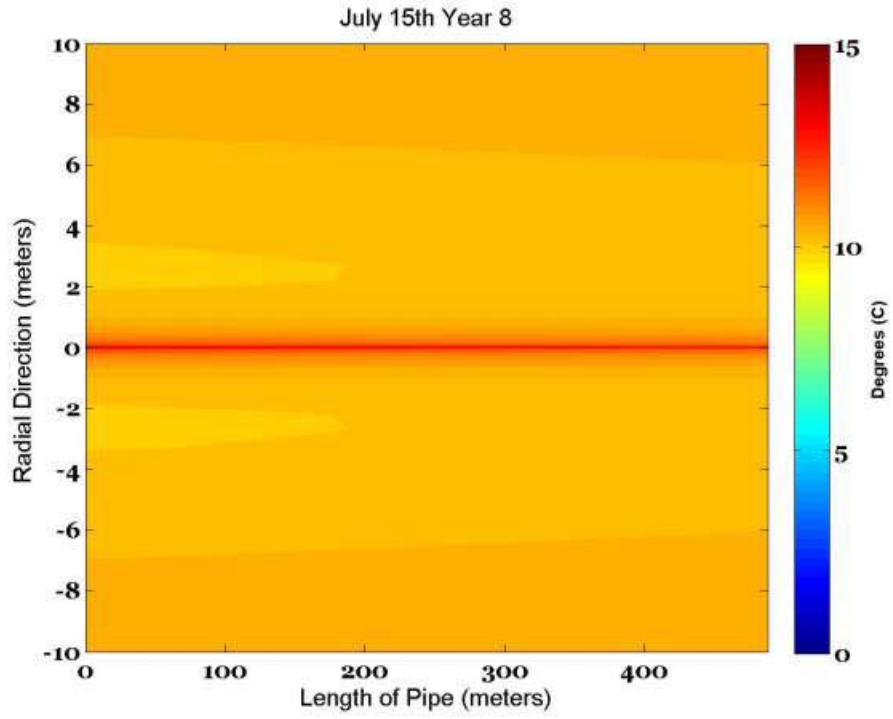


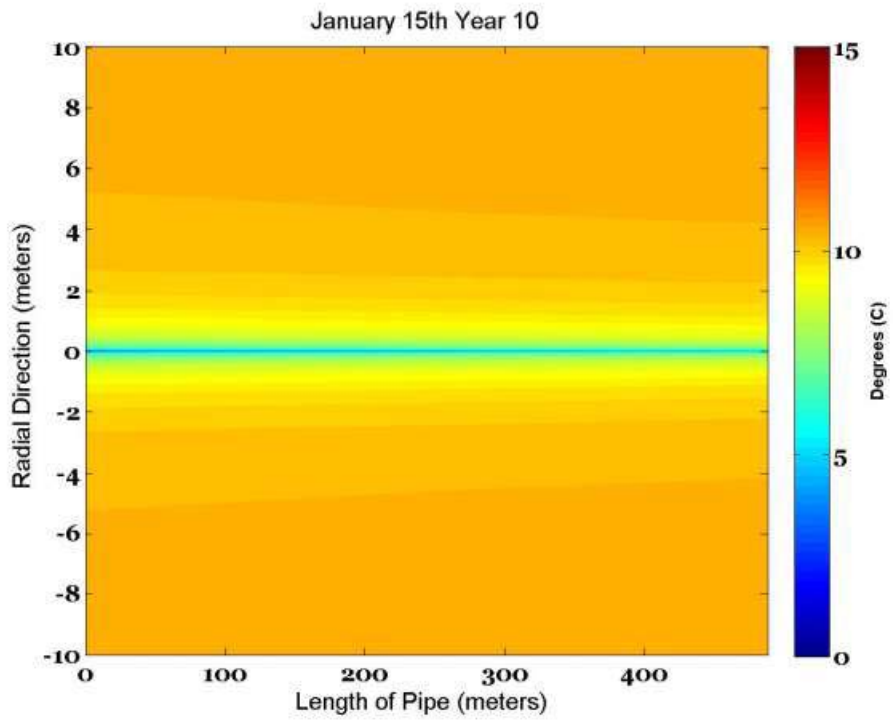
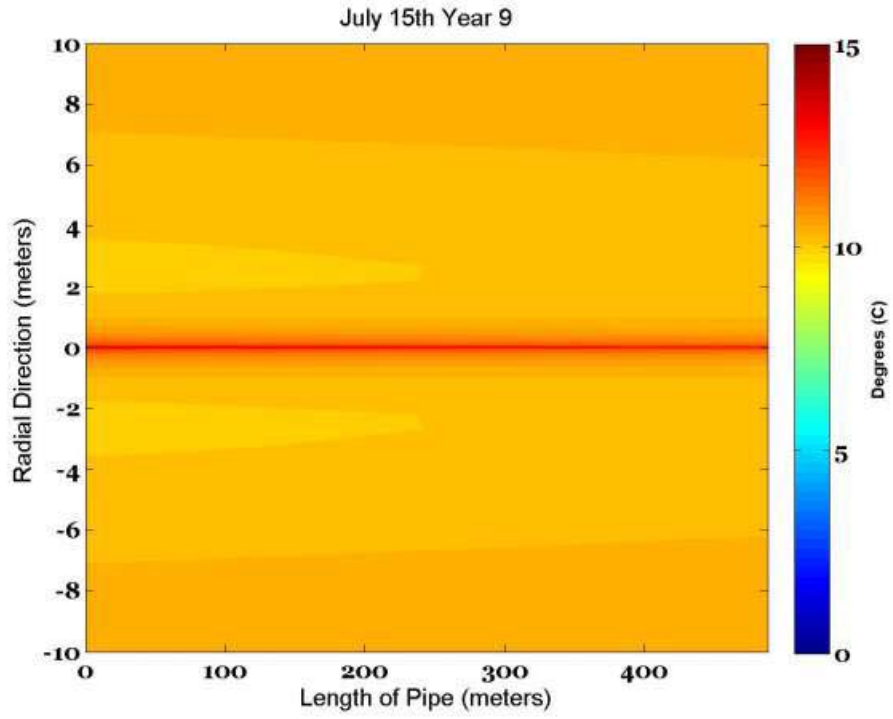


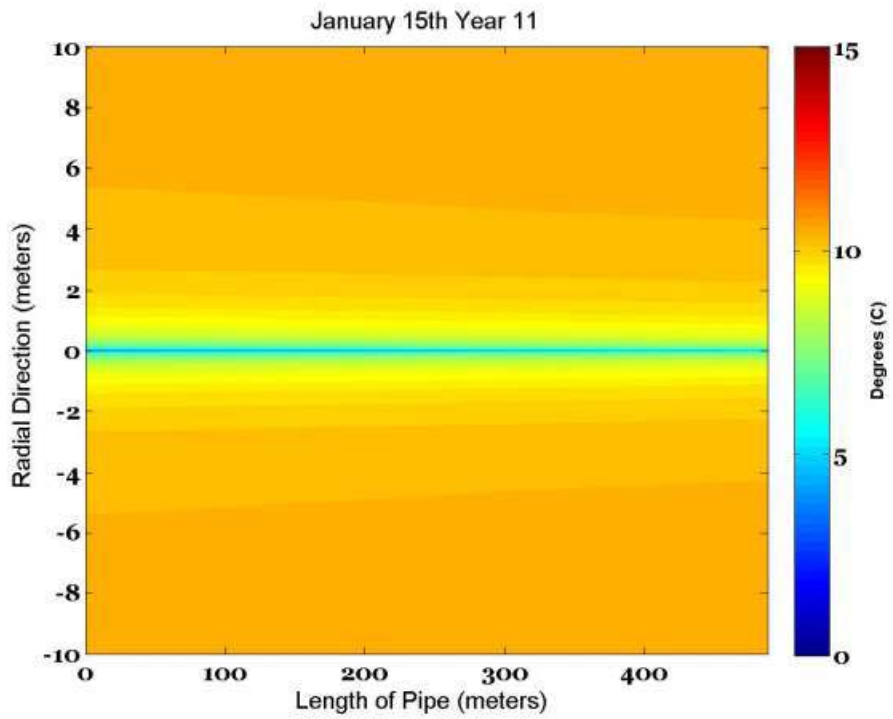
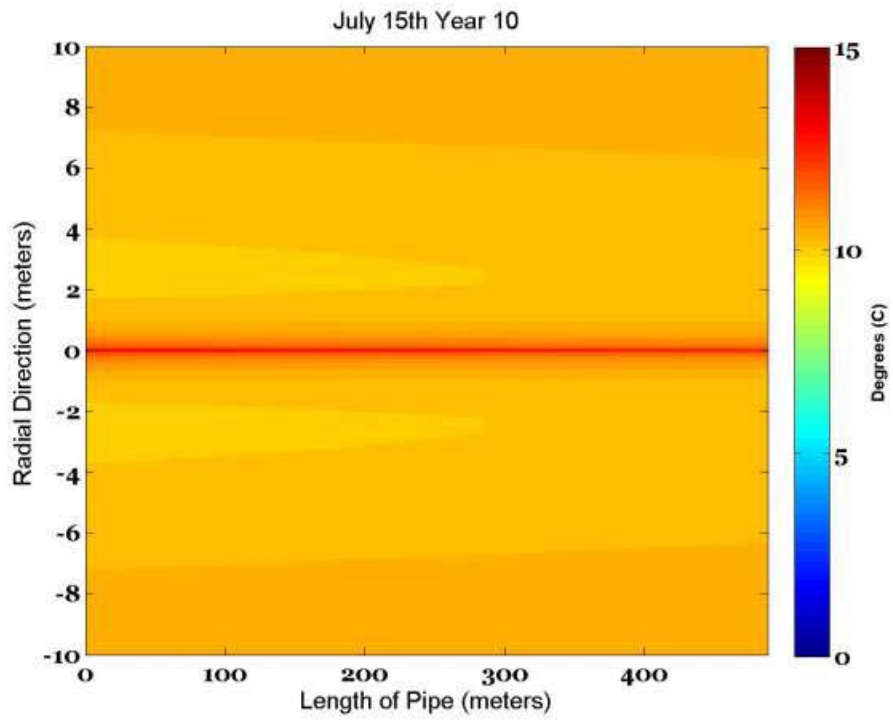


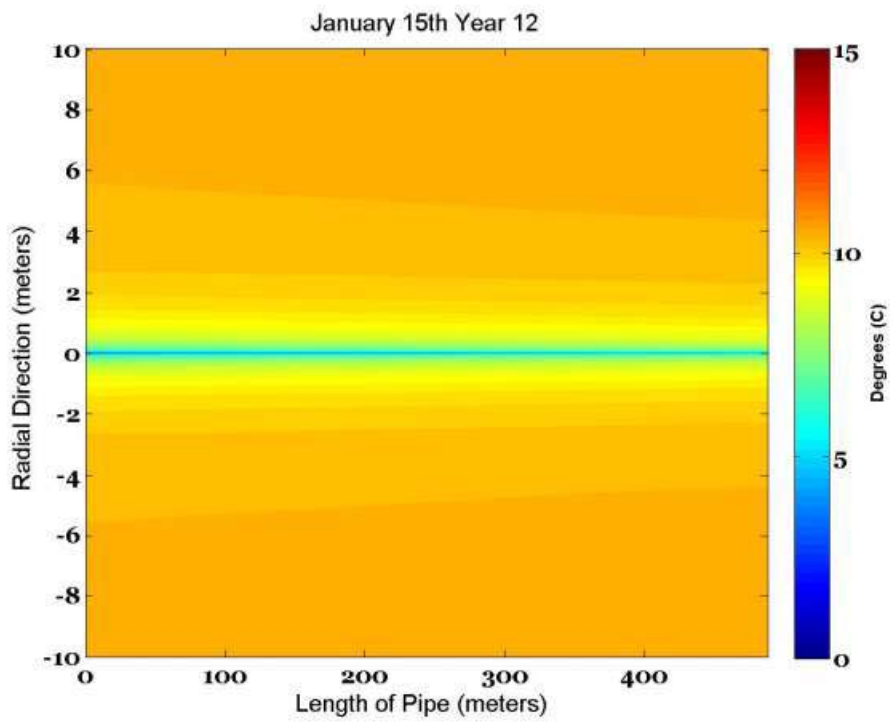
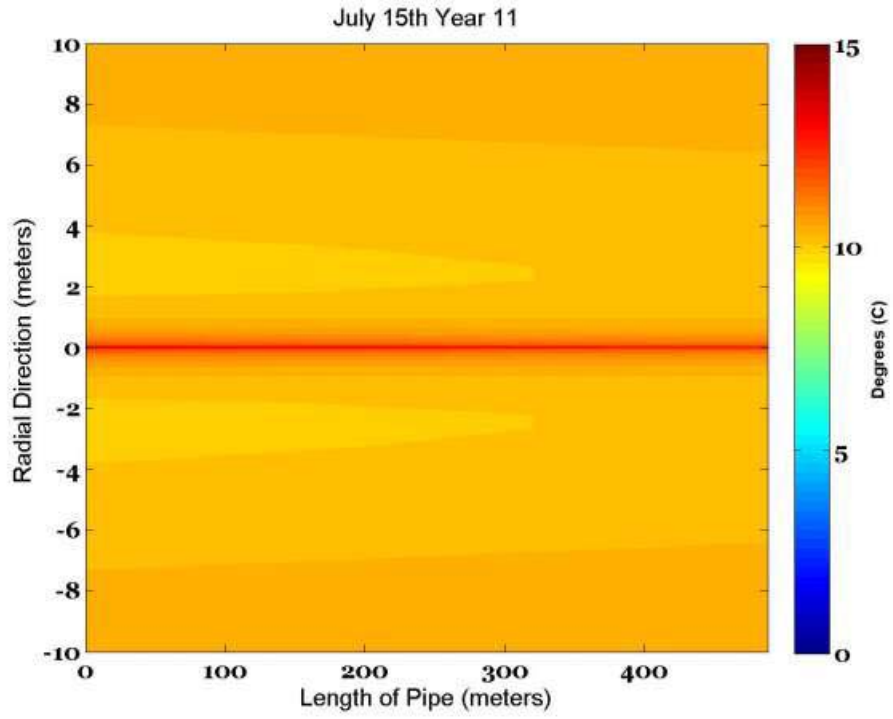


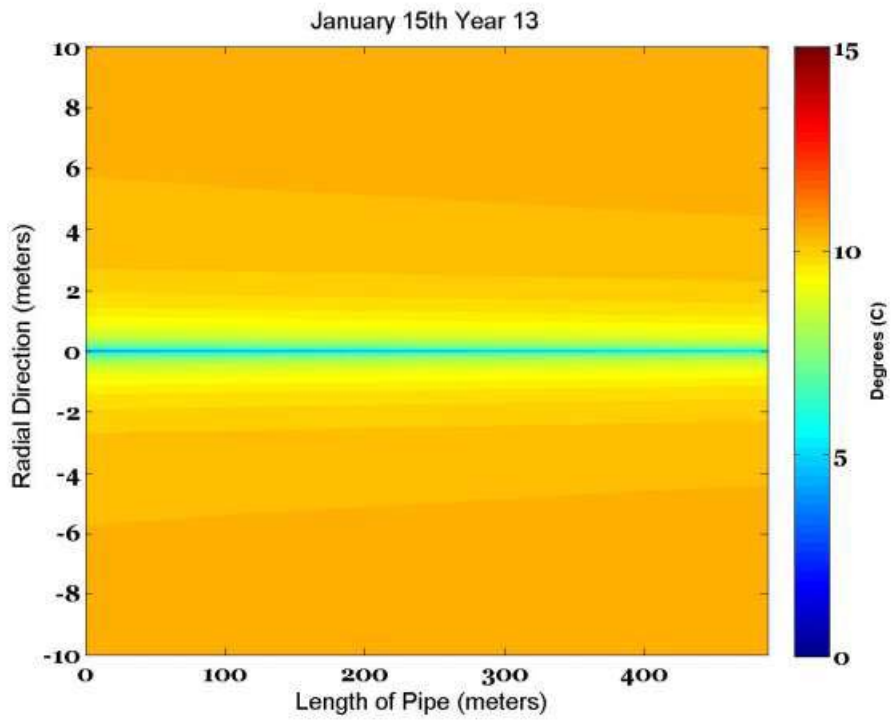
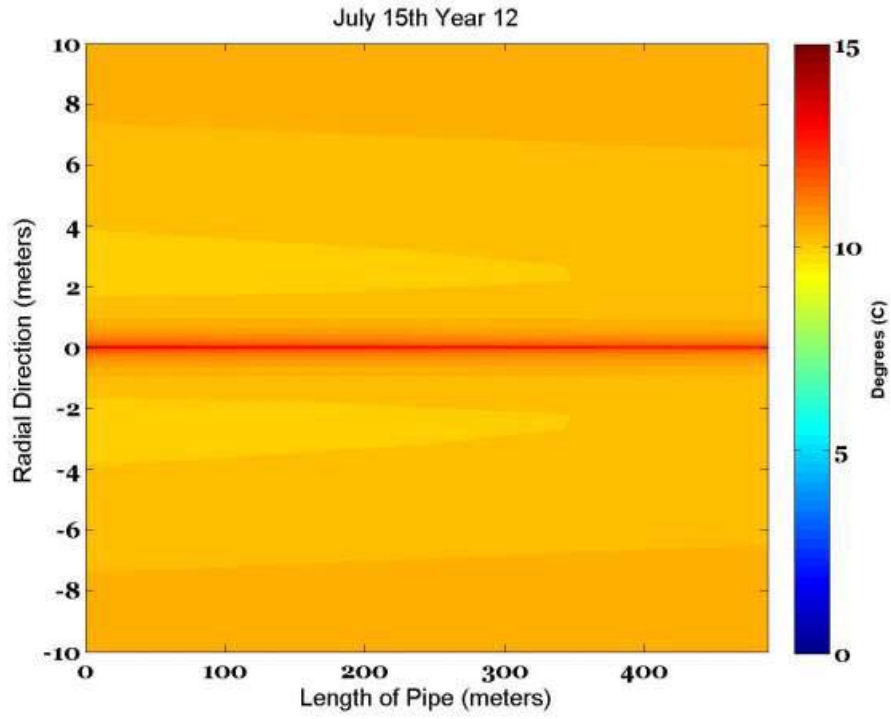


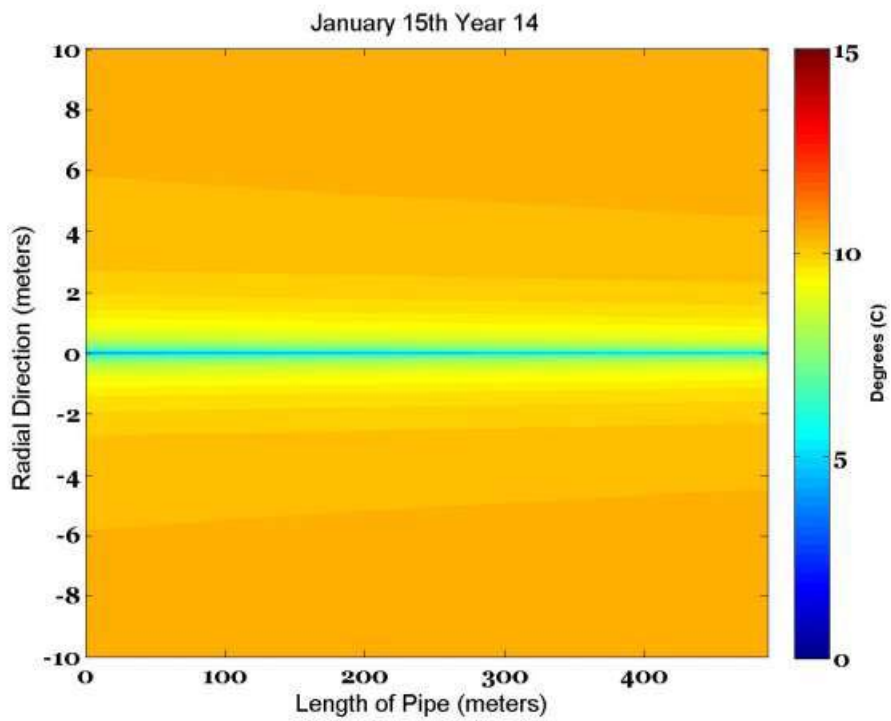
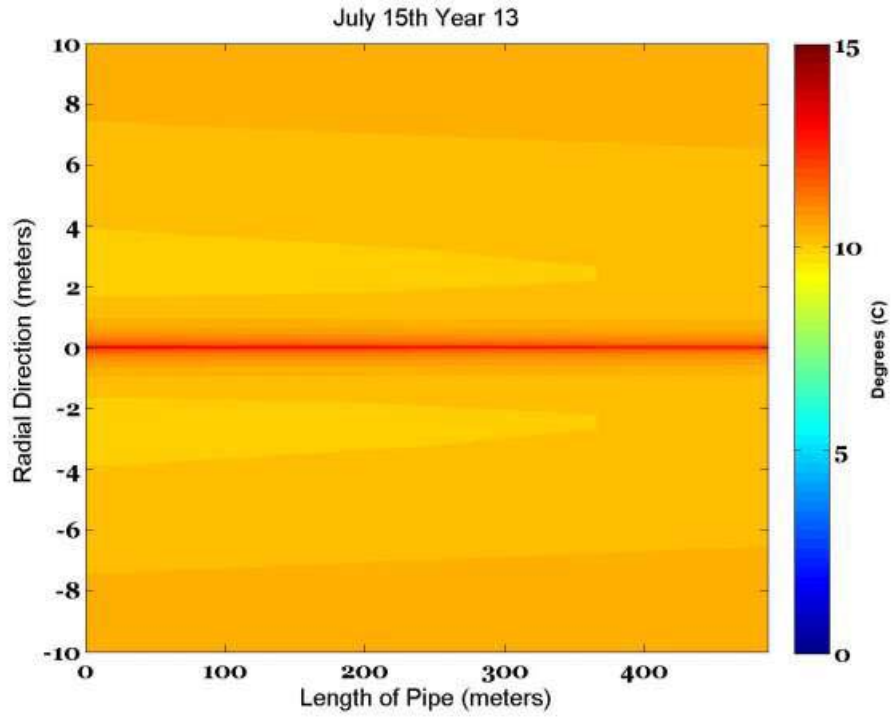


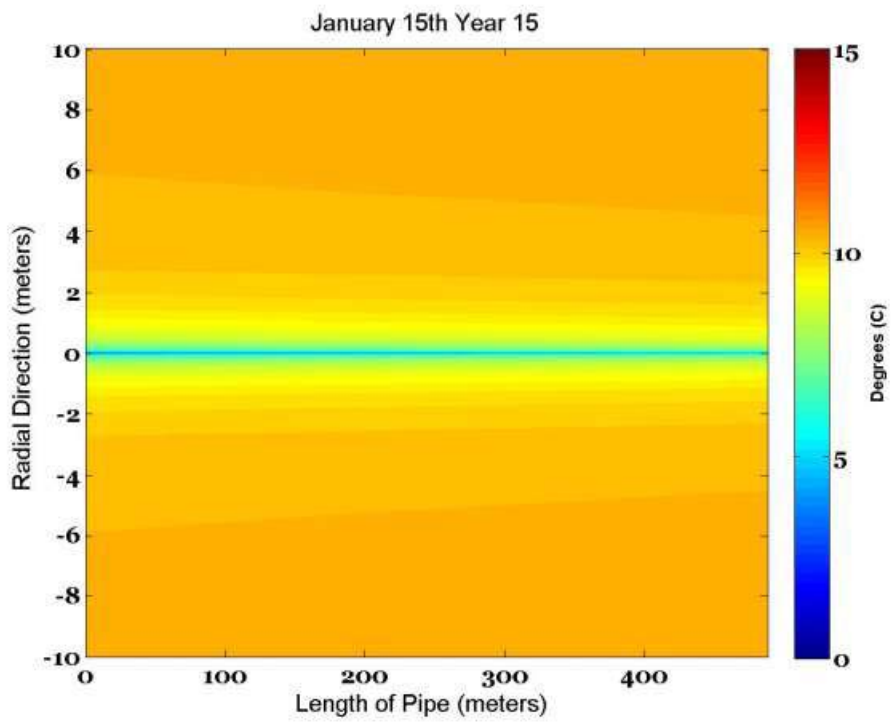
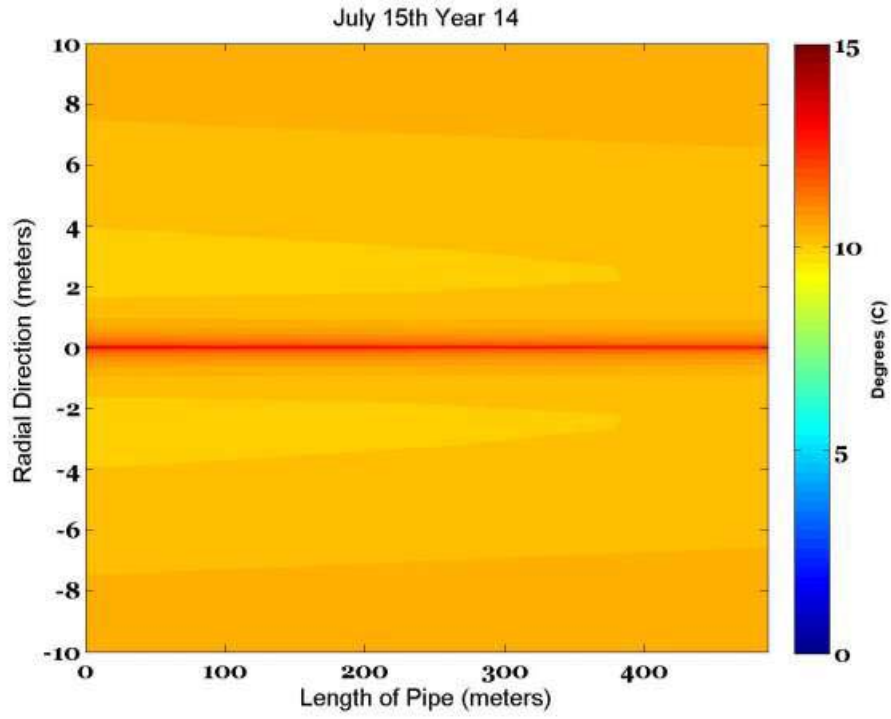


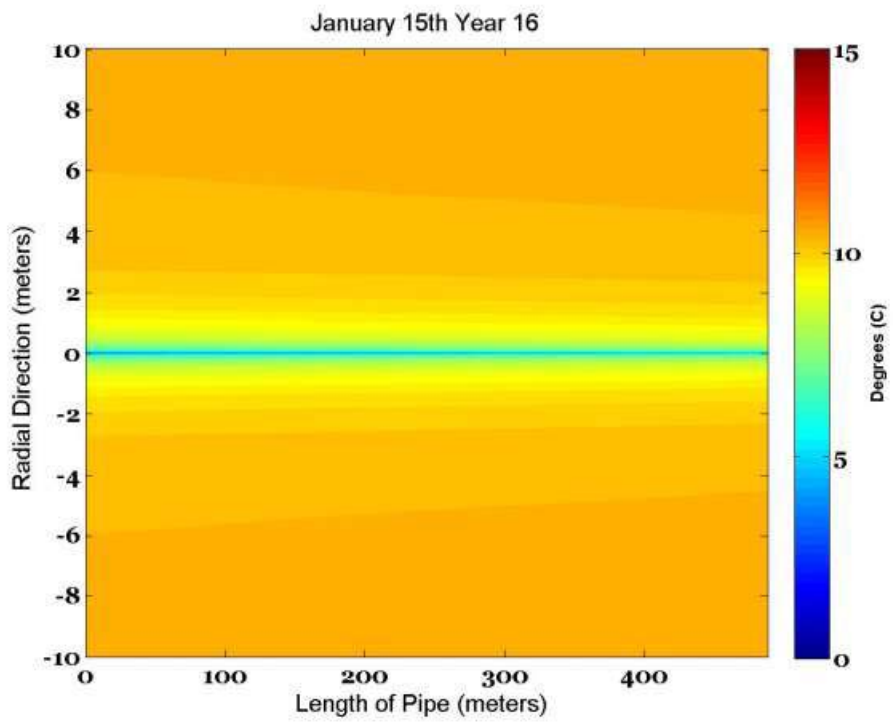
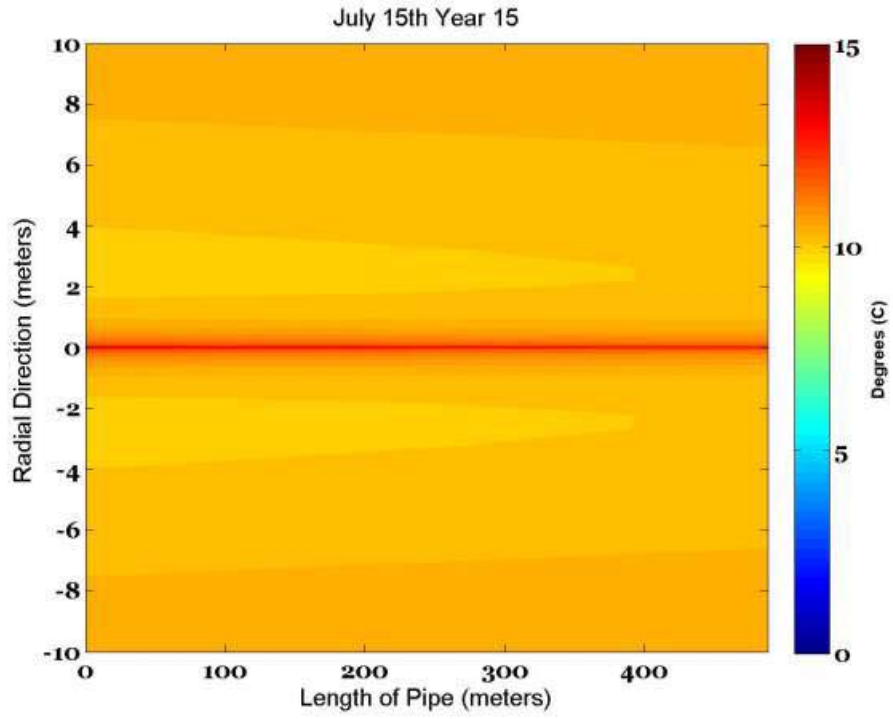


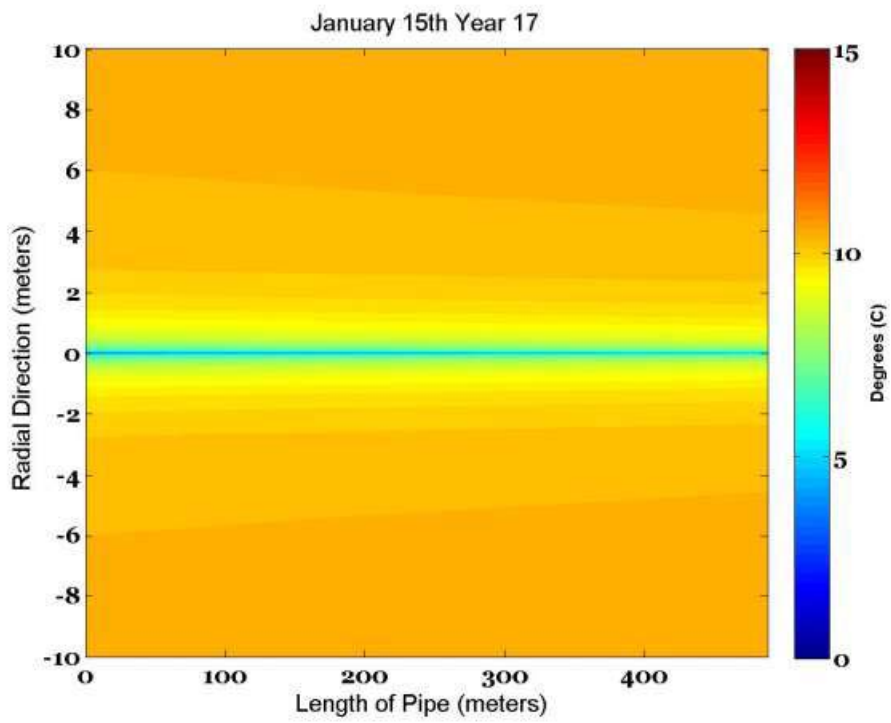
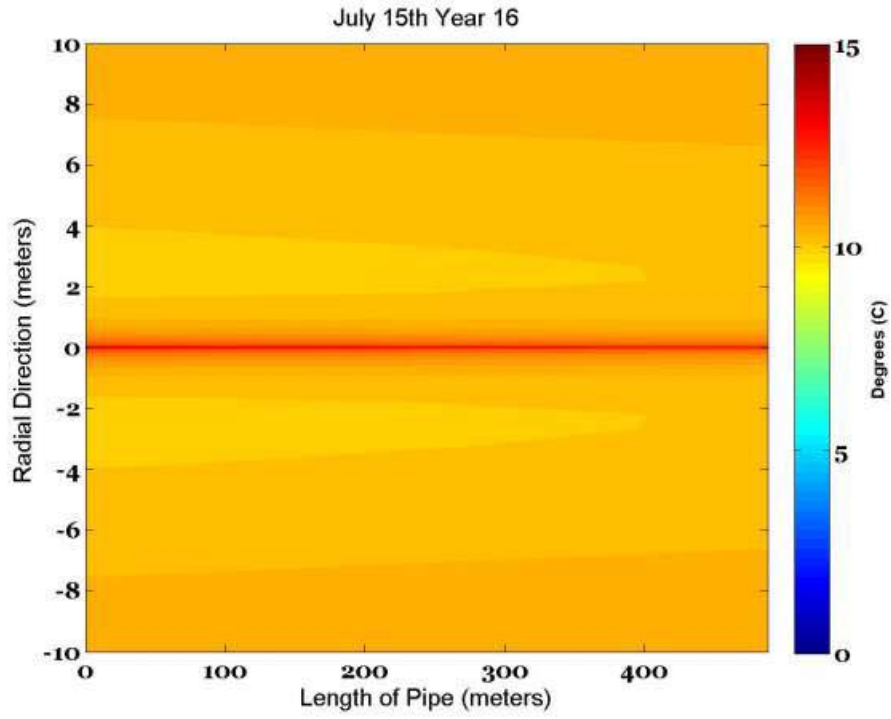


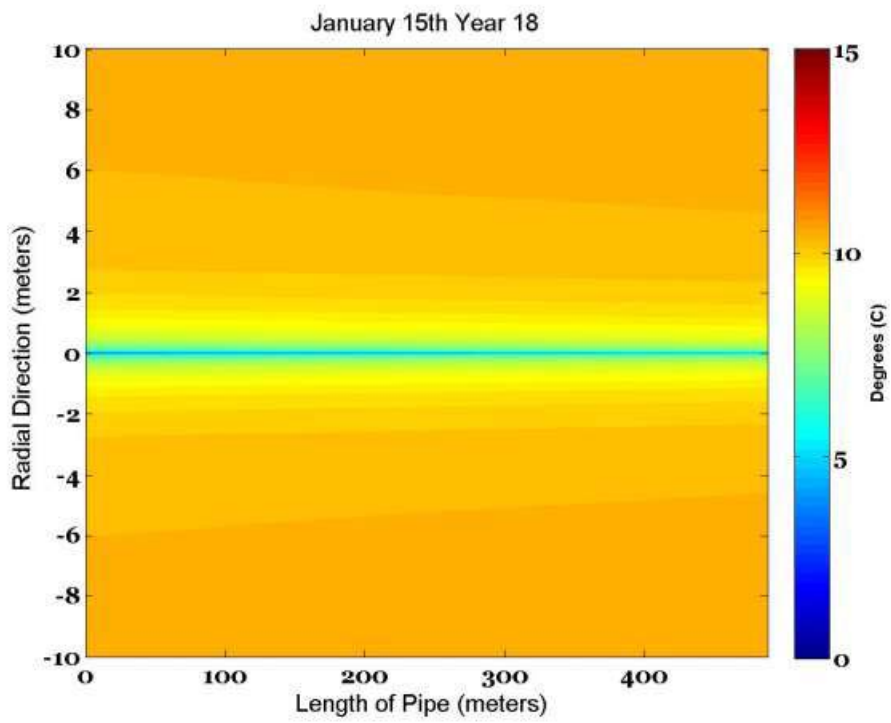
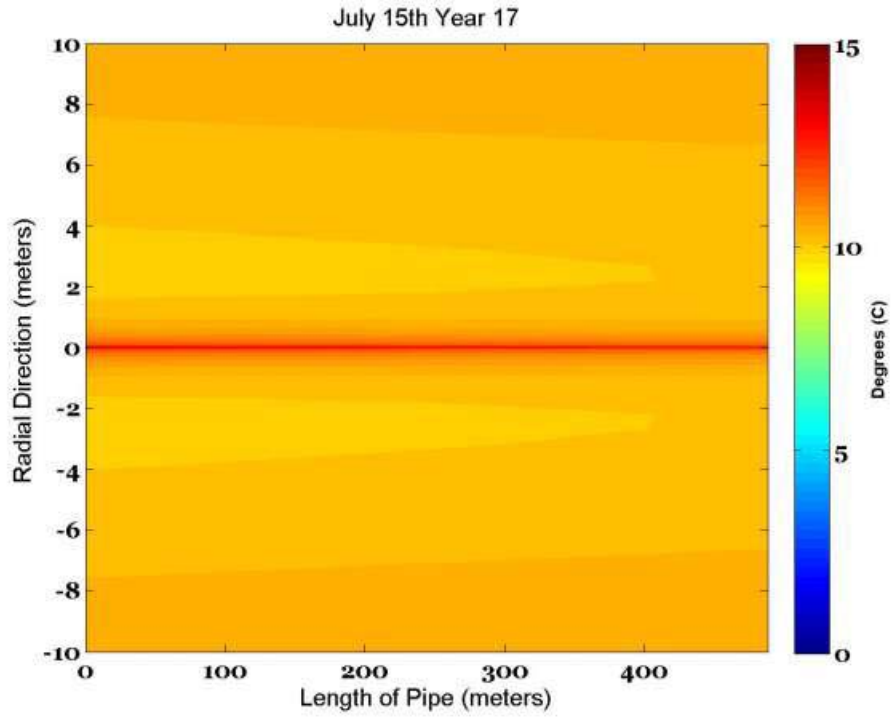


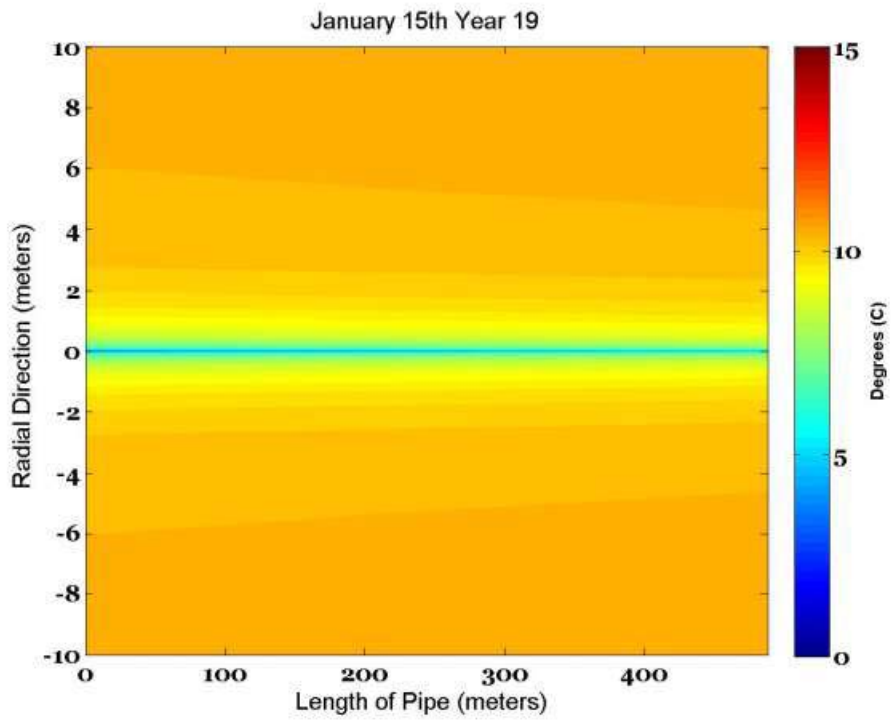
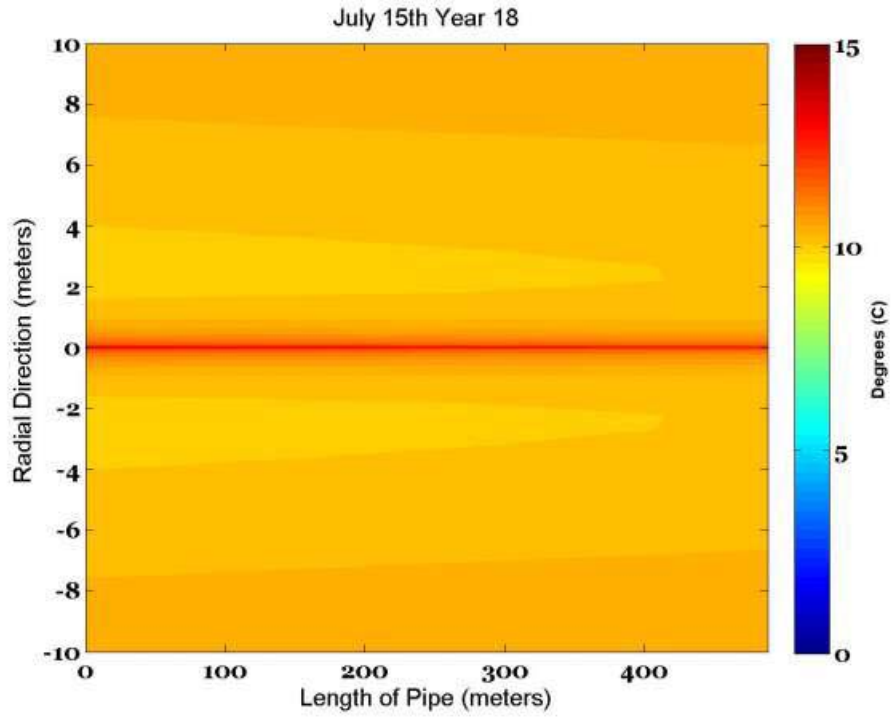


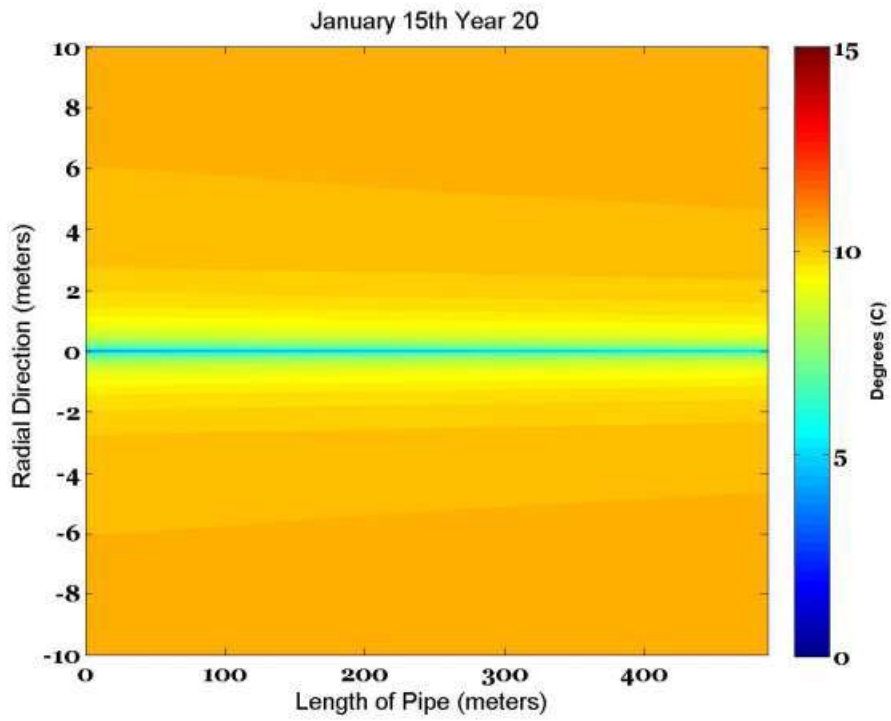
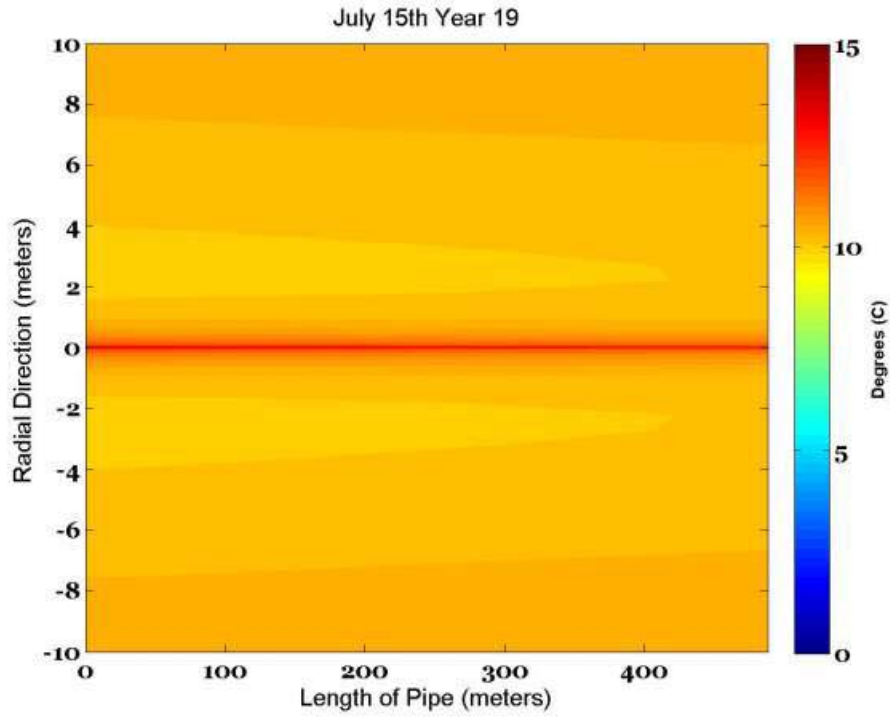


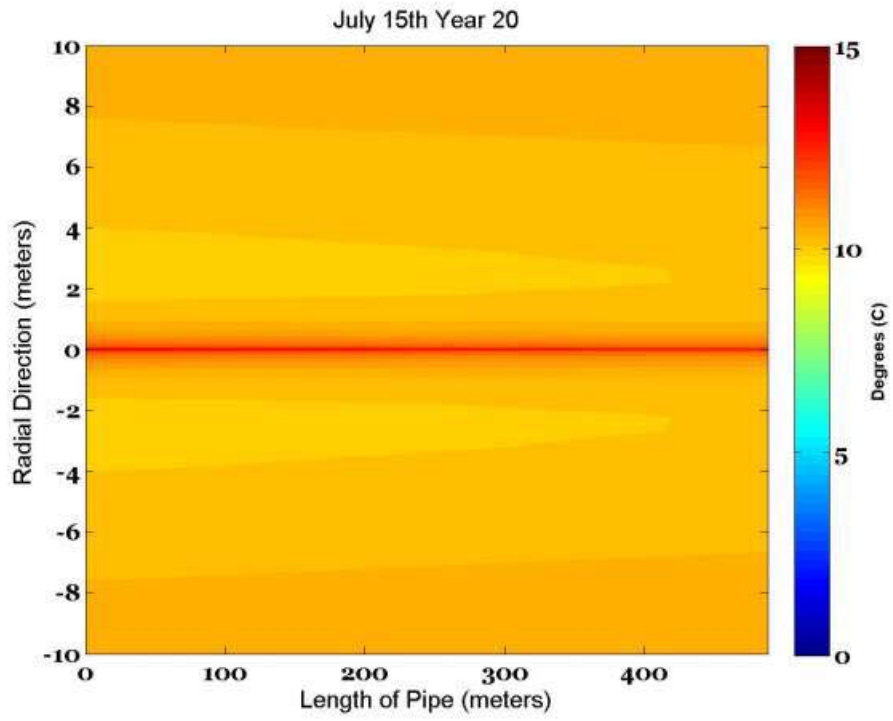












*These are temperature contour plots.

APPENDIX II: SIMULATION RESULTS FOR BOSTON, MASSACHUSETTS

Building Specifics

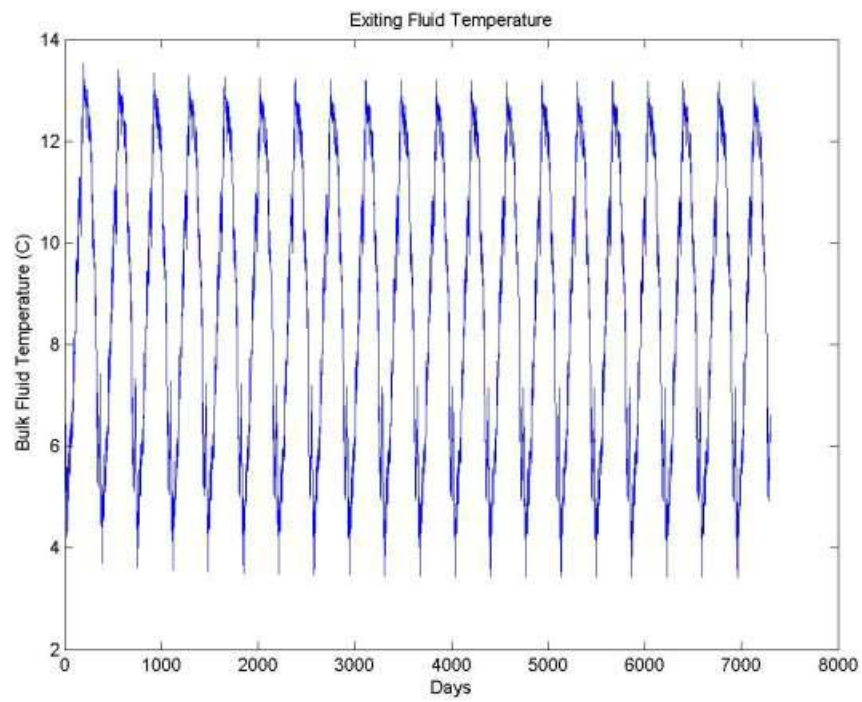
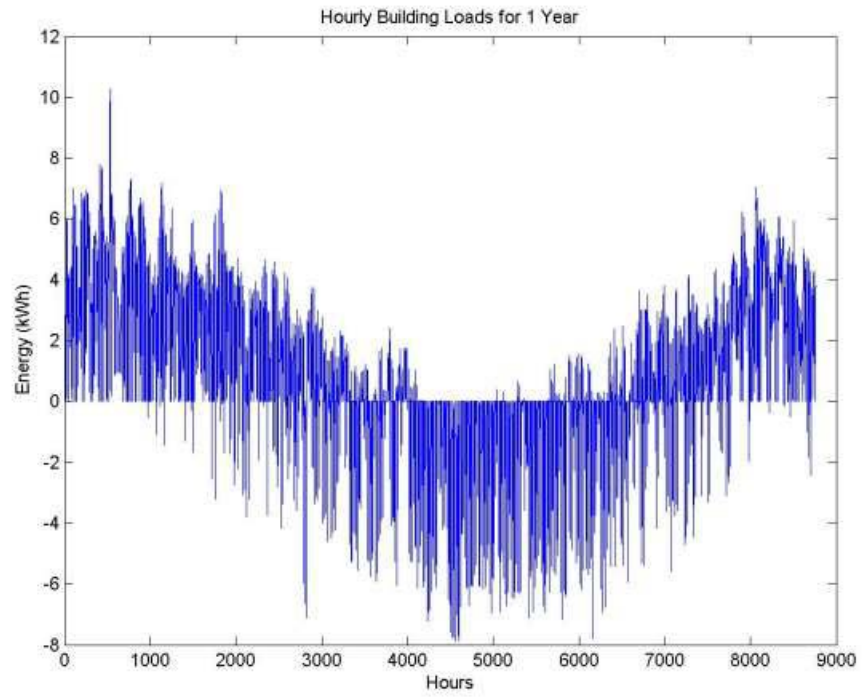
Floor plan Rectangle (18.6m x 10 m)	2000 ft ² / 186 m ²
Air Infiltration	'Moderately Sealed' (.65 ACH)
Window area	22.4 m ² / 241 ft ²
Number of exterior doors	2
Ceiling Height	8 ft. / 2.44 m
Winter Thermostat	70 °F / 21 °C
Summer Thermostat	77 °F / 25 °C
Exterior wall material layers	wood siding, 1/2" plywood, 2x4 wood studs and R11 insulation, 1/2" gypsum board
Exterior Ceiling/Attic material Layers	R-13, 2x6 wood studs, gypsum board

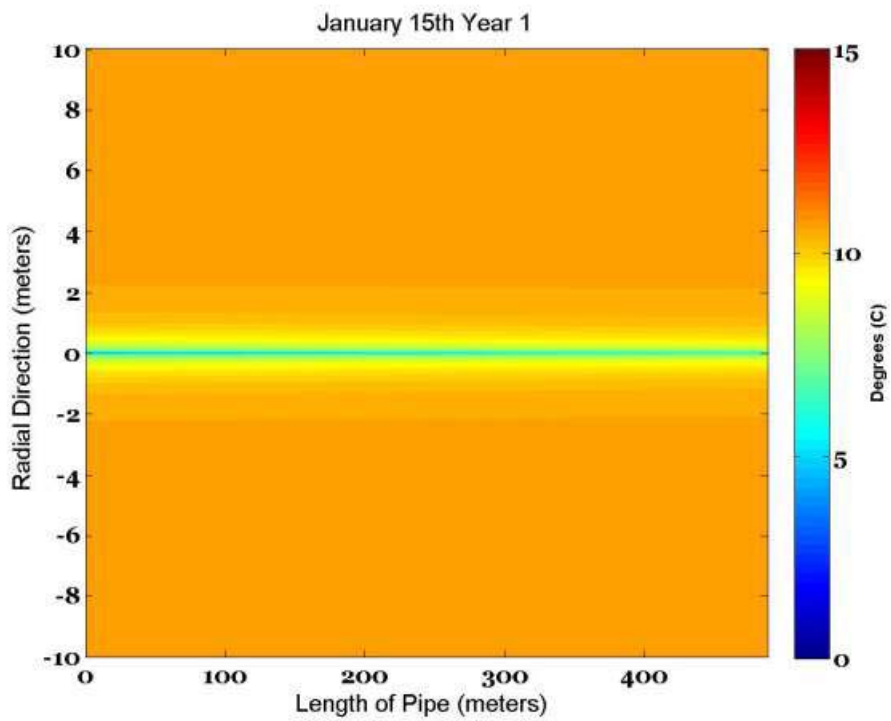
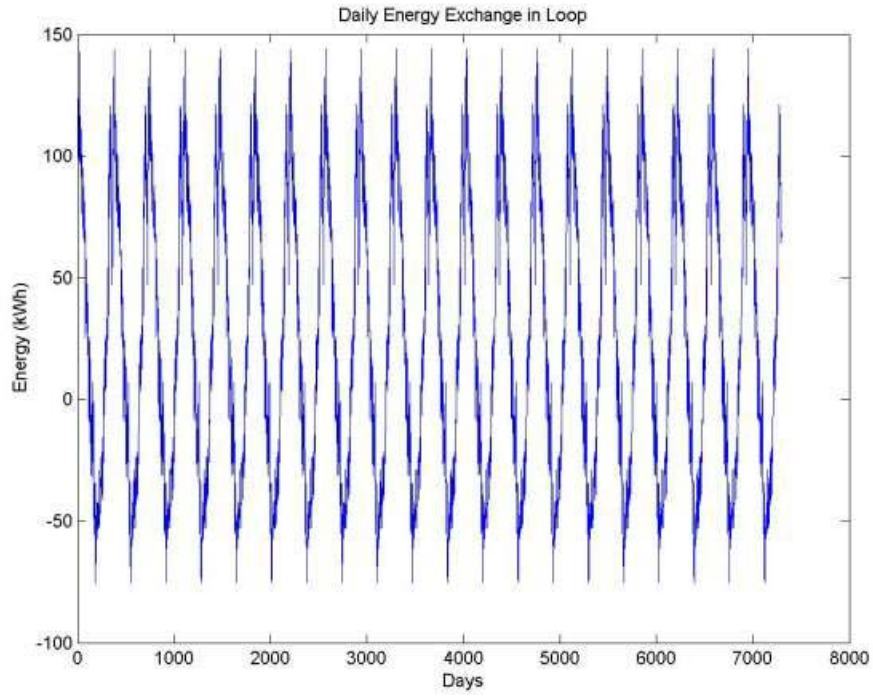
Building Load Analysis

Peak Cooling Load	7874 Whr
Peak Heating Load	10,259 Whr
Extreme Low Outdoor Drybulb	-20 °C
Extreme High Outdoor Drybulb	37.2 °C
Chosen Heat Pump Size	4 ton unit

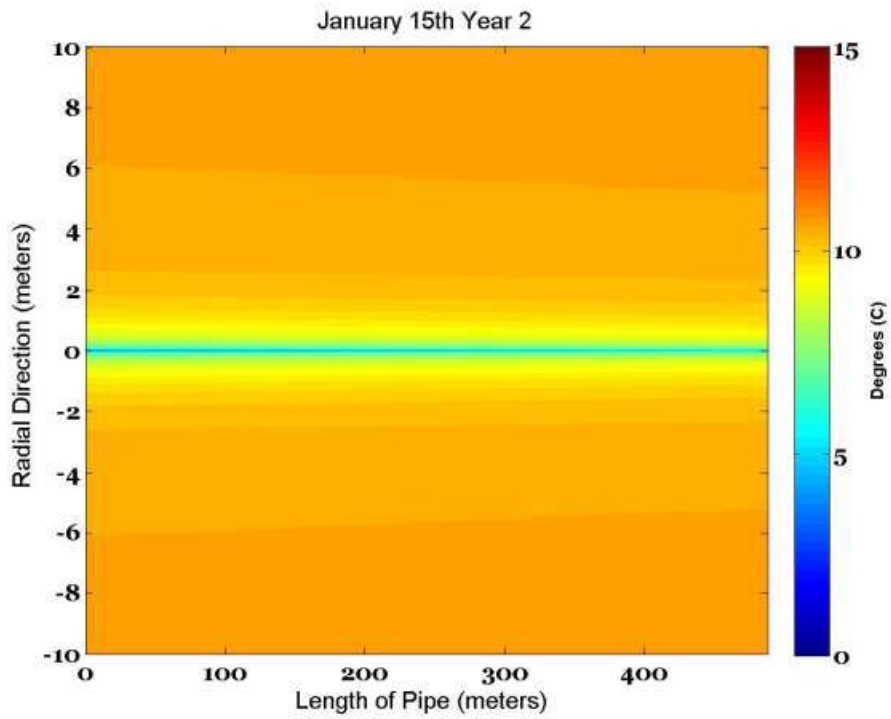
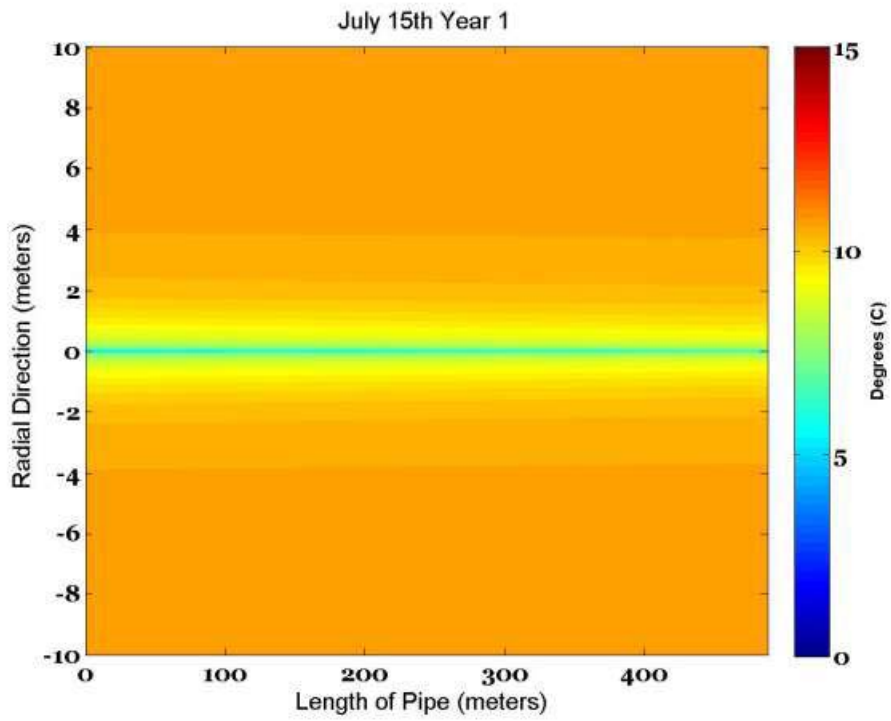
Geothermal Design Inputs

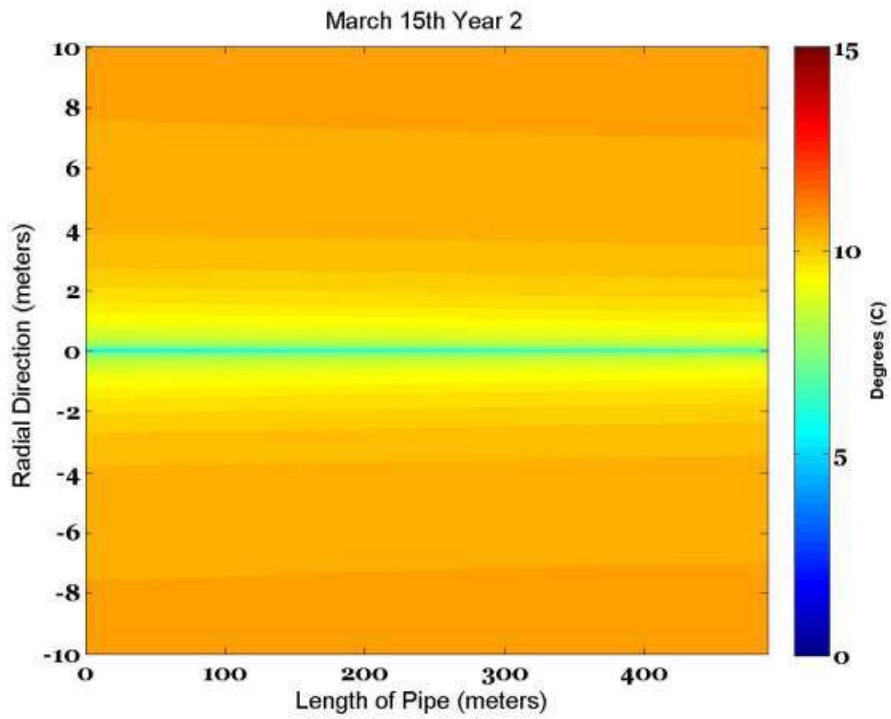
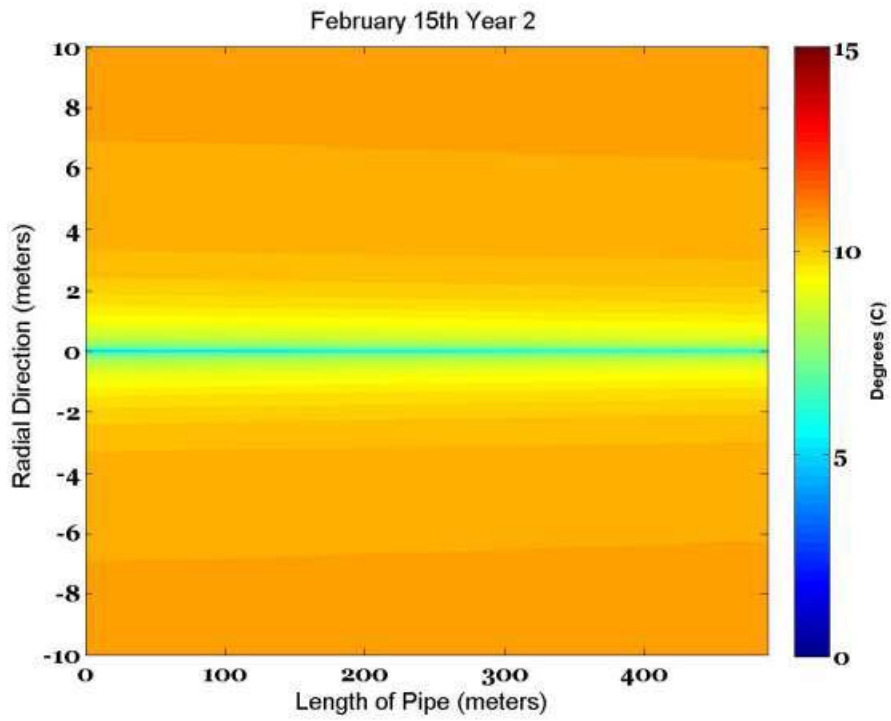
Time step	Daily
Years simulated	20 years
Length of tube	488 m
Inner Radius of pipe	15.011 mm
Thickness of Pipe Wall	3.378 mm
Fluid Thermal Conductivity (water)	0.58 W/m-C
Fluid Specific Heat	4220 J/kg-C
Fluid Density	1002 kg/m ³
Fluid Dynamic Viscosity	0.001 N-s/m ²
Tube Thermal Conductivity	0.49 W/m-C
Tube Specific Heat	1340 J/kg-C
Tube Density	941 kg/m ³
Earth Thermal Conductivity	1.3 W/m-C
Earth Specific Heat	1813 J/kg-C
Earth Density	1280 kg/m ³
Fluid Velocity	0.99818 m/s
Earth Temperature	10.6 °C
Fluid Initial Temperature	5 °C

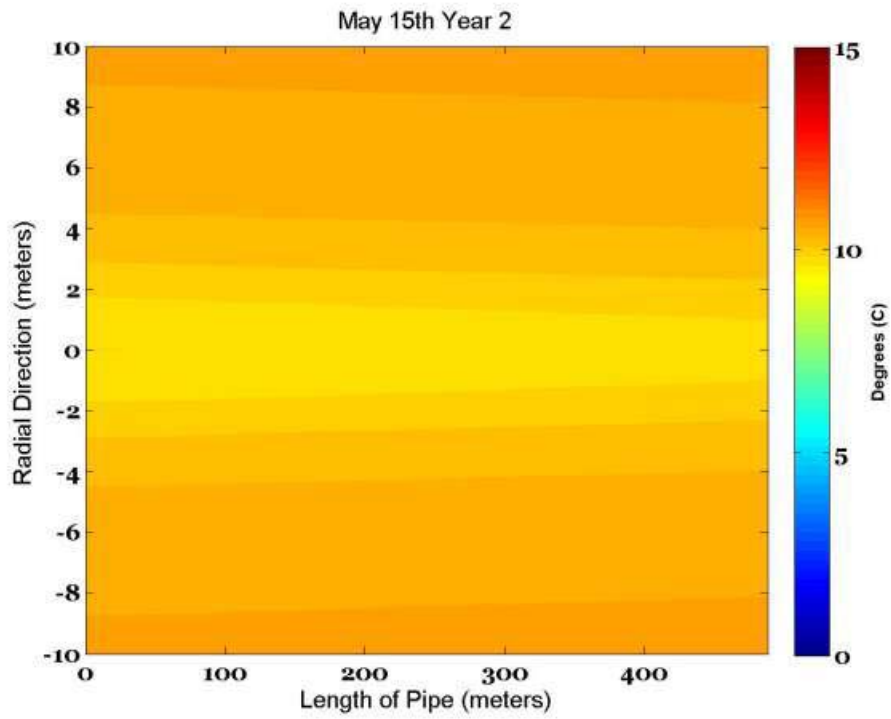
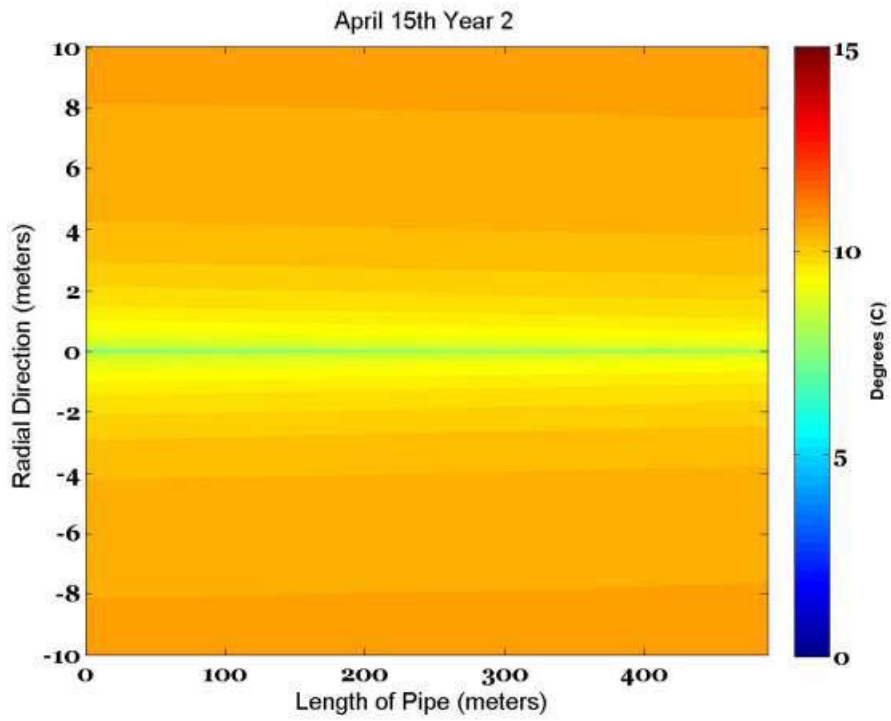


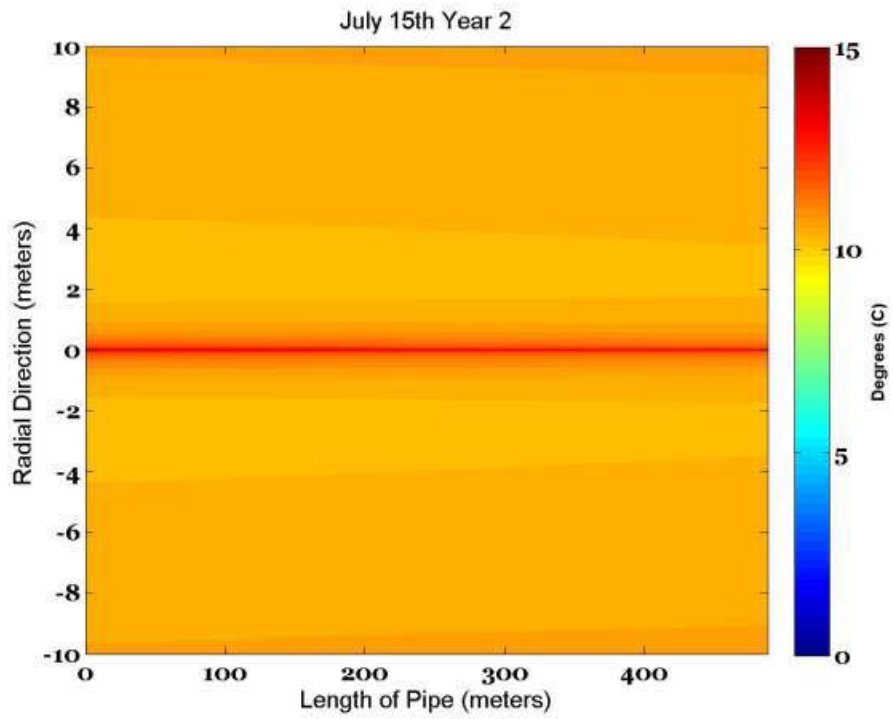
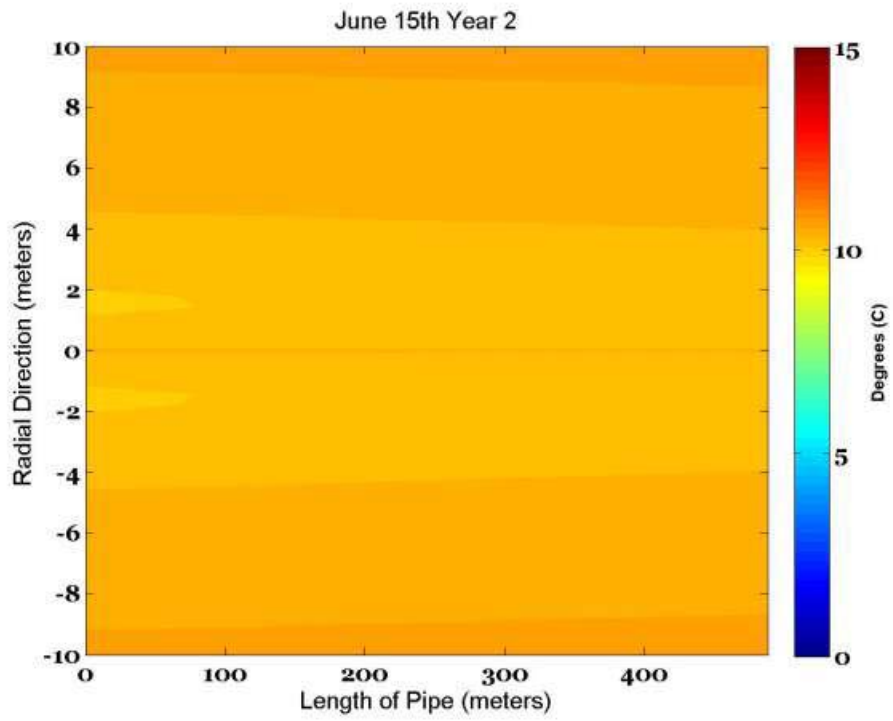


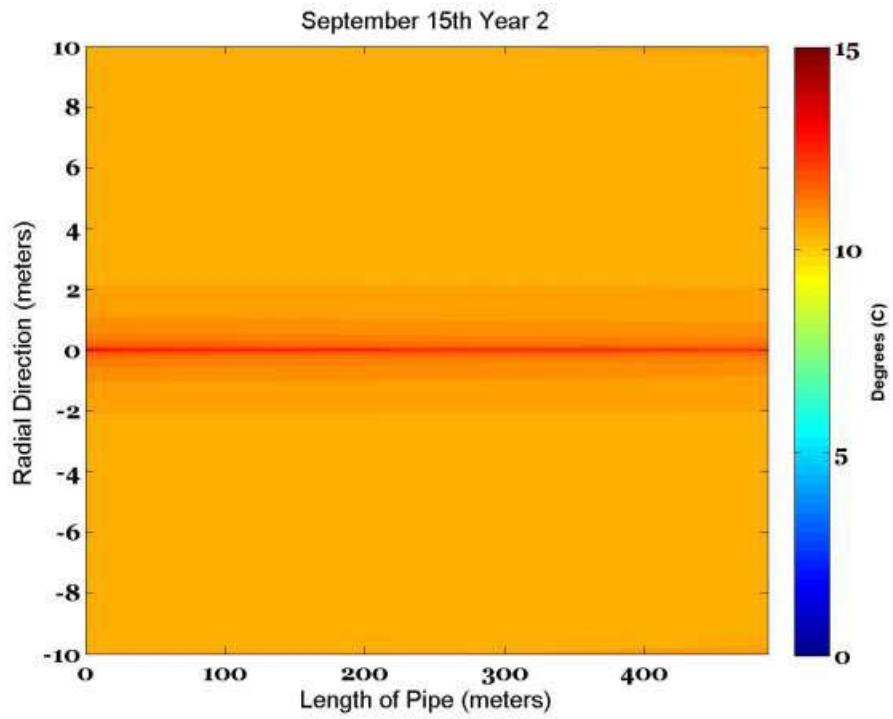
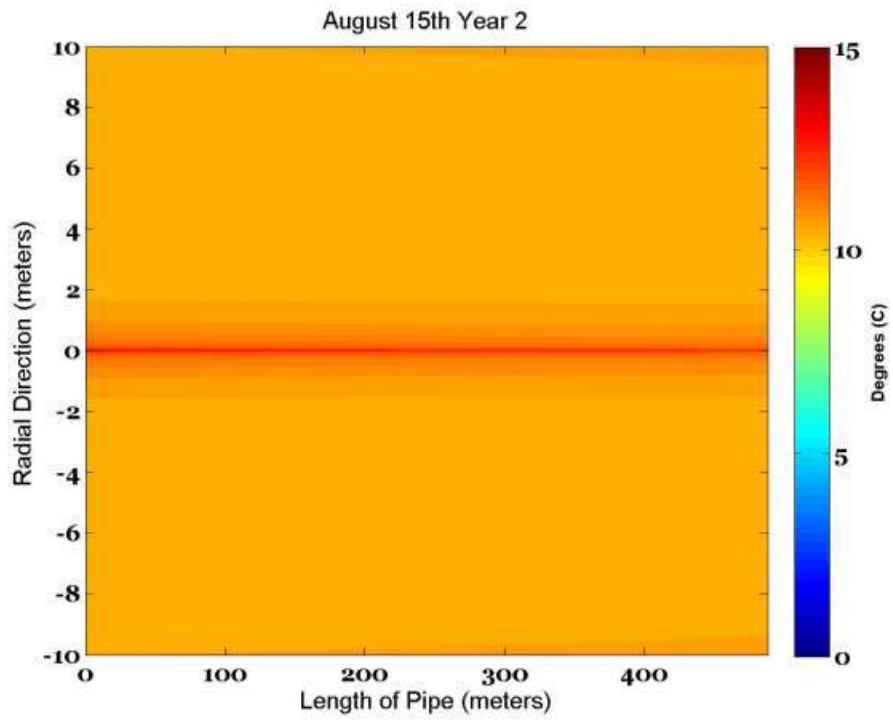
*These are temperature contour plots.

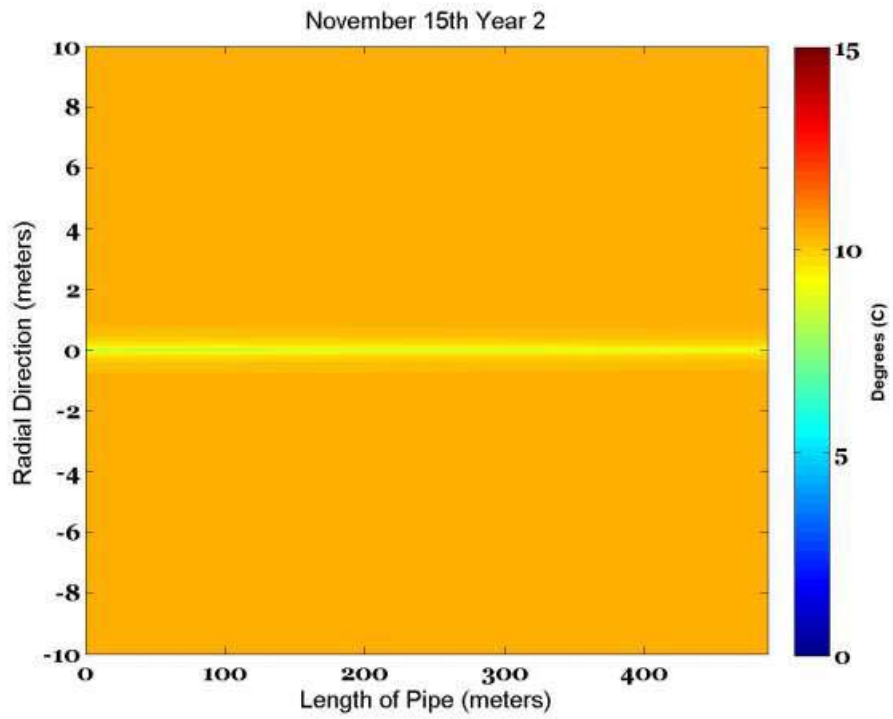
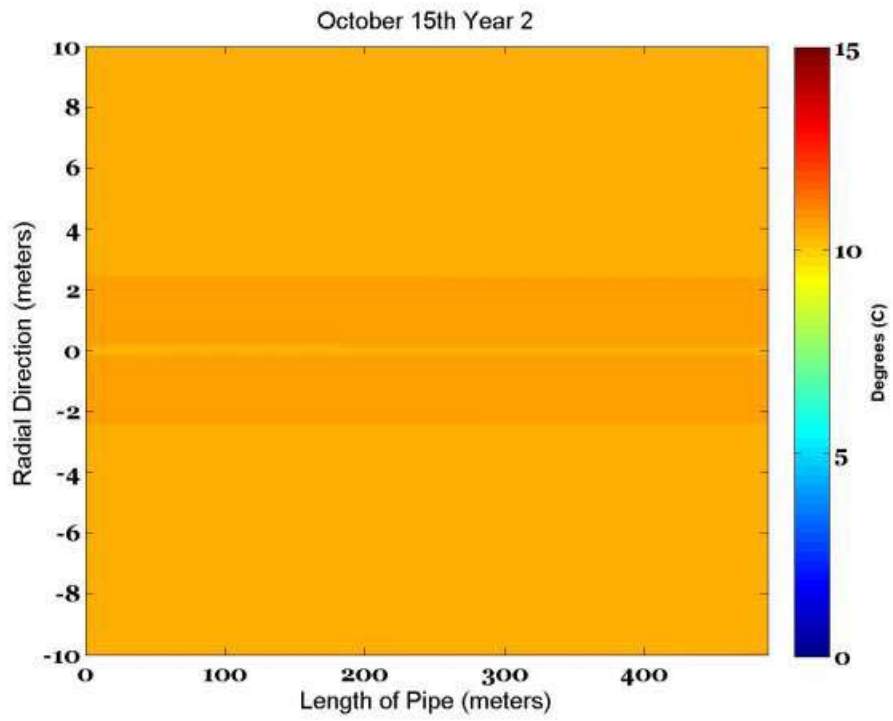


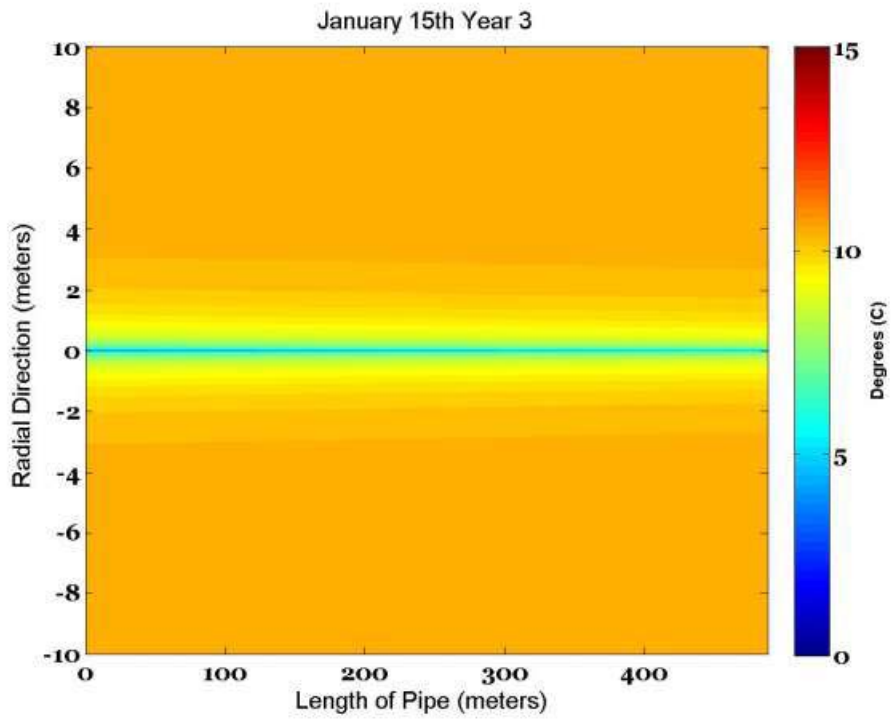
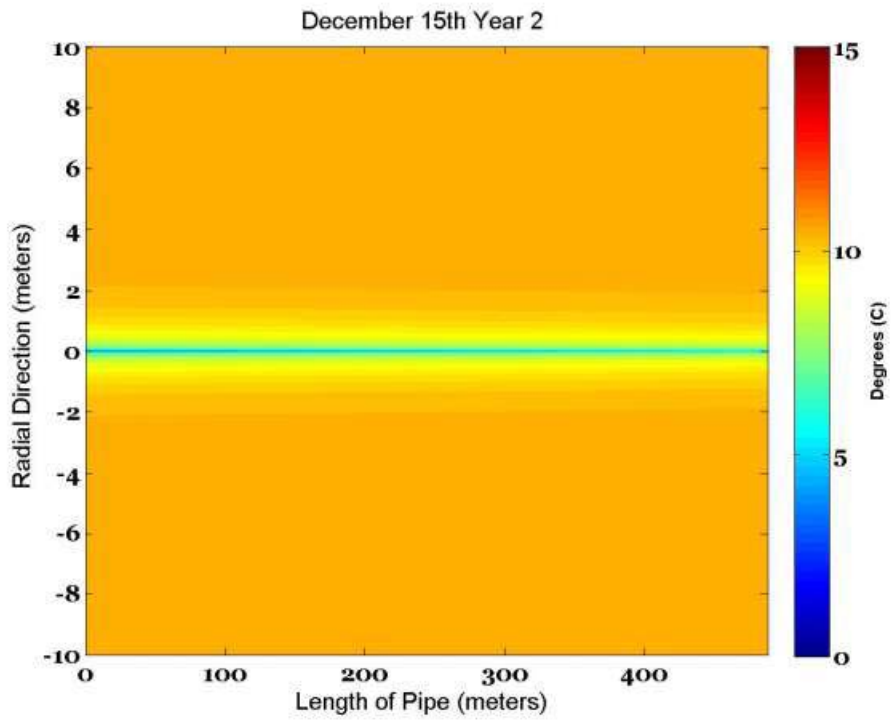


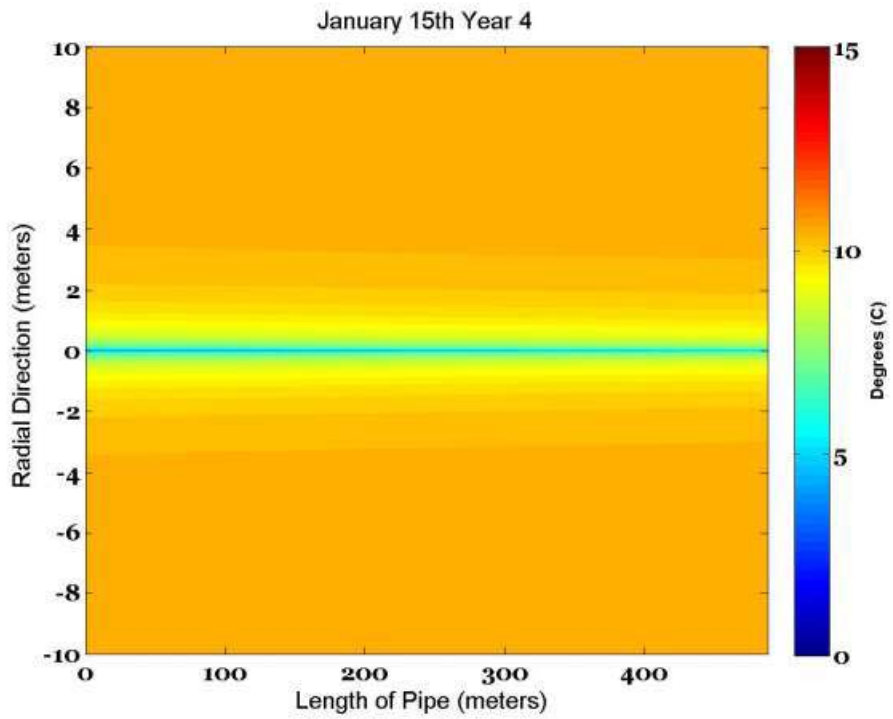
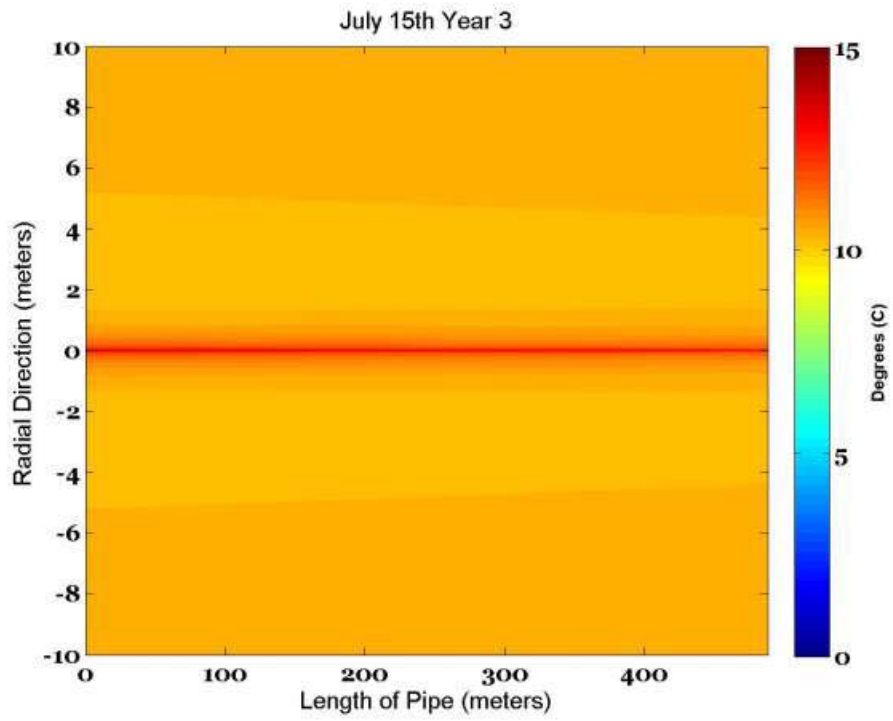


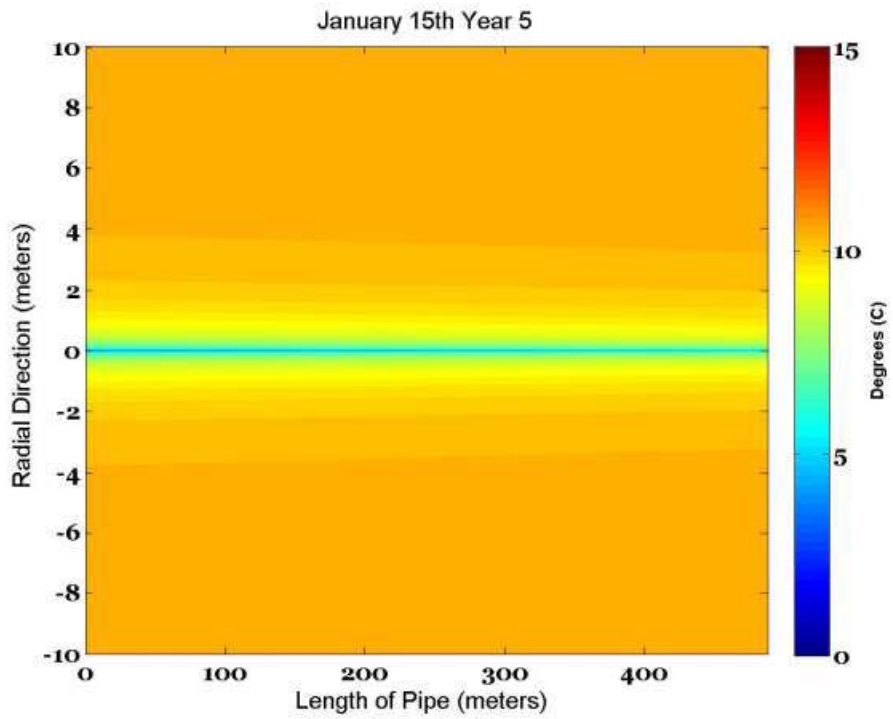
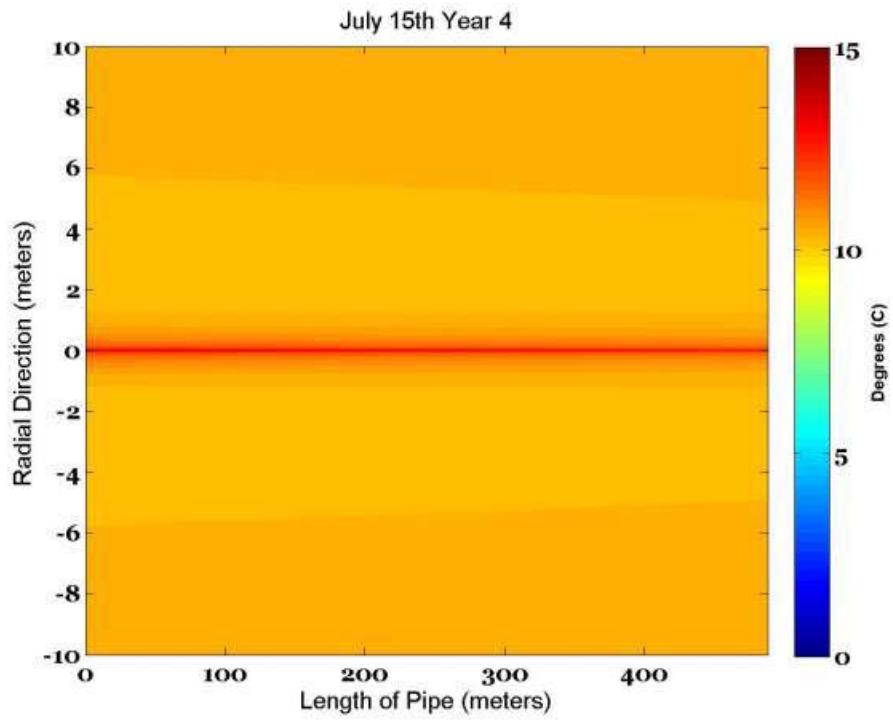


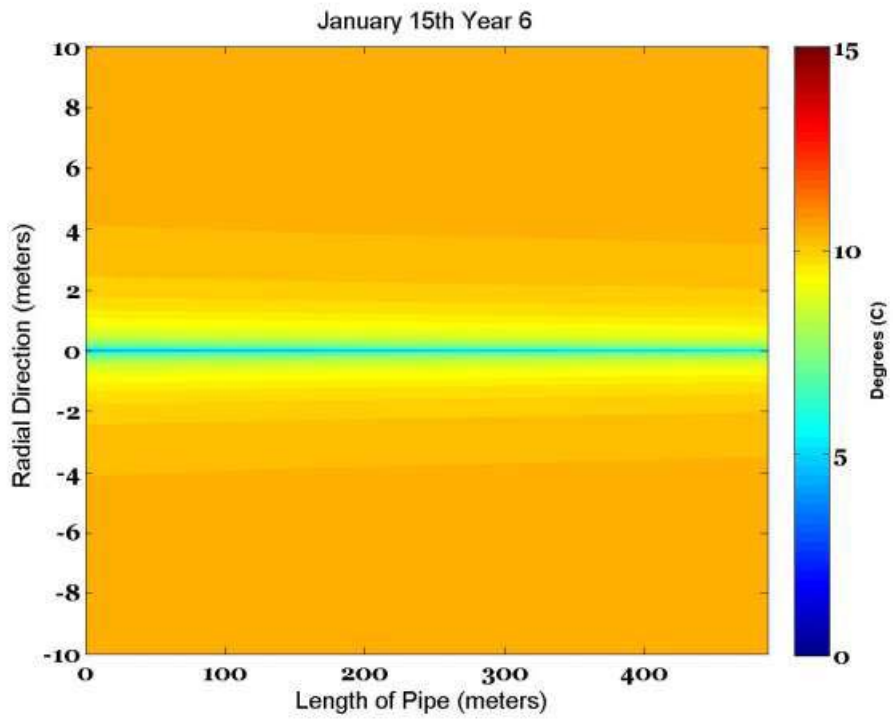
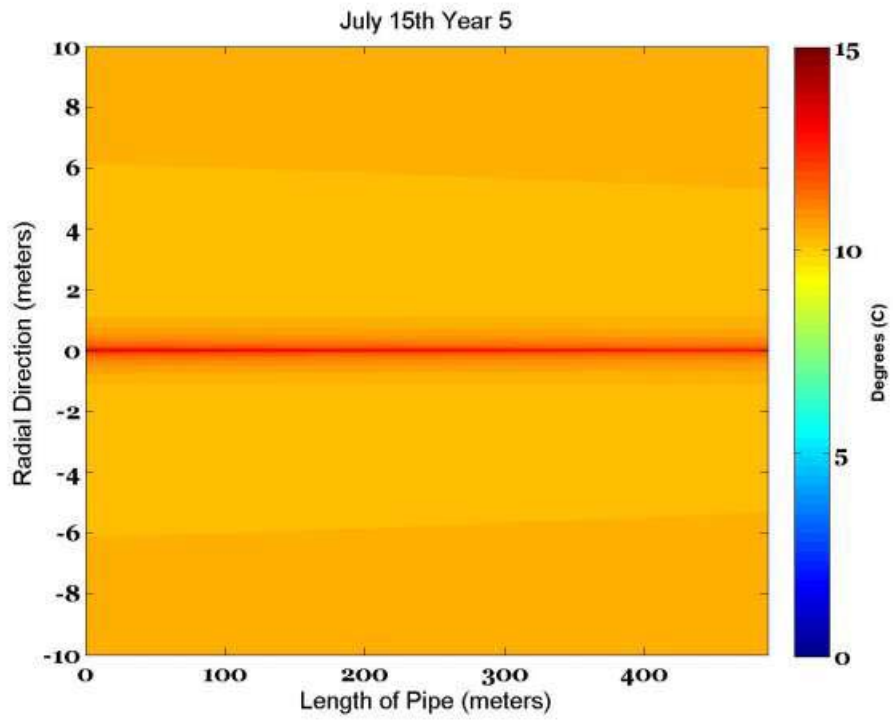


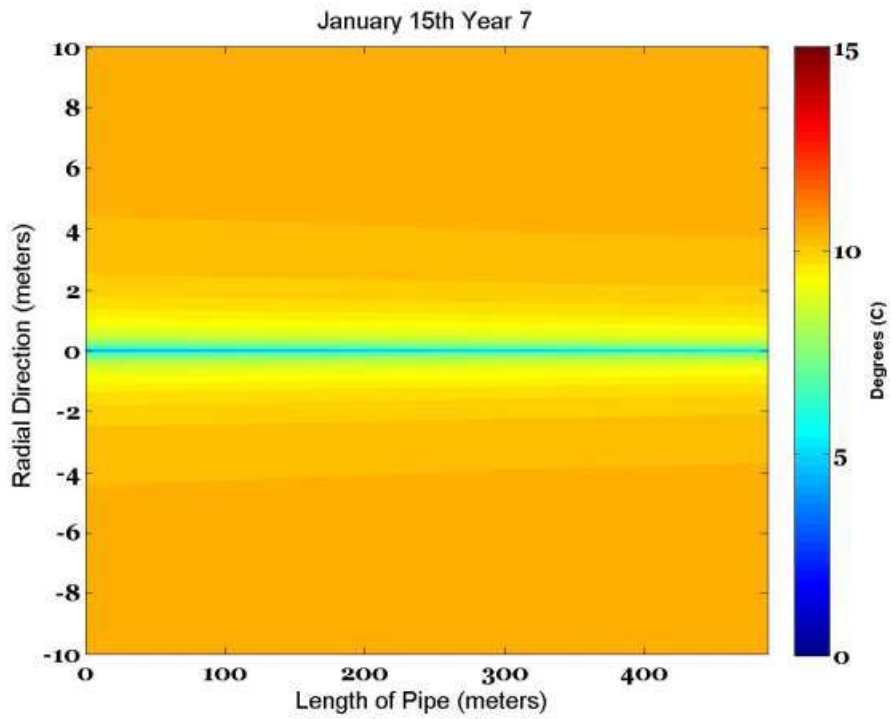
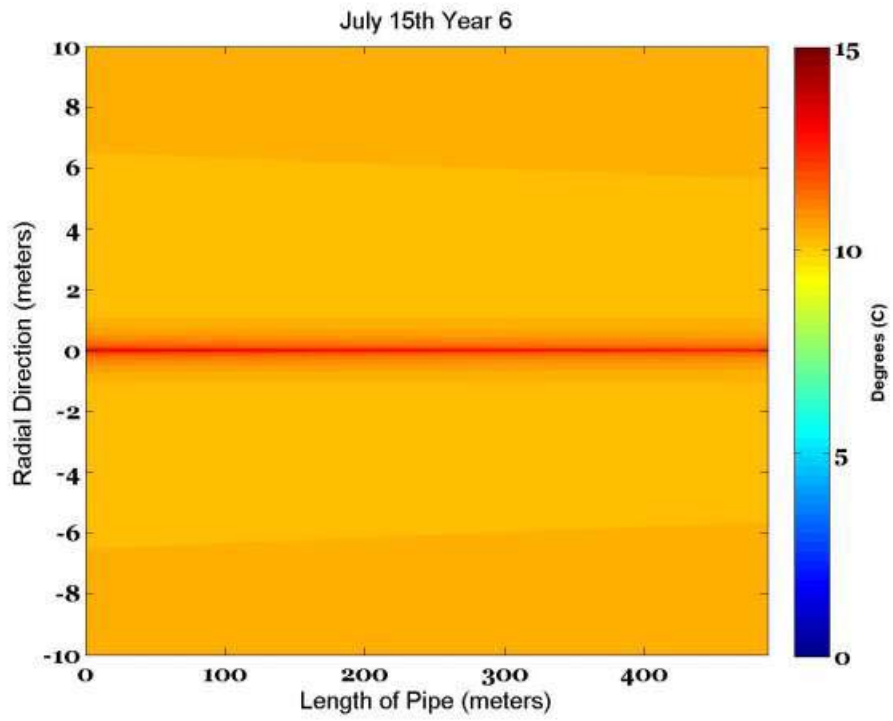


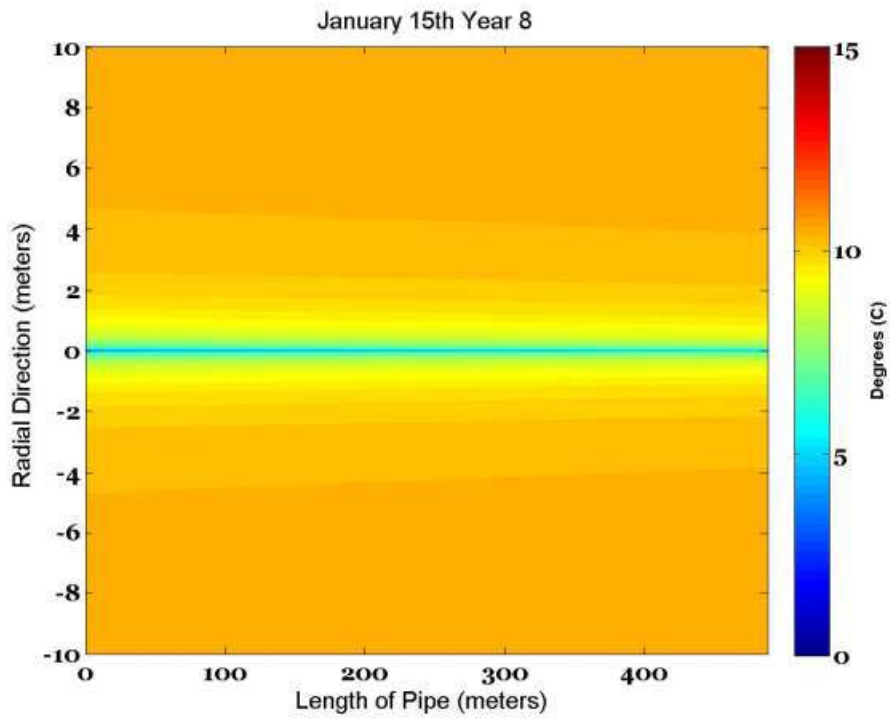
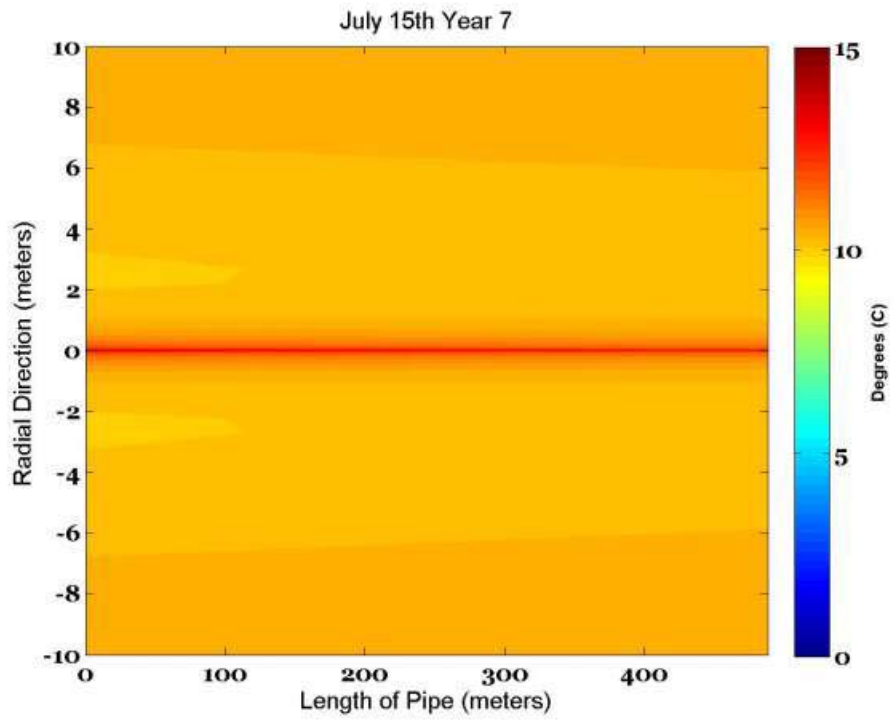


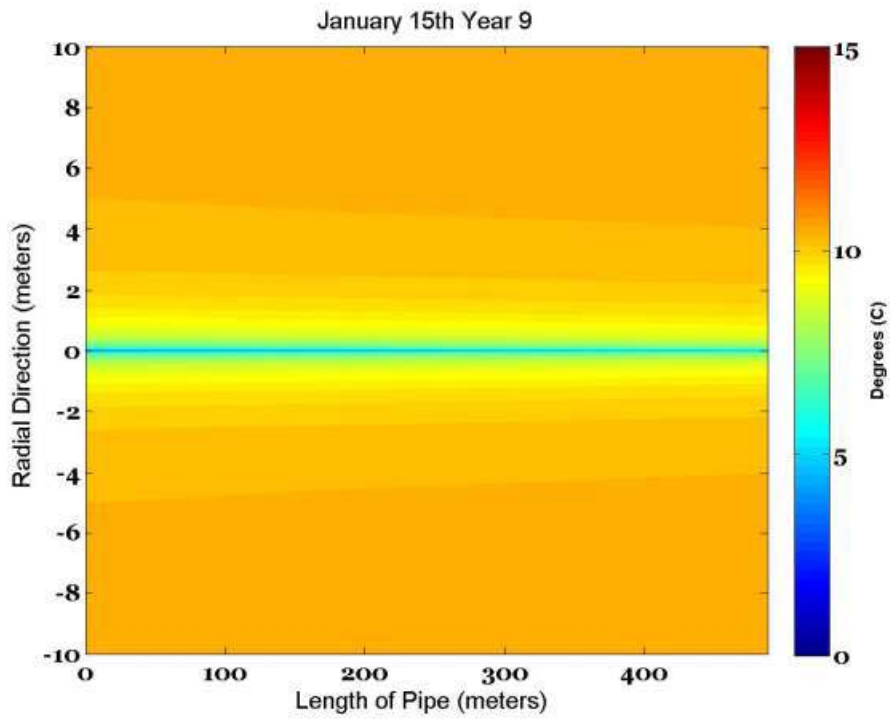
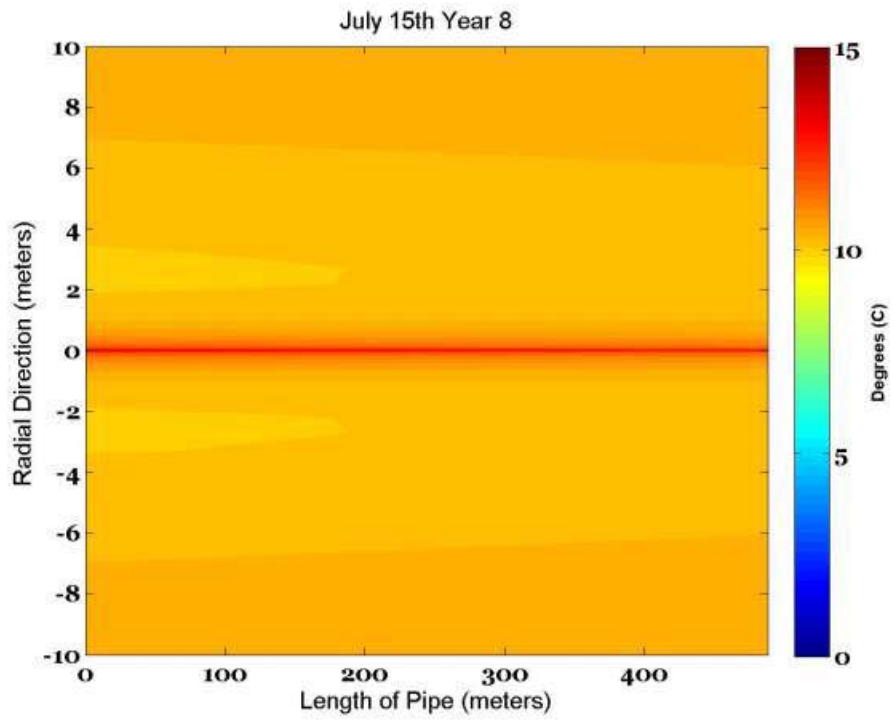


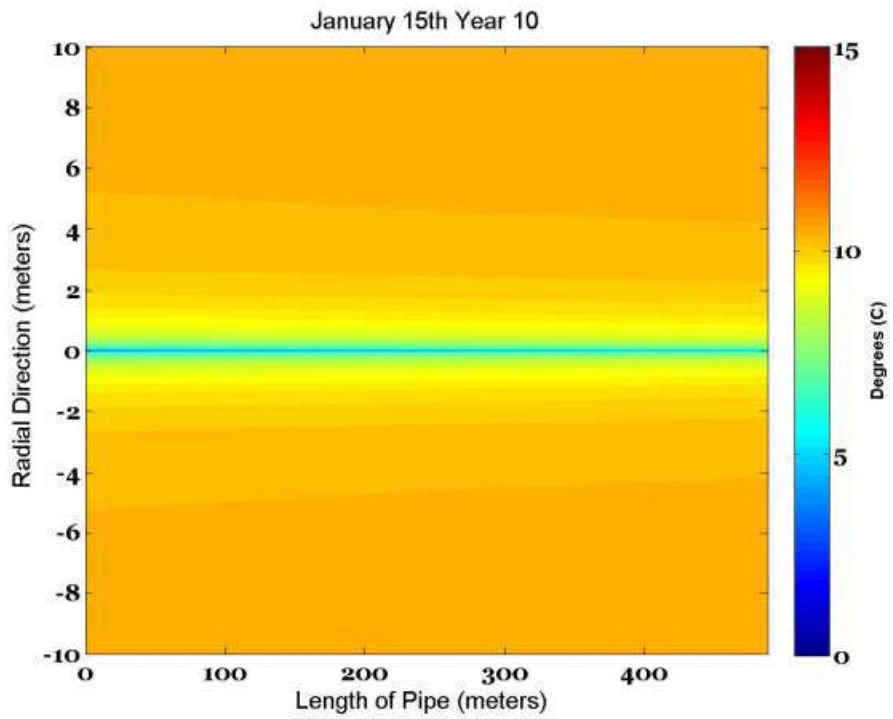
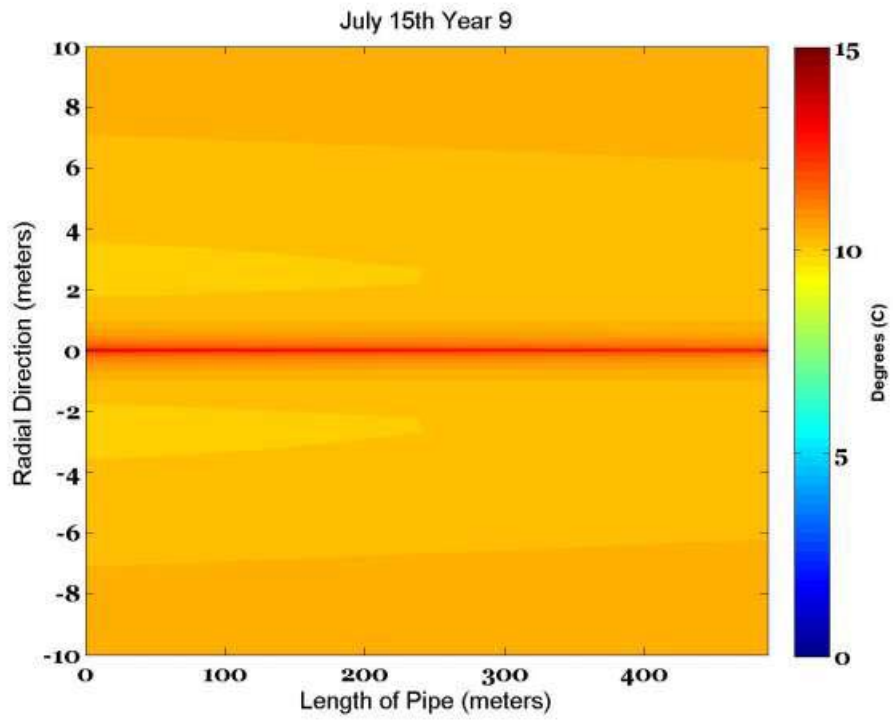


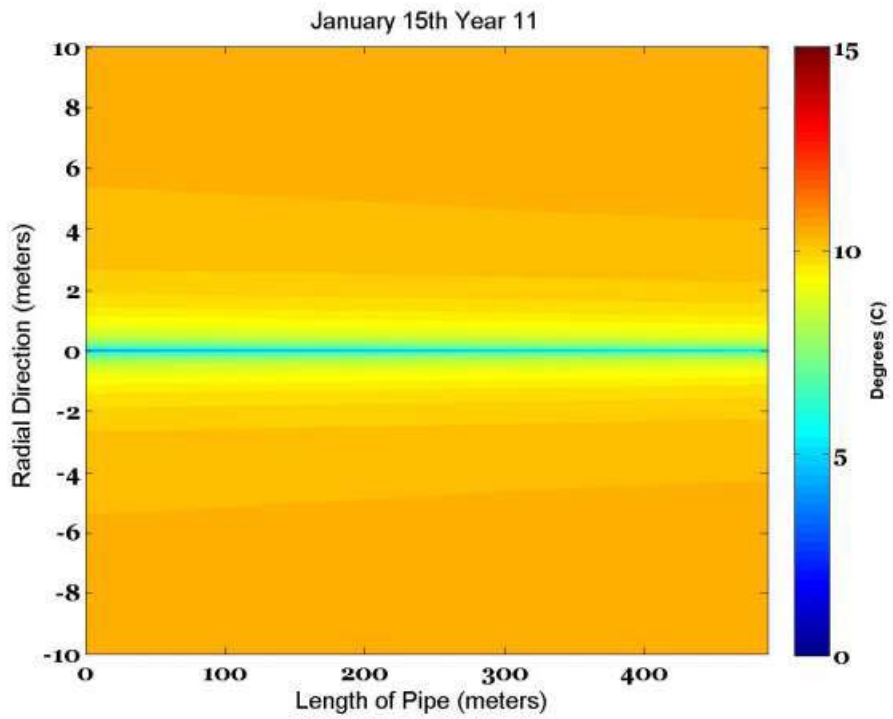
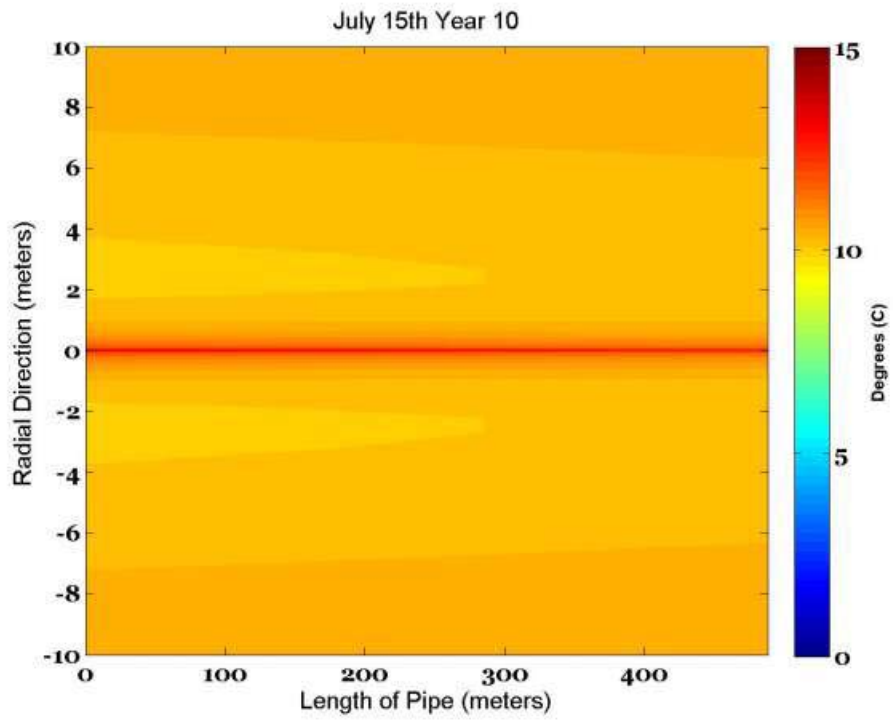


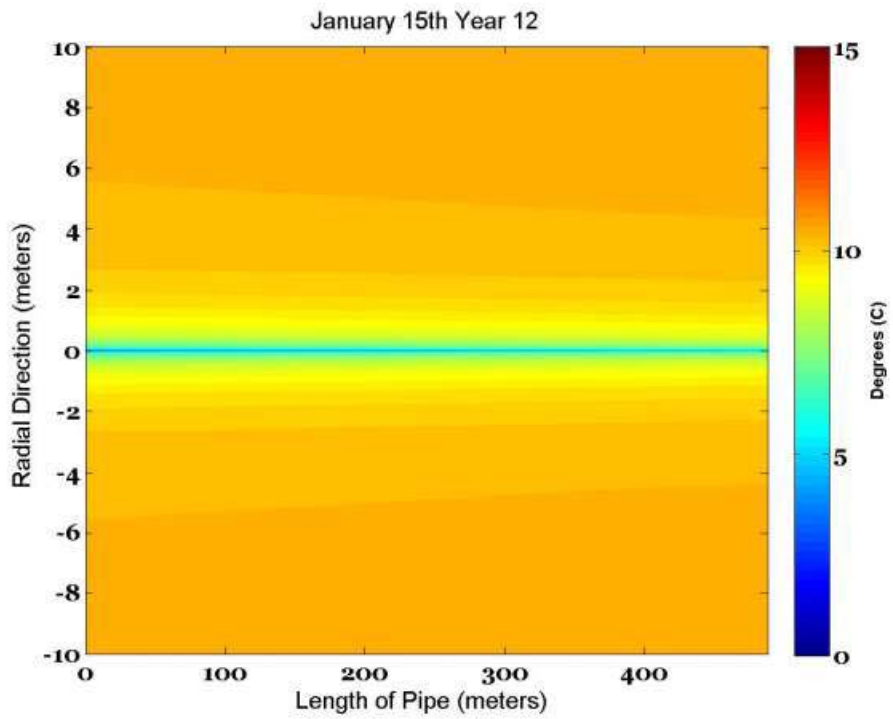
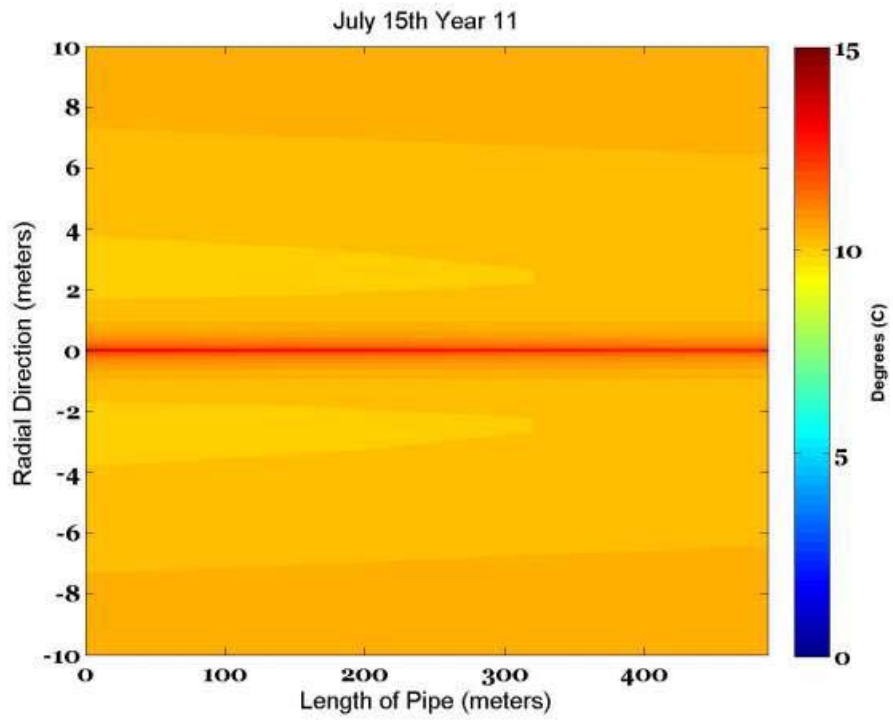


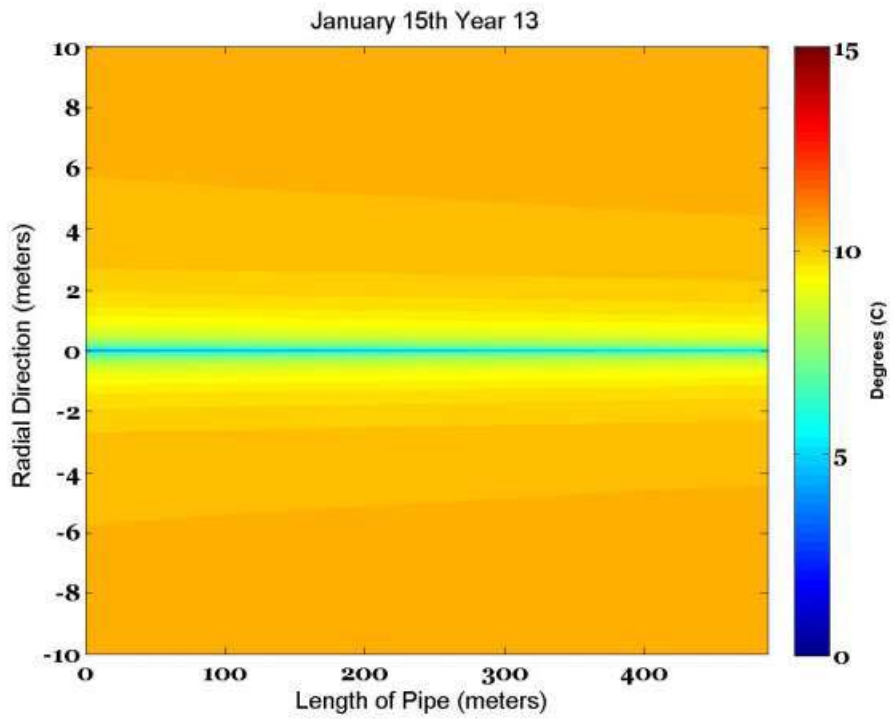
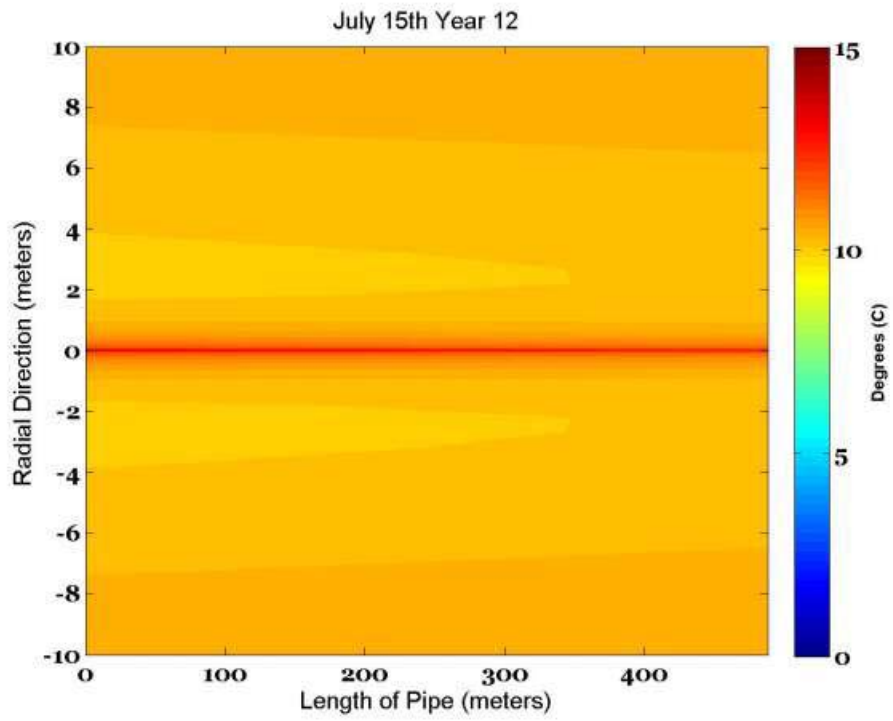


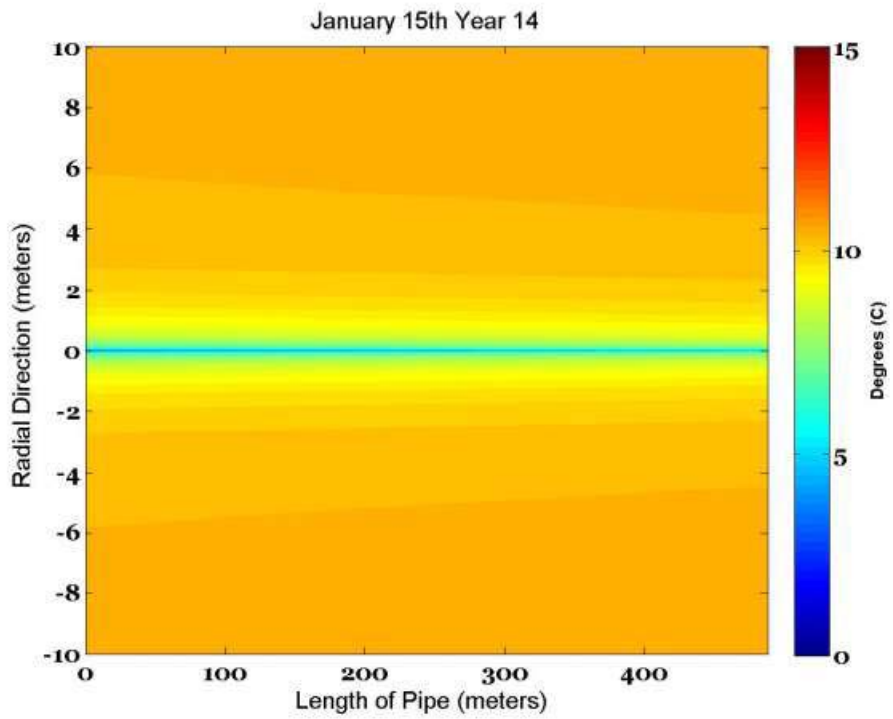
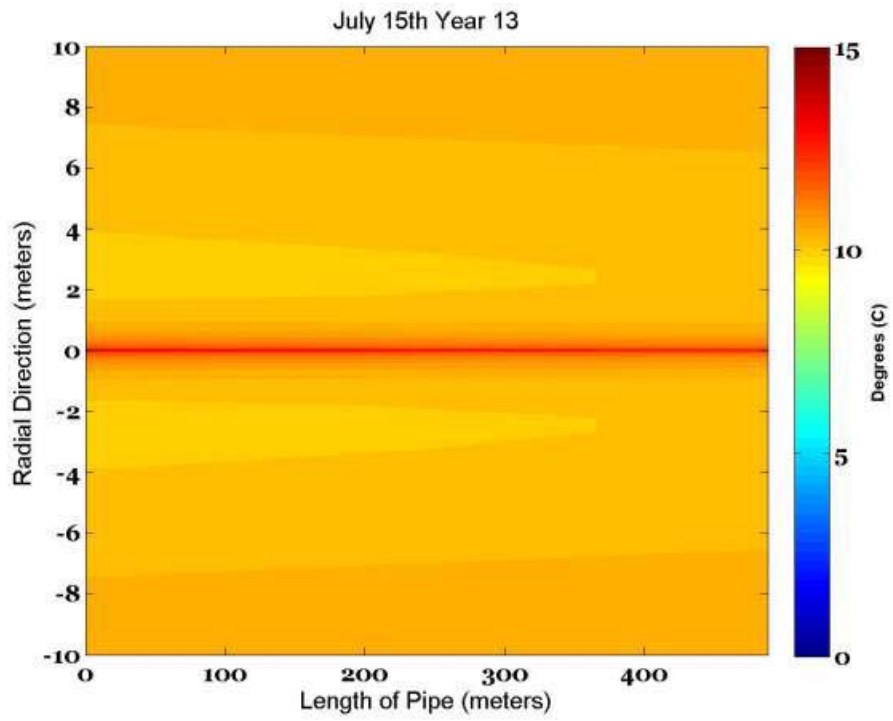


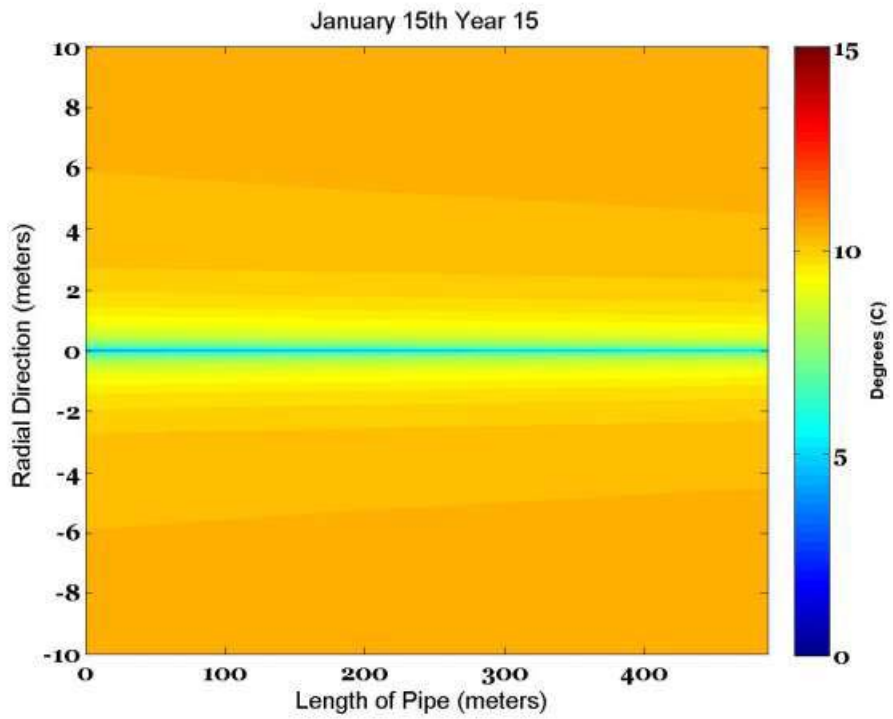
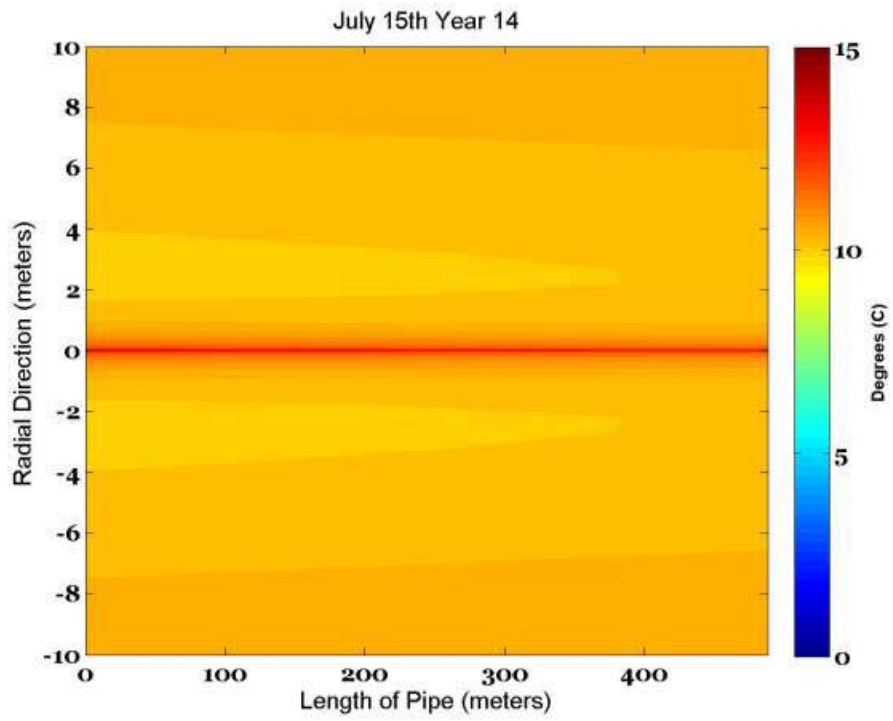


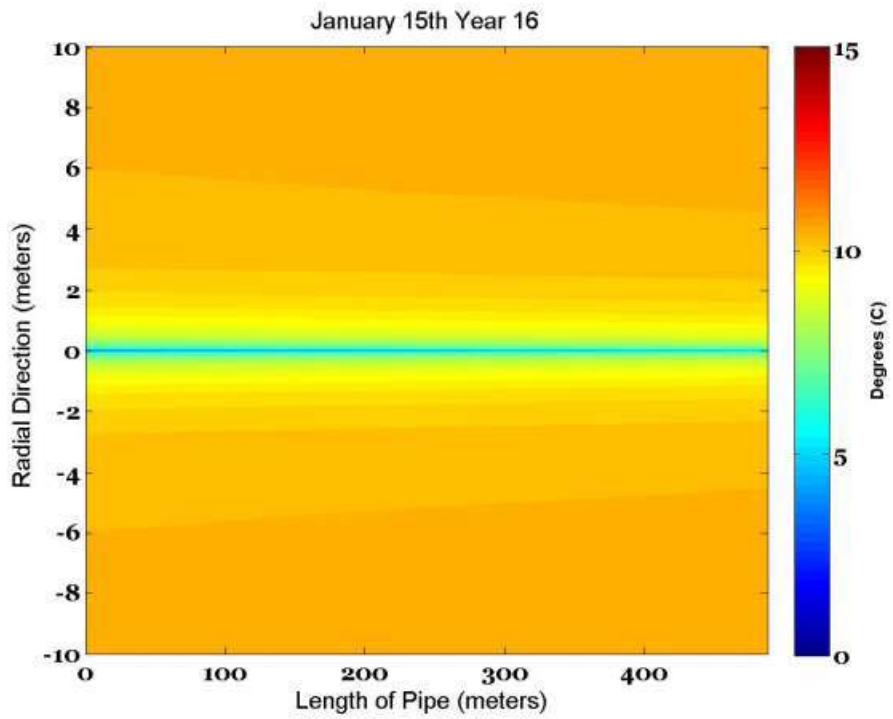
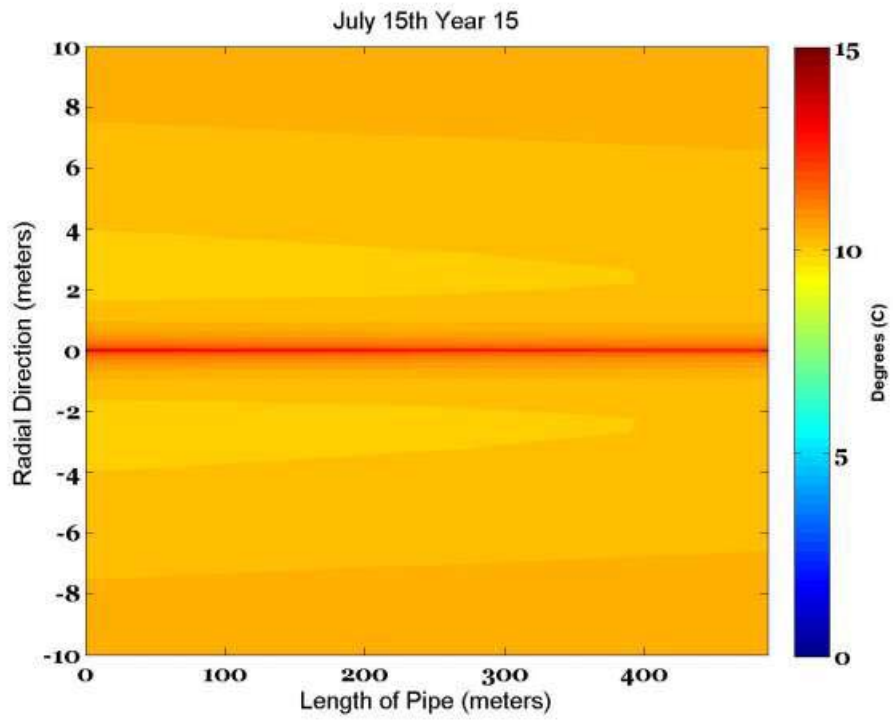


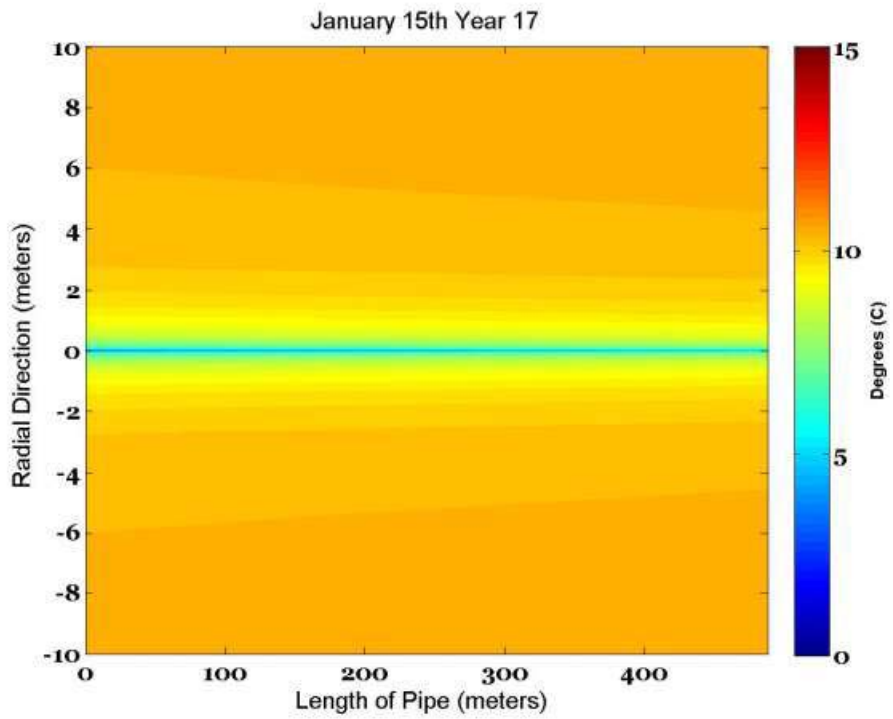
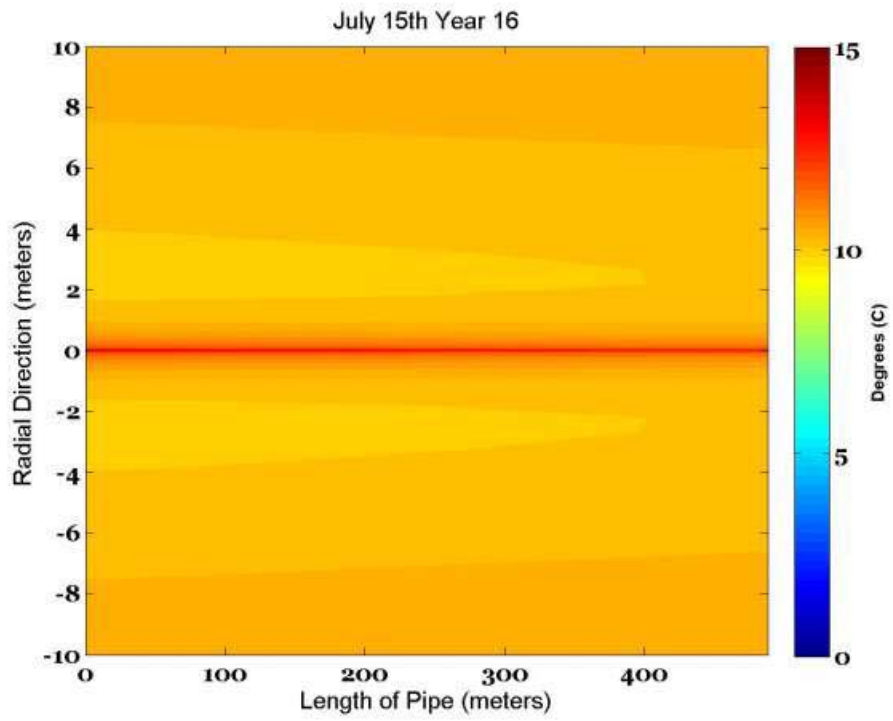


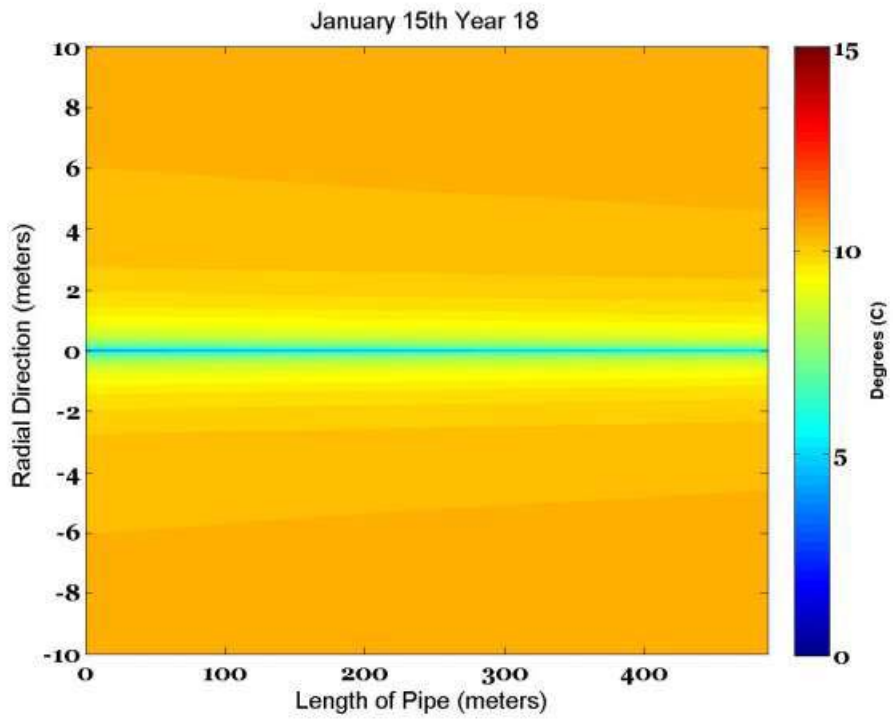
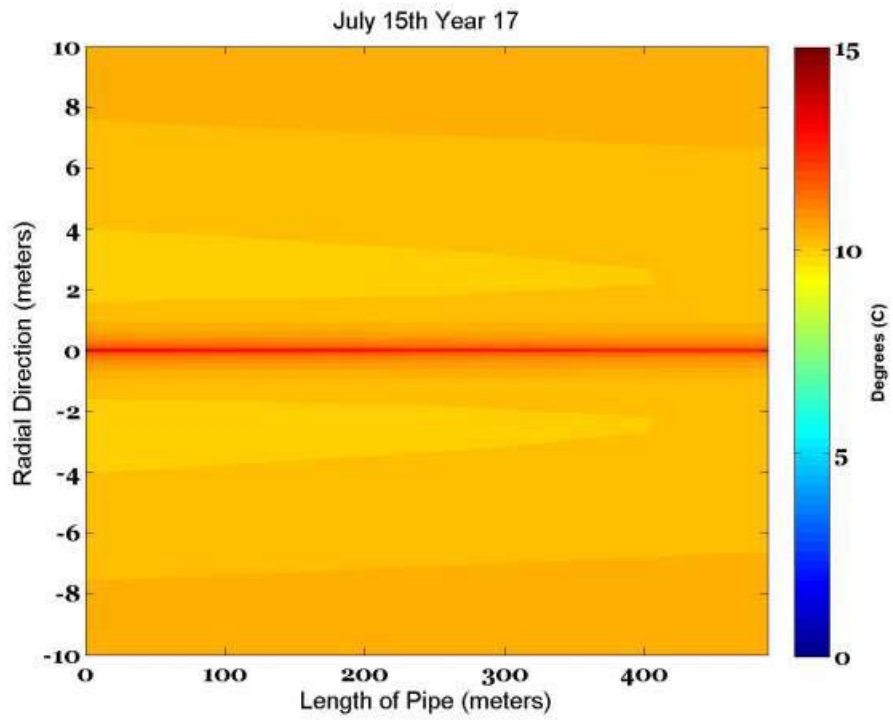


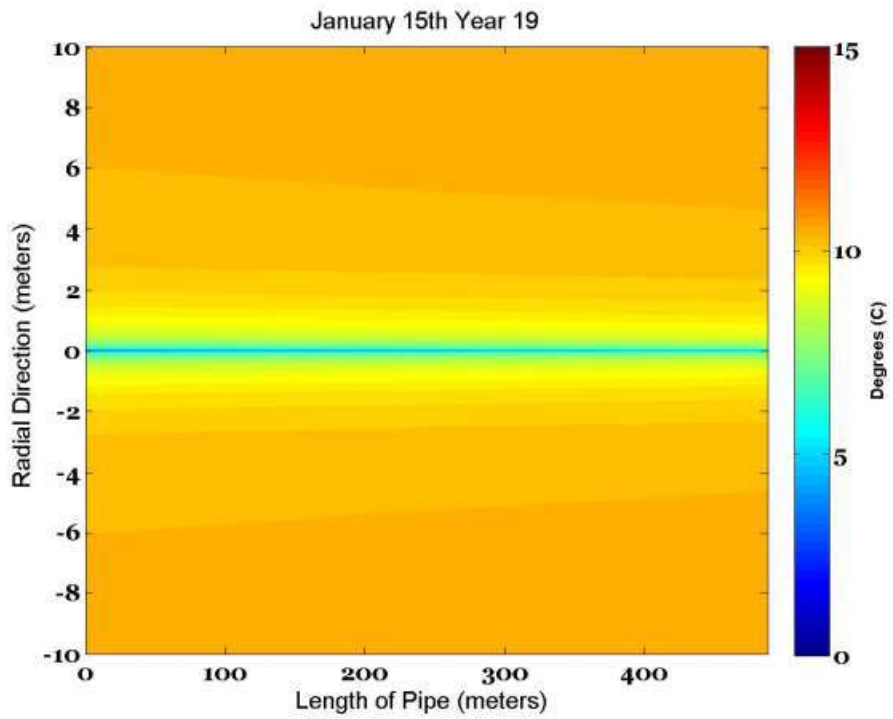
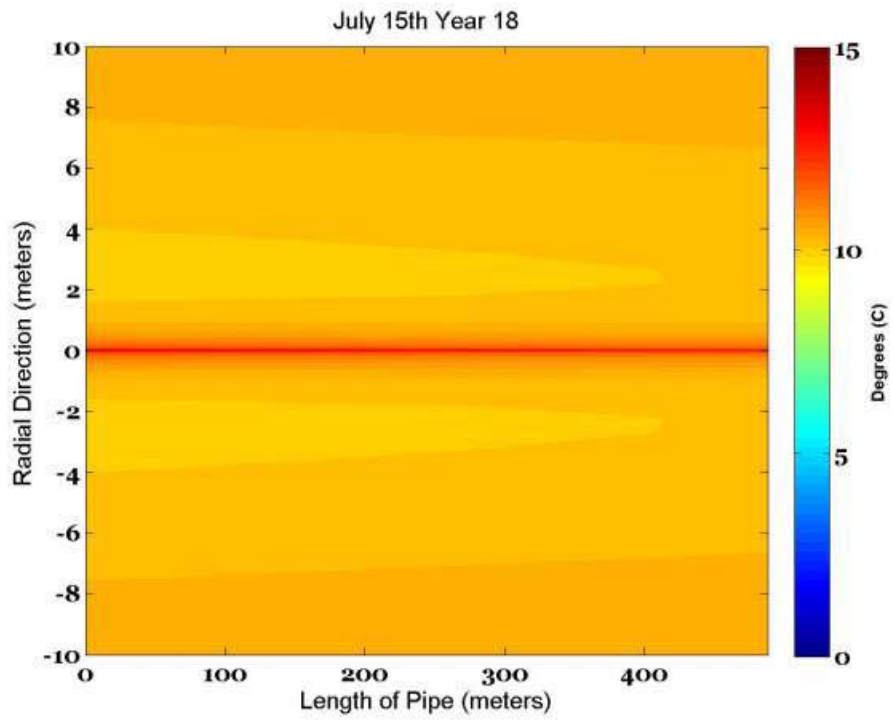


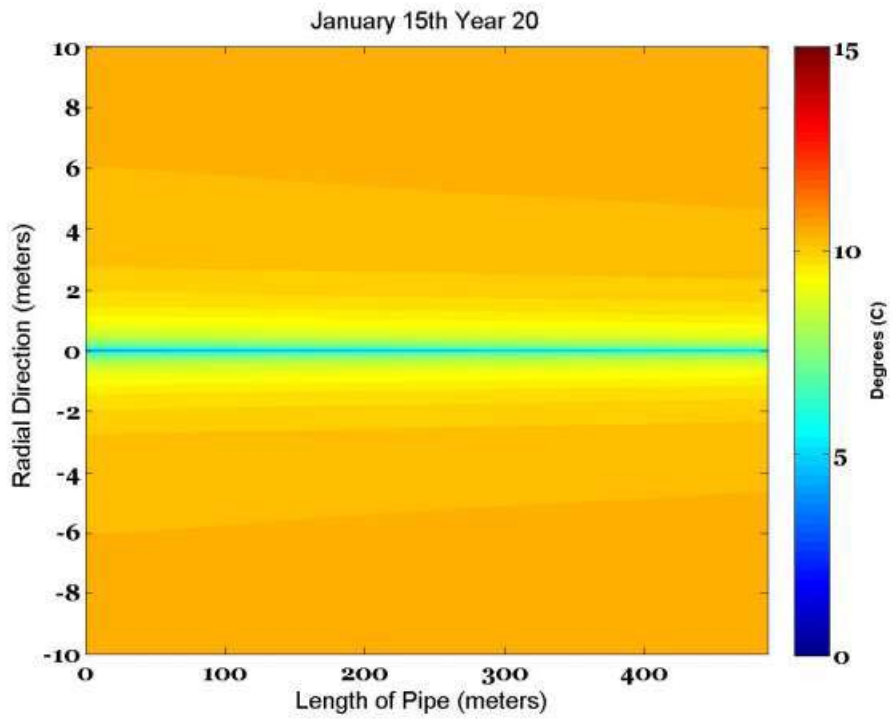
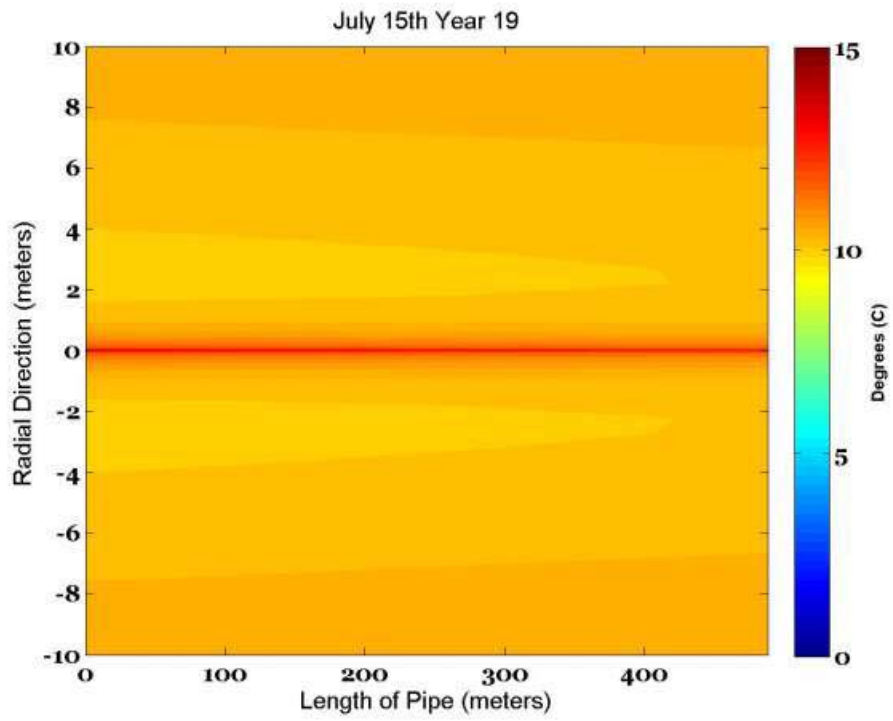


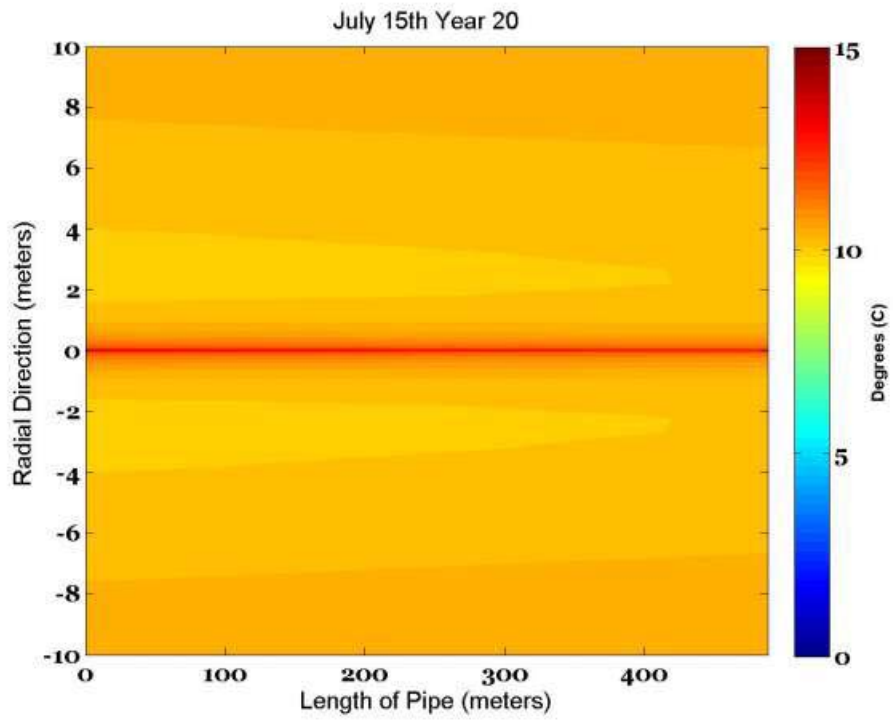












APPENDIX III: SIMULATION RESULTS FOR OMAHA, NEBRASKA.

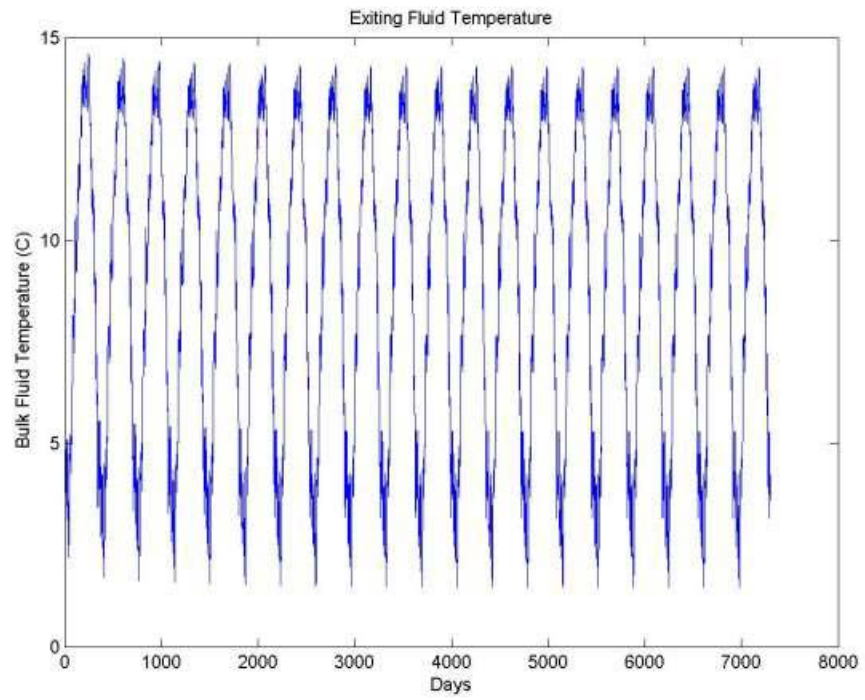
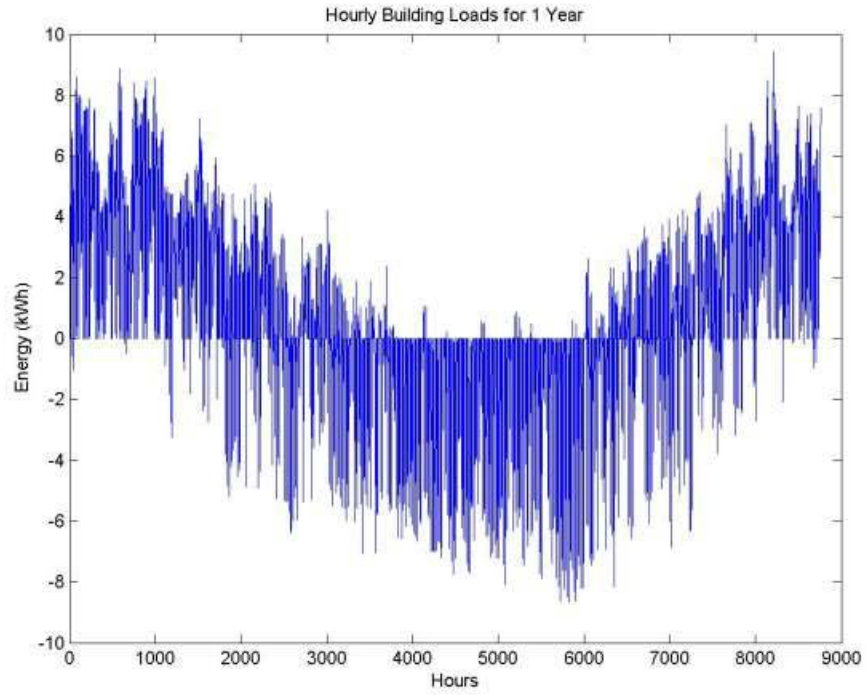
Floor plan Rectangle (18.6m x 10 m)	2000 ft ² / 186 m ²
Air Infiltration	'Moderately Sealed' (.65 ACH)
Window area	22.4 m ² / 241 ft ²
Number of exterior doors	2
Ceiling Height	8 ft. / 2.44 m
Winter Thermostat	70 °F / 21 °C
Summer Thermostat	77 °F / 25 °C
Exterior wall material layers	wood siding, 1/2" plywood, 2x4 wood studs and R11 insulation, 1/2" gypsum board
Exterior Ceiling/Attic material Layers	R-13, 2x6 wood studs, gypsum board

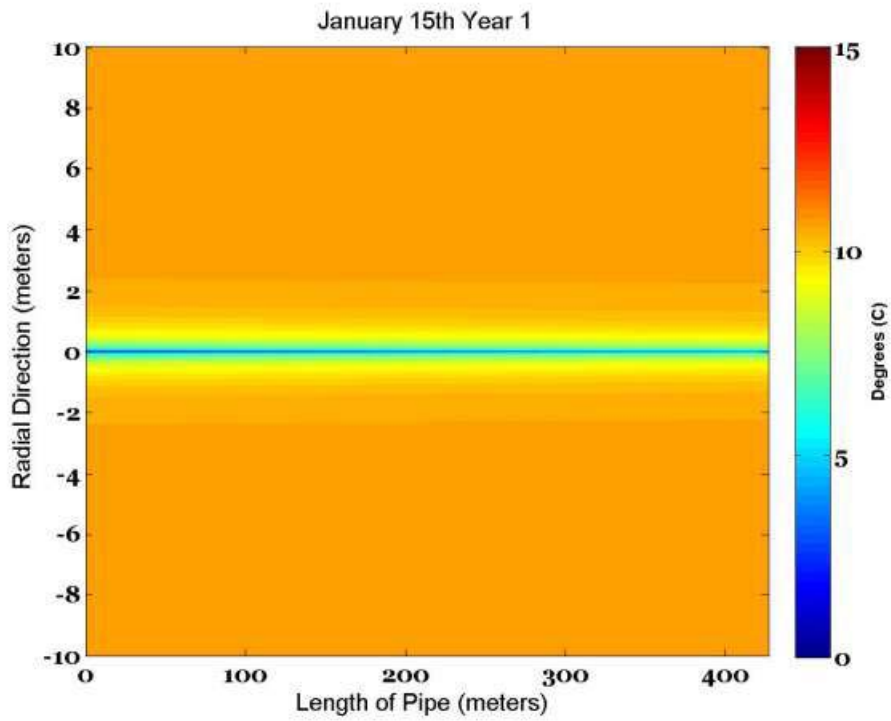
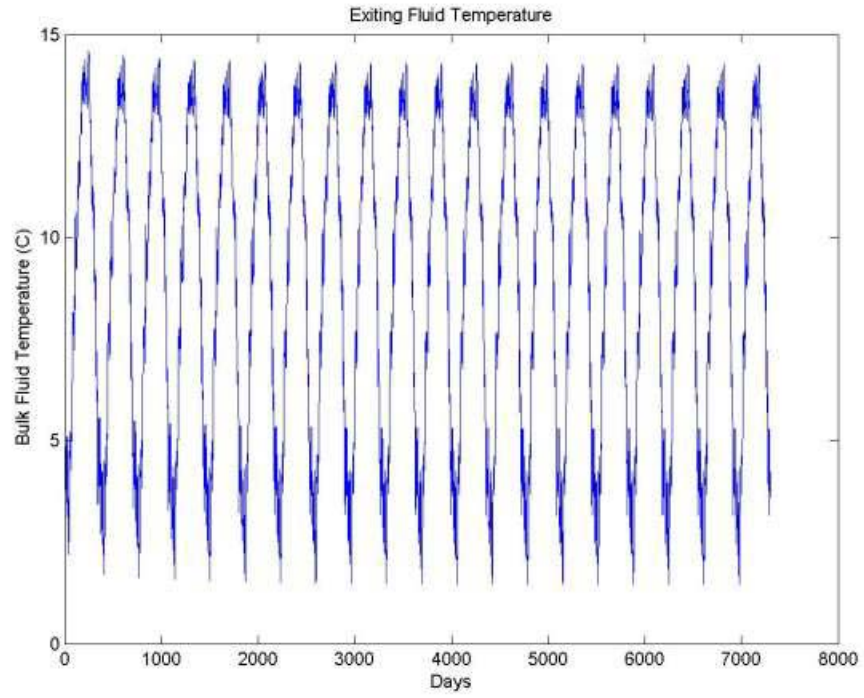
Building Load Analyiss

Peak Cooling Load	8646 Whr
Peak Heating Load	9432 Whr
Extreme Low Outdoor Drybulb	-22.2 °C
Extreme High Outdoor Drybulb	37.1°C
Chosen Heat Pump Size	3 ½ ton unit

Geothermal Design Inputs

Time step	Daily
Years simulated	20 years
Length of tube	427 m
Inner Radius of pipe	15.011 mm
Thickness of Pipe Wall	3.378 mm
Fluid Thermal Conductivity (water)	0.58 W/m-C
Fluid Specific Heat	4220 J/kg-C
Fluid Density	1002 kg/m ³
Fluid Dynamic Viscosity	0.001 N-s/m ²
Tube Thermal Conductivity	0.49 W/m-C
Tube Specific Heat	1340 J/kg-C
Tube Density	941 kg/m ³
Earth Thermal Conductivity	1.3 W/m-C
Earth Specific Heat	1813 J/kg-C
Earth Density	1280 kg/m ³
Fluid Velocity	.87341 m/s
Earth Temperature	10.6 °C
Fluid Initial Temperature	5 °C





*These are temperature contour plots.

